Delft Aerospace Design Projects 2014

New Designs in Aeronautics, Astronautics and Wind Energy

Melkert, Joris

Publication date
2014

Document Version
Final published version

Citation (APA)
Melkert, J. (Ed.) (2014). *Delft Aerospace Design Projects 2014: New Designs in Aeronautics, Astronautics and Wind Energy*. B.V. Uitgeversbedrijf Het Goede Boek.

Delft Aerospace
Design Projects 2014

Delft Aerospace Design Projects 2014

New Designs in
Aeronautics, Astronautics and Wind Energy

Editor:
Joris Melkert

Coordinating committee:
Vincent Brügemann, Joris Melkert, Erwin Mooij,
Gillian Saunders-Smits, Nando Timmer, Wim Verhagen

B.V. Uitgeversbedrijf Het Goede Boek / 2014

Published and distributed by

B.V. Uitgeversbedrijf Het Goede Boek
Surinamelaan 14
1213 VN HILVERSUM
The Netherlands

ISBN 978 90 240 6012 2
ISSN 1876-1569

Printed in the Netherlands

TABLE OF CONTENTS

PREFACE

The Design Synthesis Exercise forms the closing piece of the third year of the Bachelor degree course in aerospace engineering at TU Delft. Before the students move on to the first year of their Master degree course, in which they join one of the Faculty's disciplinary groups in preparation for their final year MSc thesis project, they learn to apply their acquired knowledge from all aerospace disciplines in the design synthesis exercise.

The objective of this exercise is to improve the students' design skills while working in teams with nine to ten of their fellow students for a continuous period of approximately ten weeks with a course load of 400 hours. They apply knowledge acquired in the first years of the course; improve communication skills and work methodically according to a plan.

Despite the fact that the final designs result from a design process executed by small groups of students with limited experience, it may be concluded that the designs are of good quality. Not only the members of the scientific staff of the Faculty of Aerospace Engineering have expressed their appreciation of the results, but also the external experts and industry, which have supported the design projects

This book presents an overview of the results of the Fall Design Synthesis Exercise 2013 and the Spring Design Synthesis Exercise of 2014, based on summaries of each of the projects. The Design Synthesis Exercise Coordination Committee, responsible for the organisation and execution of the exercise, has made this book with the aim to present an overview of the diverse nature of the various design topics, and of the aerospace engineering course itself. In addition, the book is intended as an incentive for further improvements to the exercise.

Finally the coordinating committee would like to thank the student-assistants, the academic counsellors, the educational office and all who have contributed to the success of this year's exercise.

The Design Synthesis Exercise Coordination Committee 2014:
ir. V.P. Brügemann, ir. J.A. Melkert, dr.ir. E.Mooij,
dr.ir. G.N. Saunders-Smits, ir. W.A. Timmer, dr.ir. W.JC. Verhagen

1. THE DESIGN SYNTHESIS EXERCISE

1.1 Introduction

The design synthesis exercise forms a major part of the curriculum at the Faculty of Aerospace Engineering, Delft University of Engineering. The main purpose of the exercise is the synthesis of the curriculum themes presented in the first two years of the educational program at the faculty.

Since this design exercise is organized approximately half-way through the complete five-year program (three year Bachelor of Science in Aerospace Engineering + two year Master of Science in Aerospace Engineering), the design results are not expected to be of a professional quality. Nevertheless the students and their tutors strive to create the best design they can. This is accomplished in an iterative way. Such an iterative process is a typical element of building up design experience.

The way in which a project is carried out and reviewed is only partly focused on the design result. The design process itself is of greater importance. It is especially important for the students to work as a team, since this best reflects a design process in 'real life'. In this way, the students can take full advantage of their personal qualities.

1.2 Objective

The design synthesis exercise helps to meet the faculty's requirement to enlarge the design content of the aerospace engineering course. The goal of the exercise itself is to improve the design skills of the students, in particular project management, communication,

teamwork and the application of the knowledge gathered in the first three years of the course.

The student has the opportunity to increase his experience in designing. The whole process of designing is dealt with, from the list of requirements up to the presentation of the design. Typical aspects of such a process, such as decision making, optimization and conflicting requirements will be encountered. Acquiring experience often means going through iterative processes, so design decisions can be altered to make sure that the design requirements are met. The arguments supporting the decisions are reviewed, as well as the way the project is managed. Aspects of design methodology and design management are also taken into account.

During the project the student is expected to work in a team. This means that a student learns to cooperate, to schedule and meet targets, manage the workload, solve conflicts, et cetera. In this field, effective communication is of major importance. Apart from these capabilities the student is expected to be able to communicate ideas and concepts regarding the project subject with specialists and non-specialists. By means of integrated short courses in written reporting and oral presentation, the communicative skills of a student will be developed and assessed.

1.3 Characteristics of the exercise

The characteristics of the design synthesis exercise are:

- For all students, the design component of the study is reinforced by the design synthesis exercise.
- The design synthesis exercise consists of a design project integrated with workshops and courses on oral presentation, sustainable development, systems engineering and project management.
- The exercise has a fixed end date. This means that the third year ends with the design exercise.
- All discipline groups of the faculty provide the support needed during the exercise. This enhances the multi-disciplinary nature of the exercise in general and the design projects in particular.

- The design process is supplemented by lectures on design methodology and project management, as applied to the exercise.
- Aspects of sustainable development, such as noise emission, the use of raw materials, energy consumption and environmental impact are addressed explicitly during the exercise.
- Integrating short courses on oral presentations develops the communicative skills.

1.4 Organization and structure of the exercise

Students indicate their preferences after presentations by the staff introducing all project subjects. Students are divided into groups of approximately ten persons, as much as possible according to their preferences. The exercise takes place during a continuous period of eleven weeks, the last educational term of the third year of the Bachelor course. Technical aspects of the project take up 60 percent of the time; the remaining 40 percent is spent on general topics supporting the project work. General topics are spread over the full period of the exercise. The general topics are sustainable development, design methodology and project management and oral presentations.

1.5 Facilities

To complete the exercise design within the given period of time, the groups of students can make use of several facilities. Each group has its own room, with various facilities (tables, chairs, computers, flip-over charts et cetera). Commonly used software like AutoCAD, ProEngineer, CATIA, Matlab, MS Office, MS Project, C++, Fortran, MSC Nastran and more project specific software are available. A special library is available, containing literature on typical project subjects. Finally each group has a budget for printing and copying.

1.6 Course load

The course load is measured in credit points according to the European Credit Transfer System, ECTS: 1 credit point equals 28 hours of work. The total course load is 15 ECTS credits.

1.7 Support and assistance

An essential part of designing is making choices and design decisions. During a technical design process, the choices made in the first stages are often based on qualitative considerations. When details of a design take shape, quantitative analysis becomes increasingly important.

The considerations accompanying these design choices need mentoring and tutoring, since students lack experience in this field. The execution of the project demands a fair amount of independent work of the design team. This means that the team itself is capable of executing the design process. The task of the team of mentors is mainly to observe and give feedback on the progress. The team of mentors consists of a principal project tutor and two additional coaches. Each has a different area of expertise. The method of working, the organization, the communication of the team and the collaboration within the team itself are also judged. Where necessary, the mentors will correct the work and work methods of the team. Warnings of pitfalls and modeling suggestions for certain problems during design will be given when needed, to ensure a satisfactory development of the design.

1.8 Design projects 2014

The Design Synthesis Exercise 2014 is divided into 31 different design assignments. In table 1.1 an overview is given of these subjects. In the following chapters the results of the design teams are covered in detail. For each project, the important design characteristics are covered. These are: problem introduction, design specification or list of requirements, conceptual designs, the trade-off to find the "best" design, a detailed design and finally conclusions and recommendations.

Fall DSE

Nr.	Project Title	Principal Tutor
F1	Dune MAV: Exploiting updrafts along the coast with a Micro Air Vehicle	Guido de Croon
F2	Interactive wing design using rapid prototyping	Marios Kotsonis/Richard Dwight
F3	Unmanned Aerial Vehicle Cargo Delivery System	Marcias Martinez

F4	Looking for water	Joris Melkert
F5	Inspiration Mars	Erwin Mooij
F6	Towards a Next generation of Water bombers	Paul Roling
F7	Design of a VTOL business aircraft	Sonell Shroff
F8	Rocket Powered VTVL vehicle	Chris Verhoeven
F9	Gravity explorer satellite	Wouter van der Wal

Spring DSE

Nr.	Project Title	Principal Tutor
S1	Wind turbine wake visualisation	Wim Bierbooms
S2	A new Earth observation space asset for the Royal Netherlands Air Force	Angelo Cervone
S3	All weather, all polymer Search and Rescue (SAR) UAV with hover capability	Theo Dingemans
S4	Mission to Investigate Rarefied Aerodynamics on Low Orbiting Satellites	Eelco Doornbos
S5	A320 AF (Alternative Fuel)	Arvind Gangoli Rao
S6	Birdplane	Santiago Garcia
S7	“Best of both worlds” flying car	Ronald van Gent
S8	Minimum Fly-by-wire Trainer	Steve Hulshoff
S9	IMAV 2014 – single-UAV operations	Erik-Jan van Kampen
S10	Lunar Cryogenic Sample Return Mission	Ron Noomen
S11	Twin-Lift Unmanned Rotorcraft for Aid in Disasters	Marilena Pavel
S12	Printing_the_Personal_Aircraft_of_Tomorrow	Calvin Rans
S13	Design of an Aerobatics Air Race Aircraft	Paul Roling
S14	HotFire	Ferry Schrijer/ Sander van Zuijlen
S15	Aerobatic racing aircraft design	Sonell Shroff
S16	Aerobatic racing aircraft design	Sonell Shroff
S17	High Volume Production of new Airline Workhorse	Jos Sinke
S18	World’s largest dirigible billboard	Durk Steenhuizen
S19	SAR Satellite Network for Maritime Monitoring of North Sea	Prem Sundaramoorthy
S20	Arctic wind turbines: A Cold Case	Nando Timmer
S21	Designing a Premium Business Jet	Wim Verhagen
S22	IMAV 2014 – multi-UAV operations	Christophe de Wagter

1.9 The design exercise symposium

The one-day design exercise symposium forms the conclusion to the design project, during which all student teams present their designs. The presentations cover the design process as well as the design result. The symposium is primarily intended for participating students, mentors and tutors. Other staff and students and external experts are invited as well.

A group of experts from within the faculty as well as from industry form the jury and assess the presentations in style and technical content. Three criteria determine the score of the group:

1. technical content (35%)
2. presentation (20%)
3. design content (35%)
4. sustainable development (10%)

The jury of experts this year consisted of:

Fall DSE

Jan Verbeek	ADSE
Hester Bijl	TU Delft
Bernard Fortuyn	Siemens
Hans Roefs	NLR
Martijn van Rij	Fokker
Martin Lemmen	TNO
Tineke Bakker - van der Veen	Dutch Space
Egbert Torenbeek	TU Delft

Spring DSE

Hester Bijl	TU Delft
Paolo Astori	Politecnico Milano
Richard Cooper	Queen's University Belfast
Jean-Luc Boiffier	ONERA/ ISAE Toulouse
Ladislav Smrcek	Glasgow University
Rob Hamann	SEC^2
Tineke Bakker - van der Veen	Dutch Space
Jan Rohac	CVUT Praag

Daniel Hanus	CVUT Praag
Luis Campos	IST Lisboa
Emiel van Duren	Royal Dutch Airforce
Pascal Bauer	ENSMA Poitiers
Giovanni Carlomagno	University of Naples
Hans Roefs	NLR
Bernard Fortuyn	Siemens
Arnaud de Jong	Dutch Space
Ron van Baaren	ADSE
Vassili Toropov	Queen Mary University of London
Javier Crespo	ETSIA Madrid
Jan Scholten	NLR

2. DUNEMAV: EXPLOITING UPDRAFTS ALONG THE COAST WITH A MICRO AIR VEHICLE

Students: R. Hangx, R. Keus, N.W. Klein Koerkamp, V. A. Mensink, S.F. Ramdin, M.B. Ruijs, M.A.P. Tra, Q.H. Vû, R.B. Wit, L.L. Wouters

Project tutor: Dr. G.C.H.E. de Croon

Coaches: H. Haiyang MSc, J.L. Junell MSc, F. Sluis MSc,

2.1 Introduction

Micro Air Vehicles (MAVs) are a subclass of Unmanned Aerial Vehicles (UAVs). MAVs are generally designed to have a high level of autonomy and are used for surveillance tasks. Current low weight MAVs can only fly for a maximum of two hours with a range of up to 10 kilometres due to the low volume available for energy storage and the usage of conventional systems to stay airborne. Looking at nature, birds use updrafts extensively in order to significantly prolong their flight time without having to use any additional energy, making this type of flight extremely economical. The result of this project presents a design for an MAV, which will autonomously perform long endurance beach surveillance along the Dutch west coast, by actively detecting and exploiting updrafts.

Figure 2.1: Final artistic representation of the DuneMAV

Earlier studies have shown insight on how thermal updrafts can be modelled. Ridge updrafts, which are updrafts created by wind hitting an obstacle that is large and steep enough to deflect the wind upwards, are not treated in such detail. In order to exploit these updrafts, the MAV will have to autonomously locate the dune and determine its geometry. For that purpose, colour classification and optical flow can be used, where previous applications of these methods are generally in the obstacle avoidance research field. Also, a full flow map of the wind using the geometry of the dunes and theoretical knowledge on ridge updrafts is modelled and used. Furthermore, this MAV will fly towards a point of interest in the most efficient way. This will mean that the autopilot will investigate possible routes and choose the route optimized for the lowest energy usage.

2.2 Requirements

The project started with doing a full requirement analysis. During and after the final design, this analysis is checked to ensure that the project objective is met. The most driving requirements are listed below:

- The MAV shall have a wingspan smaller than 2 m and the take-off weight shall be below 1 kg.

- The production costs shall remain below € 2,500.
- The MAV shall be able to fly from Hoek van Holland to Katwijk and back, during at least 70% of the days between June to August.
- During one day, the MAV shall be able to fly at least 12 hours.
- The MAV shall be able to provide visuals from which it is possible to recognize a person's body pose.
- Good updraft locations shall be detected ahead.
- The operational life of the MAV shall be at least 100 flights.

2.3 Concepts and trade-offs

To explore all possible solutions, different design options were conceived. This exploration is mainly fed by literature studies and knowledge obtained from the bachelor. In this conceptual phase, the launch, landing, propulsion, energy source, configurations and materials are topics that were analysed. The results of these trade-offs are discussed briefly.
Using a catapult, winch or by just throwing or dropping the DuneMAV from a certain height were considered as options for the launch. Additional weight and structural requirements are the two main criteria of a total of six trade-off criteria. Overall, launching the MAV by throwing scored best in the trade-off. For landing, a similar approach was taken. After quantifying the possible options, a simple belly landing was chosen for this mission.

A propulsion system is needed when there are no sufficient updrafts. For safety reasons, a push propeller is chosen over a pull propeller. Therefore, the MAV will be equipped with a small folding propeller, mounted on the back of the fuselage to avoid damage or injuries if the DuneMAV crashes.

An in-flight energy generation, consisting of a regenerative propeller or solar cells, were considered. After calculating the amount of energy gained using a regenerative propeller and knowing that this system adds extra complexity and weight, it is concluded that this will not be implemented in the MAV. Also, solar cells should not be included, because of the high cost, challenging manufacturability and low

added energy. This results in the choice that only batteries are used as energy supply.

The configuration of the DuneMAV is an important design aspect. Endurance and range performance, structural design, stability by perturbation, stall behaviour, manoeuvrability, subsystem placement and maintainability are the trade-off criteria. After the first iteration of the trade-off, a conventional and a tandem configuration were chosen to investigate in more depth. The second iteration was done by modelling the optimal design of a conventional and tandem configuration to the highest ratio of endurance, C_L^3 / C_D^2.

This ratio is a function of density, velocity, lifting surfaces, aspect ratio, Oswald factor and Reynolds number. Several constraints, such as a minimum Reynolds number, minimum and maximum aspect ratio, sufficient strength to withstand a landing on one wing, maximum weight and payload weight, defined the framework for the optimization. The result of the algorithm provided a clear answer; the endurance performance of a conventional configuration is higher than the tandem configuration for this mission.

The last item that was investigated was the material choice for the DuneMAV. Comparing material properties, such as tensile strength, compressive strength, Young's modulus and density, but also manufacturing complexity and cost, it has been decided to use carbon fibre reinforced polymers in combination with depron, an extruded polystyrene foam.

2.4 Detailed design

In the next phase, a more detailed design of the wing, tail, control surfaces and fuselage is made.

Layout

The model used for determining the conventional and tandem configuration is used for the initial sizing of the wing and tail,

constraining on Reynolds number, aspect ratio of the wing and tail, weight and maximum span of the wing. Input for this optimization are the tail span, set such the push propeller can be fitted in between the two booms, the length of the booms, fuselage design and weight of the subsystem. The next step is to check whether this sizing is in the margins of stability and control. This analysis is done with a software package called XFLR5, that provides several aerodynamic analysis features. It shows the result on static and dynamic stability, but also on the required centre of gravity position and the required cruise speed to achieve the maximum endurance performance. If these outputs showed a design that did not meet the requirements, the design was adjusted, until the final design of the main wing, tail and fuselage did meet the requirements.

Parallel to this sizing iteration, a trade-off was made on the tail design. After choosing for two booms, favourable for placing the propeller, a V-tail, inverted V-tail and H-tail were investigated for the best possible solution. When taking the mission profile, which will consist of heavy headwinds, into account, the H-tail is most preferable.

The fuselage design was also performed parallel to the above process. In this design, the available space, aerodynamic and structural aspects have been considered. The control surfaces (ailerons, elevators and rudder) are designed to provide adequate controllability, even with the expected side winds. This results in a final design that can be seen in figure 2.2.

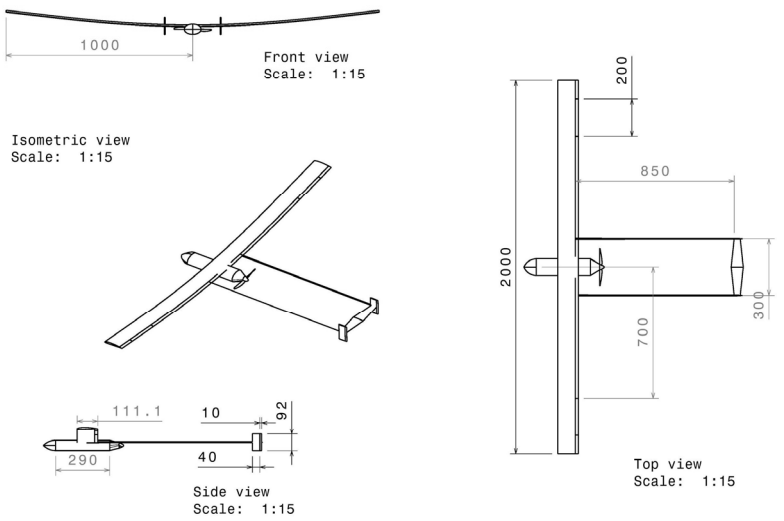

Figure 2.2: Final technical drawing of the DuneMAV

Performance analysis

To analyse the performance of the DuneMAV, a simulation was made in the "Tomlab for MATLAB" environment. It optimizes the trajectory of the DuneMAV to keep it airborne for at least 12 hours. It was found that the DuneMAV will fly at the maximum climb factor during climb, since it results in the highest energy extraction from the updrafts. Furthermore, in the updraft free zones, the DuneMAV will fly at an airspeed such that the lift over drag ratio (L/D), or glide ratio, is maximized to glide over the gaps between dunes as efficient as possible.

Aerodynamic analysis

After a second iteration, using the optimization algorithm, a third iteration has been performed. The final design has been fine-tuned aerodynamically, with the help of a 3D panel method and a vortex lattice method in XFLR5. This results in an MAV that is specifically suited for this mission. The DuneMAV will be cruising at its maximum climb factor, flying at a velocity of 7.7 m/s. The centre of gravity has been tuned in such a way that the MAV pitches to its

maximum climb angle of attack, which is equal to 7 degrees. For regions where no updrafts are encountered the DuneMAV will fly at its maximum glide ratio, 21.5, at a cruising velocity of 8.0 m/s.

Structural analysis

The aircraft should be able to withstand several load cases during its mission without failure. In order to accomplish this, four forces are investigated and the resulting stresses in the structure are examined. These load cases are: cruise with maximum wing loading, a landing on the wing tip, a landing on the tail and torsion in the wing due to the lift. The materials selected for the main wing are CFRP as a load bearing skin and depron as supporting filling of the main wing. From the analysis, it is observed that the minimum thickness needed to carry the resulting loads is less than the minimum manufacturable thickness of CFRP, which is 0.2 mm. A minimum safety factor of 1.5 is needed to account for material and manufacturing variations between the yield stress and the maximum achieved stress in the structure. For the load cases described above, a safety factor of 2.3 is achieved for the maximum Von Mises combined stress along the wing span.

Stability and control

Based on this final design, the static and dynamic stability of the DuneMAV is checked. The longitudinal static stability is achieved because the centre of gravity is in front of the neutral point. For the dynamic stability the Eigen motions of the DuneMAV have been analysed. All modes except the spiral mode are stable and certify the requirements set by FAR 23 regulation, which are very conservative regulations when translated to MAVs because actually FAR 23 regulations are for small, manned aircraft.

Surveillance and communication

To obtain images with enough detail to detect a human body pose, a high resolution camera system has been selected. This camera system consists of two 41 MP camera's, one pointing left and one pointing right, which will be able to detect a human at a distance of over 380 meters. The main disadvantage of this high resolution camera, however, is that the image size is large. Therefore communication will

be done using the 4G mobile network, which will enable a large up- and downlink. Since the DuneMAV will be flying within 4G range, this is considered the best option.

2.5 Updraft detection

To achieve the long endurance requirements, the DuneMAV must locate updrafts autonomously. The updrafts depend on the dune geometry, wind velocity and angle of incidence. Via optical flow the DuneMAV is able to detect dune geometries, after which flow mapping is used to define the updraft velocities and locations.

At first, optical flow is the pattern of apparent motion in visual scenes caused by the relative motion between an observer (the DuneMAV) and the environment. In optical flow, sequences of frames are compared to each other and the displacement of the pixels between the frames is visualized by flow vectors. Objects closer to the DuneMAV appear to move faster than objects that are located further away and will result in larger optical flow vectors. When the DuneMAV flies above the dunes, the higher parts of the dune will apparently move faster than lower parts, which will results in a larger vector between frames. With this method, 2D slices of the dune can be generated from which the dune geometry (height, width and slope) can be estimated. Combining these slices, results in a 3D map of the dune.

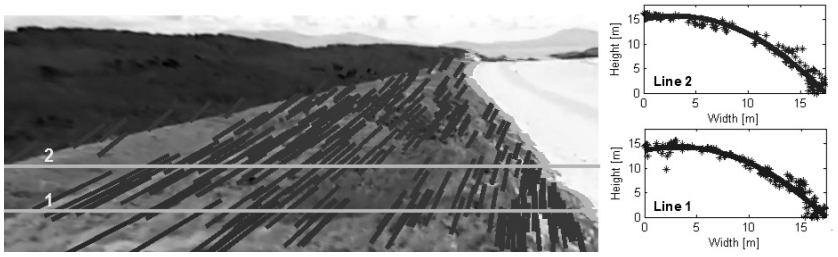

Figure 2.3: Optical flow applied on a dune and 2D Slices of the dune

The wind perpendicular to the dunes is required to define the updrafts above the dune, since the updraft velocity depends linearly on the wind speed. The wind data during a particular flight can be

obtained using an on-board wind meter. From the direction and velocity of the wind and the dune position, the wind velocity perpendicular to the dune can be defined.

Using this information, the updraft velocity can be calculated using flow mapping. This is an analytical method that can create flow patterns around objects. The dune angle, obtained by optical flow, is used as input to generate an inclined step with straight-line segments. With flow mapping, the flow pattern around the dune is visualized and the updraft velocities can be defined.

The DuneMAV should fly at the locations where the maximum updraft velocities occur, since it can extract the most energy from the wind there. From the flow pattern, these maximum velocities and the corresponding locations can be obtained. Therefore, the MAV can define its trajectory above the dunes during flight.

2.6 Autopilot

An autopilot is needed since the DuneMAV shall be able to fly fully autonomous. The autopilot consists of a guidance, navigation and control system. The guidance module handles the path planning from the current location to the intended destination. The navigation module estimates and determines the current state and the control module commands the control surface deflections and thrust setting necessary to follow the path, as determined by the guidance block.

Guidance
The guidance module handles the launch of the MAV, the path planning and thus determines the trajectory to be followed from the current location to a specified destination. The guidance module consists of the high level decision sub module and the trajectory planner sub module.

The high level decision making sub module handles the top level flight modes and deals with possible exceptions that can occur during the mission. Four flight modes have been identified: standby, take-off,

cruise and landing. The most important flight mode is cruise, in which the DuneMAV uses its optical flow system to exploit updrafts and flies at a specific attitude for maximum energy extraction. Possible exceptions that can occur during flight were investigated and predefined actions were coupled to the identified exceptions. Examples of these actions are to make an emergency landing or to autonomously fly back to a predefined home location. The output of the high level decision making submodule is a waypoint that the DuneMAV should fly to, which is used as an input for the trajectory planner.

The trajectory planner determines the path the DuneMAV should follow to travel from its current position to its destination waypoint as specified by the high level decision submodule. The path the DuneMAV should follow is determined by the total energy of the DuneMAV and by the availability of optical flow data. If the total energy of the DuneMAV is sufficient to reach the waypoint, it does not need to follow the dune line for updraft exploitation. If the total energy is not enough the trajectory planner uses the optical flow data to follow a path along the dune line.

Navigation

The navigation module consists of an estimator, which estimates the state information, and the sensors which supply the necessary data to be able to determine the state information. The autopilot needs different sensors to determine the location, velocities, accelerations and state information. The combination of these sensors is called an inertial measurement unit and is included on autopilot chips. For the autopilot of the MAV, the Lisa/S will be used. The Lisa/S, which was developed in collaboration with TU Delft in The Netherlands, is the smallest fully capable autopilot available on the market.

Control

The purpose of the controller is to translate the waypoint input to heading, altitude and airspeed set points and then to translate those set points into control surface deflections and a thrust setting. It has been decided to use an energy controller, since this controller enables

flight at a specific airspeed by controlling the pitch of the DuneMAV, without using propulsion.

2.7 Endurance check

For the endurance simulation, it is necessary to know the dune geometry and the weather conditions. To investigate the potential and kinetic energy that the MAV can extract from updrafts, the dune geometry should be known. The number of gaps, depth of gaps and the length of the dunes between Hoek van Holland and Katwijk are investigated. It is shown that the dunes have an average slope of 13 degrees, with a maximum slope of 20 degrees. The longest gap is the boulevard at Scheveningen with a length of 1800 meter. The deepest gap is located south of The Hague where the MAV should bridge a harbour.

For the weather conditions, all hourly wind speeds of Hoek van Holland between 1971-2010 were investigated. Since a high perpendicular and low parallel velocity is desired, it was concluded that the best 12-hour time interval for the MAV to fly is from 6 AM to 6 PM. The data points within this interval were further investigated to show that the MAV can fly for 70% of the time. The higher the MAV will fly above the dune, the slower it has to go relative to Earth to be able to get to 70%. This results in a trade-off between flying height and ground speed. Since the Dutch regulations do not allow for a UAV to fly so far from the controller yet, it is not known how low the MAV will be allowed to fly for maximum endurance.

When there are no updrafts available, the MAV should use its propeller to make sure it can stay in the air while flying over the areas with the gaps. Using the worst weather conditions, and the average number of times the MAV flies between Hoek van Holland to Katwijk, which is ten times, it is shown that the MAV is able to fly 70% of the time with the energy capacity for the propulsion as shown in figure 2.4.

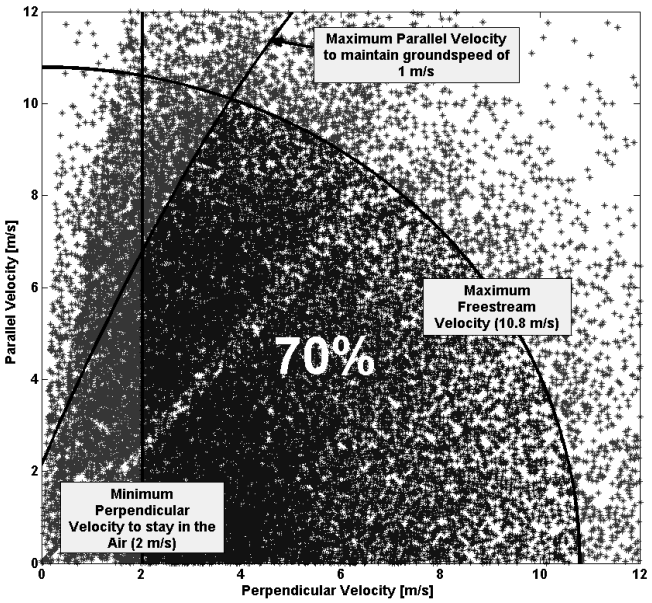

Figure 2.4: Requirement check of the DuneMAV design

2.8 Conclusions

The result of this project shows that it is possible to design an MAV, not larger than 2 m in wingspan and lighter than 1 kg, that can successfully use the energy from updrafts to stay airborne for 12 hours continuously. The design of the DuneMAV is optimized for maximum energy extraction to ensure long endurance. Furthermore, the feasibility of detecting and exploiting updrafts is shown by combining color classification to localize the dunes, optical flow to estimate the slope of these dunes and flow mapping to determine the location and magnitude of the updrafts. This knowledge is input for the trajectory planning system, that autonomously determines where to fly. This system estimates the total energy needed to get to a waypoint, where for example a photo of the beach has to be taken, and the best way to return to the optimal flight path.

The focus of further development for the DuneMAV will be the integration of the optical flow, the autopilot and the characteristics of the design. Actual measurements have to be done on the variation of the wind and gusts per unit time. Also, the stall performance of the

tail should be analysed in more detail. To ensure dune detection in regions where the distinction between the beach and dunes is not clear, different classification methods can be used. This will improve the deployability of the DuneMAV, extending to coasts across the world. Next to that, the detection of updrafts created in an urban environment, which emerge from tall buildings or skyscrapers, can be investigated in order to increase the versatility of the DuneMAV.

When this is done, the DuneMAV will be interesting for a whole new market, beside the coast guard. Also, the trajectory planning of the autopilot shows interesting possibilities for future autonomous aircraft. Conventional systems navigate from point to point in a straight line, where this report discusses how to use maximum energy extraction from updrafts to calculate the optimal route. This means that the DuneMAV will be the first aircraft to exploit this new method of sustainable flying.

3. EDDY – AN INTERACTIVE FLOW VISUALISATION TOOL

Students: J.G. Barnhoorn, S.G. Brust, D.P. van Herwaarden, J. Huibers, M.W.M. Kuijpers, I.B. van Leeuwen, K. Min, J. Ran, S.F. van der Sandt, R.J. Schilder

Project tutor: dr. R. Dwight, dr. M. Kotsonis

Coaches: dr. J. Sodja, ir. B. van Midden

3.1 Introduction

In this design synthesis exercise an interactive wing design tool prototype (Eddy) was developed by ten students in ten weeks. The complete design of Eddy includes the conceptual design, in which a concept is chosen by way of a careful trade-off. Construction of a prototype, for which € 2,500 is available, and design and programming of the tool will happen simultaneously, the results of which will be presented at the closing symposium.

Compared to conventional design synthesis exercises this project will have a shorter conceptual design phase and a larger development phase because the tool will be programmed and built.

The mission statement of this project is:

"To design, develop and build a real-time, robust, fast, profile prototyping tool, that accurately predicts and visualizes airflow behaviour around a wing profile in an interactive, intuitive and innovative way."

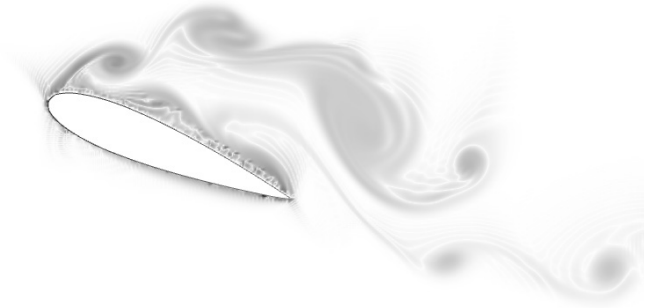

Figure 3.1: A visualization created by the CFD solver

In this executive summary a short, informative description of the content of this design project is given. It contains an overview of the early design decisions made, the more important technical details regarding the chosen design, and a conclusion with recommendations for future development of the tool.

3.2 Objectives

In developing the tool there were several main objectives that the group sought to complete. Interactivity would lead to a more insightful and intuitive tool that would increase the usability and effectiveness when using it to communicate or educate. If the tool is to be used by engineers it must first and foremost be accurate, this was an important consideration for the team. As the tool is to be used for communicating ideas, it must also be able to receive abnormal shapes as input and continue to display accurate results. In order for the tool to be actively usable it needed to be real-time; it was determined that 30 frames per second is sufficient to achieve this effectively. Lastly, a complete prototype must be brought forth to showcase the tool.

3.3 Design requirements and constraints

Constraints have been defined to be:

- For the design process, 10 people are available
- The design time-frame is bound by 10 weeks
- A budget of € 2,500 is available for acquiring hardware
- The selling price for the tool should not exceed a price of € 10,000.

The requirements for the tool are:

- The tool has to be interactive
- The tool should be fast enough to provide for 30 frames per second (fps) display rate
- The tool should have a response time of no more than 3 seconds
- The tool should be able to simulate unsteady, incompressible and viscous flow around 2D aerofoil and various other shapes.

3.4 Design concepts studied and related trade-offs

For the program several trade-offs were made with the most important ones regarding use of programming language and the various design concepts of Eddy. From a brainstorm session the group came up with eight possible concepts. In this section the different design options and the related trade-offs are explained.

Interactive whiteboard
A standard whiteboard with a camera and a PC. This requires image recognition to work. This would add the problem of image recognition to the project. Because of time constraints it was decided not to go for this option

Tablet only
A standalone tablet. Since programming options and computation power is limited compared to a regular PC it was decided not to go for this option

Standard PC/laptop
A regular PC/laptop without other possibilities for input then mouse and keyboard. In the trade-off table this solution was used as a benchmark. The other concepts are compared with this standard solution. Because this solution would lack the possibility to easily draw shapes, the group concluded that this is not an interactive solution

Smart board
A smart board coupled with a PC. Input and visualization is done on the smart board, computation is done on the PC. An excellent solution, however costs of smart boards are rather high.

PC to beamer
A PC connected to a beamer. Input is done with mouse and keyboard. The flow is visualized on a beamer. Since input and visualization is done on a different location, the group concluded that solution was less interactive and easy to use. Also drawing on a PC is more difficult compared to other solutions

Tablet to beamer
Input and computation is done on a tablet and the flow results are visualized on a beamer. This solution would lack computing power, further input and visualization is done at a different location. This would not aid in interactivity.

Megatablet
An all-in-one computer with a large touchscreen. Input, computation and visualization is done on one device. A nice solution, however this concept has its limitations on the computation power.

Interactive beamer
An interactive ultra-short throw beamer coupled to a standard PC. Input and visualization is done with the beamer. Computation is done with the PC. This solution was chosen because of its good mix of feasibility, flexibility, interactivity and it was cheaper than the smart board option.

To decide on the concept, a trade-off table was made. It was hard to quantify the different selection criteria. Therefore a discussion was held about the various concepts. The results of the discussion is summarized in table 3.1 below.

Table 3.1: Conceptual trade-off table

	Feasibility	Costs	Computing power	Ergonomics	Appeal	Applicability
Interactive whiteboard	--	-	0	+	++	--
Tablet only	0	+	--	+	+	++
Standard PC/laptop	0	0	0	0	0	0
Smart board	-	--	0	++	+	-
PC to beamer	0	-	0	0	+	0
Tablet to beamer	0	-	0	+	+	-
Megatablet	0	-	-	++	++	-
Interactive beamer	-	-	0	+	++	-

3.5 Program language trade-off

Another important trade-off was the programming language. There were various aspects which were important in this decision, such as experience, speed, possibilities and the learning curve. Another important parameter was that at the start of the project a CFD solver written in Python was already available. The programming language trade-off can be seen in table 3.2.

Table 3.2: Programming language trade-off table

	Experience	Speed	CFD available	Learning curve	Possibilities
C++	--	++	-	-	++
Python	-	+	+	+	0
Matlab	+	--	-	++	-

3.6 Details of selected concept

Input

With interactivity forming a large component of the desired tool, the input method had to be intuitive and readily accessible. It was decided to use a readymade interactive projector, which was simply an extension of a PC. The Epson projector used in this project is an ultra-short-throw system that has infrared pens that can be recognized by the projector. In this way, the graphical output of the PC is projected, upon which the pen can be used as one would normally use a mouse. Choosing this setup allowed the group to avoid the programming of an image recognition system, something, which would not have been feasible in the allotted ten weeks.

Output

With the purpose of the tool being communicative or educative, the output of the system is of high importance. A large portion of the output is visual and qualitative; this is to provide an intuitive and insightful understanding for the user. The possibility and potential for quantitative output in the form of datasheets and graphs is ready for implementation in a later version of the tool.

Basics of the vortex-in-cell method

Due to the need for real-time speeds, a Vortex-In-Cell (VIC) method was used. VIC is a type of Particle-In-Cell method that relies on a particle with a vorticity value moving over a fixed grid size and operating with a sufficiently short time step such that the particle does not leave the cell; a cell being one grid unit. As the particle carries a vorticity value, a velocity vector the particle is calculated on an Eulerian grid using Poisson solvers. The accuracy-stability of more traditional grid-based methods for CFD solvers is largely bypassed by this method.

$$\frac{\partial \omega}{\partial t} + (u \cdot \nabla)\omega - (\omega \cdot \nabla)u - \nu \Delta \omega = 0$$

Bases for the method are the incompressible Navier-Stokes equations in a vorticity-velocity format. There is a significant solver speed

increase with this method over direct, Biot-Savart law inspired integral formulas. In short, the solver consists of three major steps, those being convection, particle remeshing, and diffusion. The convection step is done to adjust the individual particles in a cell with the local velocities and vorticities that are present in that portion of the flow. The particle remeshing step is a computationally expensive portion of code which interpolates the vorticity and velocity in a cell. The diffusion step uses a particle strength exchange to cancel the slip experienced on the boundary.

Exact boundary to grid boundary

Input to the system is received as an exact boundary that is layed over the established grid. In order for this data to be usable by the solver it needs to be overlayed to the established grid; this is done by moving each point from the exact boundary to the grid boundary.

Interpolation

As mentioned, one of the more computationally expensive steps in the solver is the interpolation of the vorticity and velocity of the particle in the grid cell. In each time step each particle moves through the grid less than one cell length; the time step is adjusted such that this is the case in each iteration. In order to set the particles to the grid points for the beginning of the next iteration an interpolation is conducted which "snaps" the vorticity value back to a fixed grid point. This interpolation is based on the vorticity of the particle and its velocity; dependent upon those characteristics, vorticity is interpolated to one of sixteen adjacent grid points, four in each axial direction. A visual representation of the interpolation of a single particle can be seen in figure 3.2. After each grid point has an assigned vorticity, velocity is found using a Helmholt'z decomposition.

$$u = \bar{u} + \nabla\psi + \nabla\varphi$$

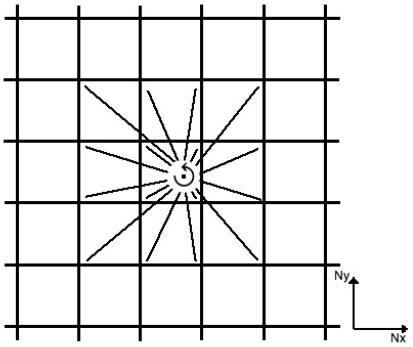

Figure 3.2 A visualization of the interpolation step

No-slip condition

In modelling a viscous fluid there is a need to meet the no-slip condition at the boundary of the solid, immersed object. Thus, velocity tangential to the boundary at the boundary of the object is set equal to zero. To compensate for the removal of said velocity a vorticity flux takes its place and is created as a fractional-step function of the local velocity, vorticity, time step, and kinematic viscosity value. Accuracy of this step is increased as the grid size increases; the method in which this no-slip condition is implemented creates an accuracy limitation for the system to low Reynold's numbers due to the thickness of the boundary layer.

$$\frac{\partial \omega}{\partial t} - \nu \Delta \omega = 0$$

$$\nu \frac{\partial \omega}{\partial n} = -\frac{u \cdot \tau}{\Delta t}$$

No through-flow

Disallowing through-flow in the immersed object is an important and necessary aspect for the accuracy of the solver. All points within the immersed boundary are known by a specific symbol, in the case of this solver that symbol is Omega. Additionally, all immersed boundary points are known by symbol Gamma. With these points known, through-flow is disallowed within these bounds.

Boundary conditions

Boundary conditions vary in different portions of the flow. The two vertical boundaries of the flow field have Dirichlet, or first type, boundary conditions and the two horizontal boundaries have Neumann, or second type, boundary conditions. The object in the flow has an immersed boundary method applied of the second type with a forcing term, g.

Computation

As mentioned in several different portions of the code, a lot of the methods presented herein are more accurate for larger grid sizes; it is thus desirable to use as large a grid size as is computationally possible. Programming efficiently and effectively and paralleled is thus an important task. Many of the calculations that are completed by the solver are individually quite simple; the shear quantity of calculations to be made is what becomes time intensive. By its nature, this problem is an excellent application of parallel programming on a graphics processing unit (GPU). As such, the solving of the Poisson matrix via algebraic multigrid method is completed on the many threads of the GPU.

Programming language

For the purposes of speed and experience within the group, it was decided that the programming would be done in C++. A fast and straightforward matrix library was found in the Armadillo linear algebra library. Parallel computing was done on the GPU using the Paralution sparse iterative solvers library and on the multi-core CPU using the OpenMP API. The GUI was created using the QTCreator IDE.

3.7 Conclusions and recommendations

In this summary the design process that led to the realization of an airflow simulation tool has been discussed. The team has succeeded in creating a prototype that is interactive and gives (near) real-time visualization outputs. The prototype is a combination of a custom made PC and an interactive beamer. The software that has been

developed is based on a CFD-solver that is robust, fast and gives accurate results. To allow for intuitive use, a graphical user interface is made that can handle hand drawn inputs and quickly responds to the input given by the pointer. The team also decided to make the tool open source, such that others are stimulated to use, elaborate and improve the prototype. The source code can be found at: https://github.com/TU-DSE2/Wing-Design-Tool.

A lot can be done in different areas to improve the tool. Such as increasing computing performance, intuitiveness of the GUI, and increasing possibilities for the display of plots. To increase the speed of the program emphasis should be placed on working on the main bottlenecks of the program. At the time of writing, most computationally intensive parts are in solving the Poisson equations. Increasing the speed in this part can be done by either using stronger hardware, more efficient coding, or finding a different method for solving for velocity and vorticity. Further creating the graphical representations of the flow continues to take extensive amounts of time and is done sequentially after computations are done by the solver. Running the graphical representations in parallel with the solver could again mean a substantial speed increase and therefore also the possibility to work with larger, more accurate grids.

4. UAV CARGO DELIVERY SYSTEM

Students: D.G. Beeftink, M.J. Bots, D.R. Hordijk, T.C.W.M. Koopman, H. Middel, R.B.A. Oude Ophuis, M. Potuijt, M.C. Schuurman, D.B. Smit, L.L.C.C. Spranger

Project tutor: M. J. Martinez, PhD

Coaches: N.F. Baltazar dos Santos, ir. D.M.J. Peeters

4.1 Introduction

An analysis of the major natural disasters showed that in the first decade of the 21st century, a shocking 2.55 billion people were affected by natural disasters; 15% more than in the previous decade. Natural disasters such as past year's typhoon Haiyan had catastrophic consequences, especially in areas with a poor infrastructure and in areas where governments were unable to support their people with medical equipment and permanent shelter. For example, four years after the magnitude 7 earthquake in Haiti in 2010, there are still more than 170,000 people living in makeshift tents.

These circumstances highlight the need for humanitarian aid to provide a permanent housing solution to the victims of natural disasters. Whilst temporary shelter and support are given to the

people affected by a natural catastrophe during the initial phase of global attention, a long-term solution is lacking.

4.2 Mission objective and requirements

Mission Need Statement:
"To perform an automated, sustainable and economical delivery of a multifunctional cargo system that provides humanitarian aid and permanent housing for three people using an Unmanned Aerial Vehicle Cargo Delivery System (UAV-CDS). The UAV-CDS has been designed to take off from an international airport in the Dominican Republic while capable of flying to a disaster zone in neighbouring Haiti."

Project Objective Statement:
"Design an automated UAV system with a modular, multifunctional cargo system that provides emergency aid in the Haiti disaster zone. Ten students from Delft University of Technology Faculty of Aerospace Engineering took on the design challenge during a ten week period."

The main requirements & constraints for the UAV were:
- Each UAV should deliver at least two cargo units per day.
- The UAV should be able to operate past line of sight.
- The mission range set by the client was of 2000 km.
- The UAV was designed to take off from an international airport runway (Punta Cana International Airport).
- The UAV should be transported by a Lockheed C-130 Hercules.
- The minimum production series was 200 UAVs, each with corresponding replaceable cargo containers.

The main requirements & constraints for the cargo were:
- The cargo delivery unit has a weight of 500 kg.
- The cargo container had to be able to be assembled into a permanent (>10 years) house for three people.
- The cargo container needs to be equipped with basic survival equipment as well as all the systems required for the permanent stay of three people.
- The cargo container needs to be dropped with a precision of 50 m.

4.3 Concepts studied and related trade-offs

The preliminary concept generation phase resulted in fourteen possible design options. They were categorised into the following five categories: lighter-than-air aircraft, aeroplanes, spacecraft, rotorcraft, and vertical take-off and landing (VTOL) aircraft. The following criteria were defined for the preliminary trade-off:

- Cargo delivery rate
- Level of automation
- Technical feasibility
- Manufacturability
- Efficiency

As a result, only three preliminary concepts remained feasible which were then further taken to the conceptual design phase. These three concepts were the airship from the lighter-than-air vehicles category as shown in figure 4.1, the tilt-rotor from the VTOL category as shown in figure 4.2 and the conventional aeroplane from the fixed wing category as shown in figure 4.3.

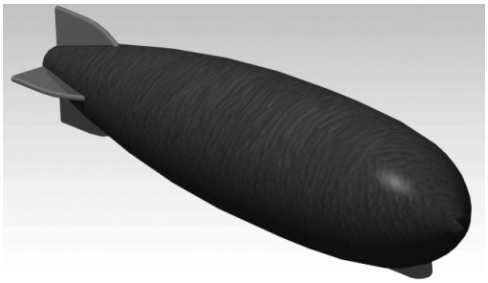

Figure 4.1: Airship concept

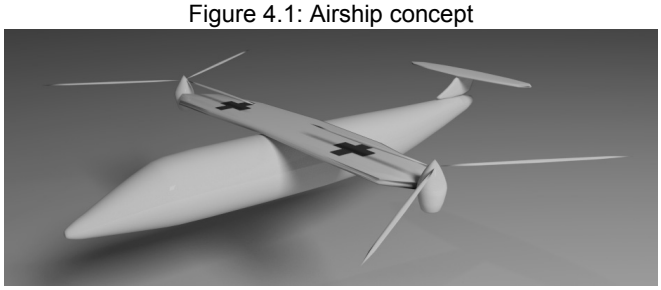

Figure 4.2: Tiltrotor concept

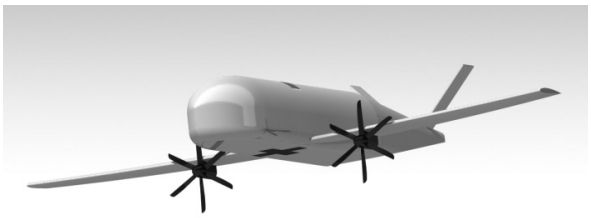

Figure 4.3: Aeroplane concept

The team divided itself into three sub-teams to generate more in-depth conceptual designs in the subsequent design phase. To be able to compare the different approaches, specific design aspects were considered during the conceptual design phase. The following aspects were considered:

- Sizing based on cargo dimensions
- Weight estimation based on cargo weight
- Aerodynamic analysis
- Propulsion analysis
- Stability and control
- Structural analysis
- Cargo delivery procedure
- Manufacturing

After these aspects were covered for each concept, a final trade-off was made according to trade-off criteria closely linked to the mission requirements. The final trade-off table is displayed in table 4.1.

From table 4.1, it can be seen that the aeroplane design obtained the highest score and was consequently the most suited concept for the mission.

A similar trade-off was made both for the delivery system and the cargo. It was decided to use a parachute deployment system for the cargo drop-off and a modular house design, since they fulfilled the requirements set by the client best.

Table 4.1: Conceptual design trade-off criteria

				Concept 1 - Airship		Concept 2 - Tilt rotor		Concept 3 - Aeroplane	
Criteria	Sub criteria	Comments	Weight	Score	Weighted score	Score	Weighted score	Score	Weighted score
Automation	Low complexity of flight control system (in case of computer malfunction)	1 statically & dynamically unstable 2 min airspeed / input required for stability 3 no airspeed / input required for stability	2	3	6	1	2	2	4
	Staff required for operating UAV on ground kept to minimum	0 if >12 1 if 8-11 2 if 4-7 3 if 0-3	3	1	3	2	6	2	6
Performance	Operational (fuel) efficiency [kg/delivery]	0 if > 4,500 / delivery 1 if 3,000-4,500 / delivery 2 if 1,500-3,000 / delivery 3 if < 1,500 / delivery	5	1	5	3	15	3	15
	Low maintenance costs	0 if > $450 / delivery 1 if $300-$450 / delivery 2 if $150-$300 / delivery 3 if <$150 / delivery	2	3	6	1	2	2	4
	Low costs of cargo drop	0 if > $750/ delivery 1 if $500-$750 / delivery 2 if $250-$500 / delivery 3 if < $250/delivery	2	3	6	3	6	0	0
Sustainability	Sustainable manufacturing	0 if totally unsustainable 1 if partly recyclable 2 if partly recyclable; no scarce materials 3 if fully recyclable; no scarce materials	4	1	4	2	8	2	8
	Long lifetime	0 if <8 years 1 if 9-16 years 2 if 17-25 years 3 if > 25 years	4	3	12	2	8	3	12
Technical feasibility	How proven is this concept [number of flying UAVs]	0 if only in conceptual phase 1 if 1-3 different types built / operational 2 if 4-6 different types built / operational 3 if >7 different types built / operational	3	2	6	1	3	3	9
	Low overall design complexity	0 if non-conventional / tilt-rotor design etc. 1 if rotorcraft 2 if conventional with jet / propeller 3 if balloon with jet / propeller	2	3	6	0	0	2	4
		Concept total weighted score:			54		50		62

high score
moderate score
low score
no score

Aeroplane concept details

The results of the detailed design phase are displayed in table 4.2. The aircraft was named AidPlane, according to the purpose of its design.

Table 4.2: Aeroplane specifications

Aeroplane features	Specifications	Value
Dimensions	Maximum take-off weight	2,448 kg
	Operational empty weight	1,021 kg
	Fuel weight	828 kg
	Wing surface area	20.8 m2
	Wing span	13.7 m
	Chord length at root	2.17 m
	Chord length at tip	0.87 m
	Aspect ratio	9
	Taper ratio	0.4
	Fuselage height	1.4 m
	Fuselage width	1.5 m
	Overall length	11.75 m
	Overall height	4 m
	Horizontal tailplane area	4.2 m2
	Vertical tailplane area	1.6 m2
Performance	Cruise speed	400 km/h
	Stall speed	105 km/h
	Cruise altitude	6,096 m

	Range	2,000 km
	Take-off distance	1,097 m
	Landing distance	877 m
Powerplant	Rolls Royce 250-B17F single engine propeller	n.a.
	Power/weight ratio	2.2
	Shaft output	2,000 rpm
	Cruise power	425 shp
	Take-off power	450 shp
	Fuel	Jet-A1, JP-8, Biofuel
	Propeller	Variable pitch, double acting, 6 bladed, aluminium
Avionics systems		
Primary flight systems	Autopilot	Lisa/L
	Computer	Gumstix Overo
	IMU (Inertial measurement unit)	Aspirin
	GPS	NexNav MAX
Telecommunications	Line-of-sight link	Microhard lpn920 UHF MODEM
	Satellite communications	SCOTY UAV SATCOM unit
Aviation system integration	TCAS (Traffic Alert and Collosion Avoidance System)	AvidyneTAS 605
	ADS-B (Automatic Dependent Surveillance - Broadcast) out	Sagatech XPS-TRB
Flight control system	Actuators	Electro-hydrostatic actuators
Others	Pitot probe heating	Dynon Avionics Heated AOA/Pitot Probe
	Wing ice detector	UTC Model 0871LH1

The overall dimensions of the AidPlane are displayed in figure 4.4.

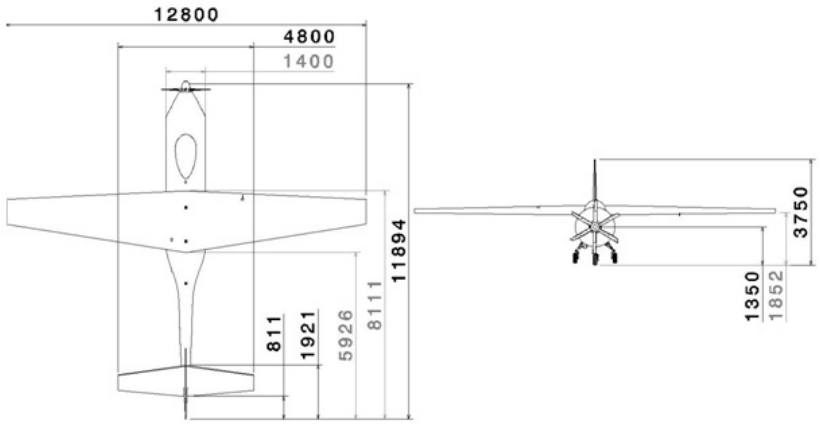

Figure 4.4: AidPlane dimensions [mm]

The AidPlane with the cargo just being released by the parachute can be seen in figure 4.5. A Parachute Low Altitude Delivery System (PLADS) was selected, which can achieve a precision drop of 50 m. The UAV with extended landing gear is visualised in figure 4.6.

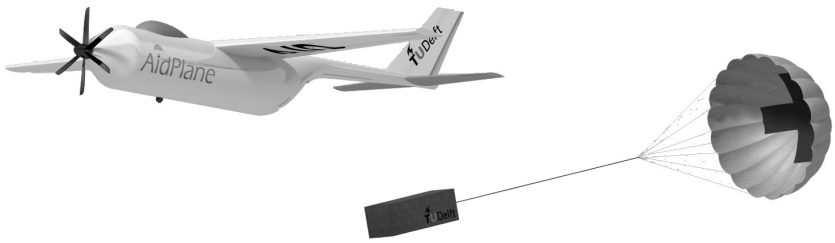

Figure 4.5: Parachute drop-off

Figure 4.6: AidPlane with landing gear extended

A special roller system was designed from which the cargo package will be extracted, as shown in figure 4.7.

Figure 4.7: Roller system for cargo extraction

The cargo can be assembled into a compact package with dimensions shown in figure 4.8.

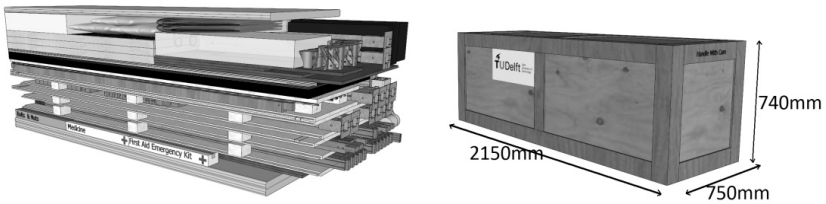

Figure 4.8: Cargo package components with dimensions

To be able to withstand hurricanes with speeds of up to 240 km/h, the house will be anchored in the ground as shown in figure 4.9. Solar cell panels mounted on the roof of the house will provide a sustainable source of energy.

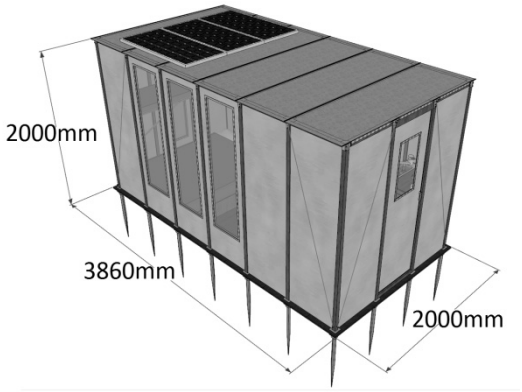

Figure 4.9: Ground fixation of the house

The house unit will be fully equipped for three people with three beds, a table unit, a bathroom and a cooking station with a sink as

shown in figure 4.10. There will be storage space for clothes etc. under the bed.

Figure 4.10: Exterior and interior of the house

4.4 Conclusion and recommendations

Conclusion

Following up from the generation and preliminary design of three UAV concepts, a detailed design of the concept best suited for the cargo delivery mission was made. This was the fixed wing aircraft, which was able to perform the cargo delivery mission with the highest efficiency in terms of the set requirements. Cruising at 400 km/h, the aeroplane easily meets the requirement of delivering two cargo units per day over a mission range of 2000 km with a block time of 7.25 h. With a total weight of less than 2.5 tons, the aircraft was optimised to carry a 600 kg-cargo payload (500 kg including contingency). Thrust is generated by a six-bladed single propeller turned by a Rolls Royce engine with a maximum power of 450 shp.

A double-tapered aluminium made wing box is incorporated in a Natural Laminar Flow aerofoil on the main wing, which was selected according to the design lift coefficient of the aircraft. To optimise the wing for cruise and to not overdesign it, single slotted flaps- high lift devices of low complexity- were incorporated along the trailing edge

of the wing to be able to generate sufficient lift at low velocities, during take-off, cargo drop and landing.

The cargo delivery system achieves its precision drop within the 50 m set by the mission requirements. The cargo is extracted from the back of the fuselage with sufficient space for the extraction parachute to safely deploy. An air bag at the bottom of the cargo package in combination with a parachute with an area of 46 m2 will ensure the smooth descent of the cargo package to the delivery zone. The cargo will be dropped from a low altitude of 45 m and a flight speed of 147 km/h so that the precision drop can be achieved without a guided parachute.

A unique avionics system has been designed which seamlessly integrates with the existing civil aviation system. Equipped with highly accurate instruments, the UAV is able to perform a precise cargo drop. Images and video can be used to record valuable data that can both provide additional information on the disaster zone and closely monitor the cargo delivery process. The core of the avionics system is the triple redundant Lisa/L autopilot, which provides the interface to communicate with the motion actuators in the UAV. The DC generator as part of the engine provides sufficient power for the entire avionic system. In case of failure, a human controlled emergency landing can be performed.

Upon delivery, the modular housing unit will provide a comfortable, flexible and expandable environment for the victims of a natural disaster. Equipped with all major components to ensure a permanent and pleasant life in one of the modular houses, each unit can cover its own power needs using a solar system. Due to its ability to withstand the harshest environmental impacts, the design of a set of units can be easily adjusted to any environment where a natural disaster might strike.

In conclusion, the cargo UAV meets all its mission requirements. In combination with its cargo delivery system and compact cargo package, its design proved to be a multifaceted engineering challenge.

Keeping the design complexity as low as possible and yet meeting all the complex design goals was an interesting task, which the team managed to fulfil.

Recommendations

To validate the functionality of the UAV and all its systems, a prototype would have to be built and tested. Especially the avionics systems and the cargo release mechanism should undergo a number of critical tests, taking effects such as strong gusts into account.

Parts of the aerodynamic shape that was given to the fuselage such as the composite dome containing the satellite communications antenna was chosen arbitrarily. Wind tunnel tests on a small-scale model should be carried out to validate the aerodynamic efficiency of the aircraft. Since the analysis tool XFLR5 used was not able to simulate the effect of high lift devices, the single slotted flaps chosen on the main wing should also be tested in a wind tunnel. Furthermore, in addition to the load distribution along the wingspan, the chord wise distribution of lift should be analysed using more advanced CFD software.

For the structural analysis the ABAQUS ™ finite element model developed as part of this design and synthesis exercise, should be refined further to incorporate the skin of the wing as a load-bearing element in order to increase the accuracy of the model. The wing as the most critical component in terms of carried loads has been analysed, modelled and verified. The fuselage should be verified in a similar fashion. To evaluate the effect of fasteners such as rivets and bolts, stress concentration factors should be used in the model and their effect on the overall model be analysed.

All open source avionics systems should undergo tests such as EMI, lightning, vibration, temperature, altitude, humidity, dust, shock and contaminants to validate their functionality under extreme operating conditions.

Although multiple safety factors have been used during the design of the parachute system, this system also has to be tested extensively to ensure the safe delivery of the cargo under extreme conditions.

5. SKYDOWSER: LOOKING FOR WATER

Students: B. Beijer, M. den Brabander, C.D. Dieleman, T.A. Heil, A.M.C. Helmer, S. Nootebos, B.J.R. Smeets, V.F. Verschuure, J. Vink

Project tutor: ir. J.A. Melkert

Coaches: A. Canet Sentís MSc, ir. A. Palha da Silva Clerigo

5.1 Introduction

A lack of fresh water to meet daily needs is a reality for one in three people around the world (WHO, 2009). This is not only a problem for present time, but all over the world this problem is getting worse as cities and populations grow and the needs for water increases in agriculture, industry and households.

Over the last few years multiple systems, such as the Winddrinker and the Windwell (www.thewinddrinker.com), have been developed to pump groundwater to the surface and desalinate this water. At this moment however, nobody knows where to find this groundwater. The faculty of Civil Engineering and Geosciences is therefore developing an instrumentation package that is able to find underground water reservoirs with the use of Frequency Electromagnetics (FEM). Current methods for measurements of these underground water-bearing layers, so-called aquifers, are either expensive (use of a helicopter) or slow (hand measurements), our

client has requested an unmanned aerial vehicle (UAV) that is able to carry the measurement package.

The Mission Need Statement of the project is therefore formulated as follows:
"Find groundwater using an autonomous, unmanned aerial vehicle by means of a low frequency electromagnetic field."

This chapter describes the design process leading to the final design that is capable of meeting the set requirements.

5.2 Objectives

There is however a difference between the mission of the project as a whole and the objectives for the Design Synthesis Exercise (DSE). Therefore the project objective statement for the DSE is formulated as: *"Develop an unmanned aerial measurement platform capable of finding ground water in remote areas, within a budget of preferably € 10,000, by 9 students in 10 weeks' time."*

5.3 Measurement system

The measurements are performed with use of Frequency Electromagnetics (FEM). In figure 5.1, a schematic drawing showing this method can be seen. A current is sent through a coil at low frequency. This generates an electromagnetic field that penetrates the ground. Lower frequencies will have a deeper penetration. Conductive materials in the ground, for instance brackish water, are excited by this electromagnetic field. Socalled Eddy currents will be induced in these conductors, creating their own electromagnetic field. This induced field is measured and is an indication for the composition of the ground.

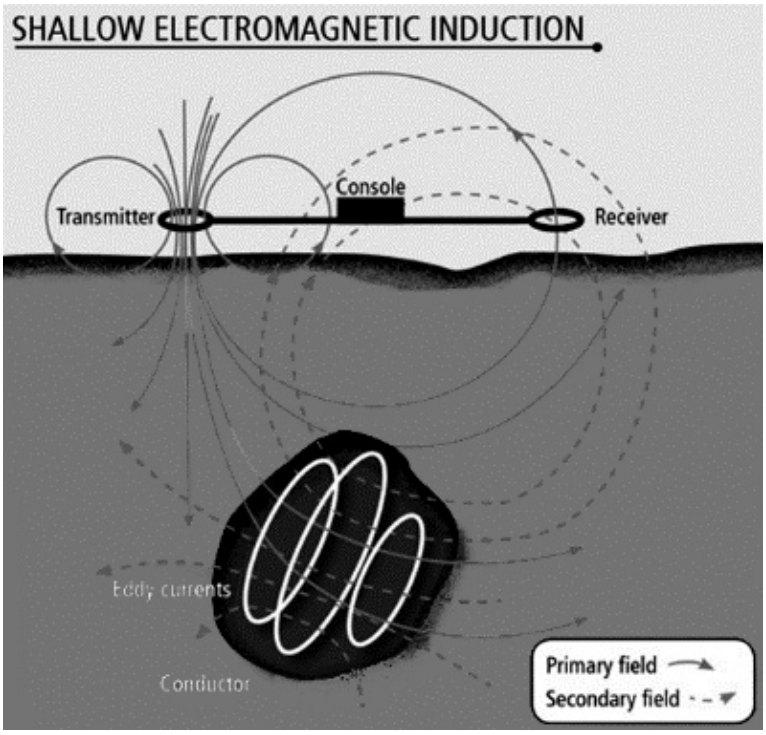

Figure 5.1: Measuring ground composition using FEM

5.4 Design requirements and constraints

The project was defined by a number of requirements. These requirements formed the start of the design phase. They can be broken down into top level requirements and additional requirements. The top level requirements are hard constraints for the project, while the additional requirements are more like a guideline. Meeting these requirements can bring the final goal of the entire project closer.

The top level requirements are:

- The UAV must carry the measurement package
- The measurement package must be able to perform measurements at a resolution of at least 10 m. To ensure this the coils should be placed at least two meters apart.
- The UAV should be foolproof.

- The UAV should be able to operate, take off and land in all kinds of environments and remote areas.
- The UAV should comply with worldwide UAV regulations.
- Additional requirements include:
- The UAV should have a unit price of € 10,000 or less.
- The UAV should scan at least 10 km^2 a day.
- The UAV should fly as autonomously as possible.
- The UAV should be able to fly continuously for at least 2 hours.
- The UAV should be easy to manufacture and should have a modular design for easy maintenance.
- The UAV should be in line of sight of the operator, while being within a range of 500 metres, at all times during operation.

During the initial design phase the requirements were expanded with conflicting requirements, such as the UAV should be able to hover. The initial concepts therefore exist of a broad range of different solutions.

5.5 Concepts studied and trade-offs made

During the conceptual design phase, seven different concepts were selected. Among those concepts were a zeppelin, several rotorcraft, a flying wing and a conventional concept. From these seven, three final concepts have been subjected to further detailed analysis. These were a conventional setup, a quad copter and even a zeppelin, as shown in figure 5.2.

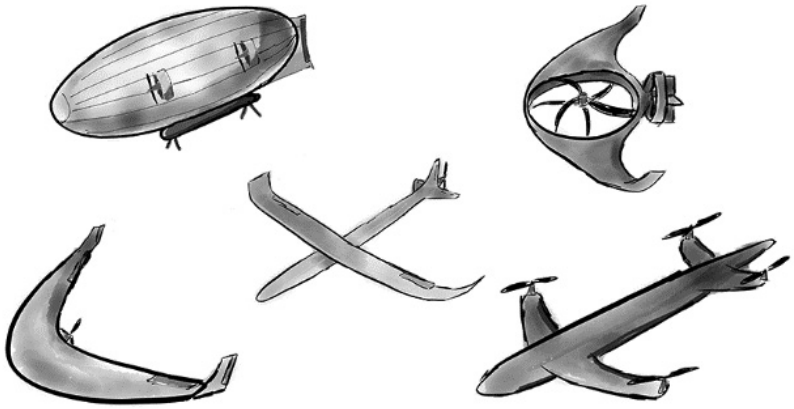

Figure 5.2: Various concepts that where designed during the conceptual design phase

In order to select the best concept, a trade-off was performed. A set of criteria was set-up to be able to properly compare the concepts. These trade-off criteria are directly linked to the requirements. The trade-off criteria categories were: minimise cost, ability to perform measurements, range, stability and sustainability. Each of these categories was divided into more detailed criteria which were graded and weighted.

After a trade-off was performed based on the criteria mentioned, the conventional concept proved to be the most suitable concept for the mission at hand. It is most cost effective, has the longest range and is flexible in terms of carrying other payload than the selected FEM measurement device.

5.6 Details of the selected concept

The final design is called the 'SkyDowser' and has a conventional layout, shown in figure 5.3. The SkyDowser has a mass of 12.5 kg, and a wingspan of 3.5 m to produce sufficient lift to carry this mass.

Launched from a catapult, the SkyDowser can be operated from nearly every terrain. A piston engine propels the aircraft, flying at a cruise velocity of 25 m/s. At this speed it is capable of flying 720 km

per day, on a single fuel tank of 1.7 litre. With the use of the coils in the wings, the SkyDowser scans an area of 29 km^2. At the end of its mission the SkyDowser lands using an on-board parachute. It lands on a rubber tail cone, to protect the fibreglass aircraft against impact damage. The production cost of the SkyDowser is € 6,500. With development cost taken into account, the unit price of the SkyDowser is € 18,500, resulting in an operational cost of approximately € 7 per scanned km^2.

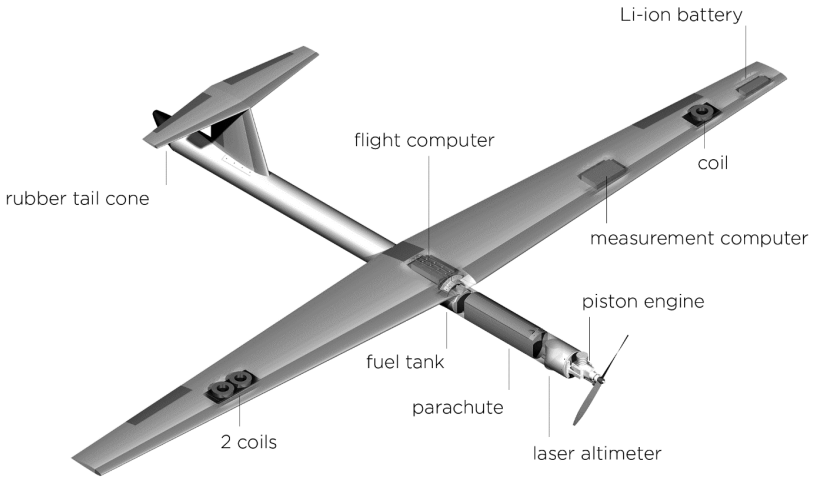

Figure 5.3: Overview of the SkyDowser including internal systems

Configuration and layout

The main wing of the SkyDowser has a span of 3.5 meters, with a total wing surface of 0.92 m^2. The wing has an aspect ratio of 13, and can be taken off in order to perform handheld measurements. Because of the operating altitude of 30 meter, the wing will be exposed to dust and insects. Therefore, the NACA 2412 aerofoil is used because of its insensitivity to roughness. Also, this aerofoil has a basic geometry, allowing for easy manufacturing, lowering the production cost. The main wing structure is a two-spar configuration, and a T-tail configuration is used. In figure 5.4, a 3-view schematic drawing is shown.

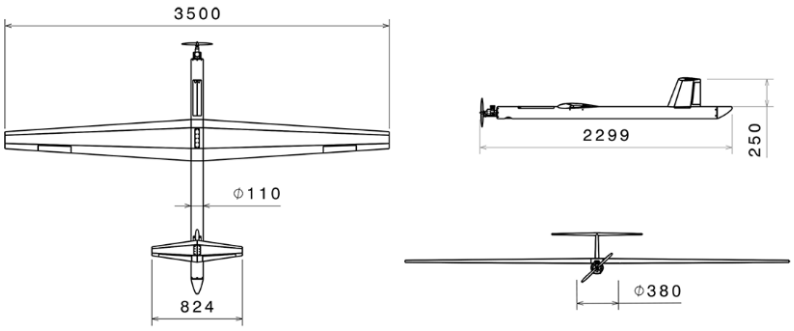

Figure 5.4: Top view, side view and front of the SkyDowser

Inside the main wing, most electrical systems and avionics are placed. The coils are placed 2.4 metres apart in an asymmetrical layout, as can be seen in figure 5.4. To compensate for the weight difference, the measurement computer and Li-ion batteries are stored in the wing. Furthermore, in the front of the fuselage a laser altimeter is placed, providing altitude determination up to a precision of a few centimetres. This, in combination with a collision avoidance system and GPS data, forms an accurate attitude determination system.

Operations and logistics

The SkyDowser has a modular design which makes it easy to assemble and disassemble on site. All the parts can easily be transported in a (off-road) vehicle. The UAV can then be fuelled and placed on the catapult which is used to perform take-off. The catapult is tensioned with the use of elastic bands and is able to accelerate the SkyDowser to a take-off velocity of 16 m/s, 125% of the stall velocity.

When the UAV has taken off it climbs to an altitude of 30 m and start scanning the area. Since the SkyDowser must always be within a range of 500 m of the observer, the UAV must fly from left to right within sight of the observer, as can be seen in figure 5.5. At the end of each turn, when UAV reaches a distance of 500 metres, the UAV will turn and scan the following “lane”. The SkyDowser scans lanes of 30 metres and then “skips” 14 metres before scanning the next one. Since the water resources we are looking for are large, this skip in lanes will not affect the results of the measurement. The observer can either follow the aircraft by car or on foot if the terrain is badly accessible for

a vehicle. In this case the SkyDowser can follow the observer, which means that the UAV will never fly away further than 500 metres.

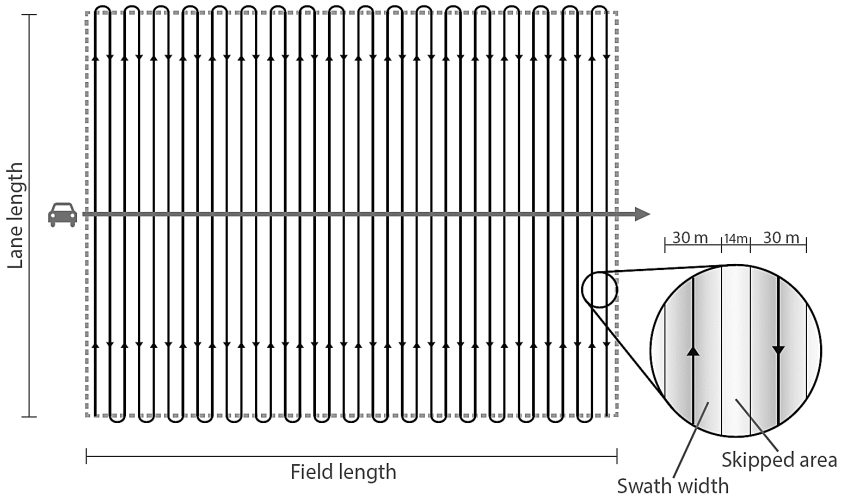

Figure 5.5: Operational route of the SkyDowser, followed by the observer.

The observer will communicate with the SkyDowser using a ground station, a laptop or an android running tablet, through Wireless Personal Area Network (WPAN) that has a range of 1.5 km. The observer can set a predestined route for the autopilot to follow by use of waypoints in Google Maps. The software of the SkyDowser autopilot can directly communicate with the ground station and enables the observer to constantly check the autopilot and change the waypoints if necessary.

During the flight a collision avoidance system is used to make sure the SkyDowser will not fly into a tall object. Two cameras on the wingtips form a stereoscopic camera system able to detect possible objects. If large objects are detected an evasive manoeuvre can be initiated. Either a climb, a climbing spiral and as last resort a sharp U-turn.

5.7 Future prospects

The FEM equipment can be used not only to find groundwater, but also landmines or archaeological sites can be discovered. Since the design is very versatile, completely different markets can be penetrated by only changing its payload. With an extended fuel tank, the range of the SkyDowser can be extended by 24 hours. This makes the SkyDowser highly suitable for various other mission, for instance; aerial surveillance for wildlife preservation or border protection.

5.8 Conclusion

The SkyDowser can be built for less than € 10,000, and has an operational cost of € 7.- per scanned square kilometre. To keep the costs down, many commercially-off-the-shelf components have been used together with open-source software. It will fly in most climate conditions and due to its catapult take-off system and parachute recovery system, operation is possible from nearly any terrain. With its full autonomous operation over 29 square kilometre can be scanned per day while using only one litre of petrol.

A modular design philosophy has been implemented in the development of the SkyDowser. It is therefore not only easy to manufacture and repair, but it can also be easily disassembled for transport by car. For detailed measurements it is even possible to take off the wing, which houses the measurement equipment and use it as handheld scanning device. The design is therefore versatile and is able to satisfy all of its requirements.

The simplicity in design and operations makes the SkyDowser an attractive solution that will suit the client better than the current alternatives, such as HEM, GEM and Proton Magnetic Resonance. Moreover it may just be the missing link in solving the global water crisis.

6. INSPIRATION MARS

Students: T. Verschoor, S. Hosseini, G. Gezels,
R. Blanco Maceiras, L.M. Kranendonk, R.M.J. Caenen,
M. Georgiev, C.D.J. Stevens, S. Ahmad,
P. Fatemi Ghomi

Project tutor: dr.ir. E. Mooij, ir. M.C. Naeije

Coaches: dr. A.M. Grande, ir. W.C.P. van der Velden

6.1 Introduction

Mars has been an object of fascination for humanity since ancient times. Up until this day, there have been numerous notable milestones from the early telescopic observations of Galileo and Huygens to the modern era of spacecraft-based exploration. Since the Mariner 4 fly-by in 1964, there have been several dozen spacecraft sent to Mars. Now, in the 21st century, a new era of spaceflight has set upon mankind as it gets its first chance to become a multi planetary species. To prepare for the colonization of Mars and taking the first step, an idea of a manned spacecraft mission to Mars and back was introduced by the Mars community. Flying a manned spacecraft to Mars could yet again give the "spark" to the Space Industry and become a catalyst for growth, education and knowledge. The mission would not only be an inspiration to the people but also a success of whole mankind.

6.2 Mission statement

The Inspiration Mars project, launched by the Mars Society, has become the innovators' beacon to contribute to this extra-terrestrial adventure. The project aims to design an end-to-end manned fly-by mission to Mars by the year 2018. Next to this mission objective, the Mars Society stated that the mission should be as cheap, safe and simple as possible.

The additional design requirements and constraints are listed below.

- Carry a crew of two, consisting of a man and a woman
- Launch shall take place in January 2018
- Fly-by altitude of 180 km
- The mission shall perform the fly-by at Mars and the return to Earth in a single heliocentric orbit
- No single-point failures are allowed
- Crew health and safety is the main design focus
- Minimize the total cost

6.3 Trajectory determination

The spacecraft's trajectory is driven by the requirements to launch by January 2018 and by being as safe, simple and cost-effective as possible. Several different transfer options were analysed to meet these requirements without exceeding the limits on the maximum time of flight, re-entry speed and change in velocity. As the trajectory imposes many of the requirements on the spacecraft's re-entry capsule, living module and all the subsystems, it was important to determine an optimal trajectory. Such a trajectory was calculated, which provided all the required information to design a "tailored" spacecraft for this mission.

Trajectory transfer option trade-off

Four main trajectory options were considered to use for the Mars fly-by mission. The first option would be an optimal Earth departure, use a fly-by at Mars and come back to Earth. The second would use the same principle, but the Earth arrival was optimized for a lower re-

entry speed. The third and fourth options would use a gravity assist from Venus in the outbound or inbound leg, respectively.

These different trajectory options were traded-off, based on five different criteria given in table 6.1. The driving criterion appeared to be the launch requirement of 2018, which made option I the winner. However, if this criterion would be relaxed option III would score higher and be possibly a better solution.

Table 6.1: Trajectory trade-off

Criteria	Weight	Option I	Option II	Option III	Option IV
Health and Safety	33.8 %	7.25	6.65	7.25	6.3
Cost	15.9 %	5.15	2.6	7.85	5.15
Simplicity	12.5 %	5.3	5.2	7.1	5.4
Feasibility	27.9 %	9.0	6.6	2.6	2.6
Sensitivity	9.9 %	5.0	5.0	4.0	4.0
Launch Opportunities	10.0 %	5.0	5.0	4.0	4.0
Total:	100 %	6.9	5.6	5.7	4.7

Final trajectory design

After determining the optimal trajectory type for the mission, a detailed trajectory design was made. This was done to define all the details and provide the input requirements for the spacecraft's subsystem design. Using the TU Delft Astrodynamics Toolbox (Tudat) and MATLAB, several trajectories between December 2017 and January 2018 were analysed as they resulted to be near the optimal solution for the trajectory. Finally, after manually adjusting the launch, fly-by and arrival dates, a final optimal transfer trajectory was determined together with a specified launch window. This launch window opens at 18 December 2017 and closes again at 4 January 2018 due to exceeding the constraints of maximum change in velocity possible and re-entry speed respectively. Finally, the mission would take around 501 days of flight, have a 4.9 km/s change in

velocity from the parking orbit and a re-entry speed of 14.2 km/s. An illustration of the trajectory is given in figure 6.1.

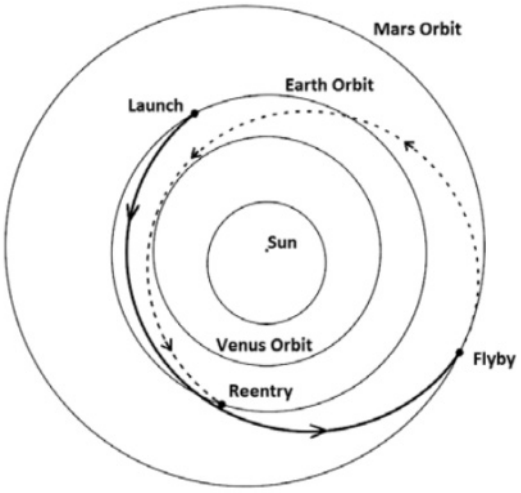

Figure 6.1: Earth departure optimized trajectory

6.4 Spacecraft concept selection

Now that the requirements, trajectory and constraints are determined it is possible to start the design process. First off all design possibilities in the broadest sense are collected. In this conceptual design phase it does not matter if the design option is viable or not. The options are categorized per mission phase and put in a clear overview, the Design Option Tree. When this phase is completed a preliminary design concept elimination is done. All concepts that prove to be non-viable are eliminated from the list, so a list of realistic design options remains.

From these design options a number of concept designs were created. Each design describes the mission from beginning to end, selecting a design option for each mission phase. The integration of the different mission elements is also assessed. Four main concepts were established, which are briefly described below.

Concept 1: Kirby

The driving thought behind this design is to fit everything into one launcher. The advantage of fitting the entire spacecraft in one launcher is that no complicated docking manoeuvres have to be performed. The spacecraft will be directly launched into the orbit going to Mars. It is possible to fit all the required payload in the launcher but the crew would be very limited in their moving space. Therefore an inflatable module is incorporated in the design. The inflatable module is the Genesis-II spacecraft, produced by Bigelow Aerospace. The rigid part consists of the Cygnus Enhanced Cargo module, produced by Orbital Sciences Corporation. The spacecraft is launched by the Falcon Heavy launcher, which will have its maiden flight in 2017. This cargo module has to be modified to be qualified for human flight. The module is deflated during launch so it can fit in the launcher. Once it is in orbit, the module is inflated to provide enough free-space volume for the crew. After fly-by at Mars a Dragon capsule produced by SpaceX is used to re-enter the Earth's atmosphere.

Concept 2: Frank

The objective of this concept was to create a design merely consisting of elements that have already proven their reliability in space. This design requires two launches. The launchers that are used are the Falcon 9 and the Falcon Heavy. First, the Falcon 9 launches a Cygnus Enhanced, a Cygnus Normal and a fuel tank into a parking LEO. Second, the Falcon Heavy launches the crew, the Dragon re-entry capsule and additional fuel. The two elements are docked in the Low Earth Orbit (LEO). At the right moment the second stage of the Falcon Heavy is re-ignited and the module is inserted into an orbit to Mars. After the fly-by and being in close proximity of Earth again, the re-entry procedure can begin: a Dragon capsule produced by SpaceX is used to re-enter the Earth's atmosphere

Concept 3: Soteria

The design approach for this concept was to make the mission as comfortable as possible for the crew, which is achieved by adding more free-space in the living module. To be able to do this, three launches will be needed to get this into space. One launch will consist

entirely of fuel, required to get the spacecraft from LEO to the right trajectory to Mars. Another launcher will launch the re-entry capsule with additional fuel, and with the third launch the living module will be launched, including the crew. Since there are two separate fuel tanks, in-space refuelling needs to be performed. The first docking is an automatic docking since the crew is not launched at that moment. They will be launched in the third launch, so the second docking can be assisted by the crew.

Concept 4: DragonHawk

The aim of this design is to only use components produced by one company (SpaceX). Two launches are used: First a Falcon Heavy fully loaded with propellant for the whole mission will be launched to a parking LEO and afterwards a Falcon 9 carrying the spacecraft will be launched into the same orbit. The spacecraft consists of a Dragon capsule with two extended trunks assembled together. The two trunks are connected and pressurized. They will provide the living module for the crew during the mission. During the launch the Dragon capsule carries the crew. In space they aid the docking during Extravehicular Activity, after which they enter the pressurized extended trunk. The module is then launched into the trajectory to Mars. When the module approaches Earth again, the crew leaves the extended trunk and moves into the Dragon re-entry capsule. The living module is jettisoned and remains in space.

Spacecraft concept trade-off

After establishing the above four concepts, a trade-off between them has to be done. The designs are graded on the following criteria: Safety, Cost, Simplicity, Feasibility, Sustainability and Sensitivity. The weighting of each criterion can be found in table 6.2. As the table shows, DragonHawk and Soteria turn out to be the best concepts. Eventually the best elements of both concepts are selected and combined into a single concept, which will be presented in section 6.5.

Table 6.2: Trade-off table of the different concepts

	Weight	Kirby	Frank	Soteria	DragonHawk
Safety	33.8%	5.1	6.4	8.1	7.0
Cost	15.9%	7.0	6.9	7.1	8.7
Simplicity	12.5%	7.7	7.7	7.0	8.20
Feasibility	23.9%	6.8	5.7	6.9	7.8
Sustainability	4.0%	7.4	7.9	5.5	6.9
Sensitivity	9.9%	4.4	5.7	8.1	7.7
Total:	100%	6.1	6.4	7.4	7.7

6.5 Final design

The final design of the Inspiration Mars mission will be described in this section, with each mission segment discussed separately.

Mission profile

The launch phase starts with the launch of the refuelling module on board of a Falcon Heavy into an Earth parking orbit with an altitude of 200 km. A second launcher will bring the spacecraft, designated Adrestia, with its crew into the same orbit. The second stage of the Falcon Heavy will remain attached to Adrestia to perform the Trans Mars Injection. To perform this manoeuvre the booster will need to be refuelled.

The refuelling manoeuvre starts with rendezvous and docking of the spacecraft with the refuelling module. The crew will perform an extravehicular activity to transfer from the re-entry capsule to the living module. During this manoeuvre the crew will assist with the docking. When successfully docked, the booster is refuelled in six hours. Thereafter, the refuelling tanks are separated and Adrestia is inserted into its interplanetary trajectory to Mars.

Once Adrestia is on its way to Mars, the booster is jettisoned. Next, the spacecraft is orientated with its back towards the Sun and the 4 solar panels are deployed. This orientation is maintained for the whole trajectory for thermal and radiation protection. After 226 days Adrestia will perform the Mars fly-by at an altitude of 180 km. It

makes use of a Mars gravity assist to transfer into the trajectory back to Earth. This second leg lasts 274 days after which Adrestia will approach Earth with a velocity of 14.2 km/s.

Two days before re-entry the crew will perform a second extravehicular activity to enter the re-entry capsule again. The living module will then be separated and continues into a heliocentric orbit for an extended mission to do additional scientific measurements. The re-entry capsule will perform a direct re-entry into the Earth's atmosphere. By controlling the flight path angle and the bank angle the g-loads remain within the required margins. At an altitude of 7.2 km the drogue chutes are deployed. The final phase of the descent will be flown under the main chutes, which slow the capsule down to a splashdown velocity of 5.6 m/s.

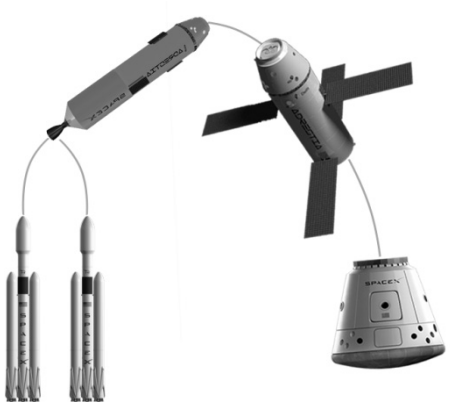

Figure 6.2: Mission profile summary

Spacecraft detailed design

The design of the different sub-systems that compose Adrestia is based on the mission and functional requirements identified for the chosen concept. The main design focus is maximizing safety, simplicity and reliability while keeping the mass and volume to a minimum. The isometric view of Adrestia, with fully deployed solar arrays, is shown figure 6.3.

To ensure the crew's health an Environmental Control and Life Support System (ECLSS) is needed. The mass of ECLSS is minimized through the implementation of advanced technologies with increased water filtering efficiency. Additionally, to increase the mass efficiency of the spacecraft, some components are combined with other sub-systems and thus used for radiation protection and power generation. Adrestia is composed of the Dragon re-entry capsule and a living module. The structure of the re-entry capsule is left unchanged, and the living module structure is designed to withstand the launch loads. The main load carrying structure is the Kevlar rear wall of the multi-shock protection shield. This shield and the sub-systems placed around the crew compartment provide enough dose reduction from galactic cosmic rays while the water tank, food and waste is placed at the rear of the spacecraft to protect the crew in case of solar particle event.

The guidance, navigation and control functions are performed by AutoNav, an autonomous optical navigation system. AutoNav takes images of asteroids against distant stars, and determines its position and velocity from these images. This information is then used to determine correction manoeuvres, which will be executed by the reaction wheels and thrusters.

Even though the guidance, navigation and control system does not require communications, the communications sub-system will be used to monitor the crew and mission development. The communication system is also used for private communication, web-conferencing and health inspections. It consists of the Dragon capsule on board component for LEO communications, using an S-Band link and a phase array antenna. For the deep space connection two extra antennas are added for a K-band link.

The power sub-system consists of two fuel cells, four solar arrays and five secondary batteries as well as power management systems. The fuel cells will be the primary power source during the LEO phase. During the Interplanetary Trajectory phase, the solar arrays are

deployed and used together with secondary batteries to produce the required power for all sub-systems.

The thermal control system makes sure that all the sub-systems work within their operating range. It is designed for the most critical thermal requirement, which is keeping the crew compartment temperature between 18 and 26°C. This is achieved by rotating Adrestia with the back towards the Sun in combination with passive and active thermal control. The passive system consists of multilayer insulation and radiators, while the active system will consist of heaters, heat pumps and pumped fluid loops.

Finally, for the last phase of the mission, the Dragon re-entry capsule is adapted for the extreme re-entry velocity of 14.2 km/s. In the first part of the re-entry the atmosphere decelerates the capsule. Below 7.2 kilometres altitude the Descent and Landing System is activated. The first step is to jettison the heat shield to eliminate the heat transfer into the crew cabin. Then the parachute system, consisting of two drogue chutes, three pilot chutes and three main chutes, is activated. Finally, the capsule will land in the ocean, where recovery ships are wating.

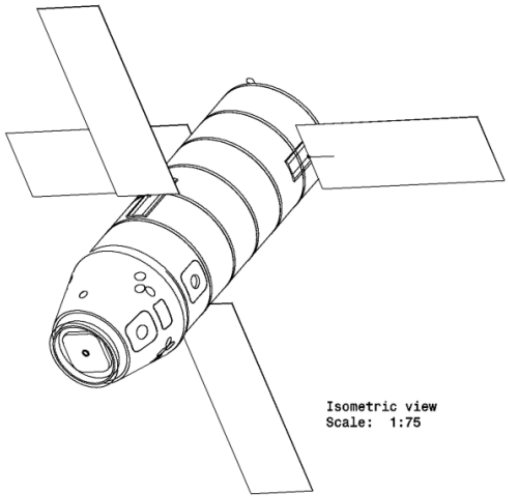

Figure 6.3: Adrestia isometric view

6.6 Cost

Two total cost estimations were made by using different cost estimation methods. A first estimation was made by using the Advanced Mission Cost Method (AMCM) developed by NASA. The second estimation used a combination of the TRANSCOST model, cost estimation relationships from Space Mission Analysis and Design by W.J Larson and readily available costs from SpaceX. The costs from both estimations were relatively close within 15% of each other. The first method resulted in an estimated cost, including reserve costs, of 4,250.83 Million Euro. The second (more detailed) method resulted in a cost of 3,772.64 Million Euro. An overview of the estimated cost is given in figure 6.4.

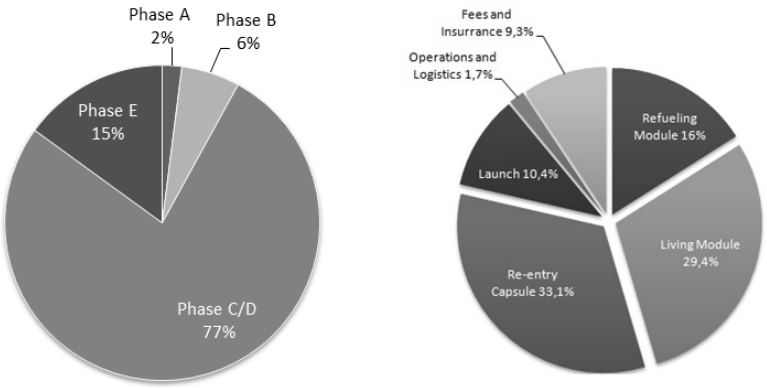

Figure 6.4: Cost estimation segment overview

6.7 Conclusion and recommendations

The mission objective is to design an end-to-end fly-by mission to Mars by the year 2018. By using existing technologies, like the Dragon capsule, the development time of systems is drastically reduced. The Adrestia design also makes use of unique design elements. On-orbit refuelling, autonomous GNC and an relatively large re-entry velocity contribute to this unique design. The sustainability of the design is achieved by including a state of the art life support system, reusable

strap-on launchers and the continuing mission of the living module. Adrestia will revolutionize space travel at an estimated cost of 4.3 billion euro.

To improve the design, recommendations are given for further studies. This design is a pre-phase A study, which means that every sub-system has to be designed in more detail further in the design process. Special attention should be given to the on-orbit refuelling and autonomous GNC sub-system. On-orbit refuelling has never been done on this scale before; this system will need extensive testing before it is ready for human space flight. Although the GNC sub-system AutoNav has already been used on the Deep Space 1 mission, it is not tested for human space flight. To ensure the safety of the crew, this system needs to be qualified for human space flight.

7. TOWARDS THE NEXT GENERATION WATER BOMBER

Students: E.V.M. van Baaren, S.A.W. van den Broek, D.A. Eisses, L.H. Geijselaers, F. Heddes, W.F.S. van Lingen , H.A. Mulder, L.A. van der Schaft, G. Stolwijk, M.C.G. van der Werf

Project tutor: ir. P.C. Roling

Coaches: ir. G. Tescione, Q. Guan MSc

7.1 Introduction

Wildfires pose a significant threat to communities living near large, forested areas. Due to biomass growth and climate change, wildfires are an increasingly common phenomenon. Common solutions to combat wildfires from the air include the use of water bombers, such as the Bombardier CL-415 and the Beriev Be-200. However, as the intensity and impact of wildfires are increasing, the need for the development of an aerial vehicle that can extinguish wildfires in a more cost-efficient and time-efficient manner has grown over the years. To meet this need, the team has been given the task to design a next generation water bomber. The mission statement of the design process has been stated as follows.

"Design an amphibious, multi-functional next generation water bomber which can extinguish fires in a more cost- and time-efficient manner than the current generation of water bombers."

7.2 Design requirements and constraints

The top-level design requirements, which have been imposed by the client, are summarized as:

- Load capacity > 15 m^3
- Water Take-off runway length < 1,000 meters.
- Climb angle > 15° at Maximum Take-Off Weight (MTOW).
- Zero payload range > 1500 nautical miles.
- Fill payload range > 500 nautical miles.
- Stall speed < 100 knots at MTOW
- Manoeuvring envelope: -2g till 5g
- 2 Pilots + 2 (other) crew.
- Water reloading on land and on water.
- Ground support equipment must be carried on board for fast deployment
- More cost efficient than current aircraft.
- Multi-functional.
- Flexible for carrying other loads.

7.3 Concepts studied and related trade-offs

During the preliminary design phase, three main concepts had been established which were considered as design options for the next generation water bomber. These concepts consisted of three different concepts, being a rotorcraft, tilt rotor and an amphibious fixed-wing aircraft. Furthermore, a different mean of intake and release of retardant had been considered for each of the three listed above. The means of intake and release of retardant for each concept, is summarized below.

As the rotorcraft concept is only able to land and take off from land, it carries the retardant in a bucket, hung from its belly. The rotorcraft subsequently hovers above the water body, dips the bucket into the reservoir and returns to the location of the wildfire. The release of the retardant will then be assisted by means of gravity.

The tilt rotor concept pumps water into an internal container, which can be done whilst hovering above a water body or standing on the ground. The tilt rotor subsequently returns to the wildfire location, hovers again and uses multiple water cannons to effectively combat a specific fire area. Similar to the rotorcraft concept, the tilt rotor will only be able to land and take off from land.

As the fixed-wing aircraft is able to operate from water, as well as from land, the fixed-wing aircraft concept is capable of scooping retardant or pumping the retardant into the retardant tanks when the aircraft is on land. The fixed-wing aircraft subsequently flies to the wildfire and delivers the retardant wildfire through either a simple open-doors drop or with a cannon system, integrated in the aircraft
A final concept choice has been made with help of the Analytical Hierarchy Process (AHP) method, which is a specific form of a weighted trade-off method. The concepts were ranked on their operational capability, reliability, availability, maintainability, safety, structural capability, costs, ease of production, sustainability and comfort.

From the trade-off, the fixed-wing amphibious concept appeared to be the most favourable concept, with the rotorcraft concept being a close second. The only criterion category on which the fixed-wing concept has been ranked less favourable, is the operational capability which can attributed to its lack of Vertical Take-Off and Landing (VTOL) capabilities, which in turn affects its drop performance. However, its better performance in terms of retardant coverage, turn-around time, fuel efficiency, ease of flight, costs, safety, lower complexity and damage tolerance, compensates for its lack of VTOL capability and therefore the fixed-wing aircraft concept has been selected as the final concept.

7.4 Mission design

The most important mission stages are the reloading and dropping of the fire retardant. The dropping of the retardant is achieved through opening release doors, enabling a gravity assisted drop. As four

separate retardant are installed, multiple drops can be performed during a single flight cycle. The opening of the release doors will be computer-controlled, during which the wind speed and direction will be accounted for. Due to separate retardant tanks and release doors, as well as due to computer-controlled operation of these release doors, different drop patterns can be achieved. For the reloading of retardant, the amphibious characteristics of water bomber are employed. In order to fill the retardant tanks, the water bomber approaches a water body of sufficient dimensions, land and start skimming the water. During this "scooping motion", two probes will be lowered which enables water to flow into the retardant tanks.

As wildfires do not occur during the entire year, the aircraft has been designed with the ability to perform multiple missions in mind so that it does not have to be grounded several periods a year, which would be a waste of (monetary) resources. Examples of other missions that the next generation water is able to perform are cargo, mail or passenger transport to hard-to-access locations as well as Search and Rescue (SAR) missions. Due to its Short Take-Off and Landing (STOL) and amphibious characteristics, the next generation water bomber also is well suited for performing human relief missions in disaster struck areas. For example, an earthquake may have damaged the local airport, rendering it useless for conventional emergency aircraft to land or take off from. In such cases, the next generation water bomber is still able to reach this area by operating from a nearby water body such that emergency goods can still be delivered to the local inhabitants.

In 2005, the US Forest Service conducted a study on the aerial application of wildland fire management, which concluded that aerial vehicles with a retardant capacity in access of 3,000 gallons (11.4 m3) continue to show significantly greater economic benefit compared to smaller platforms. Furthermore, research has shown that at least two-third of the historical fires in the U.S. were within 10 miles of a scooper-accessible body of water. Employing the scooping capabilities of the aircraft and the large retardant capacity, this new water bomber

concept is able to deliver a larger amount of retardant to the fire per hour compared to current aerial firefighting solutions.

Furthermore, as different types of suppressant are suitable for different specific missions, it has been decided to equip the next generation water bomber such that it able to drop fire extinguishant based on long-term retardants as well as on Class A foams. The long-term retardant however, cannot be mixed during flight and need to be loaded of the ground base. The Class A foam concentrate, on the other hand, is stored in small tank in the water bomber and will be mixed with water during flight. The ability to drop these different types retardants significantly increases the operational capabilities of the aircraft.

7.5 Details of selected concept

In order to start sizing the design, the customer requirements had to be translated into technical requirements. During the detailed design phase, the wing, tail, engines, hull, retardant intake and release systems have been sized.

Several performance related requirements have been imposed by the client. These include a stall requirement, take-off and landing requirement as well as a required climb gradient. For each requirement, wing- and power loading relations have been set up, from which a required power and wing area have been found. With these values known, a design lift coefficient could be determined, which ultimately led to the selection of a NACA4317 aerofoil for the wing.

The design introduces a lot of spray which can be ingested by the engines and subsequently stall the engines. In order to provide sufficient clearance between the water line and the engines, the wing will be mounted in a high-wing configuration. As the aircraft will fly at low speeds, the design will feature no quarter chord wing sweep angle, $\Lambda_{c/4} = 0^{\circ}$. The wing features an aspect ratio of 8 and a taper ratio

of 0.4. A negative dihedral angle of 1¤ is used in order to increase controllability.

Next to the main wing sizing, control surfaces and high-lift devices have been sized. For the high-lift devices, the available flap types varied from simple plain flaps to complex triple-slotted flaps. As the design of the water bomber should remain as simple as possible to improve reliability and maintainability, the complex flap systems were dismissed and a simple single slotted flap system has been selected. The flaps run from 9 to 60% of the spanspan wise, and 75 to 100% of the chord. As the flaps potentially cannot provide a sufficient CL increase during hot atmospheric conditions and the airflow does not remain attached to the wing profile at high angles of attack, the wing has also been equipped with leading edge lift-enhancing devices. Two leading edge lift-enhancing devices were available, being a Krueger Flap and a Slotted Leading Edge Flap, also known as slat. As slats were found to be the most effective leading edge devices for this design, it was decided to install the slats running from 60 tom95% of the span and from 0 to 15% of the chord. The final dimensions of the wing are listed below:

Table 7.1: Wing design parameters

Wing dimensions	
Surface area [m^2]	192.60
Span [m]	39.25
Chord length at root [m]	7.01
Chord length at tip [m]	2.80
Thickness at root [m]	1.19
Thickness at tip [m]	0.48
Flap area [m^2]	27.82
Aileron Area [m^2]	10.73

In order to ensure lateral stability during on-water operations, the wings will be equipped with floats at both tips. As they are inflatable, they will be inflated shortly before landing and deflated after take-off to reduce drag. Near the nose of the aircraft, two control canard surfaces will be added. They will function as an extra safety redundancy in case of a loss of control due to the aircraft losing or

damaging a control surface or due to the aircraft operating outside its flight envelope.

For the tail sizing, a trade-off has been made between the tail surface size and the distance to the main wing, also known as tail length. When the tail length is too small, a large tail is required which significantly increases the aircraft's weight. On the other hand, if the tail is too small, a large tail length is required which adds to the fuselage weight and subsequently to the aircraft's overall weight. During flight, the horizontal tail generates negative lift to counteract the moment created by the wings. Also, as the aircraft is able to scoop, a larger counteracting moment is required to cope with these scooping forces. Secondly, the stall angle of the tail should be higher so the aircraft will still be controllable during stall of the main wing. For these reasons, the NACA0018 profile has been selected for the tail plane of the design. The empennage consists of the vertical and horizontal tail where the horizontal tail is placed on top of the vertical tail, commonly known as a T-tail configuration. This configuration has been selected as it will provide the largest possible centre of gravity range of the aircraft. Just as for the main wing, control surfaces for the tail have been sized. The results of the tail dimensioning are summarized below:

Table 7.2: Tail design parameters

Horizontal tail	
Surface area [m^2]	43.22
Span [m]	15.06
Chord length of horizontal tail at root [m]	4.10
Chord length of horizontal tail at tip [m]	1.64
Chord length of elevator at root [m]	1.64
Chord length of elevator at tip [m]	0.66
Elevator area [m^2]	12.10
Vertical tail	
Surface area [m^2]	36.08
Span [m]	6.01
Chord length of vertical tail at root [m]	8.58
Chord length of vertical tail at tip [m]	3.43
Chord length of rudder at root [m]	3.52
Chord length of rudder at tip [m]	1.96
Rudder area [m^2]	15.13

With the selected power loading for the wing sizing and an initial weight sizing performed, it was possible to select the engines. During the mid-term phase it was decided that the aircraft would be fitted with turboprop engines, as they have better stall recovery than jet engines and operate more efficiently at lower speeds. To determine the required number of engines, the blade loadings were calculated.

For two engines, the blade loading only came within a suitable range for a diameter of 5.0 meters in combination with 10 blades. As this large diameter and number of blades are considered unrealistic, the choice for a four engine configuration was made. This configuration will ensure sufficient clearance with respect to the water and has a favourable One-Engine-Inoperative (OEI) performance. A required power of 11.6 MW was determined, which resulted in the selection of the Rolls Royce Allison T56-A-10WA engine.

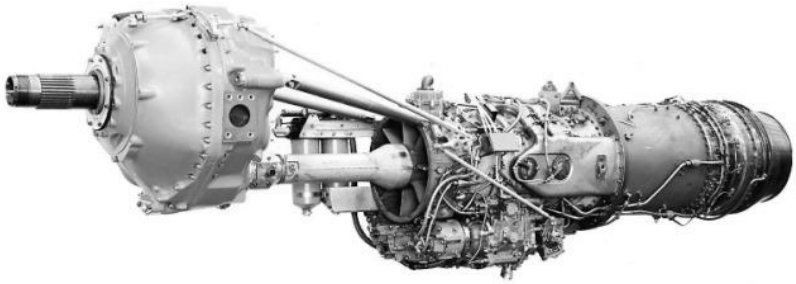

Figure 7.1: RR T56 Engine, Type A-427, from Jane's

The starting point of hull design was the estimation of the beam length, which is the width at the widest point of the hull. The load displacement was assumed to be the MTOW minus 2,500 kg, which is the loading at which the aircraft will still be able to take off with a runway length of 1,000 meters. From the beam length, an estimation for the wetted length of the hull could be determined. This length is the part of the hull that will be submerged at zero velocity and zero payload. The wetted length consists of the fore- and afterbody length, where the forebody length of a flying boat is the distance from the forward perpendicular to the main step at the keel. For the planing bottom, a V-shaped design was chosen for its ability to absorb the shock during a water landing. Also, two steps, which are abrupt

changes in the shape of the bottom of the hull, essential to break down the water suction and enable the plane to unstick from the water, have been added. The final hull design parameters are summarized below:

Table 7.3: Hull design parameters

Nose length [m]	1.50
Wetted length [m]	25.00
Length between steps [m]	7.26
Total length [m]	34.72
Length to half-chord length of the wing [m]	18.40
Maximum Hull width [m]	3.30
Height above water level [m]	4.87
Height below water level [m]	1.37
Height of the V-shape in fuselage [m]	0.60

Near the nose of the aircraft, two hydrofoils will be added which will increase lift at low speeds when the aircraft is about to take off from water.

The aircraft is designed for a retardant payload of 15.00 m^3. However, due to thermal expansion and structures within the tank and foam additive, the tank volume is increased by 6% resulting in a volume of 15.96 m^3. The tank will have a maximum height of 2.13 meters, leaving 2.75 meters of space to the top of the fuselage. The floor is positioned at 1.47 meters from the bottom of the hull, which is done such that the door thresholds are 10 cm high, enabling easier to loading of the aircraft. As a result, the water tank rises 66 cm above the floor, leaving sufficient height above the tank to stand up straight.

The water bomber will feature a retardant intake system in order to refill its water tanks during scooping. A conventional and simple way of filling the retardant tanks is by means of inlet probes. These probes will be dropped into the water during the scooping motion and water will be directed into the water tanks. The number and size of inlet probes and its dimensions depend the scooping distance, scooping velocity and the water tank volume. In order to fill the water tanks, which are located on both sides of the fuselage, two probes will be

installed with a height of 8.2 cm and a width of 15.2 cm. The release system consists of four doors, one under each tank.

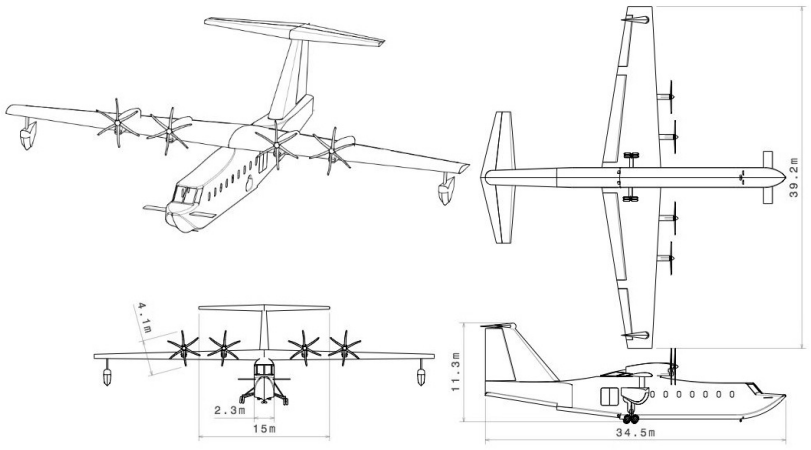

Figure 7.2: Three view drawing

7.6 Sustainability

As the next generation water bomber will accumulate significantly less annual compared to commercial aircraft, the operational sustainability has a relatively low impact on the total sustainability of the design. However, a more efficient way of aerial firefighting, efficient manufacturing procedures, material selection and the end-of life procedures contribute to the sustainability of the aircraft and are considered in the design.

The main mission of the aircraft is to extinguish wild-, forest- and bush fires. Research has shown that the wild-, forest- and bush fires in the United States in 2007, accounted for approximately 4 to 6 percent of the total greenhouse gas emissions for that year. As the next generation water bomber is able to extinguish these fires more efficiently than current firefighting solutions, it will reduce the greenhouse gas emissions and thereby contribute to a more sustainable balance in the earth's atmosphere.

3D printing is a relatively new technology and has recently been used by BAE Systems Regional Aircraft to manufacture plastic tubes for window ventilation. As 3D printing cannot yet apply, for example, heat treatments to aluminium, this manufacturing process only has been considered for the non-load bearing parts of the aircraft. The main advantage of this manufacturing process is that it minimizes the waste material and because of the small number of production aircraft, 3D printing can be more cost efficient than production with moulds.

During the material selection procedure, aluminium alloys have been selected over lighter composite materials, as the production of composites requires considerably more energy than that of aluminium. Considering the total lifetime of the aircraft, the advantage of using composites instead of aluminium will be negated by the high energy required during the production phase. Besides this, there are efficient recycling procedures for aluminium whilst the recycling of composites is still in a preliminary phase.

After a projected service life of about thirty to forty years, the aircraft will be retired from service. Before the aircraft will be parted out for recycling, all reusable parts, including engines, avionics and CADAS, will be removed. Due to the relative simplicity of the design, all of these parts can be reused in other aircraft or be used as spare parts. After these items have been removed, the hull will be parted out. During this phase, the best recovery options for different materials will be identified. During the final phase, the reusable materials will be cast into ingots for further processing, after which they can be used again as secondary raw material for manufacturing purposes.

7.7 Conclusion and recommendations

As the scale and impact of wildfires are increasing, a need for the development of an aerial vehicle that can extinguish wildfires in a more cost-efficient and time-efficient manner has arisen. Therefore, a next generation aerial firefighting aircraft has been developed, called

the Red cross Aerial Firefighting Tanker, or RAFT. The excellent flight and drop performance, its large retardant capacity and multifunctional design, enables the RAFT to outperform its competitors.

All requirements that have been imposed by de client are fulfilled and in some cases even exceeded. The RAFT is able to load and drop 15 m3 of retardant and fulfils the performance requirements, such as taking off within 1,000 meters at maximum take-off weight. Longitudinal stability and controllability are ensured by a large T-tail with large control surfaces. Furthermore, the centre of gravity is carefully located such that flight characteristics enable relaxed flight for the pilot. Finally, several innovations are integrated in the aircraft, which significantly improves the performance of the RAFT with respect to previous aerial firefighters.

Control canards
Control canards enable the aircraft to quickly recover from a stall and guarantee controllability should other control surfaces fail.

Hydrofoils
The implementation of hydrofoils to the design decreases the take-off length of the amphibious aircraft, which increases the deployment area of the water bomber.

CADAS
The Computer Augmented Detection and Aiming System (CADAS) provides the pilot with environmental information and automatic aiming. This system, in combination with current detection and aiming techniques, significantly improves the efficiency of aerial firefighting operations.

Water cannons
The RAFT has the option of two computer-controlled water cannons, which allows the release of a concentrated jet at specific targets. Although several helicopters are already equipped with a water

cannon, the high cruise speed of the RAFT yields a significantly smaller response time.

Inflatable or retractable wing tip floats

Wing tip floats are installed to enhance the lateral stability of the aircraft during on-water operations. However, as these components result in significant drag penalties during flight, inflatable floats are installed, which decreases drag during flight.

As wildfires only occur during limited period in the year, a conventional water bomber may have to be grounded during several periods per year. The RAFT, on the other hand, is designed with multifunctionality in mind, which enables the aircraft to perform different missions. The aircraft can be used to fight other kinds of fires than wildfires, being for extinguishing highway fires and oil rig fires. However, this aircraft can also be used for other missions than aerial firefighting. Due to size of the aircraft and its STOL characteristics, it will also be excellent for transporting cargo to hard-to-access areas. Furthermore, due to his amphibian characteristics, the RAFT can be used to deliver emergency supplies to flooded areas. These multiple functionalities make the aircraft more versatile and worth the initial investment.

The design of the RAFT is a preliminary design only the basic dimensions of the (sub-)system are sized. During further design phases, such as the detailed design phase, testing phase and pre-production phase, more research should be done with respect to certain aspects of the design. As currently little to no knowledge have been gathered with respect to the innovations listed above, side effects may occur that are not anticipated for. Furthermore, little research has been done regarding the lateral stability and controllability of the aircraft. Thirdly, little is known about the hydrodynamic interaction between the hull and water. Finally, additional research should be done regarding the deep stall behaviour of the aircraft.

8. InVADe - Design of a VTOL Business Aircraft

Students: V. Bontempi De Marchi, R. Dekker, H. Jaberi, R.M. Koch, J. L'Ortye, J. van Manen, S.A. van der Meijden, Q. Payanda, B.J. Pijnacker Hordijk, C. Ravesteijn

Project tutor: ir. S. Shroff

Coaches: ir. V.P. Brügemann, dr. M. Gallo

8.1 Introduction

Corporate travel requires efficient and prompt modes of transportation. However, current air travel does not meet this need as transfers between the airport and the city, waiting times at the airport and delays can greatly increase the total time to travel between two business locations. A vertical take-off and landing (VTOL) business jet would combine the advantages of a helicopter - flexibility and no need for an airstrip - with the advantages of an aircraft - fast cruise speed. InVADe (Innovative VTOL Aircraft Design) will be capable of operating in densely populated areas and will offer swift, point-to-point transportation. InVADe is designed to transport 10 people over a distance of 2000 km at a cruise speed of 600 km/h, while employing VTOL capabilities. It is planned to be flying by 2030.

Figure 8.1: Render of InVADe

Market forecasts for regular corporate jets and helicopters show that over the next two decades the market will experience continuous growth. Assuming 500 units will be sold over the next 20 years, a market share of 1.9% of this regular jet and helicopter market is achieved. Alternative markets which could increase sales numbers further include medical rescue operations, military, utility, VIP and offshore oil and gas transport. After modifications to the aircraft the UAV market can also be entered.

8.2 Concepts

The final design was chosen after the final trade-off between three different concepts was completed. The main criteria used during the trade-off include noise levels, technology readiness level and control & stability. Other criteria included specific range, weight, unit cost, operating cost, safety, complexity and sustainability. The proposed designs include the 4 Ducted Fans concept, the Heliplane concept and the TRAC concept, which are depicted in figure 8.2.

Figure 8.2: Render of the heliplane, TRAC tiltrotor and 4 Ducted Fans concept

Like the name suggests, the 4 Ducted Fans concept, which is primarily based on the Bell X-22, uses four ducted fans for propulsion. These fans can be tilted such that transition between vertical flight and horizontal flight can be performed gradually. The most prominent feature ducted fans is that they are producing low amount of noise in comparison to other propulsive systems due to the shrouding.

The heliplane is a fixed wing aircraft with a helicopter rotor mounted on top of it. In this way the vehicle can perform VTOL manoeuvres using the main rotor. The pusher props can be used to propel the aircraft forward during cruise flight. Additionally, the rotor can be used as a stop rotor or as an autogyro during this flight phase. A separate propulsion system for the rotor and propeller is implemented. The advantage is that the engines and propellers can be optimized for horizontal or vertical flight. The main disadvantage would be that a second inoperative propulsion system increases the operational empty weight significantly.

A Telescoping Rotor Aircraft (TRAC) is based on the tilt rotor aircraft, which generates lift and propulsion using tilting propellers. The most comparable aircraft are the AgustaWestland's AW609 and Bell Boeing V-22 Osprey. The upward positioning of the engines and propellers is used for the VTOL capabilities and for the horizontal flight the rotors are tilted forward. The advantage of the TRAC concept is that it

increases efficiency for each flight phase by changing the diameter of the rotor throughout the mission. Thereby, the propulsive system is optimized for each flight phases. However, the main disadvantage of this concept is the complexity of the blade design and high noise noise levels.

In conclusion, the 4 Ducted Fans concept achieved the highest score in the trade-off. In comparison to the other concepts it is able to operate at relatively low noise levels and has a high technology readiness level due to experience with the X-22.

8.3 Innovation

At this stage, the 4 Ducted Fans concept boiled down to an upgraded version of the Bell X-22. A comparison with reference aircraft and test flight data of the X-22 yielded insight in the current shortcomings of VTOL aircraft. These aircraft tend to exhibit a low maximum lift-to-drag ratio. Therefore the cruise efficiency achievable with the current concept is very low in comparison to business jets with the same capacity.
In the design of the Bell X-22, all ducted fans are sized for cruise and VTOL manoeuvres. Hence, these fans are always a compromise between good performance in VTOL and cruise. Hence, their overall efficiency is relatively low. Solving this drawback turned out to be one of the biggest innovation in the project.

8.4 Final concept layout

The final configuration of InVADe is chosen such that a higher lift-to-drag ratio is attained during cruise in comparison to other VTOL aircraft while still offering good performance during vertical take-off and landing. The main wing houses two ducted fans, which are only used during VTOL manoeuvres. During cruise these fans are turned off and covered using a shutter mechanism to reduce drag. For this reason, a higher maximum lift-to-drag ratio can be attained. Figure 8.1 depicts the final concept. A technical drawing of this concept from

different angles is presented in figure 8.3. Table 8.1 gives an overview of the main characteristics of InVADe.

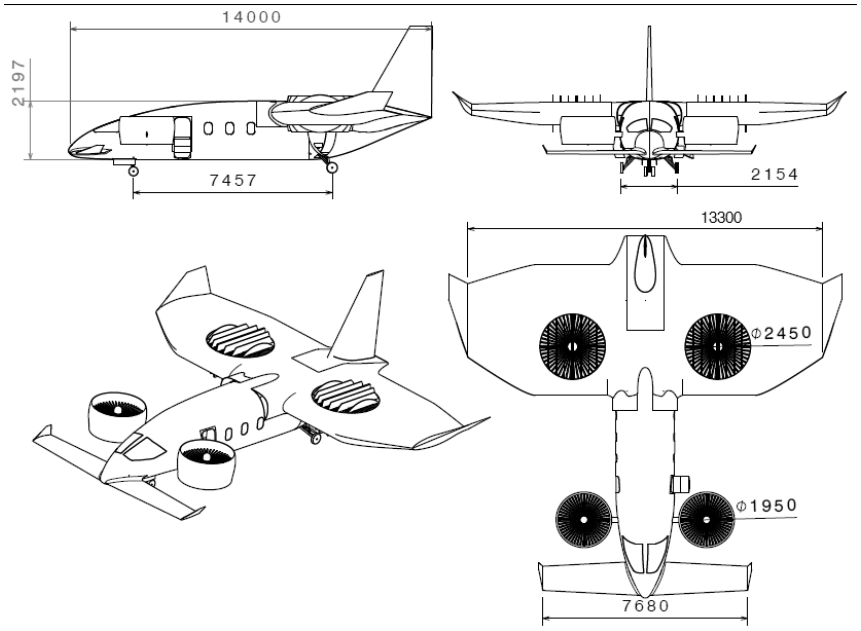

Figure 8.3: Drawing of InVADe from different angles

Table 8.1: Main characteristics InVADe

Capacity	10 Passengers
Cruise Speed	600 km/h
Range with 1000 kg payload	2,000 km
Maximum rate of Climb	19.8 m/s
MTOW	8,290 kg
OEW	5,510 kg
Wingspan	13.3 m
Noise at take-off	<81 dB
CO2 emissions	2.04 kg/km
Unit cost	6.55 million EUR
Operating cost	1,374 EUR/hr

8.5 Aerodynamics

InVADe employs four lift-generating fans during VTOL operations. During conventional flight the wing, canard, fuselage and the two tilting front ducts generate lift. The planform of the main wing consists of a rectangular inner wing, housing the ducted fans, and a

tapered outer wing section with an aspect ratio of 6.19. During transition high lift devices enable InVADe to safely perform transition at a speed of 60 m/s.

8.6 Propulsion and performance

Two turboshaft engines, housed in the fuselage, provide 3.5 MW of power to four electric generators, which in turn transmit power via electric cables to electric motors mounted in each duct. The motors then each power individual fans inside the ducts, which, together deliver enough thrust to lift the aircraft vertically off the ground.

The reasons to go for electric power transmission include that a mechanical system with shafts and gearboxes would be heavier, more complex, causes more vibrations and would need more maintenance.
After take-off the aircraft performs the transition to conventional climbing flight. While the front ducted fans tilt to provide thrust, shutters close off the aft ducts inside the wing. The rate of climb can reach a maximum of 19.8 m/s at sea level and the cruise speed of 600 km/h is reached at 75% power rating. The range varies depending on the payload from 1,082 km to 2,986 km.

8.7 Structural design

Three different structural sections of the aircraft were preliminarily designed: the main wing structure, canard, and front ducts. The outer section of the wing features a wing box, whereas the loads in the inner section are carried by two main spars and a load carrying structure for the duct. In total, this structure has a weight of 191 kg per wing. For all structural elements, Aluminium 2024-T4 was used for its high fatigue endurance limit, good manufacturability and recyclability.

8.8 Stability and control

The design is outfitted with a canard and a single vertical tail, sized for stability and control during flight. During hover and transition,

stability augmentation systems are employed. Additionally, the eigenmotions of the aircraft were examined. The eigenmotions, which include phugoid, Dutch roll, aperiodic roll, spiral and short period, were compared to the response of the Cessna Ce500 Citation. In conclusion, the dynamic stability analysis shows positive results; all eigenmodes are damped out swiftly and stable.

8.9 Financial analysis

The unit cost of InVADe is estimated to be 6.55 million EUR. With a sales price of 10.0 million EUR, InVADe is placed competitively in the market. Even though InVADe is more expensive than helicopters and in the same price range as small corporate jets, VTOL capabilities will give InVADe the edge over its direct competition. The operating cost of 1,374 EUR per hour enables a lower price per passenger than regular business class tickets, as soon as InVADe carries four passengers or more.

8.10 Sustainability

A sharp focus on sustainability, especially on noise and CO_2 emissions, motivated the design team to come up with innovative solutions and push the boundaries of the design to meet the needs of a future aerospace industry with lower environmental impact. With a CO_2 emission rate of 2.04 kg/km, on par with other modern, small business aircraft, InVADe offers a significantly lower environmental impact, particularly for short flights, since it practically eliminates the need of getting to and from the airport. Additionally natural fibres will be used for parts of the interior and also the structural parts made of aluminium can be recycled.

In the vertical take-off and landing phases, the total noise sound pressure level (SPL) produced, after abatement measures such as shielding, forward swept blades and acoustic lining, is as low as 80.7 dB at 100 m distance. This is comparable to the noise of a passenger car as heard from alongside a highway.

8.11 Conclusion and recommendations

In conclusion, InVADe is expected to offer the business market a fast, reliable and cost effective way of transportation without compromising on comfort and sustainability. However, the team identified several areas in which increased research could greatly benefit the design and its feasibility.

Up until this moment, no detailed analysis has been conducted on the vortex interference between the canard, duct and main wing and also the flow disturbance due to the shutter mechanism is not fully known. Experimental research and a CFD analysis can point out how these effects influence the performance of the aircraft.

The scarce resources available for the structural design of InVADe were used to preliminary design those parts that are critical and must be developed in non-conventional ways due to the design of InVADe. These parts include the main wing structure, the canard structure, supporting structure for the ducted fans and the duct-fuselage connection. These parts were designed in a conservative manner. Throughout following design iterations the design could be made less conservative by the implementation of stringers and stiffeners and ribs. Additionally, the implementation of subsystems might compromise the structure and must be investigated.

The sizing and detailed design of the fans and ducts are another point that should be focussed on in the future, since the fan and duct design has a major influence on the propulsive efficiency of the aircraft during cruise.

For the control of InVADe, especially during VTOL and hover the dynamics and control have to be investigated in more detail to ensure safe operation. Also the canard could be downsized if flaps on the canard are incorporated into the design.

9. MACHETE: ROBOTS ON MARS

Students: C. Akkermans, F.D. Andriessen, S. Butter, R.J. Crone, G. Galatis, R.J. Grandia, B.F. Lagaune, M.R. van Reijen, N.M. van Schoote, B.Walgaard

Project tutor: dr.ir. C.J.M. Verhoeven

Coaches: dr. A. Bhat, ir. T. Scholcz

9.1 Introduction

Ever since the manned missions to the moon in the 1970s, man has been eager to put a man on Mars. So far that dream has not turned into reality; only robotic missions have visited Mars. These robotic missions however suffered from the fact that they are fragile and limited in movement. While quite a few of the missions were highly successful relative to their design mission, they covered little ground on Mars.

One method to tackle these shortcomings would be to send a swarm of robots to the Martian surface. Swarms of robots can easily cover large amounts of surface area and offer the opportunity to explore interesting terrain features like caves. Because the fate of no single individual robot is detrimental to the whole of the mission, much higher risk operations can be performed, which potentially have a higher payoff. This study deals with the challenges involved in landing a swarm of Delft University of Technology developed six

legged 'Zebro's' (ZEsBenigeRObot) on the surface of Mars, the robots can be found in figure 9.1. It is assumed that the mission will roughly follow the pattern of the Mars Science Laboratory mission up to the point of its atmospheric entry. Central is the requirement to use off-the-shelf technologies while also pushing technological boundaries. From these first requirements a new mission is born. MACHETE: Robots on Mars; the Entry, Decent, Landing and Deployment (EDLD) of a swarm of robots on the surface of Mars.

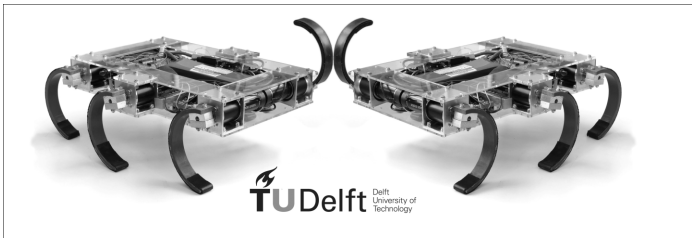

Figure 9.1 Zebro's high fiving

9.2 Mission need statement and requirements

The mission need statement and the requirements on the Martian Autonomous Critter-Housing for Extra Terrestrial Exploration (MACHETE) mission are stated below.

Mission need statement:
"Safely land a swarm of Zebro robots on the Martian surface"

The top-level requirements for the mission are as follows:

- At least 90% of the Zebro's must be functional after deployment on the Martian surface.
- Precision landing within 1 km of the target beacon.
- The mission should be performed autonomously.
- Use off-the-shelf technologies as much as possible.

The 90% survival rate and off-the-shelf technologies are on request of the customer to keep the costs as low as possible. Precision landing is required to keep the Zebro's within their maximum communication range of 1 km and to ensure that the target area can be explored in a

timely manner. Lastly, autonomy is required, because the communication delay between Mars and Earth is too long for human interference.

9.3 Concepts and trade-off

Before it was decided to go for the clustered CAESAR design, multiple deployment options and methods where considered. Entry with an aeroshell was used for every Mars mission and initial slowdown in the Martian atmosphere. The deployment of the Zebro's was the challenge. But what exactly is successful deployment? As stated three important requirements for successful deployment are: the precision landing capability to ensure swarm functionality, a survivability of 90% of the total amount of Zebro's deployed at the Martian surface, and landing autonomously. With these requirements in mind, concepts started developing. The concepts developed where then checked on their feasibility and traded off against each other to find the most cost-effective option.

Deceleration in Martian atmosphere

One of the first concepts was to use wings to precision guide a cluster or a single Zebro down to the target location. This concept proved to be unfeasible due to the large size of the wings needed to achieve a reasonable speed to land the payload on the Martian surface due to the low density Martian atmosphere. This low density also eliminates the concept of using a rotor, since the rotor tips would break the sound barrier before providing enough lift to decelerate.

Research was performed on the concept of using a parachute to slow down in the Martian atmosphere. So far every Mars mission made use of a parachute and it is thus a proven concept in decelerating.

Also a rocket descent was investigated, but using rockets to perform the whole deceleration would use too much propellant. However, the main advantage of rockets, that they give a lot of navigational freedom, could be used in combination with another deceleration concept.

At last a concept using balloons was created. The main problems with balloons are their limits in controllability and their susceptibility to wind drift. In addition they have never been proven outside the Earth atmosphere. To keep the mission development costs low, no further research on the subject of ballooning was performed.

Landing on the Martian surface

For the actual touchdown/landing four concepts were considered, all seemed feasible and further research was performed on them to support decision making in the final trade off. The four concepts can be found in table 9.1.

Table 9.1 Landing concepts for the MACHETE mission

Landing concept	Description of landing concept
Airbags	Airbags have been used before in landing on Mars, and seem to be feasible
Crumple zone	Multiple landers have been making use of crushable legs to absorb landing loads.
Bumpers	Bumpers provide a simple method of handling the touchdown impact.
Skycrane	The skycrane system as has been used for the Mars Science Laboratory, a heavy system capable of landing delicate payloads.

A crumple zone and bumper are discarded for being less volume efficient than an airbag in absorbing impact at a range of angles and the sky crane system, used for the Curiosity rover, is considered too expensive. The Zebro's are not as fragile as that rover is. The airbag system proves to be very lightweight and when employing the vented variant it is also possible to land precisely.

Final trade-off

After performing the necessary research on all the concepts and their combinations and making a preliminary design of an optimal system, the following final trade-off was performed. In this final trade-off it was also decided if the Zebro's would be dropped as a clustered or non-clustered payload. A trade-off table to support the decision for using a clustered vs. a non-clustered system can be found in table 9.2. From the iterative process the following system proved to be the most optimal configuration in decelerating and landing on Mars.

Aeroshell → Parachute descent → Clustered rockets descent → Airbags

Table 9.2 Clustered vs. non-clustered trade-off table

Criterion	Clustered	Non-clustered
Landing reliability	X	
Post landing functionality	X	
Sustainable impact		X
Landing Time	X	
Risk of maneuver at start		X
Mass of landing system		X
Redundancy	X	

9.4 Mission flight profile

The flight profile of the MACHETE mission consists of four phases. Not indicated on figure 9.1 are the launch and the transfer to Mars. These phases are not regarded as phases that needed to be designed. Nevertheless this does not mean these phases are not present in the total mission, and thus the flight profile will be given from the launch and trajectory to Mars to the last phase indicated in figure 9.2.

Launch: The MACHETE vehicle will be launched into space using a large expendable launch vehicle which is suitable for injecting payloads into a hyperbolic trajectory to Mars. A vehicle like the ULA Atlas V 541 with Centaur upper stage is likely to be used. While this study will not deal with the launch vehicle itself, it is of importance to make sure that the MACHETE vehicle is able to handle the launch loads.

Mars transfer after launch: The vehicle will be in Mars transfer for a considerable amount of time. Depending on the launch window, the transfer time may be over a year. For this study it is of importance to make sure that the payload and landing vehicle systems are properly shielded from thermal and radiation loads. The actual design of the cruise stage is not covered by this study.

Atmospheric entry / Phase 0: After arriving at Mars the vehicle will perform an atmospheric entry at a speed of around 6 km/s. The heat

shield will protect the MACHETE vehicle during its fiery deceleration in the upper Martian atmosphere. Past missions like MSL have used balance weights and/or thrusters to control the entry trajectory. While it is not part of this study to design the atmospheric entry system, it is assumed that some mass will be lost during entry.

Phase 1: After atmospheric entry the steerable parachute will be deployed at an altitude of 7-8 km at a speed of 360 m/s. At the moment the MACHETE reaches terminal velocity the heat shield will be dropped, significantly reducing the weight of the vehicle and the MACHETE starts scanning for the beacon signal. Once the signal is found, the vehicle makes his approach towards the beacon by steering its parachute.

Phase 2: After decelerating using a parachute, the parachute and accompanying aeroshell are disposed of. The eight Clustered Autonomous Extra-terrestrial Ship for the Allocation of Robots (CAESAR) will now transition to rocket powered flight in order to kill the remaining vertical velocity and to navigate toward the beacon. Disposing the main parachute and aeroshell will again significantly reduce system mass

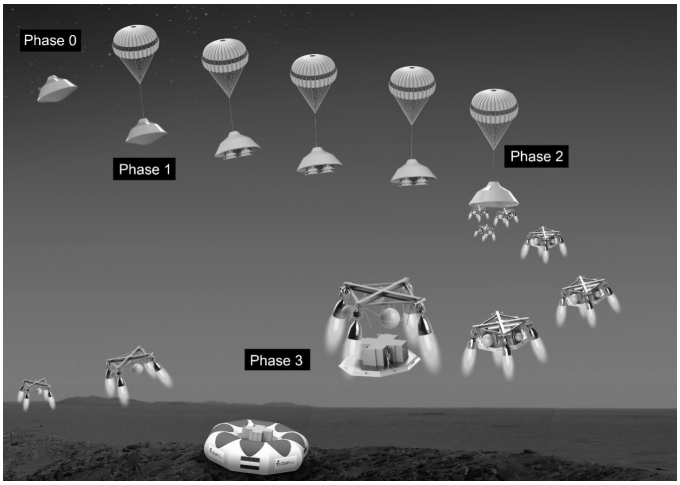

Figure 9.2 Mission flight profile of the MACHETE mission

Phase 3: After arriving at the intended landing site and hovering over a suitable landing spot the Landing Deployment System (LADS) will be deployed from each CAESAR. The LADS will absorb the final impact by using a vented airbag system. After deployment the CAESAR will start its fly away manoeuvre to safely land away from the beacon.

9.5 MACHETE design

The main function of the MACHETE is to safely transport and protect the eight CAESAR's on their way to Mars and during their fast and hot decent in the Martian atmosphere. The internal structure of the MACHETE is designed to carry two layers of each 4 CAESAR's. Once the supersonic steerable parachute has been deployed from the MACHETE and terminal velocity of 100 m/s has been reached, the heat shield will be jettisoned, and a beacon signal receiver will search and lock on to the beacon. When the beacon signal lock has been achieved the steerable parachute will navigate the MACHETE up to 2 km closer to the beacon, depending on Martian weather. Once MACHETE is at an altitude of 2.5 km the CAESAR's will be deployed from the MACHETE, and the next mission phase starts. The MACHETE will steer away from the CAESAR's and moments later crash into the surface of Mars.

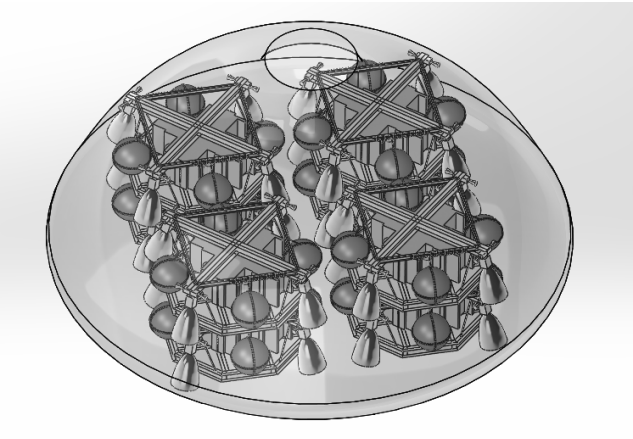

Figure 9.3 MACHETE with eight CAESARS

The MACHETE has been designed to withstand launch loads of -1g to -5g during launch and vibration loads of 2g to 15g that occur during the reentry in the Martian atmosphere. The goal was to keep the design as light as possible while still providing enough protection for the payload. During its journey to Mars the MACHETE should also protect against the radiation encountered in space. The shape and heat shield of the MACHETE have been sized according to the Viking 1 aeroshell. The MACHETE design can be found in figure 9.3.

9.6 CAESAR design

The Clustered Autonomous Extra-terrestrial Ship for the Allocation of Robots will navigate the Zebro's to the required landing area. After it has separated from the MACHETE the eight CAESAR's will continue to follow the beacon signal. However, its rocket engines allow the CAESAR much more navigational freedom than the MACHETE had. The CAESAR thus descents to the designated landing area where it employs its flash LIDAR camera to search for a landing area with rocks smaller than 0.5 m and a slope less than 10% within 1 km of the target beacon. It picks a spot and hovers above it at 30 m altitude where it drops the LADS. Afterwards it uses any remaining fuel to crash as softly as possible and fulfil its post mission function as communication relay for the swarm of Zebro's. The final design can be found in figure 9.4.

The final design is a cross shaped structure with 4 large rocket engines, 4 yaw thrusters and fuel tanks, under this structure the LADS is fastened. The dry mass of one CAESAR, including 140 kg LADS, is 230 kg and it can carry 50 kg of propellant. A nitrous oxide and ethane bi-propellant is used for its high specific impulse, self-pressurizing characteristics and non-toxicity, this is a propellant that is in development, but it has proved its performance in rocket engine tests on Earth. The other choices in this performance range are all toxic and the sustainability goals for this project prohibit the use of toxic propellants. Each of the thrusters can deliver a maximum thrust of 1200 N and provide a deep throttle setting to 5% of this. The navigational range of the CAESAR is 2.25 km.

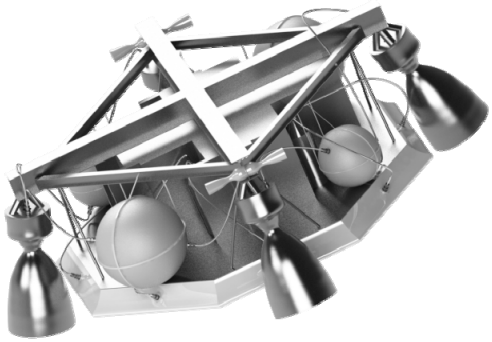

Figure 9.4 CAESAR design

9.7 LADS design

The Landing And Deployment System is the final stage of the mission. After the CAESAR has navigated to its landing area the LADS is dropped from 30 meters altitude. During its 4 second free fall its airbag is inflated with nitrogen to a pressure of 12 kPa. When its sensors detect touchdown, the vents in the airbag are opened within a few milliseconds. This allows the airbag to deflate and the payload to be put on the ground safely. With the LADS on the Martian surface it is time for the robots to be released. The shell protecting the Zebro's is lifted and by means of a radio signal the robots are activated one by one to start exploring Mars as a swarm.

The function of the LADS is to ensure integrity of the payload during touchdown on the Martian surface and to allow the payload to start performing its function. It must keep the deceleration of the payload below 30 gMars and enable the robots to get out of the system. Also the mission must be as flexible as possible, which for this system means that it should be able to land on most of the Martian surface. The Martian surface is a barren environment with two main challenges for the LADS: rocks and slopes. By designing for inclinations up to 10% and rocks up to 0.5 meter almost anywhere on Mars can be reached. The CAESAR can avoid local hazards with its LIDAR.

The final design is a 140 kg LADS which includes 28 Zebro's weighing 4 kg each. The remaining 28 kg consists of the vented airbag system and primary structure of the LADS. Cool gas generators will fill the 5.13 m^3 airbag with nitrogen and eight 0.43 m^2 vents will allow the eight compartments of the airbag to be vented separately. This separation minimizes the risk of rolling over due to slopes or high rocks. In conclusion this system is able to ensure safe touchdown at a low cost. In figure 9.5 the LADS with inflated airbags is shown.

9.8 Conclusions and recommendations

With the presented design, it is found that within the limits of currently off-the-shelf and demonstrated technologies, it is possible to land a swarm of 224 Zebro's on Mars. With a total system mass of 3052 kg entering the atmosphere, and a total Zebro mass of 896 kg, the achieved payload ratio is 29%. For the validation it is recommended that parachute deployment is tested in a supersonic wind tunnel. The parachute control performance can be tested at high atmospheric altitudes. The release sequence of the CAESAR's requires thorough simulation. A full scale CAESAR demonstrator is recommended to validate the beacon communication together with the control system performance. Full scale airbag tests should be performed to validate inflation time, airbag puncturing, and vent system performance.

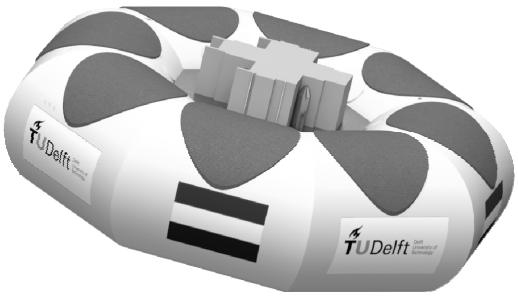

Figure 9.5 LADS design

10. THE GRAVITY EXPLORER SATELLITE (GES)

Students: C.J.E. Dohmen, A. Fattahyani, F. Grondman, D.P. Houf, B.N. Kiyani, S.J. Lubbers, E.G.A. Orsel, E. Roorda, S.H.P. Vancraen

Project tutor: dr.ir. W. van der Wal

Coaches: ir. S. Engelen, ir. Z. Xu

10.1 Introduction

For a few decades, the Global Warming phenomenon and the associated melting of the ice in the Polar Regions have become a major concern for life on Earth and understanding the behaviour of these phenomena is of vital significance. In order to have a sense of how these phenomena function, measuring the change in the mass and gravity field of Earth is essential.

Although really important, understanding these phenomena is not the only advantage of measuring the gravity field of Earth; high accuracy geoid determination, which can be done by measuring the gravity field, will improve the orbit determination of satellites and provide a global unified reference system. Furthermore, the knowledge of Earth's gravity field can be used to improve recognizing the geodynamic processes occurring in the mantle.

Currently there are satellite systems monitoring the gravity changes; however these systems are known to be very expensive and they have a limited spatial and temporal resolution. Therefore, the mission statement is as follows:

''Providing data on temporal changes in Earth's gravity field for scientific use at low cost.''

This chapter elaborates on the project by first showing the design requirements in section 10.2. The concept design process is discussed in section 10.3. Thereafter, the final design is discussed in the detailed design description in section 10.4. The financial budget is presented in section 10.5. Finally, the conclusion and recommendations are shown in section 10.6.

10.2 Requirements

The requirements for this mission are divided into technical and non-technical requirements. The technical requirements are those that give an abstract demand that can be applied directly to the satellite system, whereas the non-technical requirements are more general.

Technical requirements

- The mission should yield observations of yearly transport at a spatial scale smaller than 1000 km.
- The measurement principle to be used is the tracking of navigation satellites.
- The error in centre of mass positioning due to inaccurate pointing of the satellite should be smaller than 1 cm.
- The error in centre of mass positioning due to Global Navigation Satellite System (GNSS) measurement noise should be smaller than 1 cm.
- The temporal changes of the Earth must be monitored by covering the entire Earth within a time frame of one month.

Non-technical requirements

- The minimum operational lifetime should be 3 years.

- The cost of the satellite mission should be as small as possible given the requirements.
- The mission should be eco-friendly and all parts of the satellite must burn up entirely within 25 years of the start of the mission.

10.3 Concept design process

The main focus for the concept generation is the payload, and the subsystems that support it. Therefore, the orbit characteristics and the attitude determination and control (ADC) system have been taken in to account for the concept generation. All the other subsystems will be designed according to the payload system as the payload system prevail these systems.

The payload, orbit, and ADC subsystems are considered on their own, and a small trade-off will disclose the most viable subsystem options. These options are given in table 10.1 and are integrated in a final trade-off. From that final trade-off one concept is chosen for the detailed design. The trade criteria for the final trade-off are accuracy, availability, complexity, cost, mass, power, and reliability. The payload with one dual-frequency GPS receiver and one accelerometer, and an orbit of 650 km altitude is the winner of the final trade-off.

Since the cost needs to be as low as possible, only commercial off-the-shelf (COTS) components are used, and it has been decided that no propulsion system will be used.

In order for the satellite to have a global coverage of Earth, it has to be put in a very high inclination so that its ground track covers almost the entire surface of the planet. The sun-synchronous orbit is able to provide this. The advantages of this orbit type are that it has a small eclipse time in a dawn-dusk orbit, the thermal and power subsystems design are easier, and it is a very popular orbit, therefore more launch options are possible.

The use of dual-frequency GNSS data transmission and reception is known as a useful tool for Precise Point Positioning (PPP). The dual-frequency receiver operates on both L1 and L2 frequency band, which enables good handling of ionospheric delays. When compared to the single-frequency alternative, this option is technically more enhanced and therefore more expensive.

For the ADC an integrated system is chosen, since all the components are located on one board. From several manufactures the ADC system of Berlin Space Technology iADCS-100 is selected, due to the high accuracy, and low mass and power consumption. This system contains 3 reaction wheels, 3 magnetotorquers, 1 star tracker, MEMS sensors, and 5 Sun sensors.

Table 10.1: Options for payload, orbit and ADC subsystems

Option	Description
Payload 1	1 x dual-frequency GNSS receiver + 1 x accelerometer
Payload 2	2 x single-frequency GNSS receiver + 2 x accelerometer
Orbit 1	500 km altitude, sun-synchronous
Orbit 2	650 km altitude, sun-synchronous
ADC 1	iADCS-100

10.4 Detailed design description

To show the results of the Gravity Explorer Satellite mission, this section elaborates on the detailed design.

Astrodynamic characteristics

The geometry and characteristics of the orbit of the satellite have an important effect on all the subsystems of the satellite, therefore these characteristics have to be carefully defined. This was the main reason to have another look at the orbit characteristics from the conceptual design. Now an iterative process is done with Satellite Toolkit (STK), a program which is often used by the space community. The coverage density is simulated for different altitudes, since a requirement for this mission is to have a full Earth coverage within a month. An altitude of 580 km is chosen, which results in an orbit decay of almost 9 km in the first 3 operation years and a time to deorbit of 22 years.

The satellites orbits in a circular, retrograde, dawn-dusk sun-synchronous orbit with an inclination of 97.73 degrees, and has a maximum eclipse time of 26 minutes.

Payload

The payload's main responsibility is tracking of GNSS satellites. The accuracy by which the payload is able to measure the exact position of GES is determined by its ability to overcome measurement errors, the largest of which is the ionospheric delay. A dual-frequency GNSS receiver, operating on both the L1 and L2 frequency band, enables formation of the ionosphere-free linear combination of L1 and L2 carrier phase measurements. This combination cancels the ionospheric delay almost completely.

Many COTS dual-frequency GNSS receivers deliver a carrier phase measurement accuracy in the order of millimeters and enable tracking of both the GPS and the GLONASS constellation. The challenge lies in selecting a receiver that complies with CubeSat sizes, yielding strict mass, dimensions and power limitations.

A trade-off between various COTS dual-frequency GNSS receivers points out that Septentrio's AsteRx-m receiver performs best in terms of power consumption versus tracking performance. This receiver is therefore selected to operate on GES. Extra study in the area of shielding the receiver from the harmful space environment needs to be carried out.

Selection of the accompanying antenna type is based on the following two arguments.

- The antenna should be able to track as many GNSS satellites as possible. This implies that the antenna's directivity must be maximized.
- Data rates in GNSS communication are relatively low. This allows the antenna gain to be relatively low.

Above-mentioned points lead to the conclusion that a simple patch antenna suits the mission best. Implementing a Low Noise Amplifier

(LNA) increases the link margin such that a highly tolerant link margin exists. Based on dimensions and mass, Antcom's G5-Ant-2AT1 antenna is selected to accompany the receiver. This antenna is a COTS antenna for military aircraft applications and its heavy and large casing, designed for aerodynamic and weather-protection purposes, can therefore be removed.

The precise position measurements and their derived accelerations still need filtering for non-relevant accelerations. Those involve accelerations caused by atmospheric drag, magnetic drag, internal vibrations and many more. An on-board accelerometer could provide data that enable proper identification and removal of the non-relevant accelerations. However, a detailed market study indicated that accelerometers with the required specifications fall far outside the financial budget of a low cost mission like GES. Recently developed techniques enable modelling of the disturbance accelerations instead of having to implement an on-board accelerometer, yielding a significant cost reduction. GES will be the first dynamic gravity dedicated mission to fly at extremely low cost.

Communication and data handling

The communication architecture is sized according to the on-board generated data. The amount of data that is generated by the payload subsystem is low hence the UHF frequency band for the downlink was selected as a low cost solution. In line with the aforementioned, the TU Delft ground station was chosen as the ground segment. With a proven track record with Delfi missions and low-cost operation the TU Delft ground station fully complies with the requirements and design philosophy. To increase the amount of data that can be send over the downlink a variable data rate is implemented; the data rate will increase with increasing elevation angle between satellite and ground station at constant link margin. This will almost triple the data volume as compared to a constant bitrate downlink. The use of COTS CubeSat certified components for transceiver, on-board computer and antenna's ensures reliable operation and easy integration within the satellite bus.

Thermal control

All subsystems have their own concerning temperature. The binding hot temperature limit comes from the ADC system, with a hot limit of 40 degrees. The binding cold temperature comes from the battery with a temperature of -10 degrees as the lowest temperature at which the system will work. For a satellite in a LEO there are four major heat sources; the Sun, the albedo effect, the infrared radiation of Earth and the internal heat of the satellite. Furthermore there is heating by free molecules. The heat leaving the satellite plates is determined to be the radiator heat.

After the iterative process for finding the most favourable coating for the satellite, the materials decided upon black (Chemglaze Z306) and white (Z-93C55) paint. The panels which are facing the Sun and pointing towards the Earth are painted white. All the other panels are painted black. The highest thermal expansion is experienced by panel 2, of 0.36 mm. This is an expansion of only 1.8 %, and will not be of critical importance to the mission. The extreme temperatures for the internal components are for the hot case 43.74°C and for the cold case during eclipse -3.70 °C. The minimum temperature the system reaches does not exceed the tolerance of any of the components.

The temperature critical part of the ADC system is expected to be the star tracker, which is aimed towards the stars and away from the sun. In the performance calculations it is assumed that the entire system will have one equal temperature, however, in reality the temperature will be varying throughout the system. Therefore it is safe to assume that the temperature of the star tracker will actually stay below 40 °C, as it is located away from the main heat source and looks into cold space. With this assumption the entire system will work with the given thermal control system.

Power

The power subsystem makes sure that the system is able to carry out its tasks during mission lifetime. From all the subsystems a power budget is made. The peak power is calculated with a safety margin of 15 % applied to the quiescent power, and a total of 5.68 W and 4.93 W

respectively are used by the satellite, with an average power of almost 3 W. For a 3 year Earth orbiting mission photovoltaic energy is the most suitable and cost efficient power source. Most commonly available solar cells for CubeSat missions are triple junction Galium Arsenide solar cells with an efficiency of 28.3 %. Solar cells from Clyde Space are selected here.

The 2U solar panel contains 5 cells in series, and it includes reverse bias protection diodes, which means that when a single cell fails the solar panel will keep functioning. A solar panel is body mounted to the front side of the satellite, which is fully facing the Sun. Also a panel is mounted on the bottom side, facing the Earth, making use of the albedo, where 3 cells are used for redundancy. To make sure that the system still has enough power for minimal operation when the satellite would turn, a single unit panel is mounted at the back. To provide power during eclipse times a battery is added to the satellite. The Lithium polymer battery of Clyde Space is chosen.

Structure and system integration

Before starting with selecting a suitable structure and configuring all sub-components, the size of the CubeSat needs to be determined. A 2U or 3U size is estimated with the advantages of the 3U size being that more interior space is available and the large exterior surface allows for larger solar panels. However, with the use of CATIA 3D design software, it is determined that a 2U structure has enough interior volume available. Less surface is available for solar panels, but the available power is still within margins.

A 2U ISIS structure is selected for GES. This chassis allows easy customization to its side-panels without harming the primary structure. The configuration of the interior and exterior is shown in figure 10.1 and table 10.2.

For the configuration special attention is spend on payload performance and the attitude of GES with respect to the Sun and Earth. The GNSS antenna is placed such that it is pointed towards GNSS satellites. The main solar panel is directed towards the Sun

while the start tracker is placed opposite to the sun to avoid blindness.

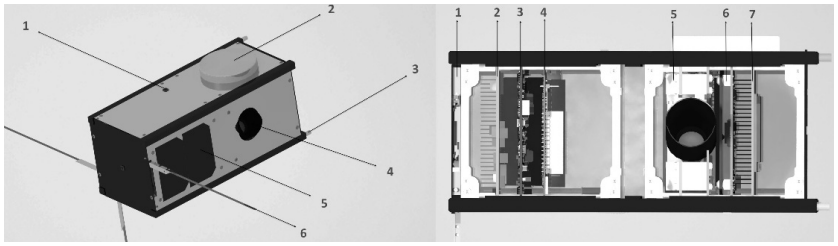

Figure 10.1: Exterior (left) and interior (right) configuration

Table 10.2: Indicated components

Indicated number	Interior	Exterior
1	VHF/UHF antenna	Sun sensor
2	VHF/VHF receiver	GNSS antenna
3	Electronic Power Unit	Kill switch
4	On Board Computer	Star tracker
5	AD&C system	Solar cells
6	Battery	VHF/UHF antenna
7	GNSS receiver	

10.5 Financial budget

Keeping the costs to a minimum has been a driving factor in the design of GES. The launch costs are reduced by opting for a piggy back launch and using a 3U deployer. The satellite being a 2U CubeSat, leaves room to share the costs with another 1U CubeSat mission. The launch costs are estimated to be 150,000 euros. The final cost of the satellite components is 100,000 euros. Being a student project and the advantage of scientific interest means free labour at the university can be utilized. The total cost remains an estimate.

A margin of 20% is added for unforeseen costs making the total cost of the satellite mission 300,000 euros. This includes all possible costs including launch, manufacturing and transportation. Comparable missions with the same objectives such as Grace-1, Grace-2 and GOCE cost 93, 327 and 350 million euros respectively. Therefore the entire GES mission costs less than 1% of missions that measure the long wavelength gravity field with comparable accuracy. Thus, the goal of

reducing costs as much as possible has been achieved. An overview of all the component cost is given in table 10.3.

Table 10.3: Financial budget

Component	Cost (Euro)
GNSS receiver	7,500
GNSS antenna	441
Integrated system	45,000
Sun sensors	7,000
Full duplex transceiver	8,500
Deployable antenna system	4,500
Onboard computer	4,300
White paint	662
Black paint	994
Battery (including heater)	1,214
Electrical power system	3,202
Body mounted 2U panel	3,312
Body mounted 2U panel	3,312
Body mounted 1U panel	1,914
2U structure	2,950
Total	94,801
Total component cost	100,000

10.6 Conclusion and recommendations

The GES can be classified as a low-cost mission that generates relevant science data with the same precision as existing missions, therefore expanding the spatial and temporal resolution at a fraction of the cost. Therefore, the satellite mission will contribute to a better understanding of climatological changes and variations on earth.

This is achieved by a 1.6 kg 2U CubeSat that is inserted into its dawn-dusk sun-synchronous orbit at 580 km altitude with a piggyback launch. The payload consists of a terrestrial dual-frequency GNSS receiver and antenna. Compared to earlier missions, the use of additional satellite navigation systems such as GLONASS and Galileo allows for a higher accuracy. A numerical model determines non-gravitational accelerations such that an accelerometer is eliminated to save cost and mass. The AD&C, C&DH and power supply are performed by a COTS integrated system, COTS on-board computer

and COTS solar panels and battery, respectively. Black and white coating paint will maintain the temperature within the satellite.
All requirements are met except for the achieved spatial scale, which is approximately 700 km less than required. The achieved spatial scale will still be better than any mission solely flying a GNSS receiver though.

The total mission cost is estimated to be 300,000 euros, several orders of magnitude less than forgoing gravity explorer missions. The Gravity Explorer Satellite mission is within university budget and could therefore contribute to both scientific knowledge and learning experiences.

There are some recommendations for improving the design that have been considered but due to time limitations could not be developed. For instance, the design could be improved with detailed calculations of the failure rates, manufacturing costs, disturbance torques, structural loads and the models used to determine the orbital characteristics and thermal system. The software applications on the mission have not been designed but needs to be investigated and implemented in the design.
Next to recommendations on the current design, some configuration possibilities that fall outside the current design concept were encountered.

Throughout the design process the requirement was to cover the Earth within a month. However, beneficial results of increasing the time resolution might be explored and implemented.

Assuming university budgets are in the order of 1 million euro, the financial budget is highly promising. The extremely low mission cost might allow for increasing the number of satellites to two or more to increase the coverage and performance.

The final design also offers two possibilities of integration with other missions: adding payload from other missions or adding the payload

to another mission. The size of the necessary components is so small that there is space left within the 2U CubeSat structure.

11. T-WRAX: VISUALISE WIND TURBINE WAKES WITH RADAR

Students: D. Bakker, M. Becker, R. v.d. Brandt, R. Corporaal, J. Janssen, J. Klein, L. Koomen, B. Omarali, D. Spengler, S. Walraet

Project tutor: dr.ir. W.A.A.M. Bierbooms

Coaches: J. Feng, MSc., dr. M.F. Motovilin

11.1 Introduction

When air passes through a wind turbine, energy is extracted from it. This creates a region of lower velocity and increased turbulence behind the wind turbine; the wake. This wake does not follow a straight line, but meanders. In a wind farm, the wake from one wind turbine can interfere with the wind turbines placed downstream of this turbine, which decreases their efficiency and increases the dynamic loads acting on them.

The goal of this project is to:

"track meandering of wake boundaries of a wind turbine during a considerable time period at on- and offshore wind farms, using a low-cost, stand-alone, durable and recyclable system."

The results from these measurements can be used to improve models for the behaviour of wind turbine wakes. These models can then be used to optimise the design and the control of wind farms, thereby increasing wind farm efficiency and decreasing the cost of wind energy.

11.2 Requirements

The top level requirement on the wake measurement system is that it must be able to make a scientific contribution to the knowledge on the behaviour of wind turbine wakes. This is the only actual requirement on the wake measurement system. There is, however, a list of design goals. This list describes an ideal system, although a system that does not meet all requirements can still make an important scientific contribution.

These design goals are:

- A measurement range of 500 m
- A resolution of 10 m in stream wise direction and 1 m perpendicular to the stream wise direction
- A sampling rate of 0.25 Hz (one measurement every 4 seconds)
- A continuous operation time of 12 hours
- An accuracy of 1 m
- A maximum allowed data loss of 5 %
- There are also some constraints on the system. Again, these constraints are design goals, not absolute constraints.
- The device should be able to operate on both onshore and offshore wind turbines
- The device should operate in a free-stream velocity range of 4 m/s to 25 m/s
- The device should preferably be mobile and applicable to other wind turbines or wind farms
- No modifications to or constructions on the wind turbine are allowed
- The device should have a lifetime of 10 years
- The device should be recyclable
- The device should be cheaper than existing measurement systems

11.3 Design concepts

After an extensive literature study, several promising measurement techniques were found that could be capable of meeting the design goals. After excluding the unfeasible design options from the list, five options remained that were analysed in further detail. An overview of each option is discussed.

Helikites with anemometers

A helikite is a kite that contains helium, thereby increasing its buoyancy. This design consists of a helikite connected to a ground station with a chord. The helikite moves around in the flow using control surfaces as well as by moving the ground station. It then measures the flow velocity and searches for the position where the boundary of the wake begins. 100 combinations of a helikite and a ground station are required to measure the complete wake. Advantages of this option are that the measurement technique is simple and straightforward, but this technique is relatively costly, polluting and risky. A helikite that breaks free inside a wind farm can damage wind turbines.

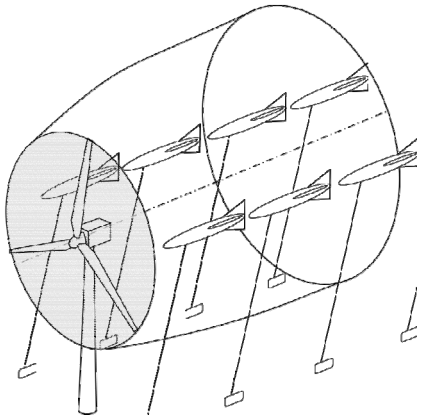

Figure 11.1: Sketch of the helikite measurement system

UAVs with anemometers

By flying a large amount of UAVs with anemometers around in the wake, a velocity field can constructed, from which the location of the wake can be determined. This system has the advantage over the

helikite system that it does not require ground stations, but flying a large group of UAVs is a risky task, especially inside a wind farm.

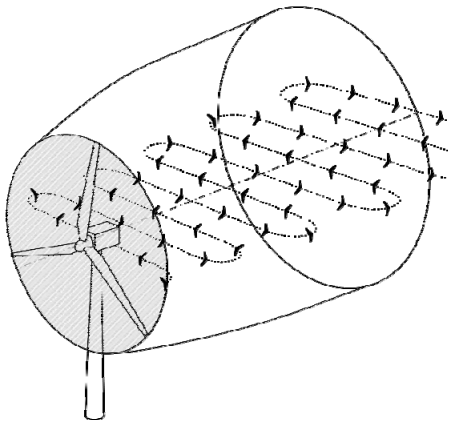

Figure 11.2: Sketch of the UAV measurement system

Acoustic tomography

Acoustic tomography reconstructs a flow field by having a sound source fly over a large amount of microphones. The propagation time of all the sound paths is used to reconstruct the flow field in between the sound source and the microphones, which can then be used to determine the location of the wake. This option is sustainable, does not consume much power and is relatively cheap, but is not a proven technology and found to be inaccurate. The large amount of microphones required on the ground could also give logistical issues.

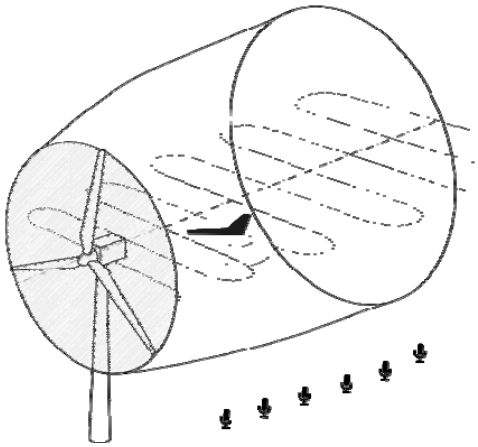

Figure 11.3: Sketch of the acoustic tomography system

Smoke imaging

Smoke imaging consists of a smoke generator placed on the wind turbine nacelle and cameras placed at some distance, looking at the wake. By analysing the images from the cameras, a flow field can be constructed, from which the location of the wake can be found. This is a relatively simple and cheap option, but the weight of the required smoke generators is high and a large amount of smoke fluid is required for 12 hours of operation. Inserting all this smoke into the environment is also not sustainable.

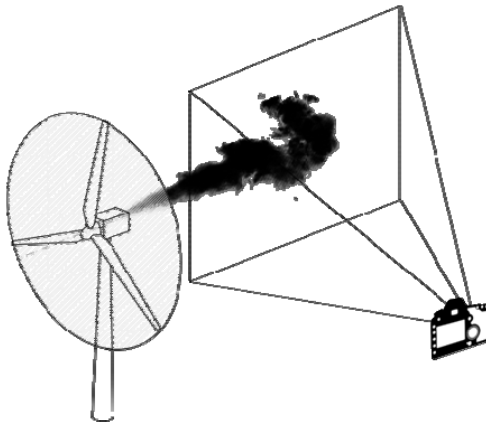

Figure 13.4: Sketch of the smoke imaging system

Radar

The proposed radar system is a radar placed on top of the wind turbine nacelle, looking at the wake of the wind turbine in the horizontal plane. The measurement result is a velocity field, from which the location of the wake can be determined. Radar was found to be a cheap, accurate and sustainable design option.

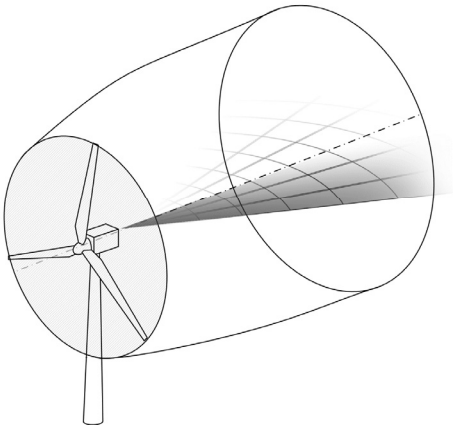

Figure 11.5: Sketch of the radar system.

System selection

These five design options were compared to each other in a trade-off to determine which option would give the best wind turbine wake measurement system. It was found that radar is the best option, since it is not only the cheapest option but also the option that would be able to meet most design goals within the given constraints.

11.4 Detailed design description

The selected radar system was designed in further detail. With this detailed design, a more accurate analysis can be made on the performance and characteristics of the radar system. The radar system is called T-WRAX, an acronym that stands for Turbine Wake Radar in X-band. The individual system components are discussed in further detail.

Overall radar design

The selected radar type is a frequency modulated continuous wave (FMCW) radar. This radar type continuously transmits a radar signal, while simultaneously receiving the echoes from objects in the path of the radar beam. The frequency of the transmitted signal is modulated to be able to determine the velocity of the wake. T-WRAX requires

some form of precipitation in the air to be able to perform measurements; measurements are not possible with clear air. T-WRAX was designed to be able to measure fog and any type of precipitation. This does, however, require a sensitive radar system. A separate transmitter and receiver antenna are used to meet this sensitivity requirement.

Electronic design

The electronic subsystem of the T-WRAX consists of commercially available radar components to decrease costs. Power for the T-WRAX is directly taken from the wind turbine where it is placed on. The T-WRAX also has a weather sensor built in to determine the current weather conditions. If the conditions are suitable for measurements, the T-WRAX will automatically start operation, allowing it to operate autonomously.

Mechanical design

The mechanical part of T-WRAX consists of a radome, a rotation system and legs to stabilise the system. The radome is a protective cover that is placed around the radar system. It protects the sensitive antennas and other radar components from the environment, but does let the radar signals pass through. For the radome, a composite sandwich material will be used. The rotation system accurately points the radar dishes in the correct direction and carries most of the weight of the radar system. The legs are used to be able to level the system if it is placed on an inclined surface.

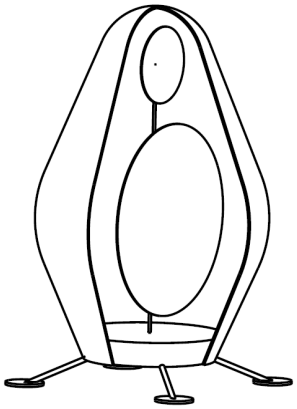

Figure 11.6: Overview of the T-WRAX design, with the radome cut open

Installation

As mentioned with the constraints, no modifications to the wind turbine are allowed. The mounting of T-WRAX on the nacelle must therefore be done in such a way that it can be fixed using the nacelle as it is. Two options are possible for doing this: If the turbine has a personnel platform, the radar system can simply be placed on this platform. If there is no platform present, the T-WRAX can be suspended under the nacelle: wind turbine nacelles have safety rails on which personnel can attach their safety cords. Since the T-WRAX weighs not much more than a heavy service engineer, it should be possible to suspend it by ropes under the nacelle.

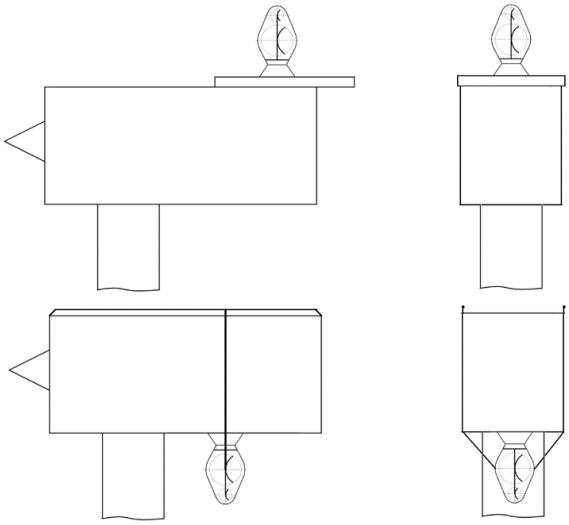

Figure 11.7: Mounting of the T-WRAX

Simulation

To verify that a radar system would be capable of determining the location of the wake boundaries, a simulation was written which models the flow field in the wake and how the radar system measures this flow field. With this simulation, it was found that T-WRAX will be able to fulfil its goal with the calculated system specifications, such as accuracy and resolution. In figure 11.8, the returned radar image is visible and the wake boundaries, as determined by the processing algorithms, are illustrated by the thin black lines.

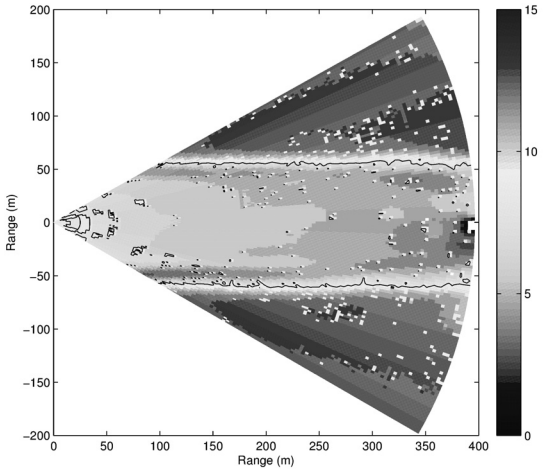

Figure 11.8: Simulation of T-WRAX performance

Design specifications

Using the detailed design of the T-WRAX system, an accurate estimation of the specifications and the performance of the T-WRAX can be made:

- System cost: € 25,000
- System weight: 132 kg
- Total power usage: 1.9 kW
- Radome height: 3 m
- Measurement range: 500 m
- Resolution at maximum range: 4 m
- Velocity resolution: 0.78 m/s
- Frequency band: 10 GHz, X-band

11.5 Conclusion and recommendations

The goal of this DSE project was to design a system that can measure the location of the boundaries of a wind turbine wake. The most important requirement is that the system can make a contribution to the scientific knowledge on wind turbine wakes and, from the analyses performed during this project, it can be concluded that this requirement is met. Most design goals are also met, exceptions are however the continuous measurement time, the accuracy, the

restriction of not placing devices on the wind turbine and the goal of making the complete system recyclable. Due to the dependency on fog or precipitation of the radar system, a continuous measurement time of 12 hours is not possible. Since the radar system is capable of operating autonomously, it is however easily possible to acquire a total time of measurement data of 12 hours. The goal of an accuracy of 1 metre is not met, but an accuracy of 4 metre is still sufficient for the validation of wind turbine wake models. The fact that T-WRAX has to be placed on top of the wind turbine nacelle is only a minor drawback since it can stay there for a long time, which makes the effort of getting it there and removing it again less problematic. A radar system requires advanced electronic components which sometimes contain special materials that are not recyclable. These materials are however used in very small amounts and, also considering the long lifetime of the system, the environmental impact of this should be minimal.

Besides those four goals that are not met, all other goals are met or even exceeded, with our stream wise resolution of 3.3 metres and our very low cost of €25,000. There is however still room for improvement. If the electronic subsystem uses more custom designed components, the cost for this subsystem can be brought down even further. The detailed design of the antennas is a complicated task: this should be performed using finite element methods to make sure that an efficient antenna design will be achieved. Real life measurements will also have to be performed to be able to fine-tune the noise filtering and other algorithms in the data processing. However, the design for T-WRAX as it currently is can already outperform competing measurement systems and techniques, with better specifications but especially with a significantly lower price. T-WRAX could be the start of big improvements in the wind energy market.

12. HIRES: YOUR EYE IN THE SKY

Students: B.J. Beckers, M.R. Haneveer, E.J. Hekma, J.B. van Ingen, D. Jiménez Lluva, D.J. Kok, A. Krikken, J.W. Lopes Barreto, P.Mesgari, L.Z.F. van Rossum

Project tutor: dr. A. Cervone

Coaches: ir. H. Khanbareh, T. Watts

12.1 Introduction

Due to recent events such as the crisis in Syria or Ukraine, there is an increasing need for visual intelligence. The best option for this is using Earth Observation satellites but since the Royal Netherlands Air Force (RNLAF) has no space asset of its own, it is completely reliant on European and North Atlantic Treaty Organization (NATO) partners. Given the structural shortage of military Earth Observation capacity within the partner nations, the RNLAF is investigating the possibility of acquiring its own independent space asset. The mission statement of this DSE is thus:

"To provide the Royal Netherlands Air Force with an independent resource to obtain Intelligence, Surveillance and Reconnaissance (ISR) information about any specific Earth location, from 2017 onwards".

The HIRES (Holland's Intelligence, Reconnaissance, and Earth Surveillance) concept developed in this project aims to provide the RNLAF with a low-cost, High-Resolution, small satellite system for Earth imaging, to be launched not later than 2017.

12.2 Requirements and constrains

The initial requirements provided by the RNLAF were the following:

- The total mass of the spacecraft at launch shall not exceed 200 kg
- The spacecraft shall be launched not later than Q4 2017
- The total cost (incl. design, assembly, testing, and launch) shall not exceed 15 M€
- The ground resolution of single images shall be 0.5 m or better
- The images shall cover an area of 1x1 km
- The image coordinates shall have an accuracy of at least 0.5 m
- The satellite shall be able to take strip search images with an area of 10x200 km
- The satellite shall provide global coverage
- The satellite shall have a lifetime of at least 3 years
- The satellite shall be disposed of no later than 25 years after End of Life

To meet the launch date requirement, additional requirements have been put on components used in the satellite design. All subsystem components must have a high technology readiness level, meaning that they have already been developed and tested by third parties. Furthermore, no ITAR restricted components can be used. ITAR (International Traffic in Arms Regulation) is a US law restricting the export of defence related products including many spacecraft components.

12.3 Conceptual design

The concept generation started by generating concepts based on three parameters: orbit, propulsion, and payload.

Orbit

For the orbit the maximum altitude was set on 650 km, based on the requirement of decay time. At this altitude the orbit will decay and the satellite will burn in the atmosphere in the time set, and therefore not end up as space debris. The first concepts where categorised in flying below 400 km, or between 400 and 650 km. Flying below 400 km greatly improves the performance of the imaging payload. The satellite does however encounter significant atmospheric drag at this altitude, which adds mass to the system for the required propulsion system to counteract orbit decay. Flying at higher altitudes reduces the need of a large propulsion system. The downside is that the imaging performance will decrease alongside, requiring a better camera to meet the requirements.

Propulsion

The need of a propulsion system is closely related to the orbit height. For the lower orbits, a continuous propulsion system is needed to counteract orbit decay and meet the required mission lifetime. The higher orbits only require a small non-continuous propulsion unit.

Payload

The imaging payload is the most important component for the performance of the satellite. The requirement on the imaging resolution was the most important factor of the design. As stated, the orbit height is directly related to imaging performance. Meeting the resolution requirements can be done of course by improving the camera. A second approach could be to use multiple cameras and use image processing techniques to achieve a single high resolution image.

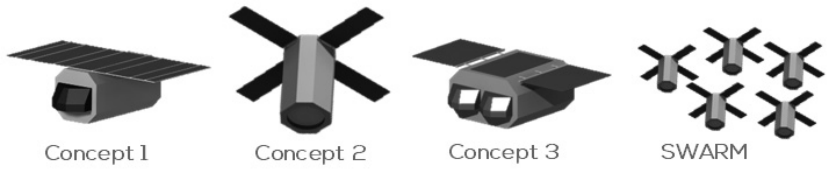

Figure 12.1: Design concepts

Concept generation and selection

Initially 24 concepts where generated, based on the three selected parameters. A preliminary trade-off based on qualitative observations was done to reduce the number to three potential concepts. Concept 1 features a single payload flying at a very low altitude and to compensate for the tremendous atmospheric drag, it has continuous electric propulsion. Concept 2 has a single powerful payload, taking pictures from 600 km altitude, and a simple propulsion unit. Concept 3 has two light cameras working together at an altitude of around 600 km and has a small propulsion unit. Alongside, a fourth concept was investigated: a swarm of nano-satellites. The great performance possibilities and highly innovative character made formation flying an interesting subject to investigate. Since a swarm is unfeasible for this project in terms of cost and development time, it was performed as a study of interesting rather than a potential candidate to give a more innovative insight to this project. After a quantitative and qualitative trade-off, Concept 3 was chosen because of its high performance, innovative character and it stayed within mass, power and cost budgets.

12.4 Detailed design

Astrodynamics

An important consideration for the orbit determination is the time it takes for the satellite's imager to cover the entire Earth in sunlight conditions. It is preferred to keep this global coverage time constant, to ensure a quick response time of the satellite at all times. A Sun-synchronous orbit can help achieve this, since it provides similar lighting conditions for every orbit throughout a year. An important consideration regarding the Sun-synchronous orbit is that for every altitude there is a corresponding inclination and vice versa.

An important sustainability concern is that the satellite must be disposed not later than 25 years after end of life, to avoid space debris from accumulating in space. This restricts the orbit altitude to less than 650 km altitude, which ensures the spacecraft will gradually decay due to atmospheric drag. At an orbit altitude between 450 and

550 km the spacecraft will be in an Earth repeat orbit, limiting the ground coverage of the spacecraft. Taking this, together with the payload performance, into consideration, an optimal orbit altitude of 565 km was found. The inclination is 97.57°, directly following from the altitude-inclination relationship in a Sun-synchronous orbit.

Another important factor is the local time ascending node. This is the local time at which the satellite passes the equator from South to North. It will determine the lighting conditions on ground seen by the spacecraft. During the winter, the areas near the poles will only receive sunlight for a few hours per day at most. The decision was made to optimise for the Northern hemisphere, since there is more area of interest in the Northern hemisphere as compared to the Southern hemisphere. Taking this into account, a local time ascending node of 13:00 was selected.

Payload

HIRES uses two identical imaging payloads combined with an image enhancement technique to provide panchromatic images with a ground resolution between 0.5 m and 0.9 m. The payloads, called Neptune, are designed and built by Elbit Systems, an Israel based company, and achieve 0.9 m resolution each. Neptune is a push-broom scanner, meaning it scans the Earth pixel-line per pixel-line, as opposed to cameras found in everyday life. The Neptune payload has been space proven on two satellites, Eros-B and Ofeq-9, and due to its country of origin is free of any ITAR-restrictions. As the spacecraft is orientated in the flight direction, mirrors are used.

The uniqueness of HIRES lies in using an image enhancement technique called super resolution. Super resolution is a post-imaging processing technique using data interlacing and interpolation of multiple images to achieve image resolution enhancement. Used on the SPOT-5 satellite since 2002, this technique is capable of enhancing the image resolution of a single payload (0.9 m) to a high-quality image with 0.5 m resolution. Basically, the two payloads are calibrated to nanometre level such that they take image samples with

an offset of 0.5 m in both the lateral and axial direction with respect to each other.

Once these images have been transmitted to Earth, interlacing of the samples and interpolation of intermediate data points result in an overall resolution of 0.5 m. Even though this technique has only been used and proven on one satellite so far, its potential enables HIRES to be much lighter and cost-efficient when compared to conventional Earth observation satellites. Theoretically, a magnification factor of 2.0 can be achieved, however due to inevitable jitter, thermal expansion in the calibration system, and assembly and calibration offsets, a magnification factor of 1.8 is assumed for the design. A visualisation of the super resolution technique is presented in figure 12.2.

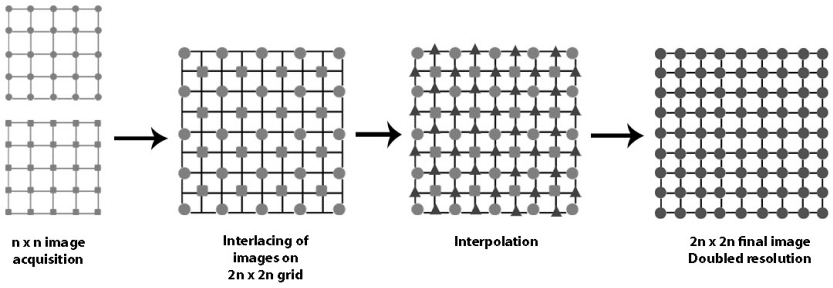

Figure 12.2: The super resolution principle

The aforementioned resolutions of 0.5 m and 0.9 m can be achieved in a total of five different imaging modes. Calibration of the system and the accompanying super resolution technique result in the possibility to achieve 0.5 m resolution 1 km x 1 km images, or strip searches of 8.9 km x 200 km. The calibration system can also be used to offset the payloads in such a manner that HIRES can produce 0.9 m resolution images of two different locations at the same time. Additionally, the imagers can be calibrated pointing next to each other and generate 17.8 km x 200 km wide view strip searches. The final imaging mode is capable of detection both velocity and direction. The imagers take pictures of the same area a few (~2-6) seconds apart. Analysis of both images can indicate magnitude and direction of object velocities.

Communications subsystem

When images are taken, they have to be transmitted to Earth. This will be done using a ground station in Vardø, Norway. Additionally, units in the field can use mobile (portable) ground stations to downlink images of their location as soon as they are made by the spacecraft above them.

Transmitting data to and from the spacecraft will be done using the X-band and S-band frequencies. The X-band will be used for sending the images, since this frequency band allows for the highest data rate. An X-band transmitter together with a horn antenna positioned on an antenna pointing mechanism will be used. Every day, 12,500 km^2 can be transmitted to the ground station in Vardø.

The S-band transmitter and receiver will be used for sending and receiving telemetry and commands. The spacecraft is equipped with two S-band patch antennas: one pointing nadir, the other zenith. By using this configuration, it was made sure that the spacecraft can always receive commands, even if it is in safe mode or tumbling. Both systems can perform each other's tasks in case one breaks down, although a malfunction in the X-band would severely limit the daily downlink budget.

ADCS

It was chosen to use reaction wheels, made by Clyde Space, as the primary ADCS actuators. These can provide a maximum torque of 0.04 Nm and a maximum momentum storage capability of 1.2 Nms. Three magnetotorquers are installed for momentum dumping, each pointing in one of the three body axis of the spacecraft. This will be done during eclipse.

As ADCS sensors, two star trackers are installed, with an accuracy of 1 arcsec. To cover the period of blinding, an Internal Measurement Unit (IMU) is installed. This IMU enables the spacecraft to determine its attitude even when star trackers cannot be used. Further, star trackers need a rough estimation of the attitude as input. This will be

provided by six sun sensors. The designed ADCS system is capable of determining the ground location coordinates with 3 m accuracy.

Propulsion unit

Atmospheric drag at 565 km altitude is low enough to fulfil the three-year lifetime requirement before the satellite reaches re-entry. However, it was decided to include a small and light resistojet propulsion unit to maintain the orbit at 565 km for the whole lifetime duration. This because there are certain altitude regions where the satellite would experience an Earth repeat orbit, which means that some locations on Earth cannot be photographed. Moreover, the Dnepr launcher has an orbit injection inaccuracy of 4 km altitude and 0.04° inclination, which the resistojet also need to correct for. The total required ΔV is 43.4 m/s ΔV. It should be noted that the propulsion system is sized for maximum solar activity for safety purposes. If solar activity is closer to average levels, drag would be less than half and the lifetime would be more than double.

The chosen resistojet is manufactured by Alta and allows for the use of different propellants as well as thrust settings. It was chosen to use the noble gas Argon as propellant for sustainability reasons as it is non-toxic and less reactive than other options such as hydrazine. The chosen thrust setting is 100 mN with a specific impulse of 110 s and this leads to a required propellant mass of 10.34 kg, which will be stored in an Aluminium 7075 T-6 tank. Moreover, there is a second resistojet for redundancy. These thrusters will be fired for five orbits every two weeks to account for orbit decay.

Power control subsystem

The HIRES satellite requires an average power of 167 W, generated using photovoltaic cells. It features one large body mounted solar array accompanied by two smaller deployed fixed arrays. These smaller arrays are stowed during launch, reducing the satellite's size at launch. Combined, these arrays have an effective area of 1.85 m2. The triple junction solar cells used have a laboratory efficiency of 30%. Including inherent and lifetime degradations, the maximum, or peak, output power of the solar arrays at end of life adds up to 540 W. This

allows charging of the onboard li-ion batteries for use during eclipse and peak power loading. Given the criticality of the power subsystem, the entire system is dual redundant and provides protection against electromagnetic interference.

Thermal control subsystem

Thermal control is in essence an energy management problem, in which the heat flux in and out need to be balanced. The spacecraft will be operating in the space environment where the residual atmospheric pressure results in a drag that is non-negligible, atmospheric heating can be safely ignored. The spacecraft does receive external heat from the Sun directly, from albedo radiation (Sunlight reflected on the Earth) and from infrared emissions from the Earth. Next to that the instruments on board generate heat as well during normal operations.

To keep the temperature within the ranges for the other subsystem, typically between 0 and 40 degree Celsius, a thermal control subsystem is needed. Using a MATLAB/SIMULINK model, an estimation of the temperature ranges was made. From this analysis a passive thermal subsystem was derived. This means that the spacecraft is covered in multi-layer insulation, some sort of blanket. The inside of the spacecraft is coated black to facilitate conduction and radiation between components. Using this thermal control the estimates of the temperature ranges between 17 and 37 degree Celsius. Locally temperatures are expected to be more extreme but further simulations should determine whether this is a problem. The mass of the thermal subsystem is around 5 kg.

Structure

The primary structure of the spacecraft is designed to meet the requirements on the points of loading, natural frequency, and deformation. The launch is the critical phase on all three points. The launch requirements are therefore leading for the structural design. Finite element method was used to size and analyse the spacecraft structure. As final design the structure is developed as a truss structure. The advantages of using a truss structure are the minimal

mass and volume that can be achieved in comparison with other structural configurations like a monocoque or semi-monocoque shell. The truss structure consists of rods made out of Al-7075-T6. This is a conventional material with the advantages of being space proven many times, low cost, and a very high strength-to-weight ratio. The structure needs additional stiffening to meet the launch requirements on natural frequency and limit the deformations. To improve stiffness side panels are implemented in the design. These panels are also used for mounting of the subsystems to the spacecraft bus. Aluminium honeycomb is used for these side panels because of the great strength-to-weight ratio, cost, and machinability.

Configuration

The spacecraft configuration depends on five factors: the subsystems requirements, launcher envelope, accessibility, prodicability, and structural integrity. The payload of HIRES consists of two large cylindrical cameras. To operate them correctly the cameras need to be placed parallel to each other. This defines the outer shape to a large extend. To have the volume, strength, and producibility optimized the bus is given an octagonal shape.

Every subsystem has specific requirements for the placement in the bus. The two deployed-fixed and one mounted solar panel are placed on top to power the spacecraft. Additional solar panels are placed at the side as emergency back-up. The resistojets are placed at the back to propel for orbit maintenance. The reaction wheels that keep the spacecraft stable are placed in the middle of the bus, one for each axis. An exploded view of the spacecraft configuration with all subsystems, except thermal insulation, is displayed in figure 12.3.

Launch and orbital operations support

HIRES will be launched on the Russian Dnepr launch vehicle, a converted ICBM from the Soviet Union. It is one of the cheapest launch services available in the world (around €8 million) and has no ITAR related issues. Moreover, the Indian PSLV is selected as the secondary back-up launcher. Both launchers have additional volume in their fairing for potential secondary payloads, which could

drastically reduce launch costs. HIRES's structure is designed such that it can sustain the launch loads induced by both launchers, resulting in fast transition time between launchers.

Once HIRES is in orbit, it has to communicate with the RNLAF, where obviously it is preferred to have the largest access time as possible. First, a location with a high latitude was selected. Within the MILSPACE agreement between The Netherlands and Norway, it is proposed to build a project dedicated ground segment in Vardø, Norway. However, at this location there would be an eight hour period per day where there would be no communication access with the spacecraft. Therefore, an additional proposition is to also use the commercial ground station in Inuvik, Canada. Using those two ground stations, HIRES can be reached each orbit. Moreover, mobile ground stations are taken into account as well. The most suitable mobile ground stations are manufactured by Rockwell Collins, which are the SWE-DISH CCT120 and CCT200. These light-weight antennae can be carried around with paratroopers and are deployable within ten minutes.

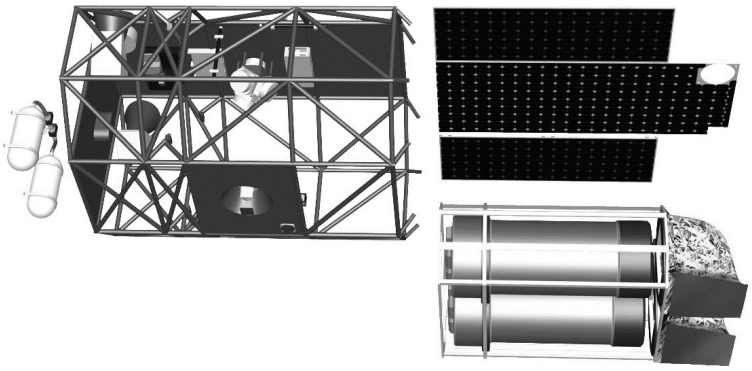

Figure 12.3: Exploded View Spacecraft Configuration

12.5 Conclusions and recommendations

Returning to the project mission statement: 'Providing the Royal Netherlands Air Force with an independent resource to obtain Intelligence, Surveillance and Reconnaissance (ISR) information about any specific Earth location, from 2017 onwards.' This goal is

successfully achieved by DSE group S2 in a phase 0/A study during eleven weeks.

The design process began with an elaboration on the requirements and functions provided by the RNLAF. Several concepts to fulfil the customer needs were generated and after several trade-offs, based both on qualitative observations and preliminary sizing, the most feasible concept was selected. This final concept was worked out further in more detail and incorporates a dual payload, a small propulsion unit, and a relatively high LEO orbit.

The heart of HIRES are the two imaging payloads. These can continuously scan a swath width of 8.9 km with a resolution of 0.9 m. The superresolution technique allows for combining the images of these two payloads into a single picture with a higher resolution to meet the requirement of 0.5 m.

Table 12.1: Main Characteristics of the HIRES Satellite

Orbit	565 km, SSO, 13:00 LTAN
Inclination	97.7 °
Orbital period	95 min
Mass	224 kg
Design lifetime	3-6 years
Average power	175 W
Resolution	0.5 m
Maximum image size	200x8.9 km
Coordinate accuracy	2 m
Data storage	512 GB
equivalent to	100 000 km2
Downlink capacity per day	75 GB
Cost	€23M-€26M

Recommendations

At this stage, the design is already quite far. Continuing HIRES means an in-depth design is to be made. This includes all subsystems of the satellite. To meet the schedule requirements there are several recommendations. It is recommended to start inquiring quotations on

the off-the-shelf components as soon as possible, especially for the payload. Furthermore, contract with the launch services is recommended to commence as soon as possible with establishing launch agreements, pricing, specific launch date(s), and more detailed launch integration and support. For the communication with HIRES frequency bands have to be allocated by the International Telecommunication Union. The formal procedure usually takes more than one year. It is therefore recommended to start the procedure directly.

A method of lowering the cost of the satellite is dual use of the available images. Selling the images commercially has economic advantages, but also allows use of commercial ground stations that can greatly increase the downlink capacity of the satellite. If selling images commercially is not an option, the use of the images by non-military government agencies could be investigated.

Swarm

In the near future, it will be possible to make a swarm of nano-satellites that work together. Making use of superresolution, this swarm could produce images with a very high ground resolution. However, this concept is still has a very low Technology Readiness Level (TRL). This implies that the time needed for development, integration, and testing is long. For this specific mission with the requirements on the launch date, this concept was seen as unrealistic. However, if there is more time available for research and development, this concept can be potentially very attractive.

13. ASAP UAV – MAKING THE SAE A SAFER PLACE

Students: D. van den Bergen, T. Blondeel, B. Durieux, D.N.E. Maxence, J.M. van Mourik Broekman, T.J.E. Schouten, S. Vial, R.S. de Wit, M. Wolken, N.J. van Wonderen

Project tutor: prof.dr. Th. Dingemans

Coaches: ir. J.A. Melkert, dr. D. Zarouchas

13.1 Introduction

In 2013, the Royal Dutch Sea Rescue Institution (KNRM) performed approximately 2000 search and rescue missions without the use of UAVs. The total costs totalled 15 million euros. A lot of research was done with respect to Unmanned Aerial Vehicles (UAV) applicable to Search and Rescue (SAR) missions, reducing the need for expensive helicopters. This will drastically reduce the costs for SAR missions and may improve the speed and efficiency with which victims can be located. In addition, these UAVs could be placed on many different types of ships, making it possible for the UAV to reach the victim's location within seconds.

A different drastic trend is the use and application of polymers in the aerospace industry for low weight solutions. Polymers are becoming multifunctional, making it possible to have electric circuits, light sources or even actuators made entirely of polymer. Therefore it is an interesting practice to design an all-polymer UAV for SAR missions.

Not before long, a working title was adapted that captured the entire scope of the project. The Autonomous Search, All-Polymer UAV, or ASAP UAV.

13.2 Mission objectives and requirements

Combining the challenges posed in the previous section resulted in the following mission statement:

"Design a concept for an all-polymer, biodegradable and autonomous UAV, deployable from ship, which locates a person in sea in any weather conditions and transfers its location to its remote command centre."

The mission of the UAV is to take off from a ship under all-weather conditions and search for a victim at sea. When a victim is found, the UAV must be able to hover over the victim or fly slow circles in the vicinity of the victim. If the UAV is lost at sea, it must be completely safe to the environment.

The initial endurance requirement was a mission endurance of minimum two hours. After consultation with the KNRM, this duration was increased to three hours as that is the maximum time the KNRM searches for victims at the North Sea.

The most important requirements are:

- 3 hour mission endurance.
- Unmanned aircraft for day and night operations.
- Operational at 7 Beaufort continuous wind with gusts up to 9 Beaufort.
- The UAV must have (limited) hover capabilities.
- The maximum non-polymer content in the construction is 5%, including the propulsive system.
- The UAV must be safe to operate autonomously, therefore it should have a See and Avoid system.
- The UAV must be safely disposable, both when intentionally being disposed and after a crash.

- The UAV must provide a stable live video connection with both visual and thermal optic cameras.

13.3 Design considerations

The killer requirements are considered to be the mission duration, polymer content and the all-weather operations. In order to be able to fly for three hours, the mass fraction of the energy storage needs to be as high as possible. The only way to achieve the 95% polymer content of the structure is by using a polymer based energy storage. Therefore, polymer based lithium-ion batteries are the only viable options.

Being operable in all-weather conditions means that temperatures can be both well below freezing point and tropical heat. The structural materials should be able to withstand these temperature extremes. However, all weather also implies that hail and rain are possible, meaning that the fuselage must be both impact and water resistant.
Strong winds are of little concern as long as the wind speed is stable. Wind gusts however, are unpredictable and lead to flight path deviations which may cause the imaging system to lose focus. The ability to cope with the windy conditions translates in the requirement to be irresponsive to gusts. This gust irresponsiveness means that the UAV should possess near neutral flight stability as it should not be an unstable aircraft but be as close to neutral stable as possible. Complementary, the design should be as compact as possible, reducing the total surface that can be affected by wind gusts.

13.4 Design options

Multiple designs have been considered which are divided among four distinct groups:

- Fixed wing aircraft
- Rotorcraft
- Lighter than air
- Hybrid

Lighter than air vehicles are considered as non-plausible as these types of aircraft are typically very responsive to wind gusts and generally cannot fly in the desired speed regime. The rotorcraft options were discarded as well. Despite of their versatility, rotorcraft cannot achieve the desired endurance at the required flight speeds. Finally, some hybrid configurations have been considered but were discarded eventually. These hybrids can consist of a rotor-propeller combination, have movable wings, motors or simply rely on a strong propeller that can act as a lift generating rotor as well. All these options have been investigated but were considered as too complex to design and too cumbersome to operate.

A wide variety of the so called 'straw man concepts' were generated and three of these concepts were further developed. A Prandtl-wing configuration, a conventional fixed wing aircraft and a flying wing with a small vertical stabilizer.

The Prandtl-wing, or box-wing, aircraft has a very low induced drag due to the shape of the wing. It has a fuselage providing a large storage area for payload and batteries. As the wing itself is less efficient due to interaction between the front and rear parts of the wing, it requires more wing surface compared to other designs. The box-wing is a compact design and therefore gust irresponsive as desired. The wings however, are relatively thin and thus fragile.

The conventional aircraft, like the box-wing configuration, has a fuselage providing the storage capacity but also relative long wings. The long wings make the design vulnerable and more responsive to gust. Furthermore the tail is considered to be a vulnerable part of the design.

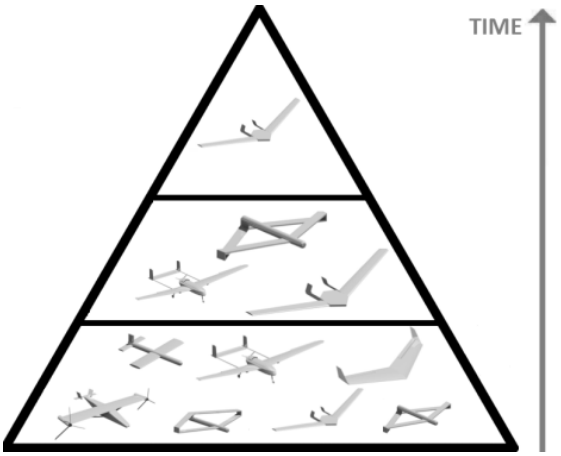

Figure 13.1: Configuration selection of the ASAP UAV

The flying wing has the least surface area of the three designs. Therefore it has the lowest parasitic drag, which is desirable for a long endurance and a high cruise velocity. The lack of a fuselage for storage area is compensated with thicker wings that provide the required storage volume.

The three remaining designs are assessed based on their inherited performance and layout characteristics. A final design trade-off is performed based on this assessment. The flying wing has the best performance on the most critical aspects. Hence, the flying wing with vertical tail was chosen as the layout for the ASAP UAV.

13.5 Operations

The KNRM performs over 2000 missions per year with a maximum duration of three hours. Therefore it is safe to assume that the UAV is to perform a mission on a daily basis with an average endurance of two hours.

In order to further analyse the required performance of the ASAP UAV, the mission is analysed. When the need arises, the KNRM sets sail into the sea, towards the last known location of the victim. During the cruise on the ship, the last known location of the victim is sent to

the flight computer of the UAV. Also, the actual meteorological information is gathered by the UAV that is on standby at the ship.
When the search starts, the UAV is mounted onto a catapult that accelerates the UAV with 5.1g over a length of 4 meters. This results in a launch speed of 22 m/s. Immediately after the launch, the UAV climbs to its cruise height between 50 m and 150 m, above the altitude of possible kite surfers and below the minimum altitude for other air traffic.

Based on the wind and possible leeway, an optimal search pattern is calculated and the UAV starts scanning for a victim. The maximum distance from the ship where the UAV operates is limited by the line of sight required for the live video connection. At an altitude of 150 m, the UAV has an operational range of 45 kilometres, that decreases to 25 kilometres at an altitude of 50 m.

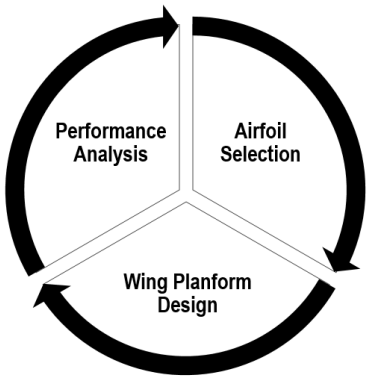

Figure 13.2: Illustration of the design iterations

The sea is scanned with both visual and thermal imaging equipment. When a computer algorithm detects an abnormality in the image, an operator is alerted. The operator can identify the victim. Now the UAV starts the station keeping modus. Here, depending on the wind speed, the UAV either flies slow circles above the victim, or when the wind speed is above the UAV's endurance velocity, it trims out for a flight speed matching the wind so it has zero ground velocity. During the station keeping modus, the UAV signals the victim with strong LEDs that the victim has been detected. When the victim is rescued,

the UAV performs a belly landing at the water surface, where it is picked up by a vessel.

Like the station keeping modus, the landing impact depends on the wind. Without wind, the landing speed is equal to the stall speed. With heavy wind, the UAV can land with hardly any ground velocity.

13.6 Performance

In order to find a victim as fast as possible, one wants the cruise speed of the UAV to be as high as possible. Contrary, during the station keeping modus and for launch stability, the minimum airspeed should be as low as possible. This leads to a contradiction in the design as these two aspects are mutual exclusive. A high cruise speed leads to a high stall speed. However, the high cruise speed is considered far more important than the stall speed, as long as the UAV can be launched safely.

The design is thus focused on a high cruise speed, and a minimum gust responsiveness, while the endurance constraint of three hours must not be violated. Gust responsiveness is quantified by a relation that expresses the vertical acceleration of an aircraft in terms of aspect ratio and wing loading, where the latter one is the dominant factor. Higher wing loadings have a positive effect on the gust responsiveness.

Hence, with a UAV target weight of 10 kg, based on a first order weight estimation, the highest possible wing loading is chosen such that the minimum flight speed constraint is not violated. Next, the lowest possible aspect ratio is chosen that allows for an endurance of three hours. As both aspect ratio and wing loading influence the endurance, but wing loading is dominant for gust responsiveness, it is better to have a higher wing loading with a high aspect ratio than the other way around. Also, a moderate amount of wing sweep is applied in order to provide some distance between the control surfaces and the centre of gravity.

After several parameter selection iterations, the high wing loading turned out to lower the total volume in the wing to such an extent that there could be no batteries stored in the UAV. Hence, the wing loading is reduced, the aspect ratio decreased and taper is applied. All these measures contributed to sufficient internal wing volume that allows for battery placement in the wings.

In order to make sure the flying wing design is controllable without a tail, a so called 'reflex aerofoil' is required. Several of these aerofoils have been selected but finally the MH81 aerofoil was selected. It offers the best stall characteristics with the required moment coefficient curve while maintaining near neutral properties. Furthermore, with a thickness of 13% of its chord, it offers the most internal volume of all inspected aerofoils.

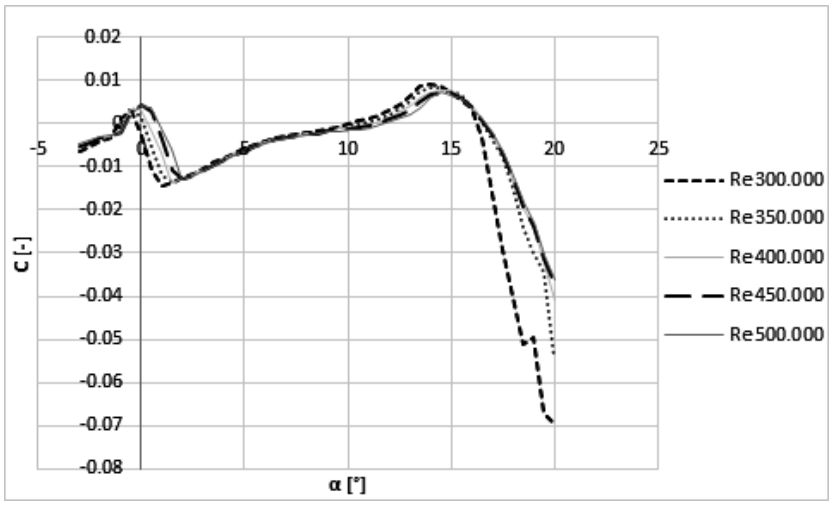

Figure 13.3: C_m-α curves of the MH-81 aerofoil at typical Reynolds numbers

13.7 Materials and structure

One of the requirements on the UAV is that it must not pose a danger to the environment after a crash. This implies that the UAV's structure must be completely biodegradable. Additionally, to further decrease the resource demand of the UAV, its shell material should also be bio-based.

Several polymers have been analysed but the Poly-lactic Acid (PLA) and its derivatives seemed to be the most promising. As the PLA derivatives generally do not differ much in structural performance and PLA has been tested extensively, PLA is chosen as core material for the structure.

Standard PLA has a Young's modulus of 3.5 GPa and a maximum tensile stress of 60 MPa. Considering a monocoque structure with a constant thickness, the wings show vibrations at a frequency of roughly 30 Hz. These vibrations cause fatigue in the structure causing it to fail at a significant lower stress. Furthermore, the glass transition temperature of pure PLA is within the UAV's operating regime.
In order to improve the structural properties of the PLA, it has to be reinforced. This can be done by either using a sandwich construction or incorporate fibres in the PLA resin. The sandwich is unfavourable as it is difficult to manufacture. Hence, as long as the structural loads allow for a fibre reinforced polymer, a sandwich construction is avoided.

There are multiple options for bio-fibres where flax, natural bamboo and viscose have been considered. Flax was chosen for its superior mechanical properties and it is widely tested and available.

A polymer can be reinforced by either matrices of continuous fibres or pre-mixed chopped fibres. The latter is easier to manufacture as injection moulding techniques are applicable for manufacturing. The maximum fibre length for injection moulding is 2 mm, this length is also the minimum allowed skin thickness for regular injection moulding. The resulting PLA-flax composite has a maximum stress of 56 MPa, which is slightly less than that of pure PLA, however, its resistance against creep and fatigue is better. Considering the wing vibration of 30 Hz, the maximum allowable stress is 12.5 MPa at the end of its lifespan.

A stress analysis was performed for multiple scenarios, where the take-off phase turned out to be the most critical one. Using the thickness of 2 mm, the maximum stress during cruise flights occurs

near the root of the wing and is 1.5 MPa, where during take-off the stress peaks at 3.9 MPa. When the skin thickness varies from 1.2 mm at the tip of the wing, to 2 mm at the root, the UAV can withstand hail impact of hailstones with a diameter of 51 mm and the maximum wing tip deflection during cruise flight of slightly over 4mm.

As polymers and composites tend to absorb water which causes its mechanical properties to deteriorate, the UAV has to be coated with a water repellant. One such coating was found which acts as a super hydrophobic layer. It is applicable on polymers and because of its hydrophobic characteristics, it helps to prevent icing on the wing.

13.8 Lay-out

Combining the results of the structural and aerodynamic analysis, the final planform parameters are deducted. The batteries are mainly stored in the wings, where the applied wing taper makes sure the majority of the batteries can be placed near the leading edge of the wing, pushing the centre of gravity forward and causing bending relief on the wing. The total mass of the UAV is 9.5 kg, where the battery weight accounts for 60% of the total weight.

Table 13.1: ASAP UAV design parameters

	Parameter	Value	Unit
Planform			
Aspect ratio	AR	8	-
Leading edge sweep	Λ_{LE}	15	deg
Taper ratio	λ	0.25	-
Twist angle (tip)	ε_{tip}	-2	deg
Incidence angle	i_w	1	deg
Dihedral	Γ	0	deg
Span	b	1.602	m
Mean chord	c_{mean}	0.2	m
Wing surface area	S	0.321	M^2
Speeds			
Minimum speed	V_{min}	18.4	m/s
Endurance speed	$V_{endurance}$	22.2	m/s
Max range speed	V_{range}	29.2	m/s
Maximum speed	V_{max}	40.2	m/s
Performance and Power			

Wing loading	W/S	275	N/m^2
Power for V_{range}	P_{Vrange}	254	W
Maximum endurance	$H_{Vendurance}$	225	min
Endurance for V_{range}	H_{Vrange}	180	min
Oswald span efficiency factor	e	0.9	-
Glide ratio	$(L/D)_{max}$	20.123	-
Profile drag coefficient	C_{D0}	0.014	-
Maximum lift coefficient	C_{Lmax}	1.421	-

Both the taper ratio and wing sweep are applied to increase the distance between the centre of gravity and the aerodynamic centre. However, these measures increase the chance of wing tip stall. In order to prevent tip stall happening, a small negative twist angle is applied.

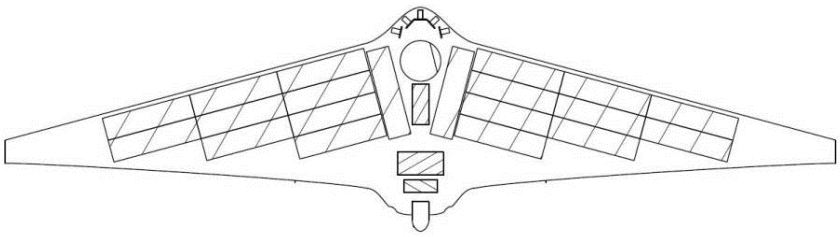

Figure 13.4: Wing platform and internal lay-out

13.9 Life cycle

The safety of the UAV is related to its reliability. Failure of critical components can cause the UAV to crash and potentially endanger its environment. To improve the reliability of the UAV, some critical components are deployed as duplex strings. By constructing a redundant servo system and equipping duplex flight computers and motor controllers, the expected mean time between failure is boosted from 900 hours to over 2,200 hours. Hence, the chance of a crash is 1 in every 1,100 missions.

As some parts of the UAV are subjected to damage and wear, a maintenance schedule is implemented. Four distinct categories are considered. Post flight inspections are performed by the UAV operator, who has to make sure the UAV is intact. There are

scheduled maintenance and repair activities which are performed by a trained mechanic. These activities are continuously ongoing and the UAV is taken out of operations for the duration of the maintenance. There is a scheduled replacement of parts that have a limited lifespan like the fuselage. Additionally, a scheduled flight envelope test is performed in order to verify the functioning of all subsystems.

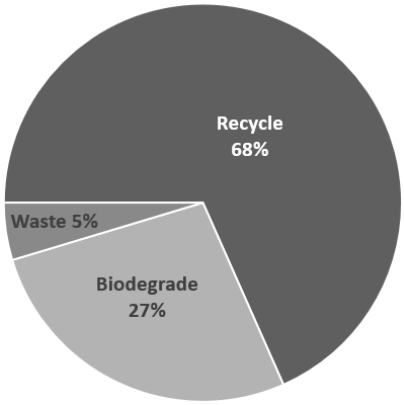

Figure 13.5: Mass fractions at the end of life of the UAV

As all components of the UAV are replaceable, it has no set lifespan. During an operational period of two years with daily missions, the batteries have been replaced twice, and the skin and servos as much as seven times.

Taking all the maintenance and replacement into account, only 5% of the materials used on the UAV is to be treated as waste. If the UAV might crash, the polymer skin will completely degrade into harmless bio-matter where the non-degradable components sink to the bottom of the sea where it poses no danger to the environment.

13.10 Costs

One of the requirements is that the UAV is affordable. In order to prove the affordability, the costs per operational hour have to be estimated. The costs consist of three parts; Research and Development (R&D), manufacturing and operational costs.

During the R&D, the dominant costs are those for labour. Estimating the total labour at 4,000 man-hours at a tariff of € 73 per hour, the R&D costs, including tests, total at € 300,000.

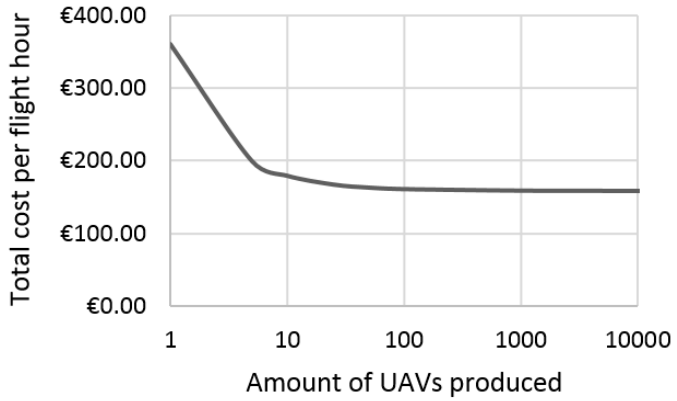

Figure 13.6: Cost per flight hour as function of the total amount of UAVs produced

For the manufacturing the UAV, the payload and labour are the most dominant factors, where the latter is subjected to the learning effect; the more UAVs produced, the more efficient the manufacturing process. This scaling effect also occurs at the R&D costs. Including the operational costs, the total UAV costs can be expressed as a function of flight hours. In figure 13.6. One can see that with a limited production of only 10 ASAP UAV's the price is more or less steady at € 175 per operational hour.

In order to verify if the ASAP UAV is affordable, the cost estimation for the UAV and all support equipment was presented to the KNRM. According to Mr M. Molenman, head of operational services of the KNRM, the ASAP UAV is not only affordable, but the cheapest of all the all-weather systems the KNRM has investigated.

13.11 Conclusion

The ASAP UAV is an all-weather UAV indeed. The design outperforms the original requirements as it can fly with wind speeds of 9 Beaufort and gusts up to 12 Beaufort. It can start its mission from a ship, search autonomously for a victim and return safe to its base.

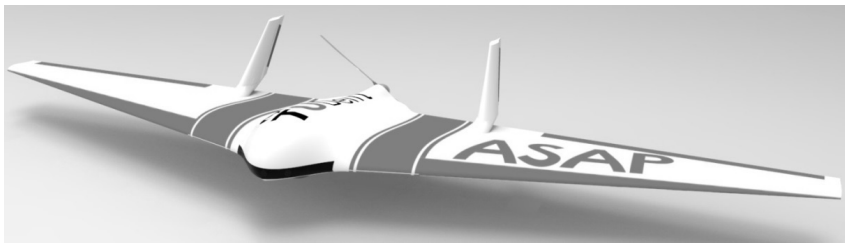

Figure 13.7: Illustration of the ASAP UAV solution

If the UAV might crash, it poses no danger to the sea life. When it is decomposed in a controlled environment, just 5% of its mass is not biodegradable, directly recyclable or re-usable.

13.12 Recommendations

Due to the restricted amount of time available for the design of the ASAP UAV, a number of aspects have not yet been adequately covered. The design team recommends a number of subjects to be investigated.

First, the results of the structural and aerodynamic performance should be verified, validated and optimized. Extensive controllability tests should be performed and in addition the autopilot must be programmed to cope with high wind operations. The hydrophobic coating should be tested for durability and anti-icing performance. However, the most challenging task would be legislative compliance.

14. MIRALOS

Students: I. A. Argyriou Tsikrikonis, R.J. de Boer, M.M.H. van den Broeck, M. Doekemeijer, J. Ehlen, J.A. Reichert, J. Rijnsdorp, P.J.T. van der Stoep, N.D.F. Verhaegen

Project tutor: dr. ir. E.N. Doornbos

Coaches: ir. A.D. Fernandez Vigo, ir. G. Liu

14.1 Introduction

For the past half century, lack of knowledge on gas-surface interactions in the tenuous upper atmosphere has resulted in large discrepancies in important mission properties such as mission lifetime, control ground tracks, and the probability of collisions. Many current drag force estimations rely on a rule of thumb approach introduced in a 1965 paper by Jacchia and Slowey, valid solely for specific shapes and solar conditions.

To cover this scientific gap, a spacecraft mission is designed with primary mission objective:

"to obtain accurate measurements of the interaction of the upper atmosphere with satellite surfaces, operational before 2020."

Additionally, the measurements will be used to create a comprehensive model of atmospheric properties and spacecraft aerodynamics. A secondary objective is included, to investigate long-term atmospheric changes. The mission will also test non flight-proven equipment and raise their technology readiness level.

In presenting order, the spacecraft orbit profile and the number of satellites used is determined based on top-level requirements and a literature study. Subsequently the spacecraft is designed including subsystems to a conceptual level, including selection of the ground station and launch vehicle. Thirdly, the design is assessed for various topics such as operational modes, risks, and sensitivity to parameter changes. Conclusively recommendations are made for continued mission design.

14.2 Literature research, concept design and concept analysis

The mission concept, i.e. the type of spacecraft, number of spacecraft, and orbit profile, was outlined in the midterm report. To allow reliable satellite drag force modelling, the following parameters are to be measured:

- Linear and angular accelerations
- Total atmospheric density
- Constituent element particle counts
- Neutral and ion temperatures
- Spacecraft surface temperature
- Particle incidence angle
- Angular distribution of re-emitted and reflected particles

An updated atmospheric model based on the NRLMSISE-00 model is developed in order to predict atmospheric conditions throughout the mission lifetime. Several high-level mission concepts were looked at, such as a guest payload mission, a single satellite, and multiple satellites missions, including and excluding a propulsion system. A single satellite mission with propulsion system was chosen for better quality of measurements, for the gained ability to perform secondary

missions, and for improved flexibility and robustness. The main disadvantage relates to increased mission costs.

Regarding the orbit profile, the spacecraft is going to be launched in December 2019 to an altitude of 650 km, where it performs scientific operations from January 2020 until June 2020. Then, the satellite descends to 500 km in July, where it performs measurements until December 2020. In January 2021, the satellite descends to 350 km altitude and performs measurements until July 2021. Lastly, the spacecraft ascends back to 500 km, and becomes available for secondary mission objectives starting September 2021. All components are designed for a mission duration of at least six years. 6.0 kg of propellant are taken on board to account for all orbit manoeuvres throughout the mission lifetime.

14.3 Spacecraft design and analysis

The second part of the final report consists of the design of the satellite, including subsystems, system integration and analysis. The following subsystems are considered up until this design phase: payload, propulsion, ADCS, power, thermal control, structures, on-board processing and communications. Next to that, an initial launch vehicle and ground station are selected.

Bus design

The bus design is strongly related to the electrical power subsystem requirement. In favour of the quality of measurements, no external panels are mounted to the spacecraft bus. This is disadvantageous for the efficiency of energy retrieval using solar cell arrays. To account for this disadvantage, the cross-section of the spacecraft is chosen to be hexagonal. The solar panels mounted radially on this spacecraft have an efficiency between 0.79 and 0.87, depending on the incidence angle of solar rays. A hexagonal bus shape also allows for a easier integration of subsystems and components. It is furthermore beneficial with respect to available launch vehicle payload fairing.

The spacecraft has a length of 3 m and a diameter of 2.2 m. This flows down from back-of-the-envelope calculations on the drag force and from payload fairing properties of feasible launchers.

Payload subsystem

The scientific operations of the satellite are carried out by the scientific payload. To that end, an adequate mass spectrometer is included in the design, which will provide measurements on composition for both neutral and ionised particles, neutral wind and ion drifts, neutral temperature, and density. The spectrometer uses a combination of magnetic sector and reflectron techniques. A second mass spectrometer is implemented for redundancy.

The accelerometer implemented is similar to the accelerometer that will be used on the GRACE-FO satellite. As part of the mission of the prior, the accelerometer will be flight-proven. Requirements on the positioning of the instrument relate to the centre of mass location of the entire spacecraft.

A GPS antenna and laser retro-reflector are used for satellite positioning. The choke ring antenna of the GPS system is responsible for precise location and orbit determination. The instrument is also equipped with a helix antenna used for occultation monitoring. Two patch antennae are added for attitude determination and redundancy.

Two configurations of the original reflectometer used on board the STS-8 mission are employed to investigate the gas-surface interactions of a plate, set at an incidence angle with respect to the incoming flow. The first configuration will ionise incoming particles, which will subsequently be detected by a distributed number of micro-channel plate detectors, placed at defined distances around the reflectometer contour. The second configuration will use an optical scanner to take pictures of the imprint of atomic oxygen particles on the silver foil.

Propulsion subsystem

Design of the propulsion system goes hand-in-hand with the concept selection. The system is included in the design to increase the

capability and flexibility of the mission. For MIRALOS multiple different types of thrusters are considered: cold gas, liquid-bipropellant, liquid-monopropellant, electric ion thrusters and electric hall. Ion-based thrusters are chosen because of their high flexibility and mass performance. Their main disadvantage is their high power consumption and cost.

The T5 Kaufman thruster is implemented because of its excellent performance in terms of power consumption.

Attitude determination and control subsystem
Highly accurate attitude knowledge and control is desired for the payload operations. The ram surface area is to be pointed in flight direction to minimise uncertainties introduced in aerodynamic calculations related to drag. Furthermore, as moving components would badly influence the performance of the accelerometer, no reaction wheels, momentum wheels, or gyroscopes are implemented for attitude control or determination.

For coarse attitude determination, two Honeywell HMR2300r magnetometers are implemented, one of them implemented for redundancy. Additionally two antennae are added to the current GPS system for redundancy providing attitude sensing with an accuracy better than 1 arcsecond.

For fine attitude determination, two sets of the extremely light-weight TU Denmark's μASC Star Camera Assembly are implemented, each with an accuracy better than 2arcseconds. A total of four optical heads are placed on the spacecraft skin pointing in different directions, implemented such that two optical heads will always be pointed away from the sun and thereby allow operation. Furthermore for redundancy, a total of four of TNO's Digital Sun Sensors μDSS are placed next to the optical units of the μASC, which can operate when star trackers cannot due to sunlight blinding.

For attitude control, two sets of three Zarm Technik's MT70-2 magnetic torque rods are implemented. The magnetometer is used in

support of these rods to accurately determine the magnitude and direction of the Earth's magnetic field. The main advantage of the magnetic torque rods are their lack of propellant, high reliability, and low mass. The disadvantage is their limited operability. However, at the Earth's poles the magnetic field changes direction, which allows for full 3-axis attitude control.

In order for the mass-trim assembly to calibrate the centre of mass, a nodding manoeuvre is performed every two months for a period of 24 hours. This procedure consists of pseudo-random milliNewton-meter torques initiated by twelve cold gas thrusters for full attitude control.

Electrical power subsystem

The electrical power system provides retrieval, storage, regulation, and distribution of electrical power to the spacecraft. First a power source has been selected based on the mission characteristics and orbit profile. A solar photovoltaic-battery system is found optimal for the MIRALOS mission. Efficiency and degradation are decisive in the choice of Triple Junction Gallium Arsenide solar cells. Lithium-ion batteries are selected based on their high capacity and efficiency.

These components are sized based on their maximum required power case, connected to the set power requirement of 975 W.

The battery size is determined accounting for eclipse times, charge/discharge efficiency, depth of discharge, and degradation over time. Taking into account the energy needed for battery charging, Earth albedo radiation, temperature degradation, design degradation, assembly inherent degradation, and annual degradation due to radiation, the solar array area and mass are calculated. The electrical power system uses three QL075KA batteries, CI ZTJ PV Cell solar array, and a Medium Power PCDU. The solar cell arrays cover 86.1% of the total surface area of MIRALOS.

Thermal control subsystem

An analysis is performed regarding thermal properties of the spacecraft. A first order estimation is made assuming that the

spacecraft is isothermal. The surface properties of the solar cell material were used in the analysis of the satellite's surfaces. This leads to a maximum temperature of 27 °C during a non-eclipse orbit with maximum operational waste heat production in the spacecraft. The opposite case, with maximum eclipse orbit and minimum operational waste heat production, yields an average temperature of -23 °C. The extreme minimum occurs during a maximum eclipse orbit under safe mode operations. In this case, the temperature drops to an average of -25 °C, with a minimum of -34 °C. This implies that numerous components require heating.

To get a better insight in the temperature distributions over the spacecraft surfaces, a thermal model is created using a finite-element program called COMSOL. By implementing all radiant heat sources, such as the sun, the Earth, the albedo effect, and the waste heat production of the spacecraft, a fairly accurate model is simulated.

The accelerometer should have a high thermal insulation. The heaters of the accelerometer cannot be placed directly on the instrument itself, since they would compromise the temperature stability requirement. Therefore, the direct environment of the accelerometer has to be accurately controlled.

The thermal control system consists of a combination of active and passive control. This is to keep thermal flexibility in good balance with reliability and complexity. A distributed processor unit controls the heated components, while the excess waste heat is radiated by a passive radiator plate.

Structural analysis

An initial design is created for the structural components of the satellite. The spacecraft bus will consist of load carrying honeycomb sandwich panels. The panels are fastened together using brackets, without an underlying frame.

The outer panels make use of 1 mm thick carbon fibre reinforced cyanate ester skins on a 10 mm thick aluminium honeycomb core. The

central hexagonal floor, on which the accelerometer is mounted, uses a carbon fibre reinforced carbon matrix composite material for both the skins and the honeycomb structure. This material has a very low and negative coefficient of thermal expansion, the former required to keep the location of the accelerometer constant.

The dimensions of the structural components are sized to withstand the loads and vibrations experienced by the spacecraft during launch. The eigenfrequencies of the spacecraft have been analysed using the finite element analysis software COMSOL. The lowest eigenfrequency in lateral and longitudinal direction is significantly in excess of the minimum frequencies required by the selected launch vehicle.

The final weight of the structure, including a margin for brackets and fasteners represents 60% of the total dry weight of the spacecraft.

Command and data handling

Three components are implemented on the spacecraft to account for command and data handling between various components and interfaces. These are an on-board computer (OBC), a central processing unit (CPU), and a remote terminal unit (RTU). The RTU has the function of offloading the on-board computer and provide redundancy.

For all three components multiple flight-proven products are investigated, upon which a final selection is made. The SCS-750 is chosen as the main on-board computer of MIRALOS satellite. The Motorola PowerPC 603e is found to be the most effective option for the CPU. Finally, the BU-63705 is selected as RTU.

Communications subsystem

The general system layout is considered, in which the spacecraft transmitter and receiver are treated. The STC-MS01 transceiver is implemented on the spacecraft, after investigating various flight-proven options. Subsequently the link budget is iterated, including all losses and gains related to communication operations. Comparing

various commercially available antennae, the SSTL Patch Antenna is selected.

Ground station selection
The ground station is to be chosen based on antennae properties and location of the station. For the uplink and downlink analysis, a ground station of the ESTRACK network is chosen. The location of the station plays a role for the number of contact periods, which has to be sufficient for transmitting all data. Because the orbit is determined to be near-polar, a ground station with high latitude is chosen, in order to optimise the number of contact periods per day. Combining this with the available ESTRACK ground stations and taking the station antenna into account, the ground station selected is the one located in Svalbard, Norway.

Launcher selection
Trading-off different launchers in different countries, for payload weight, inclination range, fairing dimensions, and launch cost, the Ukrainian Dnepr-LV is chosen to launch MIRALOS into orbit.

Resource allocation
Combining the selected components of all preliminary subsystems, an estimation can be made for the total weight of the spacecraft. This estimation relies both on the selected payload instruments and statistical data. A total spacecraft wet mass of 470 kg is estimated, of which 13 kg is fuel. The maximum power consumption that the satellite will experience is estimated at 890 W. Lastly, the total MIRALOS mission costs is estimated at €121,000,000, including a 10% contingency factor for unexpected surplus costs.

14.4 System analysis

The third part of the report contains the system analysis, in which the spacecraft operational modes, the verification and validation procedures of the design, and the mission risks and their mitigation are some of the covered subjects.

First, the spacecraft is designed to operate in six different modes. An essential mode for mission success is the Safe Mode, triggered in mission-threatening situations. All non-essential operations are thereby turned off, and the focus shifts to communication, thermal control, attitude control, and on-board computing. Other considered modes are Initialisation Mode (triggered after orbit injection), Scientific Mode, Orbit Change Mode, Calibration Mode (the ADCS cold-gas thrusters translating to mass-trim assembly drive to calibrate the centre of mass) and lastly a Drag Compensation Mode (required to maintain altitude and orbit at low altitudes).

Secondly, all instruments, subsystems, and models used for the development of MIRALOS require verification and validation to ensure proper functioning and to minimise the probability of mission failure. Components are assessed on four fronts: inspection, analysis, demonstration, and testing. In this conceptual phase of the design, most verification and validation procedures are still open to adjustments.

Thirdly, by analysing all technical risks related to mission and (sub)system design, several events exist that significantly affect the probability of mission success. As long as the financial budget allows for it, resources are to be spent with the purpose of reducing the severity of impact of these events and/or their probability of occurrence. The main risks found are related to failure of instruments, failure of the propulsion subsystem, the calibration manoeuvre accounted for by the ADCS, and communication system failure.

A top-level sensitivity analysis, investigating the relationships between design changes, showed that the current mission design is very robust. The largest design alterations originate from changes in the orbit profile. Furthermore, a RAMS analysis is carried out to gain insight for the next, more detailed phase of the design.

A market analysis shows that MIRALOS is strongly competing with other noteworthy mission concepts for acceptance and continuation of design at a space agency, such as ESA or NASA. A large financial

budget of € 350,000,000 has been assumed early in the design phase, which is disadvantageous for mission acceptance by external agencies. On the other hand, the mission has been found to be accomplishable with almost a third of the considered budget, a fact that makes the design cost-attractive.

With respect to the mission's sustainable development strategy, International Guidelines have been established to ensure fair usage of the space environment to minimise space debris, and maintain usability of frequently used regions in space surrounding the Earth. For this reason, MIRALOS is designed to burn up in the Earth's atmosphere after its secondary missions have been carried out. Additionally, the design relies on electric propulsion, thereby significantly limiting the amount of fuel taken on-board.

Until the launch in 2020, the design will be finalised, tested, and produced. Throughout operation in 2020 to approximately 2026, the resulting measurements are inspected for their compliance to the needs of stakeholders, after which the satellite is brought into a burn up orbit and ground activities are terminated. Documentation and interesting results related to both measurements as mission design are published. All activities are ended before January 1st, 2027.

14.5 Recommendations

Throughout the entire design process, risks are to be constantly identified, quantified and mitigated. The current design revolves on a single iteration, and many changes are to be made before all subsystems are fully compatible.

The methods of analysis are to be refined as the design progresses. The spacecraft bus dimensions should be reconsidered based on launcher fairing properties. Also, more research is to be performed regarding available options for instruments, components, and flight-proven solutions. Information is still lacking, thereby limiting analysis and conceptual design.

For the ADCS, two main recommendations are made. Firstly, a large risk originates from the lack of information on magnetic interference with on-board instrumentation due to the ADCS torque rods. Using literature and tests, more information on the feasibility of this design decision is to be obtained. Secondly, the calibration procedure is still unknown to a large degree, and thrusters are currently sized using back-of-the-envelope calculations. Due to the high uncertainty and design impact, this step will be asserted high priority.

Lastly, an omni-directional antenna is to be implemented on the spacecraft in order to allow communication with the ground station in case of spacecraft tumbling.

The current design is still very conceptual and is largely based on readily available knowledge and commercially available components. In further development, top-level design decisions will be minimized.

15. A320 AF (ALTERNATIVE FUEL)

Students: B. Cont, M.M. Doole, C.L.V. Driessen, M. Hoekstra, P.B. Jahn, K. Kaur, L. Klespe, C.H.J. Ng, E.M. Rezunenko, N.C.M. van Zon

Project tutor: dr. A. Gangoli Rao

Coaches: dr. C. de Servi, dr. W.J. Zhao

15.1 Introduction

Aviation is predicted to double in the next fifteen years. Therefore, by the year 2030 around four to five billion passengers are expected to be travelling annually. This large growth comes at a cost to the environment if kerosene remains the fuel of choice. One of the main issues is consequently the availability of an alternative fuel that is both sustainable and economically feasible. Several alternative fuels have been investigated and analysed for feasibility.

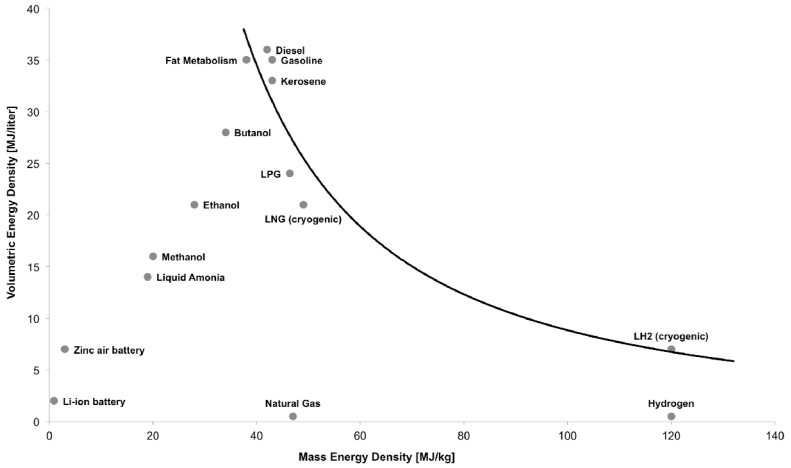

Figure 15.1 Comparison of energy content of alternative fuels for aviation

Liquefied natural gas (LNG) is a promising candidate. It provides significant reductions in carbon dioxide (CO_2) and nitrogen oxide (NO_x) emissions and completely reduces sulphur oxide (SO_x) emissions. The natural gas network already present in Europe and other parts of the world is scalable and can be used to supply airports with the gas which will then be liquefied at the airport. The liquefaction process is well-known in many industries, including shipping, making it relatively inexpensive.

There are challenges associated with using LNG. Its volumetric energy density is lower than kerosene, resulting in larger fuel tanks. Furthermore, it is a cryogenic fuel, with a boiling temperature of -161 degrees Celsius. Many systems have to consequently be modified for LNG use, primarily the engines, fuel tanks and fuel supply system. However, airports also have to be accommodated for LNG application. The changes would thus be system-wide and large scale.

15.2 Project objectives and requirements

The project objective is:

"to design the next generation sustainable A320 aircraft operating on alternative fuels for the year 2030."

A set of requirements are set to ensure that this new aircraft meets the demand of airlines, as listed below:

- Can take-off and land at all current A320 airport destinations
- Has the same stall speed characteristics
- Has a similar mission profile
- Seats the same number of passengers

A separate list of design requirements are made to assure the new aircraft is aligned with aviation sustainability goals set by the Advisory Council for Aeronautics Research (ACARE) in Europe. The sustainability design goals for this project are modified in such a way that it is suited for the year 2030, as the ones set by ACARE are meant for the year 2050.

- 50% CO_2 reduction
- 65% NO_x reduction
- 80% SO_x reduction
- 25% noise reduction
- No increase in impact of water vapour on global warming potential by the aircraft

15.3 Concept development

The process of developing concept ideas lead to a variety of aircraft designs. This was achieved by making design elements, or "ingredients" for an aircraft. The core categories involved in these design elements were the following:

- Geared turbofan or open-rotor engines
- Wing-mounted or tail-mounted engines
- High- or low-wing
- External or internal LNG fuel pods
- Different tail configurations

Eight concept aircraft were selected for a final trade-off. The trade-off had two main groups of equal weight. The first was technical and the second was emissions and noise. The final design concept consists of

open-rotor engines, mounted at the back on the H-tail, with LNG fuel pods underneath the wings.

Hybrid configuration

A study was done on 16,500 A320 flights worldwide. It was found that 75 percent of these had a range of less than 1,100 nm, which is one third of the A320 maximum range. With this knowledge and the fact that by 2030 it will be impossible that all airports will be LNG capable, it was decided to utilize a hybrid fifty-fifty configuration between LNG and kerosene. This will allow for a more seamless transition and alleviate some of the fuel tank volume penalties. However, even with this configuration for the above range of 1100 nm, it is possible to fly completely on either fuel. Therefore operational flexibility is not hindered. For longer flights, climb and descent can be performed on LNG, minimising air pollution around airports, and cruise on kerosene.

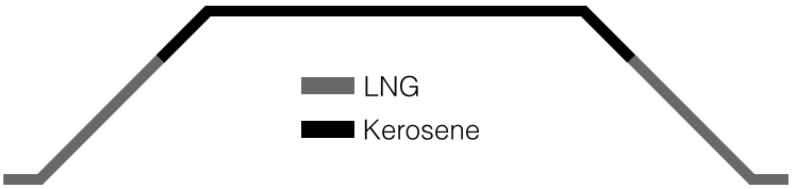

Figure 15.2 One possible mission profile for the A320LNG

Cost analysis

A breakdown of the direct operating costs (DOC) for a typical Airbus A320 is performed. Expectations are that several costs will increase due to the investment into LNG airport infrastructure and more advanced systems. The major cost saving will be due to the fuel. A market analysis preformed estimates that LNG will give 80.38 MJ/$ compared to 40.22 MJ/$ for kerosene. This makes liquefied natural gas twice as cheap compared to kerosene. Finally the discovery and utilization of shale gas will make LNG more attractive in the coming decade.

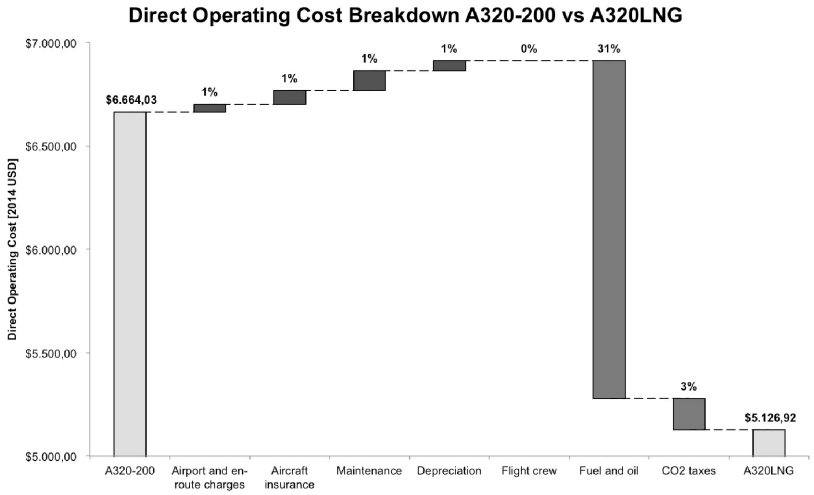

Figure 15.3 A320-200 to A320LNG Direct Operating Cost Breakdown. Total decrease in DOC is estimated to be 23%

15.4 Preliminary design

The final design concept for the aircraft has been decided. The aircraft is then designed based on the technical requirements. The different subsystems of the aircraft are presented in the sections below.

Wing

Low mounted wings are used in this design. The wing is composed of two aerofoils with similar lift characteristics. The lift characteristics are based on the lift and drag properties during cruise phase. NACA 632-615 is chosen as the root aerofoil and NACA 643-418 is chosen as the tip aerofoil. It is designed such that the root stalls before the tip, hence the ailerons will still be effective at the detection of stall. The wing has a sweep angle of 20 degrees. Also, to meet landing and take-off requirements, leading edge slats and fowler flaps are implemented onto the wing.

Empennage

The H-tail configuration is selected for this design aircraft. The main reason for this choice is that the H-tail can effectively redirect noise propagation upwards, minimizing the effect of noise from open rotors

to passengers and nearby areas. This is achieved without sacrificing flight stability and control.

Fuselage

The size of the fuselage is the same as current designs. By using carbon fibre reinforced polymers the structural weight of the fuselage decreases by 24 %. The cabin layout was modified to take up 3 additional passengers and the emergency exits were modified accordingly. To take up fuel systems, the aft fuselage was designed more spacious and reinforcements of high modulus carbon composites and Kevlar composites were implemented to withstand the impact of a failed blade.

Fuel system

A hybrid configuration is used for A320LNG. The fuel system is designed separately for both types of fuel. The kerosene fuel system is similar to current A320 fuel system layout, the main difference being that there is no longer a centre tank. As for the LNG fuel system, LNG is heated to gas form using heat exchangers, then stored in engine feed tanks. The gas LNG is then injected into compressors before fed to the engine. The insulation covering the fuel lines has to be infused with nitrogen to prevent condensation. Similarly, the LNG fuel system has to be purged with nitrogen before start up.

Fuel tank

The fuel tanks are mounted under the wing. The tank is made of aluminium 7075-T6 because it has low density and relatively easier manufacturability. Since LNG is stored at cryogenic temperatures, the fuel tanks are designed such that heat exchange is minimised. An insulation layer is added in order to achieve this. Cryogel-Z is chosen for its low weight and superior heat insulation properties. The thickness of the tank shell is also designed for potential bird strikes. To make the tank more aerodynamic and to accommodate a venting system, a fairing is built around the tank. The venting system is used to release gases from the tank when the pressure of the tank is too high. The fuel tanks have to be purged before refuelling.

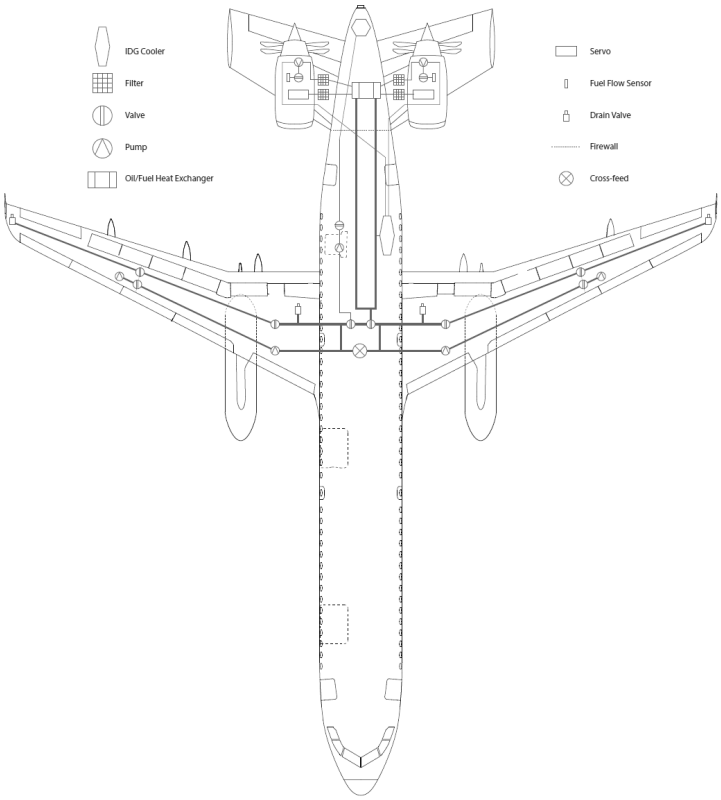

Figure 15.4 Schematic representation of the LNG and kerosene fuel systems

Engines

Counter rotating open rotor engines (CROR) are used instead of the conventional turbofan engines. This is because CROR has better propulsive efficiency and reduced greenhouse emissions. To reduce noise transmission from the engine to the cabin, a pusher configuration is used. However, certification issues regarding engine have set to be solved, as this engine has yet to be widely implemented and certified for commercial use.

Stability and control

According to the shift in aircraft centre of gravity due to the change in aircraft components, the size of vertical and horizontal stabilizers are determined. Take note that the stabilizers are designed in such a way that it serves as a shield for the open rotors to reduce noise emissions. The tricycle configuration with one wheel at the nose and two main

wheels under the wing is used for landing gear design. By preliminary flight dynamics analysis, a set of stability derivatives is produced such that A320LNG is dynamically stable in different flight modes.

Pneumatic taxi system

Ground operations of aircraft at airports produce a significant amount of emissions and noise close to homes and people. It is therefore an objective to remove these harmful effect completely. As a result two green taxiing solutions are investigated: an electric and a pneumatic system. The electrical taxiing system is found questionable as to whether it will pay off in terms of direct operational cost. Subsequently an air powered system is proposed, something that has never been done before. Initial results from the pneumatic taxiing dynamic model show that the weight and volume is acceptable and much lower than the electric system and that the air motor can deliver the required power to meet taxi requirements. This system will be able to save time due to autonomous pushback, save significant amounts of fuel and reduce noise at airports.

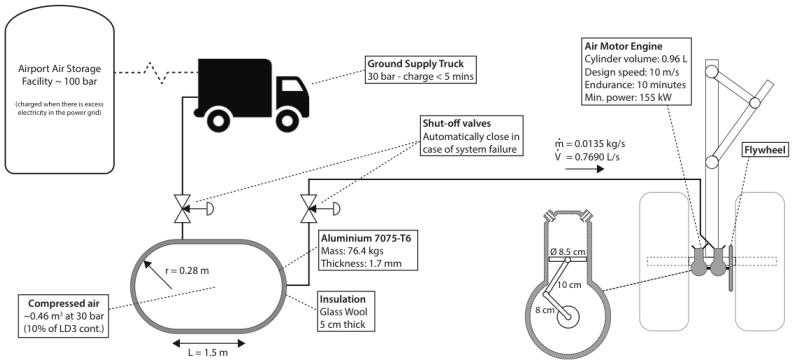

Figure 15.5 Schematic of the system design of the pneumatic taxi system

15.5 Conclusion and recommendations

To ensure sustainable air traffic growth in the future a new single aisle aircraft using alternative fuel for an entry into service in 2030 has been designed. The major alteration that is driving changes in the design is the transition to LNG, which will greatly impact subsystem

design and aircraft operations. A hybrid design is chosen which can fly on both LNG and kerosene, 50 percent of the total energy content of the fuel is kerosene and the other 50 percent is LNG. This has been chosen because LNG will not be available at all airports by 2030. Hence, a hybrid design increases operational flexibility. The design results in significant emission reductions.

There are several changes made to the A320 in order to adapt it to the A320LNG. Fuel tanks are mounted on the wings, engines are relocated and changed from turbofans to open rotors. Furthermore, the fuselage is made of carbon fibres resulting in a decrease in weight. The locations and size of the wing, tail and landing gears are considered in order to make sure the aircraft meets all control and stability requirements.

Changes of airport operations are necessary. The transportation of LNG to the airport is a major issue. As a solution the usage of existing natural gas pipelines is proposed after which the gas can be liquefied by small-scale liquefaction plants at the airport itself. This reduces the complexity associated with the transportation of a cryogenic fuel.

The A320LNG is an aircraft with a promising future. Not only will it significantly reduce the emissions associated with air traffic, it will also be attractive to operate for airlines. The total cost of the aircraft will decrease as compared to the current A320 meaning that an airline can make more profit. The A320LNG will be the aircraft of the future.

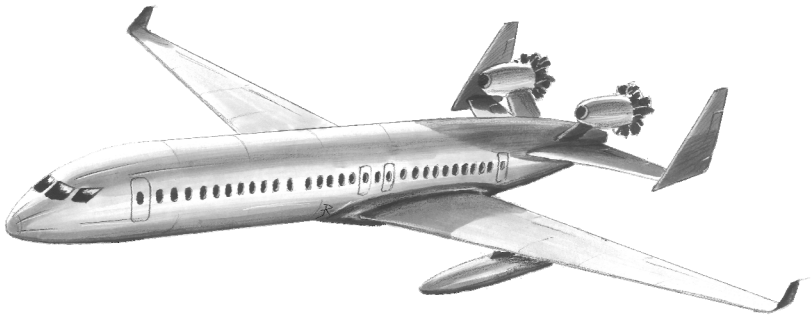

Figure 15.6 Sketch of the A320LNG final design configuration

16. BIRDPLANE

Students: J.S. van der Burgt, K.J.M. Hameeteman, J. Harms, S.H. Lee, I.A. Mkhoyan, D. Risseeuw, W.J. Schoneveld, B.Telgen, N.A. Voogt, W. Westbroek

Project tutor: dr. S.J. Garcia

Coaches: dr. G.C.H.E. de Croon, dr.ir. H.G. Visser

16.1 Introduction

Birds are remarkable creatures – Peregrine Falcons can reach the speed up to 320 km/h, and Barnacle Geese migrate over 900 km non-stop with remarkably high efficiency. In particular, the Barnacle Geese fly in formation and take advantage of the wake turbulence caused by the wingtip vortices from the birds ahead. While they are flapping their wings, they also simultaneously fold, twist, and morph their wings to maximize the aerodynamic forces and increase the flight performance. To this day, the exact flight mechanics and dynamics of the birds have not yet been fully comprehended. The decryption and mimicry of bird flight mechanics has therefore been a long-lived dream of mankind and is believed to be a possible answer to current aviation challenges.

Despite the long history of countless vain attempts to imitate the flapping flight of birds, recent developments in robotics and innovative materials have enabled us to build bird-like UAVs which

can be operated in real life; excellent examples are the SmartBird from Festo, and Robird from Clear Flight Solutions. Nevertheless, none of these current designs are capable of sustaining their flight for a long range/endurance mission.

In pursuit of acquiring better insight into the migratory birds' flight behaviour, a group of ten bachelor students have dedicated ten weeks of time to design BirdPlane, a unique flapping-wing aircraft that can fly alongside the migrating Barnacle Geese. The Mission Need Statement is formulated as follows:

The BirdPlane mission is:

"to autonomously follow and study a flock of migrating Barnacle Geese with a remotely controllable, bird-inspired flapping-wing aircraft."

In the following sections, the details of the conceptual/preliminary design and the important steps taken towards this stage are summarized.

16.2 Requirements and constraints

At the beginning of the project, a set of requirements were set by the customer, i.e. principal tutor. These requirements served as a guideline for the design of BirdPlane.

- Follow a Barnacle Geese flock from the north to the south of The Netherlands
- Unmanned aircraft for daylight operation
- Flapping wings
- Bird-like aerodynamics (passive and active drag reducing methods)
- During cruise flight following the flock, no propellers can be used
- Device should take-off and land with no human help
- Detection of bird flock to follow
- Camera incorporated to record flight and send information during whole flight to base in Delft

- Maximum wing span: 150 cm
- At least 90% of the structure must be re-used or recycled at the end of the aircraft service-lifetime
- Incorporate as many bird-like features as possible.

16.3 Conceptual designs and trade-off

In order to meet the requirements given above, different conceptual designs were proposed and evaluated. Selecting a proper configuration for an innovative aircraft design is not a straightforward process, as many different novel ideas have to be evaluated in various design and operation perspectives. Striving to achieve a reasonable balance between innovation and feasibility, five different concepts were created (fig. 16.1). In this section, a short qualitative overview is given for each of these concepts.

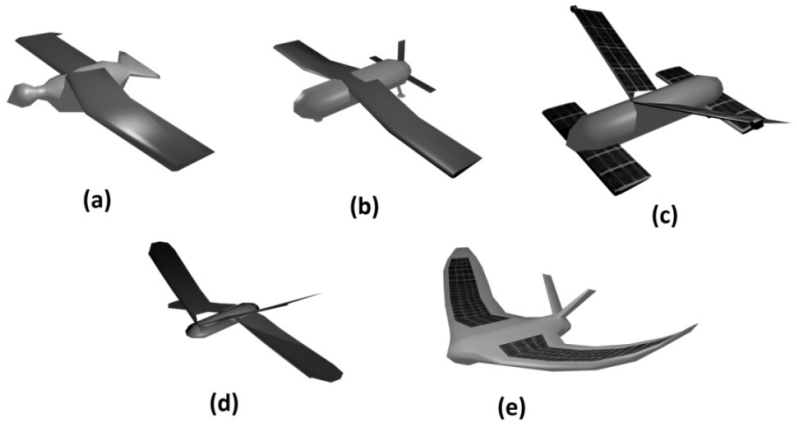

Figure 16.1: Five conceptual configurations that were initially considered for BirdPlane

Bio-inspired concept (a)

Among the five concepts, this concept bears the most similarities with the real Barnacle Goose. The wings are double hinged with a ball joint to allow movements in all directions, actuated by the artificial muscles. A triangular shaped rotatable tail is used for stabilization and control. The power is provided solely by a lightweight battery.

Conventional concept (b)
This concept incorporates simplified bird-like features. The wing is double hinged, but no ball joints are used. A gear-and-crank wing mechanism is driven by an internal combustion engine, where the twisting motion is achieved by incorporating an additional servo in the wingtip. The tail has a conventional configuration – that is, with fixed vertical and horizontal stabilizers.

Three-wing concept (c)
This configuration has two static wings (tail and canard) and one flapping wing, where the lift is mainly provided by the static wings and the thrust by the flapping wing. This setup has a large surface area which is covered by solar panels for power supply. Take-off and landing are assisted by a wheeled, non-retractable landing gear.

Dragonfly concept (d)
This concept has a double-flapping wing configuration, similar to a dragonfly. During cruise, these wings flap in opposite phase to enable station-keeping. All wings are controlled by active twist, actuated by servos mounted at the wingtip. For the power supply, hydrogen fuel cell is used. The wing material is thin, lightweight, yet stiff enough without the presence of ribs.

Futuristic concept (e)
This concept has a blended wing-body configuration, where the entire wing is composed of electro-active polymers which deflect when a voltage is applied. The power is supplied by the batteries and flexible solar panels covering the entire wings and fuselage. A V-tail configuration is used to save weight and reduce drag.

Trade-off
These five concept candidates were evaluated using a set of trade criteria which directly reflect the feasibility and technical performance of the design. The Futuristic concept had the poorest performance as the available electro-active polymers required high structural mass due to low power density. The Three-wing concept, on the other

hand, was not efficient in terms of lift generation. Also, the use of solar cells for power supply turned out to be inefficient due to the low solar irradiance in The Netherlands during autumn. The Dragonfly concept had low controllability due to the absence of control surfaces, and the limited wing morphing required a very high flapping frequency. The Bio-inspired and Conventional concept scored high in overall performances, except for the low efficiency and reliability of the artificial muscles and control issues with the combustion engine.

16.4 Final design

After the trade-off, an attempt was made to come up with the most suitable combination of subsystems from the Bio-inspired and Conventional concepts, which was then incorporated in the final configuration. In figure 16.2 and 16.3, the final layout of BirdPlane is shown. A part of the fuselage is made transparent in order to show the gear system inside.

Figure 16.2: Final layout of BirdPlane

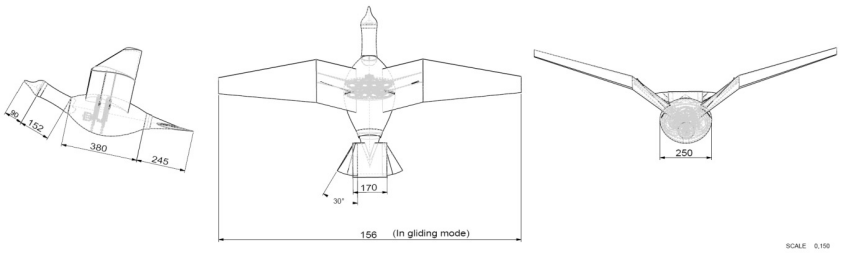

Figure 16.3: 3-view drawing of BirdPlane

The most important design parameters are mentioned in table 16.1. These values were reached after a number of design iterations and optimizations in an endeavour to meet the primary system requirements.

Table 16.1: Most important design parameters

Parameter	Value
Total mass	1.35 kg
Overall length	0.84 m
Wing span	1.56 m
Average flapping frequency	5 Hz
Maximum angular displacement of the wing root during flapping motion	60 deg
Total power consumption	130 W
Endurance	100 min
Nominal cruise velocity	18 m/s
Peak cruise velocity	26 m/s
Recyclability	62 %

16.5 Details of the final design

This section presents several notable aspects and characteristics of the final design. It should be emphasized that each of those elements are closely interrelated to one another, and cannot be considered separately.

Wing and gears design

First of all, an extensive literature study was done on the birds' flight mechanics and wing aerodynamics, which was followed by the identification of primary wing parameters - span wise twist angle, flap induced velocities, flight velocities and flap angle. Secondly, the

aerodynamic effects of these factors were formulated and quantified along the wing span by applying Kutta-Joukowski circulation theory and the Jones' method to introduce distinct scaling factors for down stroke, upstroke, and glide phases. Finally, the design parameters are optimized through iterations in an attempt to meet the requirements and constraints regarding the aerodynamic force generation. Furthermore, the wing aerofoil and planform are designed such that it resembles the wing of actual geese as close as possible.

Based on the derived design parameters, the wing mechanism is designed to allow for flapping, folding, and twisting motions. The flapping motion of the wing spars is actuated by operating the gear-and-crank mechanism, as illustrated in figure 16.4. The gears are driven by an electric motor (Hacker A20-12 XL EVO), and its RPM is varied between the upstroke and down stroke motion of the wing using a PWM controller in order to achieve more efficient thrust and lift generation. The gears which experience higher torque than the others are made of carbon steel, while the rest of the other gears are made of Nylon.

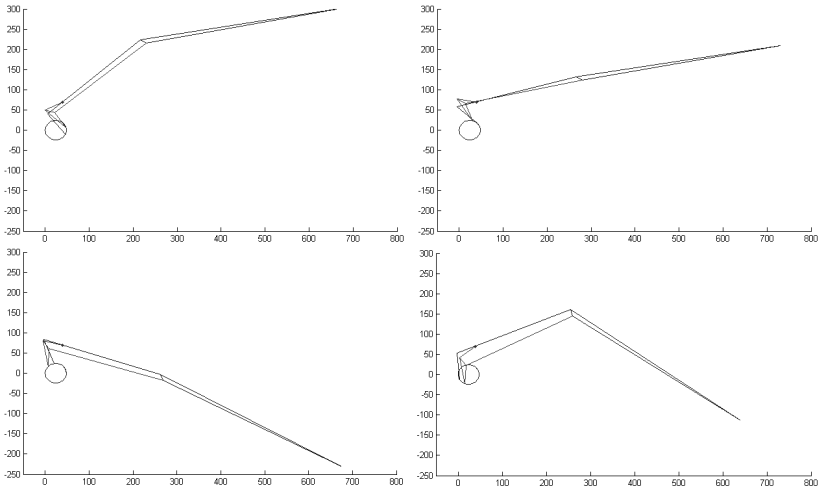

Figure 16.4: Wing flapping mechanism

In addition to the flapping and folding motion, the wing is simultaneously twisted along the span wise direction by introducing a

phase lag between the front and rear spars with a planetary gear system. This planetary gear system mounted at the rear rib is shown in figure 16.5. Each wing has two spars (made of CFRP tubes) which would move at exactly the same frequency, and thus, keep a constant phase difference if there is no ring gear rotation. The rotation of the ring gear causes a change in the flapping phase of the rear spar, resulting in a change in the phase lag between the front and rear spars, which eventually leads to a change in the linear wing twist. The loads are carried by a skeleton-like structure of lightweight carbon fibre rods and ribs.

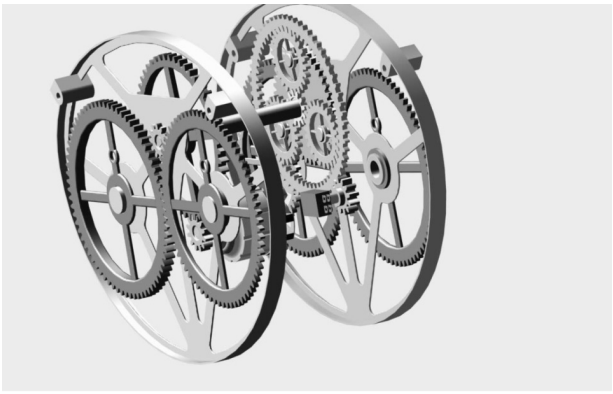

Figure 16.5: Assembled gearbox

Finally, Nylon sailcloth is chosen as the main material of the wing skin, since it is lightweight, recyclable, and moderately stiff (i.e. it allows small deformation for wing twisting, while keeping the shape of the aerofoil). On moving interfaces at the wing and tail root, a flexible skin made of self-healing polyimide is used.

Tail design

In order to provide stability and controllability, a bio-inspired rotatable tail is designed and incorporated in BirdPlane. The tail of BirdPlane is capable of several bird-like motions, such as the rotation around the longitudinal axis, deflection for pitch motion, and fanning (i.e. folding/unfolding) to change the tail surface area. These motions are actuated by three servos in total, as shown in figure 16.6.

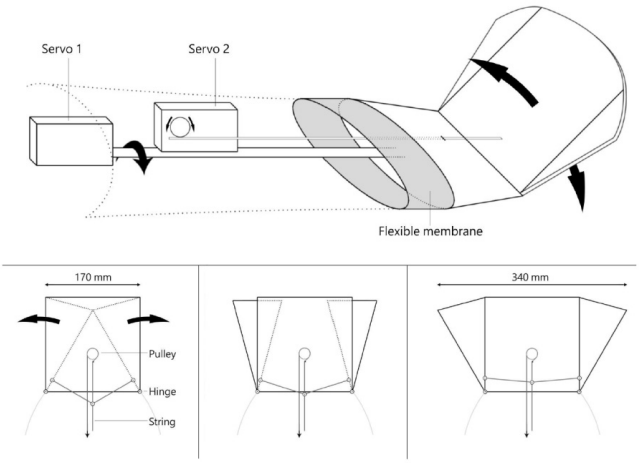

Figure 16.6: Tail mechanism actuation

Neck design

Throughout the flapping flight, BirdPlane sways up and down in response to down stroke and upstroke motions. In order to stabilize the camera platform mounted in the nose of BirdPlane, an iso-elastic neck mechanism (figure 16.7) is incorporated to decouple the motion of body and head, thereby damping the oscillation experienced by the head. Moreover, the long neck makes the BirdPlane look more like a goose, instead of a raptor.

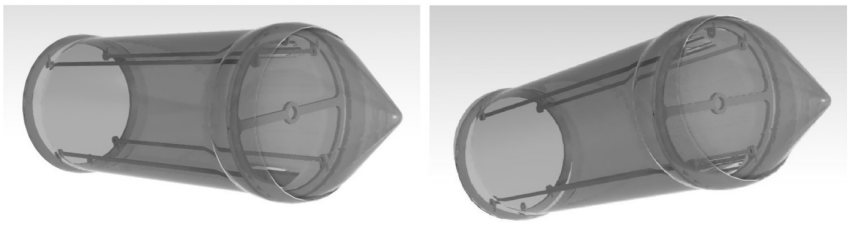

Figure 16.7: Neck structure

Fuselage design

The fuselage has in total 4 CFRP ribs which are connected by a truss structure of carbon fibre rods. The skin of the fuselage does not carry loads, and is made of 0.2 mm thick Nylon 6-6. An exception is that the "belly" of the fuselage will be made of self-healing smart rubber which can absorb the impact from landing, and recover from possible scratches and tears.

Power supply

Li-S batteries are chosen as the power source due to its high specific energy (500 Wh/kg, highest on record). Using this specific energy and the estimated energy density of 600 Wh/l, the required battery weight and volume are computed as 435 g and 360 cm^3 respectively. The batteries are divided into two packages and located such that the centre of gravity is positioned at a favourable position in terms of longitudinal stability. An electric current monitor ACS761 is used to monitor the current and voltage from the battery.

Communications

Initial analysis of possible network topologies revealed that the continuous communication link between the ground station and BirdPlane for live video stream can only be guaranteed within 20 km coverage of ground antenna network. Therefore, a continuous analogue communication link will be used for the launch and rendezvous (i.e. joining the formation flight of the Barnacle Geese) phases. For the flight phases after the successful rendezvous, the cellular 4G network will provide the possibility to give commands to BirdPlane and receive status data about the current mission state including photos. Note that 96% of The Netherlands is covered by the KPN 4G-network.

Bird detection and navigation

The navigation subsystem has to determine the BirdPlane's position in global coordinates, and specify the target location (i.e. waypoint) which will be fed to the control system. The global position of BirdPlane is measured by the GPS system embedded on the autopilot control board. Besides the position of BirdPlane, the position of the flock of geese must be known; before the launch, the migrating Barnacle Geese are detected using the weather radar system developed by KNMI. Afterwards, the flight path of the flock is extrapolated at the ground station, which is used to determine the launch moment and rendezvous trajectory of BirdPlane. Once it joins the flock and starts the cruise flight, the relative position of the flock with respect to BirdPlane is measured by the stereoscopic long-wavelength Infrared (LWIR) camera mounted at the nose of

BirdPlane. For this on-board geese detection system, feature-based optical flow method is used, and the background motion is filtered out in order to obtain distinct motion images of the geese. This detection algorithm was constructed using OpenCV in Python, and the simulation result is shown in figure 16.8.

Figure 16.8: Simulation result of Barnacle Geese detection using actual footage

Controls

Once the navigation subsystem computes the relative position of the geese and sets the waypoint to follow. These waypoints are fed into the outer-loop control system of the autopilot which computes the course and climb set-point for the inner-loop control system. Based on these set-points, the inner-loop controls the roll and pitch angle by actuating the control surfaces (rotatable tail) accordingly. Both outer- and inner-loop control operates with a PID controller and Paparazzi OSP (Lisa/M) is used for the software and hardware of the autopilot. The attitude control of BirdPlane is done by adjusting the rotation and deflection angle of the tail, and the flight speed control (i.e. throttle control) is done independently by varying the average RPM of the electric motor. The throttle control also entails an active control of wing twist which is done by adjusting the phase lag of the two spars that constitute the wing. The main motor's RPM during upstroke motion is designed to be almost twice as high as the down stroke RPM in order to produce higher lift and thrust, like actual birds do.

16.6 Conclusions and recommendations

After the iterative design process, a detailed performance analysis was carried out, and it was verified that the current design of

BirdPlane would be able to fulfil most of the key requirements without having to compromise on the initial design goals. Some of the design outcomes even suggested that BirdPlane can potentially perform better than the primary expectations in terms of flight capabilities and functionalities. Such results led us to believe that the development and application of BirdPlane can set a milestone in the field of flapping-wing UAV technology.

Innovative design features of BirdPlane are summarized as follows:

- A sophisticated lightweight wing mechanism that allows mimicking the birds' flapping, folding, and twisting to a large extent
- Birdlike tail that can rotate, deflect, and fan in/out to change the surface area for stability and control.
- Iso-elastic neck which stabilizes the camera platform at the head
- Self-healing materials on the belly to absorb the landing impact and repair itself from damages
- Advanced computer vision system utilizing chromatic and stereoscopic thermal cameras to detect and track the geese
- Fully autonomous navigation and control system during cruise flight

Even though the current design of BirdPlane suffices most of the requirements, there are still many limitations within the design, as well as potential features which deserve further research and analysis. For the future development of BirdPlane, the following potential features could be (re-)considered more in depth:

- Optimization of cam crank design for more efficient operation
- Forward flapping motion of the wing (which could be observed in the flight of actual Barnacle Geese)
- Self-take off and soft-landing by flapping the wings
- Implementation of retractable feet for better stability and turning performance
- Following different types of birds and/or UAVs
- Completely autonomous take-off and rendezvous, using on-board processors only

17. BEST OF BOTH WORLDS, FLYING CAR, VOLUCREM

Students: J.M.A. Beth, S. Doljé, D.M. van Dommelen, O. Estrela Ortega, R.O.B. de Keijzer, M.J.M. Ketelaars, E. Van Lent, D. Rodríguez Alonso, P.E. Smit, R.H. Termaat

Poject Tutors: ir. R.N.H.W. van Gent

Coaches: ir. B.D.W. Remes, S.M. Kaja Kamaludeen, MSc

17.1 Introduction

There is a need for a new way of transportation, which can minimise the door-to-door travel time for distances between 200 and 1000 km. This way of transportation should be made personal such that it is not necessary to adjust a personal schedule to a public transport schedule. A flying car would be an ideal solution to this void in the transportation market. There is a problem however; there have been many attempts at the creation of a roadable aircraft none of which truly succeeded. Previous vehicles have been a combination of a good car and a bad aircraft or vice versa or have not been safe enough for regular operation. This imposes several restrictions and design considerations such that the designed vehicle becomes commercially attractive and technically competitive.

"The objective is to design a competitive, modular, flying carver type vehicle capable of flying within a 1000 km range and 200 knots cruise speed by 10 students within 10 weeks' time."

The flying car developed is named the Volucrem and should satisfy the mission needs statement:

"There is a need for a safe, sustainable, modular, and attractive flying carver with minimum difference in operation concept, a minimal door-to-door time at 200 knots cruise speed for a 1000 km range and is available before 2025 and with a market price below 500,000 euros."

17.2 Requirements

The stakeholders for the flying car have formulated certain requirements that have to be analysed with regards to their technical feasibility. Furthermore, the requirements should restrict the design of the Volucrem such that the vehicle meets the stakeholder standards. The requirements imposed were:

1. "Carver" type of road-able vehicle
2. Detachable flight modules (flight control surfaces, flight propulsion and wings and empennage)
3. Detailed cockpit interface concept (flight controls, display usage and possibly pilot wearable avionics)
4. 2 or 3 seats
5. Standard cabin luggage per person
6. Range minimum 1,000 km (15 min reserve)
7. Maximum ease of use between the two modes of operation (conversion time and checks < 30 min)
8. Maximum safety of operation
9. Design cruise speed 200+ kts at 80% of maximum power
10. Min rate of climb 500 ft/min, 500m field length
11. Very low noise levels <65 dB within a 200 m radius during take-off and landing
12. Easily storable and securable flight equipment
13. Low CO_2 emissions (< 150 kg/h)

14. Sustainability > 90% recyclable (built for disassembly)
15. Unit cost below 500,000 EUR
16. First flight in 2025
17. Life span of 25 years
18. Design for 20,000 flight hours
19. Comply with corresponding CS23 regulations

The requirements can be classified according to their estimated effect on the design. The key requirements are requirements that must be fulfilled such that the product is commercially attractive. These include 4, 5, 7, 8, 12, 15, 16, 17 and 18. The driving requirements are those that technically limit the performance of the vehicle such as requirement 2, 6, 9 and 10. Finally, potential killer requirements are identified these are requirements that are potentially difficult to fulfil such as requirement 11.

17.3 Sustainability approach

For the Volucrem aircraft to have commercial success it is imperative that a sustainability approach is developed. The requirements for sustainability impose limits on the amount of CO_2 emissions of the vehicle and the fact that the vehicle must be 90% recyclable. Therefore for the propulsion of the Volucrem it was designed for the use with biofuels such that the net emission of carbon dioxide is lessened compared to regular fuels. Furthermore, to meet the recyclability requirement, all major structural components are made out of aluminium due to its high reusability.

17.4 Conceptual design

With these requirements and mission, different configurations should be considered. For the generation of the configurations several design option trees were made for the different subsystems. Next, a trade-off was made on the roadable and the flight design.

For the roadable vehicle an enclosed motorcycle and a three-wheeled vehicle are considered. When looking only at the weight, the enclosed

motorcycle seems to be the favourable option. The disadvantage however, is the lack of stability at low speeds. For comfort and aerodynamic purposes, the motorcycle must be enclosed. Enclosing the motorcycle means there is a need for implementing a low speed balancing system, which increases the weight. The three wheeled system is slightly heavier than the motorcycle, but gives more stability and internal volume, with an easy integration of a banking mechanism and still makes use of the lenient motorcycle/tricycle certification regulations. Hence the tricycle configuration is chosen for the roadable part of the design.

The carver could be designed for two or three passengers. It is decided to design the vehicle for two people, since the first customers would be mainly businessmen who only need a seat for themselves and for one extra passenger, ultimately saving weight.

For the flight design, at first seven concepts were considered: a conventional aircraft with high, mid and low wing, a blended mid wing, a biplane, a tandem, a closed wing and a canard. After a preliminary trade-off, the conventional low and high wing and the canard were selected.

The benefit of the high wing is the ease of attachment, the low wing has less noise, due to shielding from the engine to the ground and the canard is aerodynamically, the most efficient. For these three configurations a class I weight estimation was done with the calculation of power and wing loading diagrams and fuel fractions. One engine is used in all concepts, which is placed in the middle of the wing, on top of the carver for structural benefits. The high and low wing configurations have an H-tail, while the canard has a high wing without extra tail. All three configurations can be viewed in figure 17.1.

The categories that are taken into account for the final trade-off are the aerodynamics, structures & materials, propulsion, operations, stability & control, operative empty weight, sustainability and marketing appeal. As a result of the trade-off, the high wing configuration is

selected. This configuration is favourable for its ease of attachment, ease of operations, its stability characteristics and structural weight. Performing a Class II weight estimation on this configuration, an operational empty weight of 831 kg and a maximum take-off weight of 1206 kg is found, with the weight of the flight module of 366 kg and the weight of the carver of 465 kg. During these estimations, it is found out that flying with a turboprop would be much more efficient, and therefore a flight altitude of 7000 m is chosen.

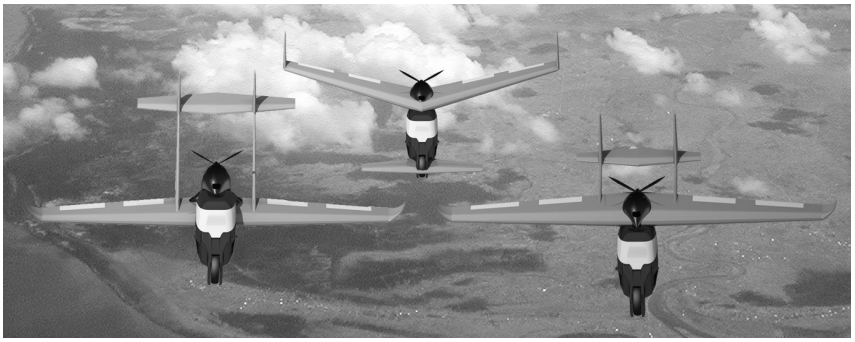

Figure 17.1: Three initial concepts

17.5 Detailed design car module

Layout

The three-wheeled banking car is designed such that it is lightweight and aerodynamic for optimal flight, with one door on the left to enter the vehicle. It has a length of 4 m, a height of 1.5 m and a width of 1.2 m. The car module has a maximum range of 230 km and can drive up to a speed of 180 km/h. It has an empty weight of approximately 465 kg. It has been given an aerodynamic shape, hiding the attachment part on the road. The roll cage is designed such that it can cope with 8g, which is the maximum landing load scenario. Figure 17.2 shows the look of the Volucrem in drive mode.

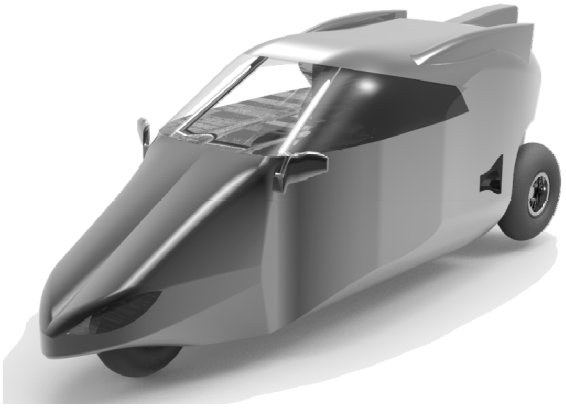

Figure 17.1: Side view of the carver type vehicle

The main customer is expected to be used to luxury as well as efficiency, therefore the Volucrem aims to fulfil the same role. Several electronic systems are dedicated to assisting the driver and improve safety and comfort. Aside from the car electronics, the flight electronic systems are stored in the car, all with their respective backup. A modern glass cockpit with a modern double-screen dashboard interface (one of which is a touchscreen) and an M-yoke control column will grant similar controls on the road and in the air.

In the car, multiple systems are implemented which can be divided into different categories: engine electronics, chassis electronics for a safer drive, safety electronics to prevent heavy injuries to the driver and passenger in case of a crash, driver assistance for easier drive and passenger comfort. In flight, most of these systems are active and can be accessed through the dashboard screens.

The wheels of the car are not only used for driving, but also for taxiing and landing. This saves both weight and complexity. As aircraft tires are under higher pressure than car tires, aircraft tires are used which are filled with nitrogen in order to prevent thermal expansion. A combined braking system is implemented for comfort, using normal motorcycle disc brakes. A modular suspension system is used for the Volucrem. It can be placed in three modes with the use of

a bleed valve: flight mode (fully retracted), drive mode (half-way extended) and landing mode (fully extended).

Control

A tilting system controls the turns and makes sure the vehicle does not tip over on the road. The dynamic vehicle control (DVC) system is implemented, which is effective from a speed of 10 km/h to 180 km/h. At lower speeds, the car turns with its front wheel and the tilting system is shut down when in flight mode, such that the wing is not damaged when performing turns during taxi. An M-shaped steering column is used for control (turning is controlled in a coordinated roll yaw motion), which is used to steer and to pitch in flight by turning and pushing or pulling. The push and pull motion is locked on the road, and due to the DVC system the conversion between the two modes is more convenient, which is also the reason why an M-shaped column is chosen. Rudder pedals are in the vehicle for redundancy purposes.

Engine

An engine similar to the Smart 880CDI engine is chosen because of its lightweight, its small dimensions and is able to deliver required power. The car engine will be used for the pressurisation and to power the electronic systems during flight, such that it's not a dead weight in the air. It weighs approximately 60 kg, has a fuel consumption of 4.3 l per 100 km and runs on diesel or biodiesel, for which a 10 l fuel tank is provided.

Pressurization

As the flight altitude will be 7000 m, pressurisation is needed in the aircraft. The cabin will be pressurised to a cabin altitude of 2500 m, which gives a difference of 33kPa. The sealing focuses on the door and the cables. Different valves are used to control the cabin pressure such that it is kept constant and safe.

17.6 Detailed design flight module

Main wing planform

The flight module that is to be attached on the car consists of a main wing, a push propeller and an H-tail. In order to produce sufficient lift for flight, a detailed design has been made for the main wing. A Joukovsky aerofoil with a camber of 1% and a thickness ratio of 17% is chosen for minimal drag and for providing sufficient space for fuel tanks in the wing. The different specifications for the wing can be found in table 17.1 and an overview of the vehicle's dimensions can be seen in figure 17.3. In order to reduce the induced drag, winglets are provided. For the tail the NACA0016 aerofoil is chosen. Plain flaps will provide extra lift with a ΔC_{Lmax} of 0.317.

Table 17.1: Wing specifications

Wing specifications	
Wing area [m^2]	13.08
Aspect ratio [-]	7.4
Wing span [m]	9.87
Taper ratio [-]	0.45
Root chord [m]	1.84
Tip chord [m]	0.83

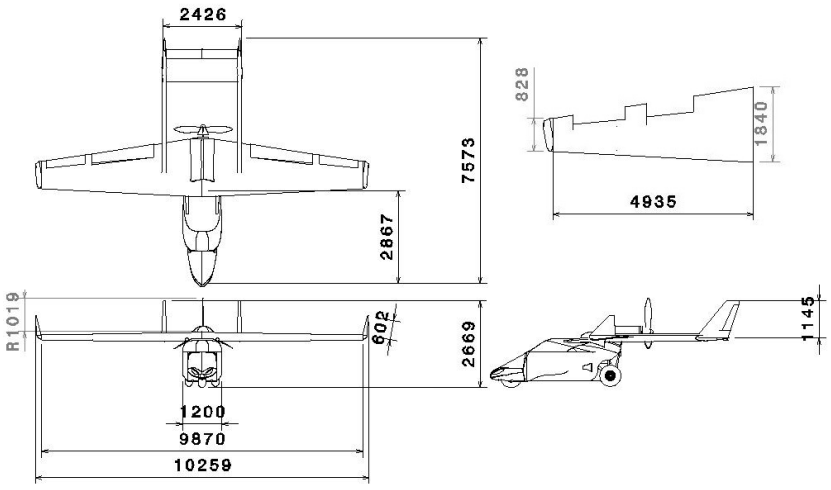

Figure 17.3: 3-side schematic view of the combined Volucrem

Empennage

First the aerofoil of the horizontal and vertical tail surfaces were determined. To reduce drag a simple symmetric aerofoil (NACA 0016) was chosen for both. The critical factor for the sizing of the horizontal tail surface was the rotation during take-off; the vertical tail was sized based on maximum sideslip. The rudder and elevator are plain flaps. The tail booms are sized for the forces during maximum manoeuvres and sideslip. The horizontal tail surface area is 2.5 m^2. The vertical tail surface area is 1.64 m^2.

Engine

Due to a higher power-to-weight ratio for turboprops compared to reciprocating engines, a turboprop engine is chosen for flight altitude of 7000 m. The engine has a mass of 57 kg and will deliver a maximum power of 180 kW. It is placed on top of the wing. 268 l of fuel is required for a 1000 km range at 212 kts airspeed, which is stored in the wing using two fuel tanks of 134 l each. A 50/50 blend of Jet fuel and Bio-SPK is used to meet the CO_2 requirement.

Performance

Since the flying car needs to fulfil different flight performance requirements, a performance analysis was done. Here the rate of climb, take-off field length, landing field length and range are determined. The theoretical rate of climb at sea level and cruise altitude are respectively 1848 and 1606 ft/min. Therefore the Volucrem can easily fulfil the stake holders' requirement of 500 ft/min. However during operations a maximum is set around 550 ft/min, because this is the human factors limit for comfortable flight. For both take-off and landing the field length was set to stay below 500 metres. It was calculated that the Volucrem's take-off field length is equal to 382 metres, and the landing field length is equal to 415 metres. Concluding the performance analysis a range of 1278 km could be achieved for maximum payload and 1698 for minimum payload (only pilot).

17.6 Attachment

In order for the vehicle to be modular, the ground vehicle and the flight module need an easy to operate attachment system, which transfers maximum loads and connects the electric systems of both modules. The solution found was a ball joint locked by an actuated securing mechanism, its main merit being the ease of operation as well as the lack of loose components. Its competitors were a pin system comparable to sail planes and a magnetic attachment system. The attachment system has been sized for the same loads as the flight module and roll cage, with the largest load occurrence at a pull-up or landing at a load factor of 8 g. Storage has also been considered; simple struts will support the flight module when a more suitable storage system is unavailable. These struts can be carried in the wings to ensure availability at the destination location. Attaching the system is done using the hydraulics present in the modular car; utilising its inherent mobility allows for ease of attachment as well as limiting supporting infrastructure.

17.7 Operations

To operate the Volucrem, an extended private pilot license as well as a motorcycle license is needed. The storage of the wing module is performed by means of a stacking system. The refuelling can be implemented in the stacking system. The conversion between modes can be performed within 30 minutes. When creating a business model, the unit cost of the Volucrem was estimated to be around 480,000 euros. Using the innovative flight module sharing method, the operational costs were drastically reduced. Finally, this product has been designed using sustainable materials and is expected to be 90% recyclable in 2050.

Manufacturing, testing and certification

The car module will be manufactured as a fuselage since the cabin is pressurised and the rear wheels will serve as landing gear. An important difference with an aircraft is the testing procedure; each product must be tested in flight as well as on the road. As an aircraft

flying en-route IFR, the Volucrem is certified by CS-23 regulations and carries the corresponding instrumentation. The road vehicle module is certified as a motorcycle or tricycle. The corresponding licences required from the operator are a private pilot licence extended with pressurisation and turboprop systems. To drive the ground vehicle a motorcycle licence with no limitation to power is required.

Storage, maintenance and business approach

When the Volucrem reaches the mass production stage several infrastructure facilities will have to be made available. Stacking the flight modules in a hangar will significantly lower storage costs and space. It also allows for centralised maintenance, further limiting operational costs and increasing availability of flight modules. Future opportunities for business plans include a shared ownership principle which lowers operational cost due to maintenance and unavailability of the flight module, online flight plan determination and automated refuelling, all aimed at reducing conversion time and ownership cost.

17.8 Conclusions and recommendations

The objective of this project was to design a roadable aircraft with capacity for at least two occupants and their corresponding hand luggage. It must have a range of at least 1000 km with a cruise speed of approximately 200 knots. As presented before, the result of this project is the Volucrem, the evolution of personal transport, a vehicle capable of joining the advantages of an airplane and the convenience of a car, leading to a low door-to-door time.

The designed roadable aircraft is based on a three wheeled vehicle with capacity for two occupants with their corresponding hand luggage. It is capable of flying within a range of 1278 km and 212 knots cruise speed. It will be available on the market by 2025 with a price below half a million euros and can be seen in figure 17.4.

Regarding its controllability, it is able to turn on the ground in a roll motion thanks to its banking mechanism. This reduces the operational

differences and allows the occupants to have similar sensations on the ground and in the air. Simplicity is also present in the attachment procedure. This allows the conversion between modes to be performed within 30 minutes. The market price of the Volucrem was estimated to be around 480,000 Euros. However, using the innovative flight module sharing method, the operational costs were drastically reduced. Finally, this product has been designed using sustainable materials and is expected to be 90% recyclable in 2050. All this makes the Volucrem to be the outcome of the evolution of transport.

Among the recommendations for future design modifications, a thorough analysis of the structure may be beneficial. In addition, a more comprehensive analysis of the controls and human-machine interface is necessary. Regarding the operations, a more detailed operational analysis is needed. With respect to the aerodynamic behaviour, a more in depth analysis could increase the aerodynamic efficiency of both modules and therefore the operational costs.

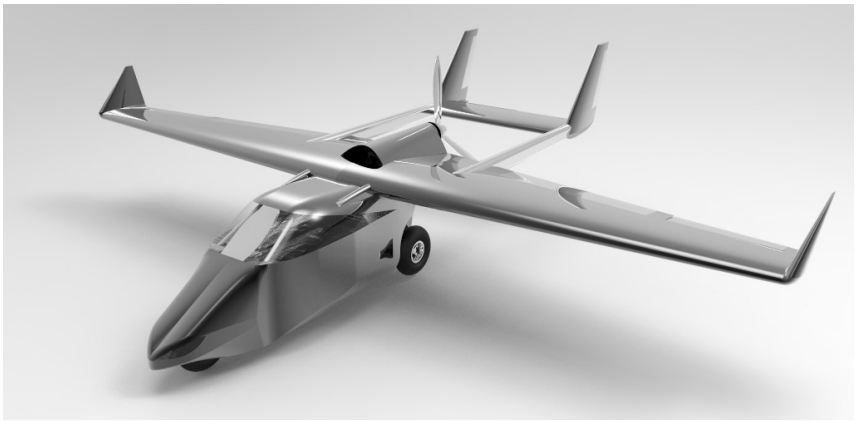

Figure 17.4: Volucrem Aircraft

18. MINIMUM FBW TRAINER AIRCRAFT

Students: N.O. Abuter Grebe, N. Barfknecht, A.J. van den Berg, M.J. van den Broek, J. van den Elshout, L.J. van Horssen, W. Jousma, F.G.J. Rijks, D. de Vries

Project tutor: dr. S.J. Hulshoff

Coaches: ir. O. Stroosma, dr.ir. A.Viré

18.1 Background

Accident rates in general aviation are 10 to 40 times higher compared to commercial aviation. On the one hand, this stems from pilots flying infrequently due to financial restrictions. This lack of practice may lead to inadequate responses in difficult flying conditions, potentially with fatal consequences. On the other hand, the high accident rate is caused by the increasingly dense aerospace, challenging coordination of airspace participants, especially in loitering circuits. A solution to this problem is the implementation of a fly-by-wire (FBW) system, which provides flight envelope protection (FEP) and decreases the pilot's workload.

Currently, the cost of FBW systems is a major drawback to the development of full fly-by-wire aircraft. The SAFAR project aims to develop the state of FBW technology to the point of practical application in light aircraft. Aurora Flight Sciences has already fitted a DA-42 with FBW/autoland and Diamond Aircraft is planning on

introducing FBW options on some of their aircraft in the near future. All of them feature full FBW operations with mechanical back-up.

18.2 Mission statement and requirements

The objective of this design synthesis exercise is:

"to perform the preliminary design of a FBW light training aircraft with minimum direct operating costs."

The incorporation of FBW systems into light aircraft will increase their usability in future airspace environments, ensuring general aviation remains possible. The aircraft will tackle the safety issues within general aviation using flight envelope protection and optional autoland functionality. A FBW trainer aircraft will also allow for more cost-efficient training of commercial airline pilots for the larger FBW aircraft. This design aims to provide the benefits in safety of FBW to the light aircraft market, whilst minimizing operating costs to compensate for the inherently higher costs of FBW systems over the conventional mechanical options.

Several requirements and constraints were given within the project definition, a minimum cruise speed of 90 kts, a minimum demonstrated crosswind of 15 kts, a minimum rate of climb of 800 ft/min, a minimum range of 800 km in solo training configuration, a minimum take-off distance (50 ft obstacle) of 500 meters, a maximum landing distance (50 ft obstacle) of 400 meters and emissions at or below the level of a Diamond DA-20.

18.3 Concepts studied and related trade-offs

Four concepts were considered before an aircraft configuration was chosen. These concepts are low wing aircraft with a t-tail, high wing with a conventional tail, a low wing combined with pi-tail and a low wing with v-tail.A class-I weight estimation and sizing was done for these concepts, which served as the basis for a trade-off. This trade-off was based on two criteria, namely low development risk and low

direct operating cost (DOC). The first criteria comes from the higher development risks induced by incorporation of FBW. For that reason, additional risk should be mitigated as much as possible. In the trade-off, the v-tail configuration was rejected because of the high development risk. The pi-tail appeared to be inefficient and was also rejected. The other two concepts scored equally in performance and therefore an additional trade-off was made between these concepts. This was done based on a market analysis and customer preferences. At the moment no new two-seater high wing aircraft are sold, since Cessna discontinued production of its new Cessna 162 due to technical problems. This presents a market opportunity for a new high wing aircraft. Another advantage of a high wing configuration is that it offers good visibility, which is important for VFR training. It is also more suitable for flight students learning to land because of the large wingtip ground clearance. Finally, a high wing enables easier (dis)embarking as pilots will not have to climb over the wing. This is advantageous as many general aviation pilots are of higher age due to financial and time constraints.

A high wing configuration with a conventional tail plane was chosen based on these trade-offs. In addition to the low development risk and DOC, this conventional configuration is also more suitable for ab-initio training. Training pilots in an unconventional configuration would not be sensible. Value increases because of this conventional configuration as market acceptance is improved.

For the landing gear a fixed tricycle configuration is used. The landing gear on this aircraft will be non-retractable, because of the low operating speeds. The additional aerodynamic drag will not outweigh the increase in weight and complexity that a retractable system incurs. Similarly, the tricycle configuration is chosen over a tail dragger because of the mission objective, which includes ab-initio training; tail draggers are harder to control and provide lower visibility on the ground.

A nose mounted tractor propeller is chosen for two reasons. Firstly, there is more room for the engine in the nose than in the tail, where

the vertical and horizontal tails are mounted. Secondly, the tractor configuration is the most conventional for trainers, improving the market acceptance. Furthermore, a side-by-side seating configuration was chosen, which is better for instructional purposes than a tandem configuration. The instructor will be able to closely monitor the actions of the student.

Table 18.1: Main design results

Design Parameter	Value
Surface [m^2]	11.43
Aspect Ratio [-]	10
V_{cruise} [m/s]	58
W_{empty} [kg]	419
W_{MTOW} [kg]	637.7

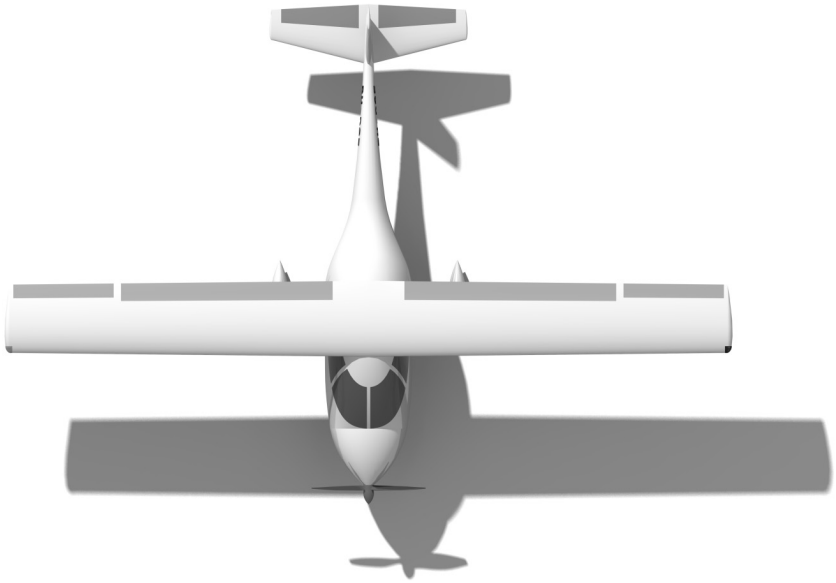

Figure 18.1:Topview aircraft

Figure 18.2: Sideview Aircraft

Figure 18.3: Frontview Aircraft

18.4 FBW concepts

In this section, the different options for the FBW system are presented and their advantages and disadvantages are discussed.

One of the safest options for the FBW system in terms of development risk is the FBW with a mechanical back-up. The advantage of this configuration is the high certainty of certification. The aircraft is controlled through FBW, but it may be disengaged to allow the aircraft to be flown with a conventional mechanical system. According to ARP4761 for certification, any failure that could lead to a catastrophic consequence should have a maximum probability of occurrence of 10^{-9} per flight hour. With a mechanical (back-up) system, the FBW could be designed for limited authority. This kind of system is only allowed to apply a limited control surface deflection on top of the mechanical output.

The other option considered is a full authority system. A full authority system is allowed to apply the full range of control surface deflections. Having a limited authority system is easier to certify than when full authority is applied, because the pilot can still overrule the FBW. If the choice is made for full authority FBW with mechanical back-up, a clutch has to be designed to disconnect the FBW in case of failure. Due to the lower redundancy level used in the limited authority FBW system, the cost of hardware of the FBW system is much lower compared to the full FBW systems. Therefore, the global market share needed to break even for FBW with mechanical back-up is 8.3% in a bad market. This is the lowest market share required by the different FBW configurations.

There are, however, also some disadvantages to the option of FBW with mechanical back-up. Firstly, the handling characteristics should be designed for control with mechanical flight controls. This means that use of a reduced stability margin is not possible when using a mechanical back-up system. Another disadvantage is that with a mechanical back-up system one is restricted to use soft limits (i.e. the pilot can override the flight envelope with excessive force) to maintain an acceptable actuator size. Because with hard limits (i.e. the pilot cannot override the flight envelope) the actuator need to overrule the force exerted by the pilot on the control surface.

The third disadvantage of using FBW with mechanical back-up is that in case of a failure the FBW is disengaged and the control is purely mechanical, which could lead to safety-related issues. The last disadvantage of having a mechanical back-up system is that it needs more maintenance, which leads to increased operating costs.

The second option that is considered is a full FBW system. With a full FBW system there is no mechanical backup, however the requirement to have a safety critical system still remains. To comply with this requirement, a full FBW system needs either triple or quadruple redundancy.

In the worst case approximation, a 12.5% and 16% global market share is needed to break even for triple and quadruple redundancy, respectively. Therefore the required market share for a trainer with quadruple redundancy will be probably too high for a newcomer with a high-cost product. As technology is developed further, reliability of components increases, and triple or maybe even dual redundancy can provide the reliability needed for certification.

A disadvantage of having a full FBW system is the difficulty of certification. Although FBW systems are already widely used in commercial airliners, business and fighter jets, such systems are still in the research and development stage for light aircraft. There are no specific certification specifications in CS-23 yet, therefore certification issues should be handled in close relation with certification authorities. Especially software reliability is subject to common scepticism, inducing certification difficulties. Another disadvantage is the additional complexity and power demand from an artificial force feedback system, which is necessary because of the CS-23 stick-force regulations.

The major advantage of FBW however, is that FEP is relatively easily integrated. Furthermore it also has more value as a safety system than FBW with a mechanical back-up, because the FBW system by itself will already have the safety critical failure probability of 10-9 per flight hour. This means that there is no need to switch to a back-up system, increasing overall safety. Another advantage of having a full FBW system is that the maintenance of the mechanical back-up system is not needed anymore, which potentially decreases the direct operating cost. Finally, the advantage of a relaxed stability margin can be explored with a full FBW system. Control surface areas can then be reduced, thus lowering drag and imposed stresses.

The last option which is considered is having a full FBW with graceful degradation. With graceful degradation the control surfaces are split up into several sections. All sections will have their own actuator, which can be downsized because of the lower hinge moments. In case of failure, the aircraft can still be controlled with the other partitions.

The main advantage of a system using graceful degradation is that there is no need for clutches in the FBW system. This could lead to a less complex actuation system, and thus could reduce the weight. Reducing the weight of the aircraft leads to a lower fuel consumption, which is beneficial for the direct operating costs. Another advantage is that a moving part is removed from the FBW system. Fewer moving parts can increase the reliability, since fixed parts normally need less service and last longer than moving parts. On the other hand, a disadvantage of graceful degradation is that, when an actuator is stuck, the aircraft manoeuvrability is reduced. Therefore the development cost and certification risk of full FBW with graceful degradation potentially increases. Based on the obtained results, it might be possible to obtain weight savings and cost reductions by using graceful degradation. The exact effects of using graceful degradation should be researched and certification possibilities should be discussed with the certification authorities.

18.5 Flight envelope protection

One of the main goals of this project is to reduce the amount of catastrophic failures in general aviation, especially with small aircraft. To reduce these failures, the use of flight envelope protection (FEP) in general aviation is investigated. There are two main methods, in which FEP can be incorporated. One being hard limits, meaning that the pilot can never override the FEP unless it is disconnected. The second being soft limits in which the pilot can still override the flight envelope with excessive force.

Both of these FEP philosophies have their own advantages and disadvantages. The main advantage of a hard limit system is that aircraft will always be in a safe flight regime, where with soft limits the pilot can still bring the aircraft in unsafe flight conditions. Especially for less experienced student pilots, it would be useful to have a hard limit FEP system. Student pilots are more likely to get confused about the aircraft state in a stressed situation. If the pilot does not know the aircraft state, he could still bring the aircraft in

unsafe conditions. The disadvantage of having a hard limit system is that it is hard to integrate into an aircraft which utilizes FBW with a mechanical back-up system since a hard limit system should be able to override the forces introduced by the pilot. A soft limit FEP does not have this limitation and could thus be used in a full FBW system and FBW with a mechanical back-up.

Another disadvantage of a hard limit FEP compared to soft limit, is that with hard limits the pilot cannot fly the aircraft at its full capability. This can have catastrophic consequences; for example when flying directly into a mountain, the pilot might want to overrule the flight envelope protection in order to save his life. Using soft limits, the pilot is able to override the FEP and could thus overstress the aircraft when needed. If hard limits are applied, an option to disconnect the FEP should be fitted. The pilot should however realize in what state the aircraft is when disengaging the FEP, otherwise it could have catastrophic consequences.

One of the main failures in general aviation is the failure to maintain airspeed. Therefore it is recommended to have a way to increase the airspeed of the aircraft. This can be done by either lowering the nose or increasing the throttle. Most accidents happen at low altitudes, where maintaining altitude becomes priority. Therefore it is recommended to have an auto throttle function in the FEP.

The way FEP is handled in aircraft is just a matter of philosophy. Where Boeing uses a soft limit FEP, Airbus aircraft use a hard limit FEP. When using a mechanical system, full authority is not recommended, due to the large forces the actuators should be able to give. When using a full FBW system however, it is a matter of preference which FEP system to use. Therefore, if full FBW is considered for the final design, one might propose to make it something that can be chosen by the customer.

18.6 Autoland system

One of the requirements of the trainer aircraft is to have autoland in solo training mode. Several autoland systems, such as Instrument Landing System (ILS), Microwave Landing System (MLS), Ground-Based Augmentation System (GBAS), Satellite-Based Augmentation System (SBAS), Visually-Guided Landing System (VSGL) and the Parachute Landing System were investigated.

The most feasible option was the SBAS system. The SBAS system is an enhanced global navigation satellite system (GNSS), which uses cross-continental ground stations. These ground stations ensure that differential corrections can be made for the GNSS, improving the accuracy of the whole system. The main disadvantage of SBAS is that it is only certified for CAT I approaches at this time, which does not cover the touchdown. Beechcraft and Aurora have investigated autonomous landing with the Athena 411 integrated flight control system, however development was cancelled due to the collapse of the general aviation market.

Since a full autoland is considered not to be feasible at this moment, an alternative solution was found. This alternative solution is a precision approach, which will only fly the approach till 250 and 200 ft altitude, for Europe and the USA respectively. A precision approach is less expensive than a full autoland system. The major advantage of having a precision approach is that it is already certifiable. Later on, when autoland for general aviation is closer to certification, it could be implemented in the aircraft instead of a precision approach.

18.7 Conclusion and recommendations

General aviation aircraft have an accident rate 10 to 40 times higher than commercial airliners. Therefore a study has been done, researching the feasibility of a fly-by-wire (FBW) aircraft with flight envelope protection (FEP) and autonomous landing capabilities. The whole FBW system has been integrated with the design of a general aviation aircraft.

The preliminary design study resulted in a two-seater, single engine, high-wing aircraft with a conventional tail. The aircraft has a maximum take-off weight between 628.8 kg and 681 kg, depending on the chosen FBW layout. The layouts considered are FBW with mechanical back-up, full FBW and full FBW with graceful degradation. When a mechanical back-up is used, a market share between 6.3% and 8.3% is needed to achieve the maximum selling price of 400k€. When full fly-by-wire is used triple redundancy is probably required. This results in a needed market share of 9.4% and 12.5% to achieve the maximum selling price. To protect the pilot from unsafe flight conditions, flight envelope protection is implemented. This can be done either using hard or soft limits. When using a full FBW system it is just a matter of philosophy on which system can be used. When using a mechanical system however, it is more logical to implement soft limits. For complementing the FEP, an auto throttle function is suggested for low altitude airspeed control. Another method for inducing an increased airspeed is lowering the nose, which is not advisable at low altitudes where most crashes happen.

The autoland system, as a "digital parachute", seems unfeasible with current hardware techniques. Certification of such a system will depend on research of other companies. Therefore, a precision approach feature has been chosen which will only fly the approach till 250 and 200 ft altitude, for Europe and the USA respectively.

To conclude, it can be said that development of a full FBW trainer aircraft is technically possible. Certification and financial feasibility remain uncertain. Therefore it is up to the investor to choose whether or not he wants to take the risk of investment in a full FBW system. The more safe option, in terms of certification risk, is to have a mechanical back-up system. The main disadvantage of using a mechanical back-up system lies in the associated limitations, such as the required stability margin and difficulties in applying hard limit FEP.

In order to actually achieve the use of FBW systems in a small trainer aircraft and improve safety in general aviation, some future research

is suggested. First of all, this is only a preliminary design study. Therefore, the general aircraft design should be further refined and detailed. An interesting field of research may be the reduction of hinge moments on the control surfaces by adding balance horns or smartly placing the control surface hinge lines. This may decrease the power consumption of the FBW system and ease certification. It is recommended to do extensive research on the hardware layout of the FBW aircraft and gather more specific information on FBW components. In this study detailed information, on actuators in particular, is still sparse. Manufacturers of such actuators, sensors and flight computers may be contacted in order to gain more information in terms of weight, dimensions, power consumption and reliability of these components. Especially the reliability of all FBW components is an important issue which demands more specifics. More advanced knowledge of reliability figures is required to interact with certification authorities and thus directly influences the success of the FBW trainer.

Finally, additional research is suggested on different methods of employing FEP and its potential for accident and fatality reduction. This information can help to convince flight schools and private owners of the enormous advantages a FBW trainer has to offer and help strengthen the position on the market.

19. 4-PROP: FOR PERFORMING RESCUE OPERATIONS PERSISTENTLY

Students: I.K. Ashraf, M.C. Butijn, Z. Liu,
M.P.R. van Moorselaar, M. Pfahler, M. Scherff,
M. Siddiquee, S. Unni, J. van Wensveen, P.L. Wyzen

Project tutor: dr.ir. Erik-Jan van Kampen

Coaches: Q. Guan MSc, D. Mehta MSc

19.1 Introduction

Micro Air Vehicles (MAVs) recently received a lot of interest due to their small size, low weight and wide range of applications like aerial photography and remote observation. Their ability to traverse ground obstacles and to provide an aerial overview whilst being small enough to fly inside makes them particularly suitable for Search and Rescue (SAR) missions. They can provide useful information such that emergency services can take safe and efficient action. This will ultimately prevent injuries and safe lives. A SAR mission is the objective of this year's International Micro Air Vehicle (IMAV) Conference and Competition.

IMAV is organised to stimulate the focus on research that can be used for real life scenarios while allowing the various research groups from around the world to share their knowledge. This year the competition consists of a single mission that combines both outdoor and indoor mission elements with a focus on the following tasks: surveillance,

object recognition, endurance, and multi-MAV operations. During the mission a jury will judge the design of each team based on a number of different criteria. Examples of these criteria are the level of autonomy, overall performance and the dimensions of the UAV (Unmanned Aerial Vehicle).

19.2 Project objective and design requirements

The goal of this Design Synthesis Exercise (DSE) project is to design a single-UAV system that will compete in the IMAV 2014 competition. The objective of this DSE project has been stated as:

"To design a single-UAV system that will impress the jury of the IMAV 2014 competition."

The IMAV competition poses a number of top-level requirements on the UAV system design:

- The system shall have a mass smaller than 5 kg.
- The system shall have a maximum momentum smaller than 20 Ns.
- The system shall have a maximum dimension less than 150 cm.
- The system shall comply with the Dutch law.
- The system shall use an electrical propulsion system.

Additionally, following from the DSE assignment the system cannot cost more than € 5,000. Within the team it was decided that the MAV should be able to perform all mission elements of the IMAV competition. This year (2014) the mission consists of the following elements:

- Create a map of a small village hit by a major natural disaster indicating possible road obstacles.
- Quick visual inspection of buildings to recognise house numbers and find possible entry points.
- Detailed inspection inside buildings searching for survivors and objects of interest.
- Landing on a roof to observe and report a number sequence of a digit panel across the street.
- Precision landing at specified landing zone.

19.3 Conceptual design and trade-off

During the initial design phase, several straw man concepts were generated individually by all group members. These concepts were then grouped into five broad categories, based on which five different concepts were chosen and further developed. A preliminary design of the five concepts as well as a trade-off of these concepts is presented below.

Ducted fan

As the name suggests, this configuration is primarily composed of a fan which allows the MAV to generate lift. Control surfaces are placed underneath the duct and are sized to counteract the maximum torques that occur during forward flight. Four control surfaces are used in order to provide controllability in all directions while also allowing for yaw control. An illustration of the concept can be seen in figure 19.1.

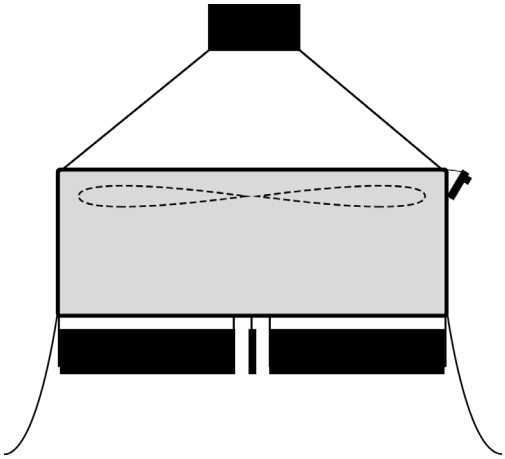

Figure 19.1: Ducted fan

Flapping wing

The flapping wing concept aims to make use of wing flapping so as to generate lift and thrust. After evaluating insect-like flapping and bird-like flapping, the latter combined with a jumping mechanism is found to be best suited for the mission at hand. The concept is designed such

that it is longitudinally stable and is controlled using the tail, the flapping rate and the twisting of the wing.

Flying wing

The flying wing is the only fixed wing concept evaluated during the conceptual design phase. The concept makes use of two counter-rotating rotors place on the wing itself to allow for vertical take-off, with two propellers on the front for forward flight, as seen in figure 19.2. Furthermore, the presence of a fixed wing makes this choice extremely appealing for covering long distances efficiently.

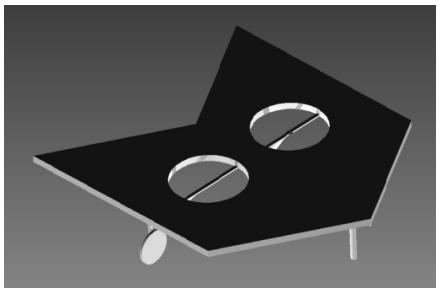

Figure 19.2: Flying wing

Helicopter

The helicopter aims to generate lift efficiently while providing a high level of agility and manoeuvrability. A classical configuration consisting of a single rotor with a tail rotor is selected.

Multirotor

Various multirotors were evaluated, at the end of which the conventional quadcopter is found to be the optimal design. The preliminary design can be seen in figure 19.3. The quadcopter is the most common design for MAVs that require hover capabilities. It is controlled by changing the torque on the four rotors, depending on the motion that is desired. Although unstable, this concept is highly controllable and has good manoeuvrability characteristics.

Figure 19.3: Quadcopter

Concept trade-off

In order to determine which concept was best suited for the mission at hand, a trade-off was performed based on the criteria that were found to be most relevant in terms of completing the mission effectively. Each concept was given a score from 1 to 5 by every team member (5 being the best), which was then multiplied by the normalised weight for each criterion. The results of this weighted sum trade-off are presented in table 19.1. It is worth noting that the winning concept, the quadcopter, has a total score that is 8.5% higher than the next best concept, the ducted fan. This sizeable difference suggests that the results of the trade-off are conclusive.

Table 19.1: Concept trade-off

	Ducted fan	Flapping wing	Flying wing	Helicopter	Quadcopter
Speed	14.25	24.94	47.50	35.62	58.19
Dimension	83.33	18.33	40.83	45.83	63.33
Safety	49.35	49.35	44.54	12.04	32.50
All weather	37.88	26.40	29.85	33.29	51.66
Ease of deployment	37.98	21.10	33.76	37.98	47.48
Agility	37.46	13.29	24.17	48.33	58.00
Payload capacity	70.08	16.76	39.61	60.94	63.99
Maturity of concept	30.22	12.09	25.18	48.35	44.32
Total	360.56	182.27	285.44	322.39	419.46

19.4 Detailed design

During this phase of the design, the selected design is elaborated. As explained in the previous paragraphs, the quadcopter is the winner of the trade-off. The detailed design is driven by the following criteria: perform all missions, autonomy, reparability and modularity and lightweight.

Structure

The structure of the quadcopter consists of four beams, two centre plates, four feet, a payload bay and fasteners. Sandwich panel material is used for the beams (foam and carbon fibre reinforced plastic). The beams are designed such that the MAV can fall from 50 cm high without breaking. The four beams are screwed together between the centre plates. This choice was driven by the maintenance criteria. The plates are composed of carbon fibre reinforced plastic as well. They were designed to minimize the deflection as much as possible.

The same material is used for the V-shaped feet. This shape provides structure stiffness during landing on rough ground. The length of the feet is 150 mm. The VDECS (Vibration Damped Electronic and Camera Structure) houses the main on-board electronics. It is located below the centre plate and connected through rubber dampers. Nylon bolts are used to hold all parts together. These cheap and lightweight bolts are sized to break before the structure does. Once again, maintenance has driven this design choice. A 3-view drawing of the designed MAV can be seen in figure 19.4.

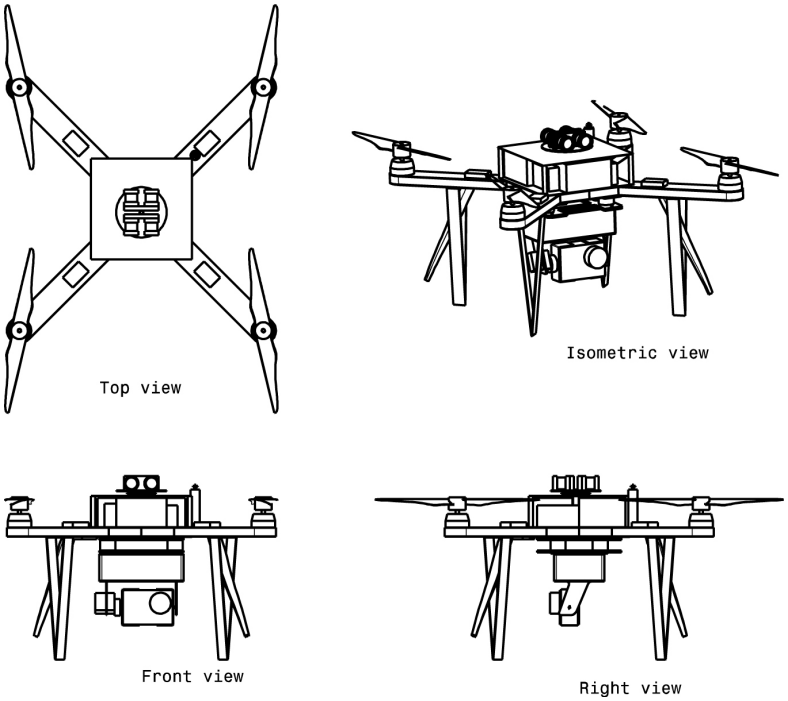

Figure 19.4: 3-view drawing of 4-PROP

Propulsion and power

Different rotor configurations were studied by the propulsion group: variable pitch blade, (fixed) tilt rotor and a conventional configuration. For the sake of simplicity and robustness, the tilt rotors and variable pitch blade configurations are pushed aside before the trade-off. The remaining possibilities are the conventional and fixed tilt configuration.

A trade-off showed that the conventional configuration was best suited for the mission at hand. Subsequently a second trade-off was performed to select an appropriate aerofoil, which yielded the Arad6-il aerofoil as the most suitable for the propellers. The propeller itself was designed using QProp. It has a diameter of 200 mm and a typical rotational velocity of 9150 RPM during hover. The use of electric engines is compulsory by the competition rules. From online catalogues, a brushless DC motor manufactured by Turnigy was selected. It can reach 15,000 RPM and has a motor velocity constant of 1080 RPM/V. The flight performance is calculated with a simulation in

Solidworks: 155 W are required to reach a cruise speed of 14 m/s. This will be the maximum speed allowed by IMAV regulations during the competition.

Besides the propulsion of the MAV, the power subsystem was also designed. Three lithium-ion battery packs are taken on-board and each pack contains 7 cells providing 3.8 V. These were selected based primarily on power requirements and operational time. Additionally energy density, voltage and discharge rate were considered. The batteries have a mass of 700 g, almost half of the total mass of the MAV.

Communication

Different types of communication technology exist, for instance laser communication, radio, WLAN and 3G. The selection was based on the range and the bandwidth. FSO (Free-Space Optical) and radio communication were the winners of the trade-off. However, since FSO requires a clear line of sight, it was decided to only use radio communication. The data to be transmitted are divided into four packets: command, control, status and imagery. The two first packets are data from the ground station to the MAV and the two last packets from the MAV to the ground station. The imagery packet uses the 1.3 GHz frequency while the others use the 2.4 GHz frequency spectrum.

The frequencies were selected in order to meet the range requirements and to comply with European regulations. The imagery packet has the largest data volume as the pictures and the live feed are transmitted to the ground station. The data rate for this packet is just under 60 Mb/s. The packages are in the order of kilobits. Since different frequencies are used, different transmitters and receivers have to be used as well. However an antenna diplexer allows the use of the same antenna for all frequencies. The final stage of the communication subsystem design is the antenna selection. After the first iteration a pair of whip antennas is selected to provide an optimal radiation pattern. A budget link analysis was performed for outdoor and indoor communication. It showed that the MAV can communicate through a 30 cm concrete wall.

Sensors and processing unit

The quadcopter requires sensors, a processing unit, an imaging system and a navigation system for both indoors and outdoors. Two categories of sensors are established: the primary and secondary sensors. The primary sensors are the Inertial Measurement Unit (IMU) which consists of accelerometers, gyroscopes and magnetometers. The barometer and the GPS also belong to the primary sensor group. They are related to the MAV's behaviour and attitude.

The secondary sensors are mission related: RGB cameras, ultrasonic sensors, LIDAR system and gas sensor. This last sensor is a personal touch which goes beyond the competition. Knowing if dangerous gasses are present in the catastrophe area allows the emergency services to take appropriate actions.

The processor selection is driven by the required processing power and the interfaces. From those criteria the Hummingboard / Navio combination was selected based on a trade-off. The Hummingboard has a 1 GHz quadcore processor. The Navio system hosts the autopilot. This whole operating system is Linux based.

Mapping the area and detecting objects are the primary goals of the imaging system. In addition it provides a live video feed. To achieve these goals two cameras are used: a small lightweight camera for object avoidance and a high resolution camera which will be tasked to map the area, provide the live feed and recognise digits and other objects. The selection for the camera configuration is an optimisation between mass and image quality. The high resolution camera is a 12 MP GoPro Hero3+, while the lower resolution camera is the Raspberry pi camera module which has a resolution of 1080p.

Finally the indoor navigation is ensured by a LIDAR (LIght Detection And Ranging) system located on the top of the MAV. It is placed on a rotating platform to cover a 2D plane of 360 degrees. Optimised algorithms will be used for the indoor mapping and navigation, also called Simultaneous Localisation And Mapping (SLAM).

Guidance, navigation and control

Before planning a path to its destination, the MAV needs to know its position. The GPS, IMU and camera are used for outdoor navigation, while the same IMU and camera, the LIDAR and the ultrasonic system are used for indoor navigation. The GPS attenuation is too high through the walls and the roof to provide a sufficient accuracy. The autopilot collects measurements form GPS, IMU, LIDAR, camera and ultrasonic system, merges them with all their errors and makes a state-estimation which exceeds the accuracy of all the individual measurements. Additionally it can compensate for time-dependent errors of the IMU by compensating for it with an external, independent measurement (GPS).

Object avoidance and trajectory planning are part of the guidance subsystem. To guide the MAV to its destination the camera, the LIDAR and the ultrasonic system are used. The Scale Invariant Feature Transform (SIFT) algorithm handles the collision avoidance with static or dynamic objects. The data generated by the SIFT and the SLAM algorithm are used to create the 3D trajectory. It also plans the velocity trajectory and can even plan the take-off and landing procedures.

The guidance subsystem sends commands to the electrical speed controllers which converts them to voltage inputs which change the rotational velocity of the propellers. This modifies the thrust and torques, which lead to a change in motion.

A linearization is applied to the equations of motion for a simpler gain tuning among other reasons. The controller has been designed for stabilisation: when an input is given, the controller will give the answers such that the velocities and the angular rates are equal to zero. This is done by first tuning of the gains of the inner loop (angular rates), followed by the angle loop, then the velocity loop and finally the position determination loop. To have a full working autopilot, it still needs to be designed in more details.

Ground station

Two people are mandatory to operate the Unmanned Aerial System (UAS) by Dutch law, however one operator is sufficient since everything is portable in one backpack. The MAV is controlled using a laptop. It has a shielded screen to retain visibility in bright light. Additionally it has a movable antenna to establish the data link with the MAV. All the data received by the ground station are stored to be reused later.

On the screen of the laptop the status of the MAV, batteries and sensors are displayed. The main item on the screen is a map on which you can give specific tasks to the quadcopter. The high resolution pictures taken by the MAV are processed on the ground station to make a map of the disaster struck area.

Finally the ground station also keeps in stock spare parts to repair the quadcopter or maintain it. This is a great advantage of a modular MAV.

Mission planning

The UAS will be able to perform the different mission elements as described above. All these tasks have to be performed with a certain level of autonomy. This level of autonomy has a large influence on the way the MAV is operated. A general mission process is described below.

After the technical checks the operator switches the quadcopter on. It initiates itself and awaits the input command from the operator. As soon as the mapping area and resolution have been determined and the take-off clearance given, the drone takes-off and flies over the area. The images are sent to the ground station computer where they are stitched into a map. The operator can then analyse the map and communicate the location of possible road blockages to his colleagues.

The next mission is a visual house by house inspection for survivors. The MAV is autonomous and therefore able to avoid obstacles and find its way through and out of the building. The emergency services

will be provided with floor plans of the buildings. The operator is able to control (redefine) the mission from the ground station at any time. The live video feed is also useful for the next mission element which consists of the observation of a building that represents a potential hazard to the emergency services.

The last portion of the mission is a safe and precise landing close to the ground station where the operator can collect the memory devices to analyse the high definition imagery. The user can replace the empty battery. The whole mission is performed in 30 minutes.

19.5 Conclusions and recommendations

4-PROP is a MAV that can perform SAR missions autonomously. It will provide emergency services with useful information such that they can take safe and efficient action. This information consists of:
A map of the area indicating possible road blocks, the location of buildings and corresponding house numbers.
A floor plan of a building indicating the location of survivors and other objects of interest.
Location and concentration of flammable gases.
Location and feature of user specified features recognisable with image feature recognition.

During the mission there will be a live video feed on the ground station. Additionally the MAV can land or hover to observe a specific building or area. The MAV designed consists of the following main design features:

- Maximum dimension of 610 mm.
- Total mass of 1442.5 grams.
- Maximum thrust-to-weight ratio of 1.75.
- Cruise speed of 20 m/s, maximum speed of 28 m/s.
- Consistent climb speed of 6 m/s, maximum climb speed of 8 m/s.
- 30 minute flight time.
- 12 MP high resolution camera.
- On-board LIDAR system for building mapping.
- Total MAV cost of € 1,643.

The ground station consists of a laptop, spare parts, a toolkit and additional batteries. It has a mass of 12,460 grams and a cost of €1,347.

The following recommendations are most important for further development of the design.

Currently, the propellers are designed using the same aerofoil throughout. However, since there is a high variation in the flow at different parts of the propeller, there is a significant possibility to optimise the propeller efficiency by making use of different aerofoils at different sections.

Currently, there is no investigation into the effect of the heat generated by the battery, the motors and the various other on-board systems. In addition, there is little knowledge about the operating temperature range of the product, and under what conditions it performs most efficiently. This is an important aspect to analyse further.

Currently, the LIDAR system has not been tested or even built. It will need extensive testing to measure its performance. It should also be tested in combination with the indoor navigation algorithms.
Currently, a linear DC-DC converter is used. In future development a switch mode controller should be considered. Although this system is more complicated, it will also be more efficient and will therefore increase the flight time.

Currently, the autopilot is only partially developed. In future work it should be elaborated and expanded for both hover and moving flight conditions.

20. THE LUNAR SECRET: LUNAR SAMPLE EXTRACTION AND CRYOGENIC RETURN FEASIBILITY STUDY

Students: N.O. Bernving, D. Brinkman, B.F. Gellert, A. Gonzalez Puerta, R.A. Makhan, A.M. Pronk, M. Smeets, M. Vergaaij, B. Verheijen, Y.H.J van Weersch

Project tutor: ir. R. Noomen

Coaches: ir. J.A. Pascoe, dr. M. Pini

20.1 Introduction

The Moon: a familiar sight to all. Ever since the dawn of mankind myths and theories have been put forward to try and explain her presence in the night sky. To test the current theories on her creation, detailed knowledge of the chemical composition of the lunar soil is needed.

The Lunar SECRet mission has been designed to recover exactly this information. It will extract a 2 m deep drill core from the lunar South Pole, store this sample below 120 K to prevent loss of the volatiles captured in the ice and return it to Earth for the scientific community to analyse. In short, it will unveil the lunar secrets.

20.2 Mission statement and requirements

DSE group 10 was assigned to conduct a feasibility study on a lunar cryogenic sample return mission. The mission statement was defined as follows:

"To retrieve a two meter deep sample from the Moon's surface without allowing its chemical composition to change."

After discussions with the customer, the following main requirements were agreed upon:

- The project shall choose a sampling area within 370 km from the South Pole of the Moon.
- The sample shall consist of a drill core down to at least 2 m depth.
- The sample shall be kept at temperatures lower than 120 K until retrieval on Earth.
- The sample shall be kept at temperatures lower than 120 K for at least 12 hours after landing on Earth.
- The mission shall launch no later than 2025.
- The life cycle cost of the mission shall not exceed €800 million including launch cost.

Sampling will take place at the South Pole of the Moon, due to the high probability of ice present in the lunar soil and due to the reduced helium-3 surface contamination caused by the Sun. The recovered samples will have to remain below 120 K in order to preserve their chemical composition. In order to ensure that the mission is competitive in the market, it will launch no later than 2025 and will not exceed €800 million.

20.3 Conceptual design and trade-off

In order to explore conceptual designs, a design option tree was created. This tree included all options, from tried-and-true options to theoretically possible ones. Several options were discarded after preliminary research, such as a manned mission, which exceeded the cost budget. To create the concepts that would be investigated, two

distinct variables were defined. The first of these was the choice of landing at or away from the permanently shaded sampling sites in the pre-selected craters. These craters are the Wiechert J, the Amundsen, the Shackleton and the de Gerlache. The other variable considered was the mission layout. The three options considered were to leave the re-entry vehicle in low Earth orbit, low lunar orbit or have it descent to the lunar surface. These variables were divided over five concepts, which are discussed below.

Concept 1
This concept is designed to land outside the permanently shaded area of the Amundsen crater, and therefore uses a rover powered by fuel cells to retrieve the sample from a permanently shaded area. This concept explores the scenario landing the entire spacecraft, including the re-entry vehicle, on the Moon. Since the concept lands inside the crater, direct line of sight to the Earth is impossible. Therefore this concept includes a communications-satellite.

Concept 2
This concept is designed to land near the edge of the Wiechert J crater and uses a walking hexapod rover to retrieve the sample. The rover makes use of radioisotope thermoelectric generators (RTG) to power and heat the system. This concept explores the scenario of leaving an orbiter equipped with the re-entry vehicle in a low lunar orbit, similar to the Apollo missions.

Concept 3
Concept 3 is designed to land near the edge of the Shackleton crater in a near permanently lit area. This concept also uses a rover, only in this case an already developed rover, specifically designed for this crater. This concept explores the scenario of leaving the re-entry vehicle in low Earth orbit.

Concept 4 and 5
These concepts are designed to land a stationary lander inside the permanently shaded area of the Wiechert J crater, and will therefore collect their sample at the landing site. Both concepts individually

decided to leave the re-entry vehicle in low lunar orbit, similar to Concept 2. The difference between both concepts is that Concept 4 uses RTGs to power the lander and Concept 5 uses a fuel cell.

Trade-off and final concept

A trade-off was performed using the following criteria (and their weights): sample quality (35 %), cost (25%), reliability (20%), development risk (10%), mission expansion (5%) and sustainability (5%). After this trade-off, Concept 4 and 5 were identified to be the most suitable candidate for further design. The mission makes use of a lander for operations on the Moon, consisting of an ascent stage and descent stage, and an orbiter which houses a dedicated re-entry vehicle. The Wiechert J crater at the South Pole of the Moon was found the most suited for both Concept 4 and 5 and was therefore chosen in the final concept.

20.4 Detailed design

After the trade-off process, a detailed design of all stages and modules were created. The outcome of this process is depicted in figure 20.1.

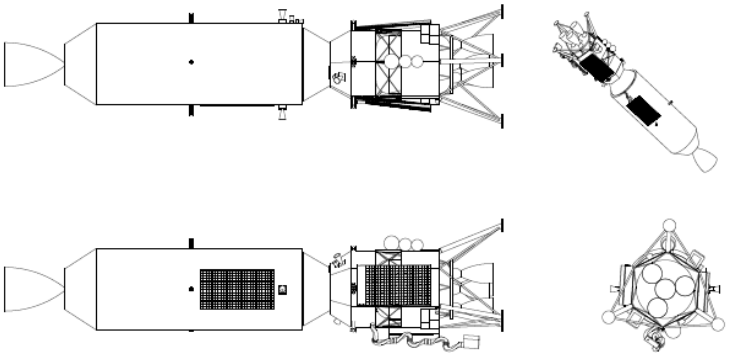

Figure 20.1: Three-view drawing of the complete spacecraft

Ascent stage

The ascent stage, as depicted in figure 20.2, serves to transfer the sample from the Moon to the re-entry vehicle. To this end it contains five major subsystems. The first two are the propulsion system [1] and

attitude and orbital control system (AOCS) [2] for the descent to, and ascent from the lunar surface, as well as for the docking manoeuvres. Third, the ascent stage contains part of the system needed for docking with the re-entry vehicle [3]. Fourth the cryogenic system used for sample storage [4] is housed in this stage. Last is the robotic arm located within the ascent stage [5]. This arm is used to transport the samples from the drill to the cryogenic system on the Moon and to place the cryogenic system into the re-entry vehicle after docking.

A support system consisting of struts is used to keep the connection between the ascent stage and the orbiter stable under the induced launch vibrations. These struts are removed after separation from the launcher.

When the ascent stage is on the lunar surface, it receives its power and heat from fuel cells located in the descent stage. During ascent and docking operations it is powered by solar panels and batteries.

Descent stage

The descent stage serves as an operational platform for the lander vehicle, as depicted in figure 20.2. Its hexagonal shaped body [6] is wrapped around the ascent stage's engine configuration and is attached to the latter's payload compartment. In the first place, it contains the structure required for the landing on the Moon. Most prominent in this are the lander legs [7]. These legs will firstly handle the shock loads induced by the landing and secondly ensure ground clearance for the engine during landing and take-off.

The descent stage also houses the fuel cell system [8] used to provide the lander with power during its decent and the operations on the Moon. The waste heat of this fuel cell will be used to keep the system at operational temperatures. The final main subsystem, the drill system is attached to the side of the decent stage [9]. This drill is an adapted ExoMars drilling system and will be used to retrieve the sample from the lunar surface.

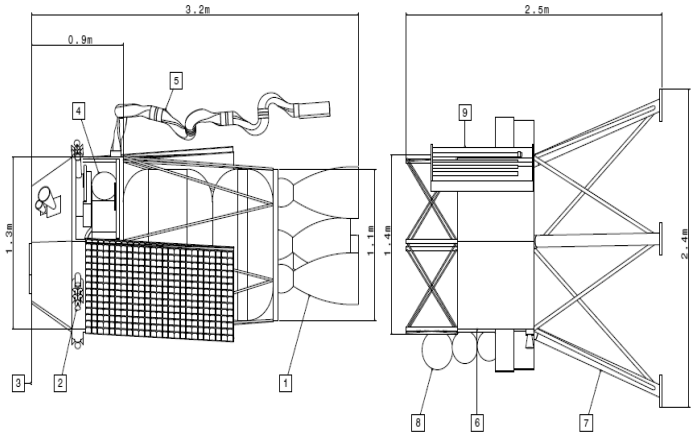

Figure 20.2: Exploded view of lander with dimensions with left the ascent stage and right the descent stage

Re-entry vehicle

After the ascent stage has docked to the orbiter, a hatch in the re-entry vehicle will open which allows for the placing of the cryogenic system with the sample, after which the ascent stage and docking mechanism are detached. Nearing Earth the re-entry vehicle is released from the orbiter.

The re-entry vehicle will enter Earth's atmosphere with a velocity of 10.93 km/s and a spin rate of 15 rpm for flight path stability. During its ballistic re-entry, the vehicle will experience high thermal loads and a maximum deceleration of 29 g. In order to cope with the thermal loads an ablative heat shield made from PICA was designed. This heat shield ensures the temperature inside remains within operational limits. The layout is presented in figure 20.3.

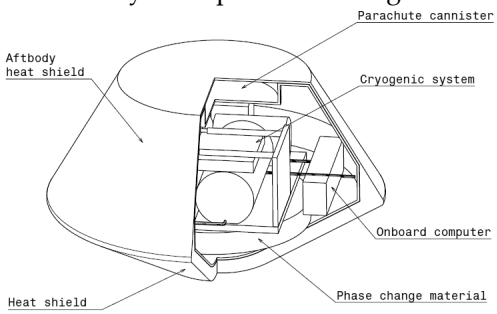

Figure 20.3: Overview of the re-entry vehicle

Orbiter

The purpose of the orbiter is to support the ascent stage, the descent stage and the re-entry vehicle during transfer to the Moon and transport the re-entry vehicle back to Earth. In order to perform these tasks, several subsystems are included. First, a propulsion subsystem performs the major orbital manoeuvres. This propulsion subsystem consists of a main LOX/RP1 engine and two large propellant tanks. Second, an AOCS system is present which ensures accurate pointing during the engine burns and the docking procedure. Prior to re-entry, the AOCS is also used to induce the aforementioned spin for re-entry. Third, solar panels provide electrical power to the orbiter and the coupled re-entry vehicle during the whole mission life, which is expected to be about 40 days from launch until re-entry. Lastly, a structural adapter keeps the re-entry vehicle in place and ejects it to initiate the re-entry procedure.

An overview of the orbiter can be seen in figure 20.4.

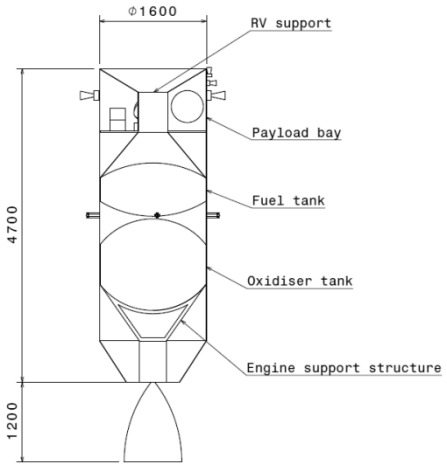

Figure 20.4: Overview of the orbiter with dimensions

The launch vehicle

The Falcon Heavy launch vehicle has been selected for this mission. This choice has been made, primarily because this launcher will be able to directly launch the spacecraft into a trans-lunar injection. This fact saves significant amounts of propellant and reduces the

spacecraft's complexity, since no additional kick stage is required. Furthermore, sustainability considerations played a part, since the Falcon Heavy is a partially reusable vehicle. Finally, the Falcon Heavy's fairing size and launch mass capability were an important factor.

The cryogenic system

To preserve the sample in compliance with the customer requirements, it needs to be stored at temperatures below 120 K at all times. These temperatures have to be maintained up to 12 hours after the landing on Earth.

To ensure the sample remains at cryogenic temperatures a cryocooler is used. For this mission, a two stage reverse-Brayton cycle cryocooler is selected and adapted to the specific mission needs. According to a conceptual study by NASA the maximum estimated thermal power input encountered will be 12 W, whereas the Brayton cooler provides a cooling capacity of 13.6 W at a temperature of 100 K. The cooler's mass is 32 kg and its power consumption is 480 W.

In space, the cooling flow used by the cryogenic system rejects heat into space using radiation. However, after re-entry, whilst in the atmosphere, this is not possible. Therefore a heat sink is used here to absorb the heat from the cooling liquid. This system allows for the extraction of large quantities of energy from the cooling liquid, without heating up notably.

The thermal power input drastically increases in atmospheric conditions due to convection and conduction to the ground. An aerogel insulation layer, placed around the cryogenic system, is therefore used as thermal insulator. The layer's required thickness is 6.6 cm and the mass of the insulation material is 7 kg.

The cryogenic system, which is a closed and insulated system during nominal operations, is designed to be able to open up and receive samples from the robotic arm. Furthermore, the whole cryogenic system is designed such that it can be transferred from the ascent

stage to the re-entry vehicle by the robotic arm. After this transfer, the orbiter and re-entry vehicle, now housing the cryogenic system, return to Earth.

Moon operations

After the lander has touched down on the Moon, the drilling operations start. The drill is lowered to the surface of the Moon using two linear actuators and when in place, drilling commences. The drill is designed to penetrate down to 2.2 m depth within six hours. After drilling the sample must be retrieved from the drill and placed into the cryogenic system. The first step in this process is to retract the sample from the ground to the top of the drill. Here a tool, attached to the robotic arm, is used to separate 10 cm sections from the rest of the sample. The robotic arm then transports this section to the cryogenic storage and places it in the sample container. This process of separating and storing 10 cm sections is repeated until 20 samples are retrieved. The last 20 cm of the sample taken from the surface and the tool used for storing samples are then left behind on the surface of the Moon, when the ascent stage returns to the orbiter.

Ground segment

The spacecraft will be launched from Cape Canaveral, Florida. ESA's ESTRACK ground stations will be used when the orbiter is less than 30,000 km away from the Earth (which is both after launch and before re-entry). NASA's Deep Space Network will be used when the orbiter is further away from Earth. Using these two networks, the orbiter can be tracked during the entire mission, except for the time spent in lunar eclipse. The spacecraft will, upon re-entry, land at the Soyuz landing site, which is located in the steppes of Kazakhstan. Here the sample will be recovered.

20.5 Mission evaluation

After the detailed design phase, a performance analysis of the spacecraft was performed. In this analysis, the reliability and risk, mass, power and cost were considered.

Reliability and risk

The reliability of the whole system was found by applying statistical failure rates. Data for individual subsystems were applied to an exponential reliability function, which yielded a reliability for the entire spacecraft of 96%. A risk analysis of the spacecraft's technical design was also performed. From this assessment, it was obtained that the drill system, robotic arm and the cryogenic system were the subsystems with the highest risk. The risks associated with these items will be mitigated by using proven technology, outsourcing detailed design to specialised companies and insuring the spacecraft against failure scenarios.

Mass and power

In table 20.1 the mass and power generated are shown for the four spacecraft modules. In the first row the total dry mass is shown, which includes a 20% ESA system level margin for every stage or module. This total dry mass is then used to compute the required propellant, which yields the wet mass as shown in the second row. The third row shows the total design power, which contains a 20% ESA system level margin as well. This design power is then used to compute the mass and size of the power supply system.

Table 20.1: Mass and power budget overview of the Lunar SECRet spacecraft. Total spacecraft power is not applicable

	Ascent stage	Descent stage	Orbiter	Re-entry vehicle	Total spacecraft
Total dry mass [kg]	665	417	777	433	2292
Propellant mass [kg]	1,766	0	2,469	0	4235
Wet mass [kg]	2,431	417	3,246	433	6527
Total power required [W]	1,672	247	1,283	937/738	N.A.

From table 20.1 it can be seen that both the decent stage and re-entry vehicle contain no propellant. For the decent stage, this is because the ascent stage engines are used for all manoeuvres of the lander. As a result, all propellant required for the lander is stored in the ascent

stage. Furthermore, it should be noted that two values are given for the total power required for the re-entry vehicle. This is due to the fact that the re-entry vehicle requires less power when awaiting retrieval than during re-entry.

Cost

The total life-cycle cost of the Lunar SECRet mission is evaluated using the unmanned spacecraft cost model (USCM8). This model is derived from the cost of 44 Earth-orbiting satellites and was validated using lunar and sample return missions to determine the offset for planetary spacecraft, which was found to be 23%. As part of the risk mitigation, the launch cost, production cost and flight support cost are insured for launch and in-orbit failures. Furthermore, the Falcon Heavy launcher is expected to have a launch cost of 135 M$. Using this launch vehicle and the cost model, after adding the 23% offset, the total life-cycle cost was found to be around 477 M€ for 2014 economic conditions.

20.6 Conclusion and recommendations

The total spacecraft design consists of an orbiter, ascent stage, descent stage and a re-entry vehicle. This spacecraft is designed to be launched into a trans-lunar injection using a Falcon Heavy launcher, which is anticipated to be operational well before 2025. In the worst case, if the Falcon Heavy would prove unavailable, the spacecraft could also be launched using an Ariane V with an additional kick stage. The expected mission time from launch to re-entry is 40 days.

Upon arrival at the Moon, the lander, which is composed of the ascent stage and descent stage, descends into the Wiechert J crater, which is located on the South Pole. There 20 samples, each of 10 cm length, are retrieved using the drill system and loaded into the cryogenic storage system using the robotic arm. The ascent stage uses the descent stage, which is left behind on the lunar surface, as a platform for take-off from the lunar surface.

Once in orbit the ascent stage will dock with the orbiter and transfer the cryogenic system containing the samples to the re-entry vehicle. The orbiter will then initiate a trans-Earth injection and the ascent stage is left behind in lunar orbit. Upon arrival at Earth the orbiter separates from the re-entry vehicle and burns up in the atmosphere, to reduce space debris caused by this mission. The re-entry vehicle continues to land in the Soyuz landing site, located on the Kazakh Steppe in Kazakhstan.

After analysis of the design, it became apparent that there are still some challenges left for the design to overcome. The biggest of which will be the cryogenic system which needs to withstand the g-loads and thermal loads that are produced by the re-entry procedure. In spacecraft, cryogenic systems are generally used for cooling propellant tanks and lenses, and are therefore not designed for the 29 g loads associated with ballistic re-entry. Other elements in the spacecraft which needs more research are the drill system and the robotic arm. These will be stored and operated outside the body of the lander, as can be seen in figure 20.2, which means it will have to operate in environmental temperatures below 120 K.

If during more detailed design phases, additional resources are used to ensure the cryogenic and drilling system, and the robotic arm will perform as expected, it can be concluded that this mission is feasible. A 2 m deep drill core can be obtained from the South Pole of the Moon, it can be stored below 120 K and it can be safely returned to Earth. Using the Lunar SECRet spacecraft, the secrets of the origin of the Moon can be unveiled.

21. LIFT^2 – LIFTING INNOVATION FOR TRANSPORTATION: TAKING TRANSPORTATION TO A HIGHER ORDER

Students: M.J. Beuker, M. Bevernaegie, J. Büskens, P.J.H. Deldycke, K. Krieger, P.F.R. Massart, R.N.J. Rousseau, A.J.G.T. Scholtes, T. van Hemelen

Project tutor: dr. M.D. Bos-Pavel

Coaches: dr. W.N. Anderson, dr. D.Wang

21.1 Introduction and background

Natural disasters have increased in frequency and severity in recent years. Especially poorer and less developed countries struggle to cope with these problems on their own and require help from the international community. The Netherlands Red Cross has made it its mission to step in in such cases, providing resources and manpower to help mitigate the consequences for those affected. With support of the Netherlands Red Cross, the Hospitainer Company designs mobile hospitals capable of rapid deployment. One mobile hospital is made of six standard sized shipping containers for smooth transportation by land and sea.

As experience has shown after the typhoon Haiyan (2013) in the Philippines, this is still not sufficient to reach an adequate response time. Together with the Netherlands Red Cross, Hospitainer

Company issued the request of designing an aerial vehicle configuration capable of transporting containers to the disaster area and hence enabling a faster deployment of medical aid. This in combination with the TU Delft's scientific interest in unmanned multi-lift system has triggered the launch of the LIFT^2 project.

The top level requirements originating from the stakeholders are specified in the following list:

- twin-lift technology.
- autonomous flight
- transport a payload of 10 tons
- cruise velocity of 80 kts.
- maximum velocity of 100 kts.
- transport its maximum payload over a range of 200 km and return (200 km) after the load is dropped, without refuelling.
- hover for 30 min. during the mission.
- perform six missions per day

21.3 Conceptual design choice

In the conceptual design phase different types of rotorcraft were analysed in order to choose the best solution to the problem under consideration. Therefore current rotorcraft technology was evaluated with respect to the required mission, which revealed three possibilities. Furthermore different ways of payload attachment to the rotorcraft were investigated. Below the most feasible concepts are highlighted and illustrated in figure 21.1.

Concept 1

The first concept consists of conventional helicopters. This technology is most mature and has proven to work. A conventional helicopter consists of one rotor and one tail rotor. Another possibility with this concept is the tail rotor to be in a duct. This is called a fenestron. Fenestrons have the advantage of being less noisy and are generally less dangerous because the rotor is encased.

Concept 2

The second concept was chosen to be a coaxial helicopter. This type of helicopter consists of 2 main counter-rotating rotors. As the induced torque by the main rotors is cancelled out, there is no need of a tail rotor which leads to the main advantage of a compact configuration. Most existing unmanned rotorcraft are coaxial helicopters.

Concept 3

The third concept is the ducted fan. Here the main rotor is encased in a duct. Despite relatively few existent operational examples, this innovative concept is appealing because of its reduced power consumption thanks to the minimization of blade tip losses. Another advantage with respect to safety is the fact that when flying in twin lift configuration a collision will not necessarily result in a disaster.

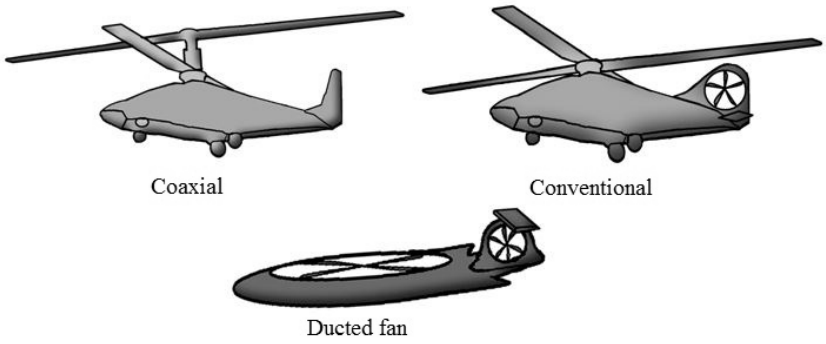

Figure 21.1: Conceptual design options

Trade-off

A trade off study has been performed between the different concepts. This study considers a quantitative comparison on the initial performance, cost and sustainability estimations of the systems, while the risk and RAMS (Reliability Availability Maintainability Safety) are qualitatively compared. The study indicated that the performance in hover and cruise as well as the sustainability levels are the main disadvantages of the coaxial concept, while the operational characteristics, such as cost and RAMS, demonstrate to be either

comparable or lower with respect to the other concepts. This gives sufficient reason to discard the coaxial design.

The selection of either the conventional or the ducted fan design proves to be less definitive, as both have a complementing set of advantages and disadvantages. The respective advantages of the ducted fan and conventional helicopter can generally be distinguished in the following two categories; performance and design maturity. The ducted fan shows considerably better performance and sustainability characteristics, while the design immaturity affects the estimated risk, reliability and maintainability characteristics. Whereas the proven design concept is associated with better RAMS characteristics. The performance and sustainable focus of the innovative ducted fan concept has been given preference over the mature conventional concept within the LIFT^2 development.

The inter-rotorcraft-payload connection method

In accordance with our mission the transportation of standard sized shipping containers is the main goal. There are again three possible options for attaching this payload to the rotorcraft. In order to choose the best option both stability and weight needed to be taken into account. Below the three options are stated.

Option 1

The first option is the so called pendant configuration. Figure 21.2 illustrates this concept. The lateral inclination of the rotorcraft result in a tilted lift force which in the end results in an increase of payload weight.

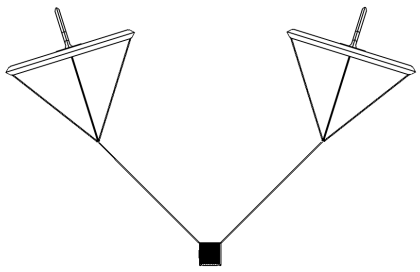

Figure 21.2: Pendant configuration

Option 2

This option consists of a rigid bar attached to both rotorcraft. This however has several disadvantages with respect to controllability and complexity. As the rotorcraft are meant for multipurpose use, the rigid bar needs to be able to disconnect.

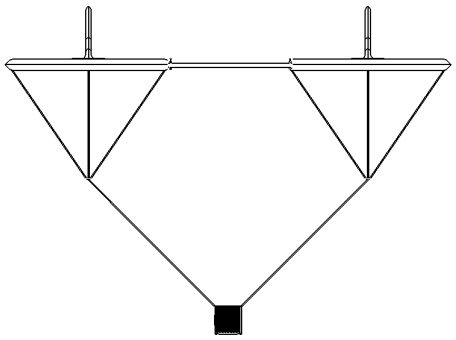

Figure 21.3: Rigid bar between rotorcraft

Option 3

The second option consists of implementing a spreader bar between the tethers below the rotorcraft and above the payload as shown in figure 21.3.Extra weight due to the bar is accounted for, but the main advantage of this configuration is the lift force that remains vertical.

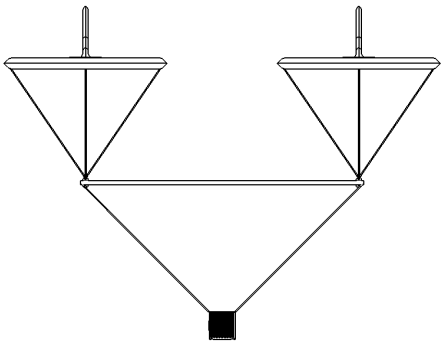

Figure 21.4: Spreader bar configuration

Payload connection trade-off

Option two will lead to structurally complicated attachment points, this would also lead to an unacceptable weight increase and therefore

is discarded. The addition of the spreader bar decreases the stability characteristics of the system with respect to the pendant configuration. As the control system of the collective unmanned system shall account for the total system stability in either method, hence more attention is paid to the weight increase. Thorough analysis pointed out that the increase in total weight was the smallest using the spreader bar configuration and hence this was chosen to be the best option.

21.3 Design

Fuselage

The fuselage serves as the main rotor duct so therefore its dimensions depend almost entirely on the size of the main rotor. The required volume for subsystem storage and fuselage drag considerations determine the height of the fuselage. While the width of the fuselage is sized by the main rotor diameter, the necessary arms for the tail rotors set the fuselage length. Figure 21.5 gives the main fuselage dimensions.

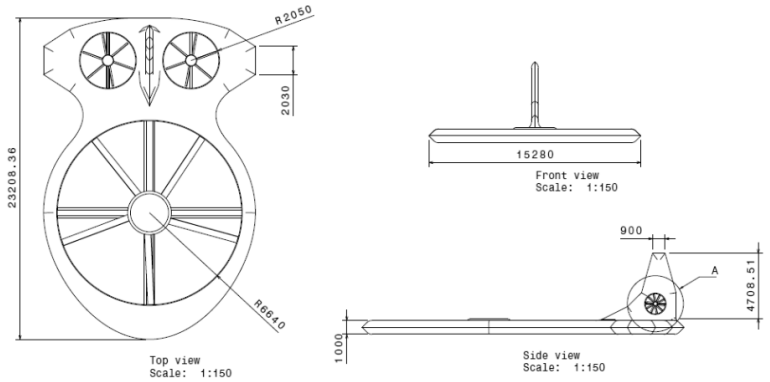

Figure 21.5: Main fuselage dimensions

The main load bearing structure in the fuselage is a ring beam. It has been modelled with the finite element method in order to determine material and thicknesses required to withstand the loads acting during the different phases of the mission. Aluminium has been chosen as fuselage material for weight and cost benefits. The tendency

of aluminium to form air- impermeable oxide layers gives corrosion resistance to LIFT², essential for operations in humid environments. The material choice leads to maximum take-off weight of 9.3 tons per rotorcraft. On the ground this weight is supported by a three-point landing gear made of aluminium. Wheels are favoured over skids to improve on ground handling.

Propulsion

Ducted fan technology has been chosen to increase propulsive efficiency for all rotors. The main rotor and horizontal tail rotors provide the thrust required during all phases of the mission. In accordance with the American convention the advancing side is on the right for the main rotor. The tail rotors turn against each other to reduce yaw-pitch coupling. For all rotors the sizing is optimized for the critical mission phase, which has been identified as cruise with payload. Blade twist has been chosen to enable optimum performance of each blade segment while limiting the twist to a polynomial distribution for ease of manufacturing.

The main rotor has 5 carbon fibre blades that are attached to a bearing-less hub made of the same material. Due to the hub choice the blades have a large flapping angle. As the shroud makes cyclic pitch unnecessary the total blade deflection from the normal horizontal is well within the limits for the shroud. As an additional safety measure the blade tips are made of an easily abrasive material to avoid severe consequences in the unlikely case of blade-shroud contact.

Two T700-GE-701 engines provide the required power for the main and all tail rotors. The engines are connected to the rotor by a drive shaft that runs through the fuselage cross. Per mission 1710 kg of standard aviation fuel are required to feed the engines. The use of an electrical engine has been investigated, though the amount of power required and the turn-around time have made this option unfeasible.

Control

Control inputs are generated by the three tail rotors: two horizontal fenestrons and one vertical. Equal thrust change of both horizontal

tail rotors causes a pitching moment while differential thrust induces a roll. Besides generating control moments the horizontal tail rotors aid the main rotor in providing the required thrust. The vertical tail provides anti-torque and yaw control. In cruise flight the tail rotors are unloaded by the corresponding tail surfaces.

Longitudinal static and dynamic stability have been investigated for a single vehicle and for the system. The equations of motions have been linearized around different flight conditions and the inherent stability of the ducted fan can be overcome with a PID controller. For the system more complex control algorithms are required to achieve stability.

Performance

Rotorcraft performance is best explained using diagrams, the most important of which is the flight envelope which shows the operating limits of the vehicle in terms of speed and altitude. Figure 21.6 shows the flight envelope of the entire system (i.e. two rotorcraft with payload). It can be seen that at 1,500 m altitude (i.e. the cruise altitude) the maximum velocity of the vehicle is 70 m/s. This velocity is dictated by the rotational velocity of the rotor which always operates below the drag divergence Mach number in order to prevent a huge increase of drag. The maximum altitude is reached at an altitude of 2,750 m.

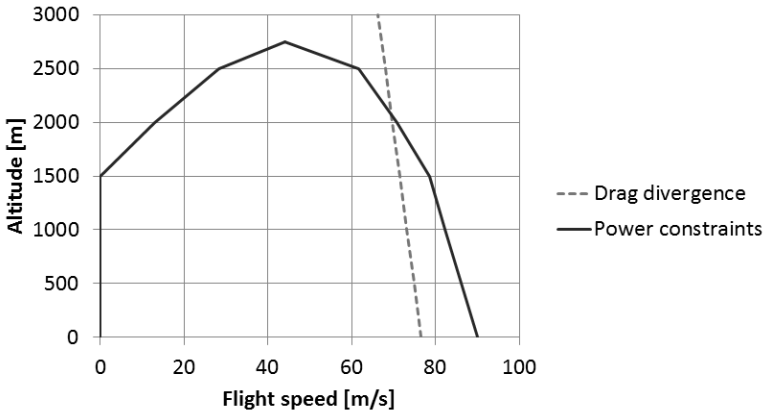

Figure 21.6: Flight envelope

Payload attachment

As outlined earlier a spreader bar configuration has been chosen for the payload connection. Steel cables are used to connect the spreader bar to the payload and the rotorcraft.

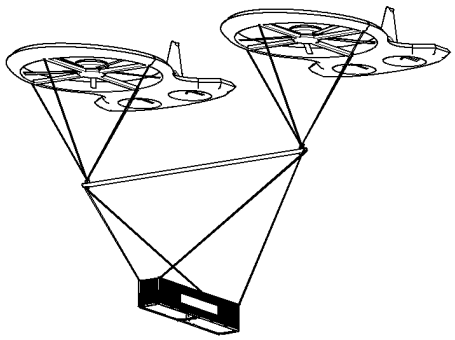

Figure 21.7: Rotorcraft with payload

The spreader bar is connected to four reinforced locations of the fuselage, where the fuselage cross intersects with the main structural ring. For payload attachment the rotorcraft take-off independently and hover while the spreader bar and later the containers are attached.

Communication and autonomous operation

Although the LIFT^2 system operates autonomously, a constant data link with the ground station is maintained for monitoring. The rotorcraft operate in a master-slave configuration. Commands and mission changes are communicated from the ground station to the master, which relays the commands to the slave. For line-of-sight communication the C-band is used, while beyond line-of-sight communication is achieved via satellite relay on the Ku-band.

Cost and risk

Three innovative concepts are combined in this design: twin-lift technology, ducted fan propulsion and autonomous operation. Innovation is always associated with risk and it has been a conscious decision to accept this for the design of the LIFT^2. For design and

operation of the LIFT² system the two major risk factors have been identified: the horizontal fenestrons and the control system. Both concepts are working theory models, which have not been proven in flight, and their failure would be catastrophic for the mission.

Innovative concepts require a high amount of research and testing, which has led to the design cost estimation of 7.1 billion US dollars.

Market

Although this project has been designed based on the needs of a humanitarian mission, the LIFT² system has possible applications in other markets. It is important for the system to establish itself outside this niche market to make the project a success and collect revenue. The offshore market, oil platform and offshore wind parks, is expected to have an increase in demand for rotorcraft. The demand is for medium to heavy lift rotorcraft with a range similar to the LIFT². Companies in this industry segment are possible investors, who can provide funds which are outside the possibilities in the humanitarian aid segment.

21.4 Conclusion and recommendation

The innovative design of the LIFT² has three major benefits compared to existing products: multi-purpose use, autonomous operation and fuel efficiency.

Autonomous operation increases the safety of the flight crew, which increases mission safety, especially for medical aid missions in war zones, while the fuel efficiency of the system lower the operation cost for the operator.

The conceptual design presented in this report complies with all stakeholder requirements and the preliminary design can commence. Based on the insight gained in the conceptual design, the following recommendations can be made for the project commencement:

- More iterations should be performed with the methods outlined to achieve higher efficiency.

- The degree of simplification used in the structural analysis of the load cases should be traded for more accuracy. Loads originating from vibrations need to be account for.
- Deflections of the structural elements (especially for the blade analysis) should be taken into consideration
- A detailed model of the flow over the fuselage needs to be developed in CFD. This model should then be validated with wind tunnel experiments.
- The investigation of dynamic stability should be extended to include lateral stability and control for both the single rotorcraft and the system.

22. PRINTING THE PERSONAL AIRCRAFT OF TOMORROW

Students: K.P.A.M. Barten, M. de Bie, T.P.A. Cheylus, I. van de Grift, I., C. Jux, S. van der Linden, M.M.J. Opgenoord, S.H.M. Peelman, K.F.S. Stoter, F.J. van Zanten

Project tutor: dr. C. Rans

Coaches: F. Tian, ir. H.J. Tol

22.1 Introduction

Additive Manufacturing (AM) technology uses a layer wise deposition of material to build up a part. Conventional production methods typically take a solid block of material and subtract material until the final geometry is achieved. It is a relatively new technology that could radically change aircraft design. DSE group 12 has investigated the opportunities and advantages of using Additive Manufacturing in the design of a small aircraft. The project mission:

"Design a manned experimental aircraft that has an airframe constructed using Additive Manufacturing technologies"

It is our mission to show what great possibilities are available using AM. Every project starts with an objective. In this case, this is to

design a manned experimental aircraft that has an airframe constructed using only AM technologies. To prove the concept, an aircraft that is able to take-off and land at Lelystad airport is designed. This aircraft should be a single seat demonstrator that is able to loiter for two hours at 4,000 ft with a speed of 85 kts. Furthermore the aircraft has to be in-line with the FAA requirements for a Light Sports Aircraft (LSA).

The most important constraint is the relatively small sizes at which the different AM techniques can print. Another limiting factor of AM is that there is a lack of knowledge on the properties of the materials after printing a part.

AM offers many opportunities, the first is in the material efficiency of AM because it does not remove material. The fly-to-buy ratio is increased dramatically. Where conventional production methods have a buy-to-fly ratio of 15-20, AM can get close to a ratio of practically one.

22.2 Concept development

The concept development and selection stage was split up in three general phases. Phase 0 comprised of an extensive literature study. One sub-team performed specific research into the application of metal AM products, while the second sub-team investigated components made of plastics. In phase I the team was redistributed into three sub-teams, each generating their own set of concepts. These three teams had their own subject to focus on. These are aerodynamics, conventional aircraft design and structural optimization. Firstly the three groups individually performed a trade-off between the concepts they generated. In phase II the final concept for each group was worked out in more detail after which a final trade-off was performed between these last three concepts as can be seen in figure 22.1.

Figure 22.1: Renders of phase II concepts

The aerodynamics group introduced a Blended Wing Body (BWB) design, in which the wing and fuselage are merged into one. One of the most striking advantages is its increased fuel efficiency because of its high aerodynamic performance. Since the "fuselage" is also generating lift, the lift is more concentrated to the middle of the aircraft. This decreases the bending moments on the structure allowing for a lower structural weight and for using low-strength materials. Furthermore, a BWB usually has complex curved shapes, especially for the "wing-fuselage" integration. Therefore, AM could offer some exciting opportunities for this concept.

Conventional design was defined as an aircraft with a main wing and horizontal stabilizer in the rear. The main strengths of this design can be found firstly in the use of an elliptical wing, which is an aerodynamically efficient planform that is relatively difficult to manufacture using conventional methods. Secondly, the wing, cockpit and landing gear are joined in a single location. This introduction of practically all major forces in a single joint, leads to a relatively simple load case for each part. They can therefore be more easily optimized individually. Also, bending loads in sub-parts are reduced due to this central load application.

Using a structural focus to generate concepts the idea of a tandem aircraft naturally arises: Two smaller wings can produce just as much lift as one larger wing though with a much lower bending moment at the wing root. This concept is configured with one forward wing in a low-wing configuration and one aft wing in a high-wing configuration. This configuration allows a reduction of the effects of downwash on the rear wing, increasing aerodynamic efficiency. Overall this configuration shows many advantages: It is structurally

efficient, very well suited for AM and the absence of a tail plane reduces the trim drag. The stability and more specifically, stall behaviour due to blanketing are challenges that needed careful consideration though.

22.3 Trade-off

To determine which of the three final concepts will become the final design that is worked out in the detail design a trade-off is necessary. For the trade-off itself the Analytical Hierarchy Process (AHP) was used. Graphical comparison was used to verify the AHP outcome. AHP is a mathematics and psychology based process that is used for multi-criteria decision making. It was decided to structure the trade-off criteria in correspondence with the following classes: Performance, Manufacturing, Structural Layout, Scheduling, Regulations, Sustainability and Others. It is however important to note that these have different weights in the final trade-off matrix as is indicated in table 22.1.

Table 22.1: Trade-off criteria and weights

Criteria	Weight [%]
Manufacturing	30.34
Performance	18.22
Structural	18.22
Regulations	9.45
Scheduling	9.45
Sustainability	9.45
Others	4.86

Finally, each of these criteria is evaluated for each concept. The results of this matrix are given in table 22.2.

Table 22.2: Final trade-off table for three concepts

Criterion	Parameter	Weight [%]	Elliptical wing	Blended wing	Tandem wing
Manufacturing	AM benefits	21.23	o	+	o
	AM focus	9.10	+	-	+
Performance	L/D	14.58	o	+	o
	Stability	3.64	+	-	o

Structural	OEW	12.75	-	+	o
	Assembly	5.47	-	-	+
Regulations		9.45	+	o	o
Sustainability		9.45	+	-	o
Others	Innovation	1.94	-	+	+
	Academic value	1.94	o	+	+
	Aesthetics	0.97	o	+	+
Final grade			0.0203	0.2575	0.2887

As can be concluded from table 22.2 the tandem wing concept that was generated by the structures group has the highest score. This concept continued to the detailed design phase for further development.

The tandem wing aircraft is specifically tailored to the needs of AM. It limits the loads on joints by distributing the lift over two lifting surfaces. Thereby it allows for greater use of non-metal parts which in turn is more sustainable, considering energy consumption during production. Furthermore, it fits well in the scope of the project. For this concept, a class II weight estimation has been performed. This leads to the weights and sizes as can be seen in table 22.3. Figure 22.2 shows the geometry of the final design.

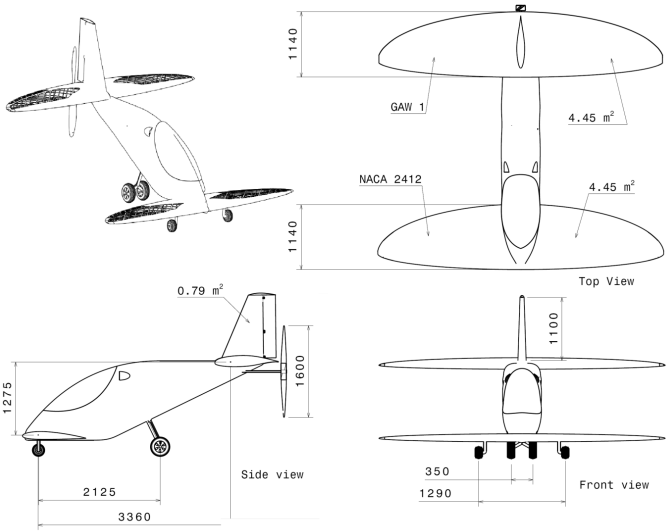

Figure 22.2: 3-view drawings of final design

Table 22.3: Component weights resulting from Class II weight estimation

Parameter	Value	Unit	Parameter	Value	Unit
Wing	83.5	kg	Furnishing	5.4	kg
Vertical tail	6.1	kg	Engine	64.0	kg
Fuselage	66.2	kg	Propeller	10.0	kg
Nacelle	9.2	kg	Operational Empty Weight	301.2	kg
Landing gear	28.6	kg	Fuel	44.7	kg
Fuel system	3.0	kg	Payload	100	kg
Flight control system	7.2	kg			
Electronics	17.9	kg	MTOW	455.9	kg

Table 22.4: Geometrical properties of final design

Parameter	Value	Unit	Parameter	Value	Unit
Lifting surface area	8.9	m^2	Fuselage length	4.5	m
Aspect ratio	5.5	-	Aspect ratio, vertical tail	2	-
L/D	11	-	Surface area, vertical tail	1.64	m^2
Wingspan	4.95	m^2	Take-off power	54.85	kW

22.4 Additive Manufacturing

While AM technology is praised as the revolutionizing future manufacturing technique, one large misconception is spread: AM allows one to create any part or product. This is not entirely true. Indeed, AM technologies enable the creation of complex and revolutionary structures in single parts, but still, AM technologies have their limitations as well. To better understand the difficulties encountered during the design process of the tandem aircraft, it is important to point out the most restraining limitations. These limitations are mainly: build volume, overhang angle, materials, anisotropy, tolerances, surface finish and production time.

Besides the limitations that are encountered in AM it still provides great design freedom compared to conventional manufacturing technologies. Precisely this design freedom proved to be a harmful factor in the aircraft design and development process: The variety of design options that can be considered is extremely large, and thus,

trading off all design possibilities becomes a time consuming process, if not impossible. Furthermore, design methodologies, analysis methods and sizing tools taught in academia are tailored to conventional designs. These are mainly based on the use of sheets, beams and columns. It proves difficult to escape this way of designing and sizing of structural components. Thus, inspiration for design solutions of some components is obtained from nature, also known as biomimicry.

The design freedom of AM translates into different design philosophies which can be used. The first philosophy considered by the team is the use of Topology Optimization software. This software determines the optimal material distribution, given a certain design space, the material properties and the several applied load cases. After obtaining the computer generated geometry this model is smoothed and subsequently validated using a Finite Element Analysis. This first design philosophy is implemented in the design of the vertical tail and wing roots. This design approach is promising as it can provide unconventional and lightweight designs. However, the big drawback of this design philosophy is its time requirement due to the suboptimal pipeline between Topology Optimization software and CAD software. Therefore another design method is required for this 10 week DSE project.

The second design philosophy is used for all other aircraft components. A conventional design strategy is chosen, mainly due to time-constraints. First, the applied loads under operating conditions are defined, and internal forces on a predefined geometry determined. From this, internal stresses are calculated and critical locations identified. From these, the geometry or material can be changed such that the maximum stresses are not exceeded. Once a conventional design has been made it is investigated how this can be fine-tuned such that advantages are drawn from using AM technologies. Examples include using smart edge fillets, introducing longitudinal offsets or cross-sectional gradients. For some parts, sub elements which are loaded in a single load-case are optimized in

Topology Optimization software on a small scale. This is done for instance for the fuselage-shear panels.

In conventional structural design, joints are often critical parts since load transfer from one section to another often leads to peak stresses. The major restriction of many AM methods is the size of which the components can be manufactured. This means that the aircraft has to consist of multiple sections which are connected at certain transition planes. The joining methods are therefore a crucial aspect of the design. The freedom offered by AM allows for more complex joints than those used in conventional design. Geometrical interlocking is for instance one of the options. In total there are three main joining areas: the wing-roots-to-fuselage connections, the wingtip-to-wing-root connections and finally the vertical-tail-to-wing-root connection. For the wing-roots-to-fuselage connections a geometrical interlocking slide system with an overlapping nut is used. The wingtip-to-wing-root connections are constructed using a system that both overlaps and uses a pin for interlocking. The vertical-tail-to-wing-root connection also uses interlocking with pins to keep the geometry in place. Of course every joint is individually customized for its load case.

22.5 Final design

Designing a tandem aircraft does not come without a thorough stability and controllability analysis. Contrary to traditional aircraft layouts, with a main wing and an empennage, the tandem aircraft has two lifting surfaces on both extremities of the fuselage. In addition both lifting surfaces generate approximately the same amount of lift and the exact distribution needs to be determined for aircraft controllability. To achieve static stability, the neutral point needs to be located behind the CG and different parameters affecting its location are investigated. The method used to determine the stability of the aircraft is based on the DATCOM method. Based on this method, the aircraft is statically, longitudinally stable. For controllability also the DATCOM method was used and confirms the aircraft is controllable

with the current control surface layout. For control actuation, a simple cable system is used as is custom in small aircraft.

From the final concept as came out of the concept development and selection the overall aerodynamic shape has been determined and the vertical tail has been sized. The aerofoils for these aerodynamic surfaces had to be selected. For both wings distinct aerofoils have been selected for stability reasons while the vertical tail also requires an individual aerofoil. The vertical tail uses a NACA 64A015 since it offers very good structural opportunities while the stall behaviour is beneficial and drag is kept to a minimum.

Concluding, five aerofoils were selected from a larger pool of 35 aerofoils. These five aerofoils continued to a separate trade-off for the front and a separate one for the back wing. The most distinct difference between the two is that for the front wing a low Cl_α is considered better, while for the back wing aerofoils with a high Cl_α have a clear advantage. Eventually, the NACA 2412 is selected for the front wing, while the GAW-1 proves to be most suitable for the back wing. The NACA 2412 is one of the most widely used aerofoils in the LSA category due to its good overall performance. The GAW-1 aerofoil's main advantages include low drag at the design condition, but a high C_{lmax} allowing the rear wing to stall later than the front wing, with the only large disadvantage its highly negative moment coefficient.

The final aerodynamic design is evaluated to see whether it meets all requirements and whether there are any issues associated with it. At high angles of attack, the blanketing effect has been identified as a high risk. One of the main reasons for performing an extensive CFD analysis of the aircraft was to investigate whether blanketing was indeed a problem for this aircraft. From this CFD analysis it can be concluded that the L/D ratio of the aircraft is very close to the value used for all preliminary sizing of the aircraft and requires no further design changes. One of the initially identified risks was the so-called blanketing effect. When at high angles of attack the front wing stalls, the rear wing has to operate in fully separated flow. This leads to the

stalling of the rear wing too, at which point the aircraft has no lift anymore. However, the blanketing effect is less of a problem than anticipated. Only at an angle of attack of 25 degrees it becomes an issue, though this angle is never reached in normal flight conditions.

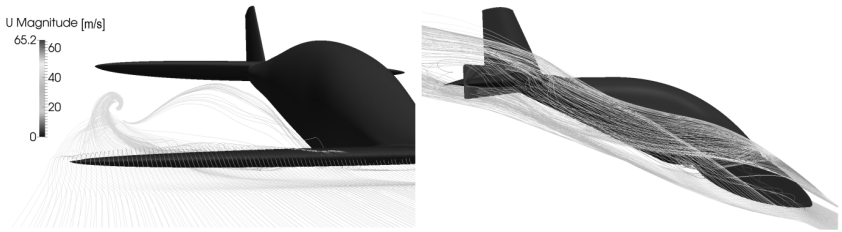

(a) Streamlines at α = 15° (b) Streamlines at α = 25°

Figure 22.3: Aerodynamic analysis of final design showing streamlines at 15 and 25 degrees

Calculations have shown that the aircraft will remain stable on the ground even if pilot and fuel are absent. Furthermore, in case the pilot weighs less than 100 kg it is possible to add weight in the nose of the aircraft to increase the stability margin during flight even more. The aircraft has been designed to be both statically stable and controllable during flight. However longitudinal dynamic and lateral stability have not been checked thoroughly. This would require a much more in-depth analysis and thus has not been developed due to time constraints and because it is not in the scope of the project.

Parts of the design relied heavily on certain software packages. Mainly the Topology Optimization software had a great influence on the structural design process. To properly understand the limitations and accuracy of the results provided by the software a case study was performed. The ultimate goal of validating the TO software would be to determine whether the results are indeed the most weight-optimal structures. To properly perform such a test would require extensive testing of multiple models which iteratively converge to an optimal structure. To test the limits of the software it was decided to create a model that was loaded in shear, torsion and bending.

A cantilever beam that is loaded slightly off centre was chosen. The test specimen was printed with a Builder 3Ddesktop printer. The

Topology Optimization simulation ran with a load of 200 N. The displacements of the final model according to the FEM used in the TO simulation are shown in figure 22.4 along with the experimentally established validation data.

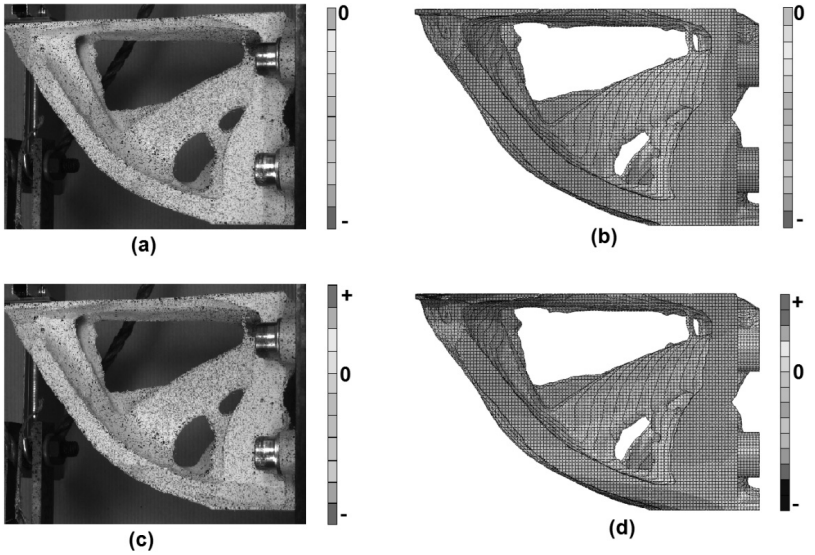

Figure 22.4: Comparison between FEM results and validation data from case study

When the displacement distributions of the test and simulation are compared it can be concluded that they are quite similar. On the left size the test data is plotted; on the right the FEM calculations. On the top the displacement in x-direction is shown and on the bottom the displacement in y-direction. The test results are obtained using Digital Image Correlation. It was found that the results obtained by the TO software showed the correct displacement distributions. The most important regions are those with the peak stresses, which were at the correct locations.

Another conclusion was that it is very difficult to directly use the output from TO software for further analysis. The final simulation was performed at a load of 500 N instead of the original 200 N because the measurements had too much noise. Finally, it was confirmed that the anisotropy due to the layer wise build-up of the

model was indeed the reason for failure. The anisotropic properties could however not be determined as the stresses at this load could not be calculated with a FEM analysis. A recommendation for further research is to design the same load carrying structure with the same restrictions and the same mass using conventional structural sizing methods. Stress distributions and failure loads for this model could provide further insights on the benefits of Topology Optimization and Additive Manufacturing.

The sustainability aspect of this aircraft is difficult to evaluate. Using AM will limit the carbon footprint the aircraft produces during production and transportation, but on the other hand AM machines require much more energy than conventional manufacturing equipment. The real environmental impact of such an aircraft would require an intensive investigation on all components of the aircraft's life and all of the assumptions stated should be taken into account.

Furthermore, the aircraft's design, production plan and operational lifetime should be completely known and quantified. Such an evaluation is not possible at this stage of the design. The aircraft's life time is only 20 flights; hence the aircraft's use contributes little to its overall carbon footprint. Obviously, this aircraft is designed to demonstrate the feasibility of AM in aerospace engineering and sustainability is not the focus of the project. It can however further be improved by choosing AM facilities that use electricity from clean power plants. Finally, this aircraft is unique and produced in a batch size of one. Compared to a large batch as is customary in LSA, a single prototype can never compete in sustainability.

22.6 Conclusion

The Design Synthesis Exercise's purpose of group 12 was to assess the feasibility of designing a personal aircraft using only AM techniques for the airframe construction. As for most engineering problems, given enough time and money, everything is possible, but more interesting is to determine whether the technologies' benefits are worthwhile to invest further research into them.

Although AM offers immense freedom of design, enabling highly efficient structural and aerodynamic solutions, it also brings along its own limitations. At the moment, the build volume is largely process dependent and for the majority of technologies it is rather small (≤ 1 m^3), resulting in a larger number of joints required.

Regarding the design process, AM requires a rethinking of the approach strategy to a design problem. Compared to classical manufacturing processes, AM provides almost total design freedom; so much, that it proves difficult to find a starting point in the design phase. Thus, the concept selection process in this particular project has often been intuitively driven. Furthermore, the various opportunities can stretch the conceptual design phase and thereby, prevent progress into the detailed design.

Furthermore, once a novel concept has been developed, conventional analyses and sizing methods may not be applicable to the desired design. At the same time, it is inappropriate to initiate a full FEM analysis at such an early stage in the project. To cope with this new design environment, adjusted or even revolutionized systems engineering methodologies are required to assess the feasibility and to perform the initial sizing of a concept. In designing the final concept, two major design philosophies were created. The first uses a computer simulation to determine an optimize geometry after which smoothing and FEM validation is applied. This is however a very time consuming process, which is why the second design philosophy was created. This uses conventional design methods, with subsequent incorporation of features that exploit AM benefits.

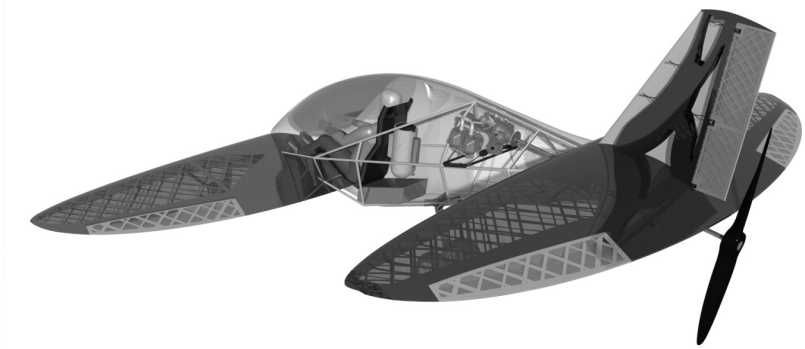

Figure 22.5: Final design render showing internal structure of wings, fuselage and vertical tail

In conclusion, Additive Manufacturing has shown its potential and the possibility to print a complete airframe structure, but for the moment it is advisable to only use AM as a tool to add value to specific aircraft components. The high costs associated with it make it suitable for parts with a high impact on the overall weight of the aircraft. In the aerospace industry a minor weight saving can already yield a large fuel reduction, justifying the higher cost for the part in the long term. That does however not mean that everything should be printed, for example the skin for the aircraft. The keyword for the future of AM in the aerospace industry is therefore “added value”.

23. AVINYA

Students: J.A.P. Borst, M.L. Hoogendoorn, J. Kaminski, S.B. Latooij, M.J. van der Lelij, P. Poudel, S. Sachdeva, J. Spans, S. Tandon, J.A. Tuitert

Project tutor: ir. P.C. Roling

Coaches: dr.ir. S. Hartjes, K. Javonov MSc

23.1 Introduction

After a three year break for safety improvements and reorganisation the Red Bull Air Race (RBAR) has made a spectacular return in 2014. The Red Bull Air Race is an international series of air races in which competitors have to navigate a challenging obstacle course in the fastest time. Pilots fly individually against the clock and have to complete tight turns through a slalom course consisting of pylons known as air gates. The aircraft currently used for these races are modified aerobatics aircraft that were not originally designed with aerobatic racing in mind.

With the return of this legendary race, the Delft University of Technology initiated a project for the design of a no compromise racing aircraft. The project objective statement was defined as:

"Design a customisable aerobatic race aircraft, to win the Red Bull Air Race competition, by ten students in eleven weeks."

The aircraft is required to exceed performance capabilities of current competitors while satisfying the RBAR regulations. The result of this project is Avinya.

23.2 Design requirements

In order to realise a successful design a clear mission need statement had to be defined based on the high level requirements. Avinya, a word from Pali language, means to achieve the extraordinary which cannot be achieved by ordinary intelligence or perception. Therefore, it fits our mission need statement:

"Design a lightweight and customisable aerobatic race aircraft with performance characteristics that exceed those of current competitors."

The performance characteristics of the current competitors form the basis of the client requirements. The client performance requirements are given in table 23.1. An additional client requirement was that of aircraft customisability. As each race track is different, the configuration of the aircraft needs to be able to be optimised to the specifics of the track being flown in order to get the best possible performance. Since the objective of the aircraft is to compete in the Red Bull Air Races, the top level requirements do not only consist of the performance desired by the client, but also of the limitations imposed by the Red Bull regulations. These regulatory imposed design restraints are given in table 23.2.

Table 23.1 Client requirements

Requirement	Value
Maximum speed	> 230 kts
Maximum ROC	> 4700 ft/min
Maximum roll rate	> 420 ° /s
Maximum load factor	10 g
Empty weight	< 700 kg

Table 23.2 Red Bull regulation constraints

Requirement	Value
Empty mass	> 540 kg
Race mass	> 698 kg
Stall speed	< 61 kts
Take-off distance	< 500 m
Landing distance	> 500 m
Wing span	7-8.5 m

23.3 Concept selection

With the client requirements and regulatory constraints clearly defined, multiple concepts were generated that could potentially fulfil the mission need. Together with the client four of the generated concepts were selected for a more detailed comparison. These four substantially different concepts are: a biplane, two aircraft with conventional configuration, of which one with an elliptical wing and the other a forward swept wing, and an aircraft with a canard and pusher-propeller configuration.

Biplane

The biplane concept is a highly manoeuvrable aircraft, its two wings enable the biplane to have a substantially smaller wing span relative to the other three concepts. Because of the smaller span, the inertia about the longitudinal axis is lower, resulting in a better roll performance. Biplanes suffer a penalty in the aerodynamic efficiency due to the interference between the two wings; this reduces the maximum rate of climb that can be achieved. A sketch of the biplane concept is provided in figure 23.1.

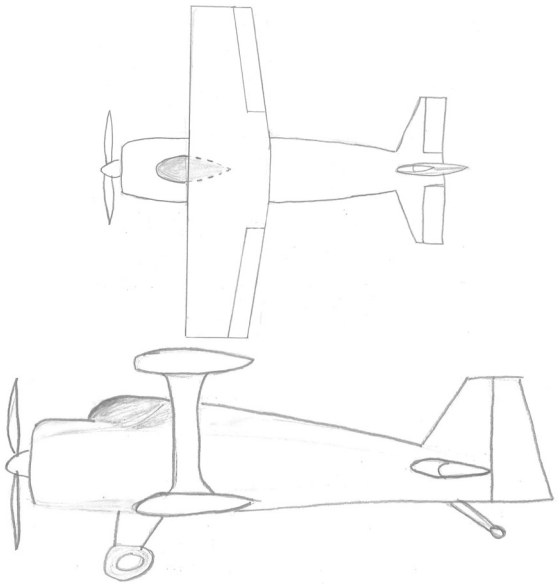

Figure 23.1: Top and side view of the biplane concept

Elliptical wing

During the Red Bull Air Race one of the main influences on aircraft racing performance is the so called 'bleed off speed'. This is the speed a pilot loses when performing high-g manoeuvres. The main cause for this loss of airspeed is the induced drag which increases proportionally with the load factor. Since an elliptical wing planform minimises induced drag, it was chosen for one of the designs. One of the disadvantages of using an elliptical wing however is the simultaneous span wise stall. This stall is characterised by a sudden loss of lift over the entire span, creating very unpredictable aircraft behaviour. Considering the low altitude at which the races are flown, meaning little stall recovery time, this is considered a very dangerous occurrence. A sketch of the elliptical wing concept is given in figure 23.2.

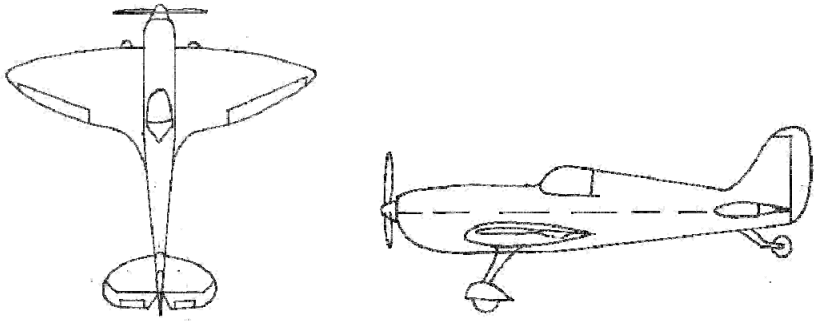

Figure 23.2: Top and side view of the elliptical wing concept

Forward swept wing

The main aspect of the Red Bull Air Races that distinguishes it from other air races such as the Reno Air Race is the fact that the pilots need to manoeuvre through a tight course of obstacles. To optimise for track time, the aircraft not only needs to be fast, but also highly manoeuvrable. Sweeping the main wing forwards increases the manoeuvrability of the aircraft. This however means, that the aircraft in itself tends to be unstable, a problem that is usually solved by installing artificial stability. Because of the aerobatic nature and the corresponding need of the pilots to feel the response of the aircraft, artificial stability is not an option. Apart from the forward sweep of the main wing, this concept, as illustrated in figure 23.3 does not differ significantly from the aircraft currently competing in the RBAR.

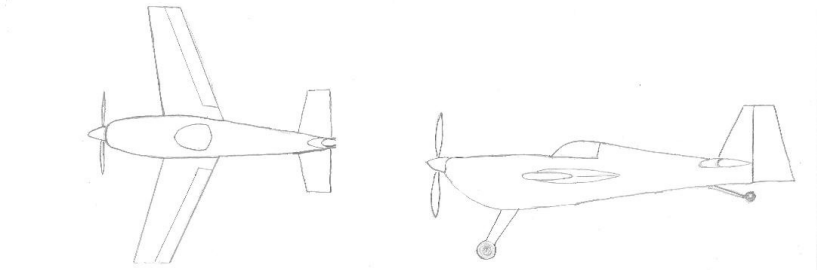

Figure 23.3: Top and side view of the forward swept wing concept

Canard concept

The last concept considered, depicted in figure 23.4, has a canard configuration and pusher style propeller. Just as the forward swept wing concept the canard is highly manoeuvrable, and additionally it has the benefit of the canard generating, useful, positive lift. This is

opposed to a conventional configuration where the tail is mostly creating negative lift, or down-force. This results in the canard offering the same performance whilst requiring a smaller wing, thus reducing the overall weight of the aircraft. It is however more difficult to design a canard aircraft for stability, as the canard itself is destabilising.

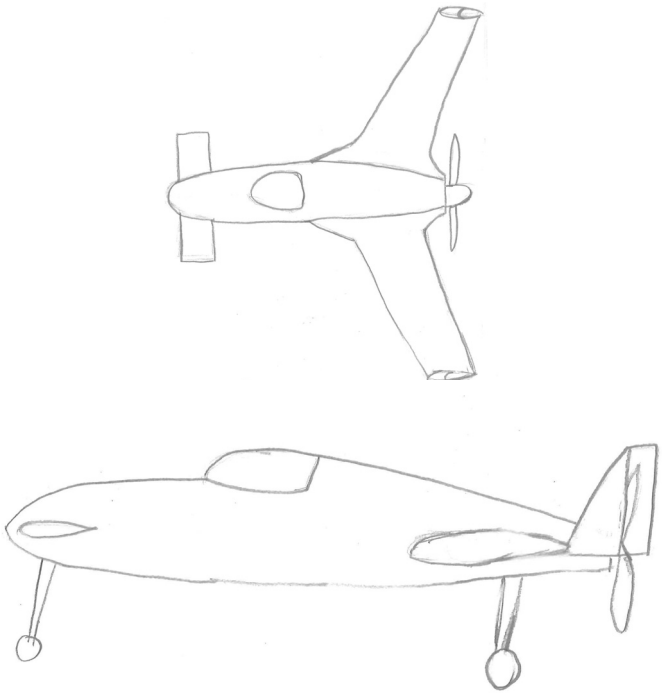

Figure 23.4: Top and side view of the canard concept

After establishing a comparable estimate of the performance characteristics of each concept, a trade-off was performed in which the best concept was chosen. This trade-off compares not only the performance of the different concepts, but also the stability characteristics, structural efficiency, the possibility for customisation, the compliance to the regulations, and several other aspects.

The trade-off resulted in a draw between the forward swept wing and the canard concept. These results were presented to the client and after extensive deliberation the concept carried over to the conceptual design phase was based on a heretofore undiscussed criterion: how

original is the design compared to the current competition. Based on the client preferences, and also based on the performance characteristics, the forward swept wing was forgone in favour of the canard concept.

23.4 Trajectory optimisation

A sensitivity analysis has been performed using a trajectory optimisation tool in order to generate guidelines to find the optimal design. The analysis is performed by simulating a lap around the 2014 Abu Dhabi track, featuring a chicane, half-cuban eight, s-turn and a 180 turn. The influence of certain performance characteristics on the track times is investigated by changing one parameter at the time, whilst others are kept constant. However, this analysis does not take into account the interaction between variables, for example: an increase in wing span limits the roll rate that can be achieved. The interaction between variables needs to be analysed in the future. The parameters analysed are pitch rate, roll rate, aspect ratio, operative empty weight, zero-drag coefficient, stall speed and never exceed speed. It is found that the most important parameters are the roll pitch rate, zero-lift drag coefficient (C_{D0}) and aspect ratio.

Here, one would have the change of a particular parameter as input and have the time penalty as output. The time penalty is the amount of seconds the aircraft flies slower around a predefined track; a negative time penalty means the aircraft performs the track in a shorter amount of time. The time penalties are given in table 23.3.

Table 23.3 Design guidelines

Time penalty [s]	Input unit
$-0.0014\Delta p$	°
$-0.079\Delta q$	°
$0.026(\Delta A)^2-0.48\Delta A$	-
$-0.0013\Delta OEW$	kg
$50\Delta C_{D0}$	-

Table 23.4 Performance characteristics

Parameter	Wing 1	Wing 2
Rate of climb [m/s]	24.7	25.0
Roll rate [◦/s]	420	398
Pitch rate [◦/s]	93.8	94.2

23.5 Performance characteristics

The design guidelines as discussed in section 23.4 are used to design one aircraft with two modular wings. The first wing being optimised for roll rate and the second for rate of climb and aerodynamic efficiency. Both are checked to comply with the requirements on the roll, pitch and climb rate. Also, the control surfaces needed to achieve those rates, are designed.

The surface area is determined by finding the wing loading. This is done by generating the wing versus power loading diagram based on the available power, MTOW and the requirements. The engine is provided by RBAR and therefore the power available is set. The weights are taken from the class II weight estimation, combining these two led to the required surface area. Next, the wing planform is designed such that the climb and roll rate requirements are met. A high rate of climb is mainly driven by a high aspect ratio. Whereas the aileron authority ($C_{L_{\delta_a}}$) and the roll damping coefficient (C_{L_p}) are leading for the roll rate. The major parameters for the pitch rate are the load factor and design speed. The achieved parameters are given in table 23.4.

Finally, the control surfaces are sized, mainly based on lateral control considerations. The ailerons are sized such that the required roll rate can be achieved with a minimum size, while taking into account the limited space due to the rear spar. In detailed design phase, balancing spades have to be added to the ailerons in order to reduce the stick force and allow the pilot to more accurately control the aircraft.

The rudder is sized based on the spin recovery requirement, when parts of the rudder become ineffective. To avoid having the rudder in

the stall the winglets extend above and below the wingtips making them approximately symmetrical about the wingtip. This is beneficial as the side force produced by the rudders does not cause a large moment about the aircraft x-axis and lateral control coupling is reduced. The rudder starts behind the chord of the wingtip, such that it can move freely through all deflections without interfering with the wing.

23.6 Aerodynamic analysis

With the surface area and aspect ratio determined in section 23.4, a 3D aerodynamic analysis is performed to find the optimum taper ratio and sweep angle. 2D analysis is performed to select the aerofoil. Both are performed using the interface of XFLR5. Which allows to perform a 2D analysis for different aerofoils over a range of Mach and Reynolds numbers. The advantage of using XFLR5 for the 3D analysis is the option to use the vortex lattice method, lifting line theory and the 3D panel method.

The aerofoil is selected based on the performance aspect, as well as the feasibility. The performance parameters taken into account are, from most important to least important; the stall angle, C_m during cruise, L/D ratio, C_{Lmax}, camber, LE-radius and thickness. The NACA 2414 has a stall angle of 21 degrees and a C_m of -0.052. This, combined with good scores on the other parameters made this the best aerofoil in terms of performance. For the canard aerofoil the same parameters are analysed, in the same ranking. Though the requirement on the stall angle changed from the highest possible to an optimum angle. From this trade-off the best aerofoil is found to be the NACA 2.5411.

The disadvantage of a cambered aerofoil is that the regulations do not allow it, due to the lower performance in inverted flight. However, inverted-flight-time is very short and therefore not considered a main concern. Analysis shows cambered aerofoils are feasible. From the 3D analysis performed on the wing planform it is found that the wing stalls at 19° with a C_L of 1.5. The lift gradient of the wing is found to be lower than for the canard. The analysis shows that the canard

causes an unstable moment to the aircraft, though the main wing is compensating and therefore the aircraft is longitudinally stable. These parameters can change due to the control surfaces as sized in performance analysis. It is found that each aileron can cause 0.6 increase in lift coefficient, enough to achieve the required roll rate. For stability during landing, the elevators cause an increase in lift coefficient of 0.8, which is quite high due to the undisturbed flow over the canard.

Furthermore, the fuselage is designed to minimise the drag. The largest contribution of fuselage drag is the parasitic drag. Reduction of this drag can be achieved by having a fineness ratio around 2.7 to get a natural laminar flow over the body. The exact shape and size of the fuselage are also dependent on the components which have to fit in, mainly pilot and engine. Once the fuselage, wing and canard were sized, the zero-drag coefficient was calculated to be 0.0254. This takes into account surface roughness, pitot tubes and the interaction between wing and fuselage.

23.7 Stability and control analysis

Stability and control analysis is performed to guarantee the aircraft can be flown safely. Since the aircraft has to be highly manoeuvrable, while safe to fly, neutral stability is considered as being the optimum. But, before performing stability analysis, class II weight estimation is done. From this weight estimation the component weights are found. The heaviest parts are the wing, fuselage and engine. The c.g. position of these components is of major influence on the stability of the aircraft.

The centre of gravity positions are based upon the Rutan Long EZ and the configuration as after the first trade-off. The canard is located as far in the front as the fuselage structure allows, while the wing is entirely in the back. The engine is located in the back of the fuselage. After these components were placed, the most forward and aft c.g. position are computed, which depend on the loading sequence of fuel, pilot and additional weight.

Once a first estimation of the component c.g. positions and weights is made, the stability and controllability curves are plotted to size the canard surface. The stability curve is determined for cruise conditions, whereas the critical condition for controllability is during landing. There are multiple parameters that affect both curves, changing these parameters does not help in achieving a feasible design. Though, some of the parameters that can be influenced in order to achieve a feasible design are the fuselage length, canard planform, position of the wing, canard and engine as well as the aerodynamic parameters $C_{L_{\alpha_h}} / C_{L_{\alpha_{wf}}}$, C_{L_h} / C_{L_w} and ΔC_L due to the elevator. These parameters are changed and iterated with the performance and aerodynamic departments until an optimum design is found. Using the canard size the planform is designed based on literature, an optimum is found with a high aspect ratio, while there is no sweep, taper or dihedral angle applied.

Next, the landing gear length and position are determined. The main constraints for the landing gear position are the longitudinal and lateral tip-over criteria and the longitudinal ground clearance. Based on these constraints, the main gear is positioned at an angle 15º behind the most aft centre of gravity. The nose gear is positioned using a moment balance around the aft centre of gravity. Afterwards, the vertical tail is sized assuming an inherently stable aircraft combined with the required tail volume coefficient. The arm length required for this coefficient is highly dependent on wing span and sweep. Therefore the vertical tail size changed with every iteration.

Finally, the stick force due to the elevators is calculated. This force is dependent on a lot of parameters, such as elevator deflection, dynamic pressure, wing loading, c.g. position and elevator size. Also the trim tab has influence on the stick force, however it is assumed that no trim tab is installed. Furthermore the balancing spades are not taken into account, therefore the forces calculated are too high. Though the forces found appeared to be reasonable for general aviation aircraft, so adding the balancing spades will leave reasonable forces.

23.8 Structural analysis

The stresses within the aircraft structural components, being main wing, canard and fuselage, are analysed, after which these are sized and the material selected. The structural strength of both the wing and the canard is ensured by a wing box, that consists of two spars going from one wingtip, through the fuselage, to the other wingtip. The wing box has to be able to resists high loads and torques. The main contribution to the loads comes from the lift, causing both shear forces and bending moments. The ailerons and the vertical stabiliser with its rudder, when deflected, cause additional forces and moments. These forces and moments result in stresses in the wing box, which are used to calculate the wing box thicknesses and perform a material selection. For the canard however there is no vertical tail and no wing(box) sweep introducing additional forces and moments. The elevators deflect simultaneously and therefore no torque is introduced into the fuselage

The maximum moment with respect to the fuselage longitudinal axis at the root of the wing box for both main wings and canard is 97.38, 102.4 and 8.124 kN respectively. The material chosen as a result from iterations between wing box geometry, resulting weight and ultimate yield stress is Epoxy/high-strength carbon fibre, quasi-isotropic. Chosen due to its specific strength, low density and sufficient impact strength. The weight of the wing boxes are 41.2, 44.4 and 9.55 respectively.

Next, the fuselage is designed. A trade-off is made between a (semi)monocoque and truss structure. It is found that a truss structure has the most advantages. A skin is placed over the trusses and will be effective in shear loads. The cross section is modelled by a cone with a radius ranging from 0.4 (nose) to 0.5 m (aft). It is assumed that deformations take place around the centre of gravity and the cone is thus clamped at its c.g.

The moment over the length of the fuselage ranges from -80.0 to 60.0 kN. The thickness is set and the stress determined by using Von Mises

to add the aileron torque and bending stress due to the wing. The material chosen is AISI Steel 4130 since its yield strength is higher than the ultimate tensile stress present during its mission. Finally, using the mass moment of inertia the size of the rods is calculated and the conceptual design of Avinya completed.

23.9 Final concept

The result from analysis performed is a conceptual design. This conceptual design has to be taken into a detailed design phase before it can be produced or operated, however it shows that the idea is feasible. A first impression of the design can be found in figure 23.5. Although two wings are designed the render of only one wing is provided, since the overall layout is similar. The planform of each wing is given in figure 23.6. It can be seen that both wings have the same root chord and surface area to make them interchangeable and allows optimising the aircraft per track. The expected track times of the aircraft on the tighter Abu Dhabi track and the longer sample track are given in table 23.5. Although wing 2 does not comply to the required roll rate, its time is still faster on the sample track and therefore not meeting the requirements can be overcome. The remaining client requirements are met by both wings, however the concept as a whole does not comply with the Red Bull Air Race regulations. Though, the aircraft is safe to fly and reasons to convince Red Bull of allowing a canard aerobatic race aircraft are apparent.

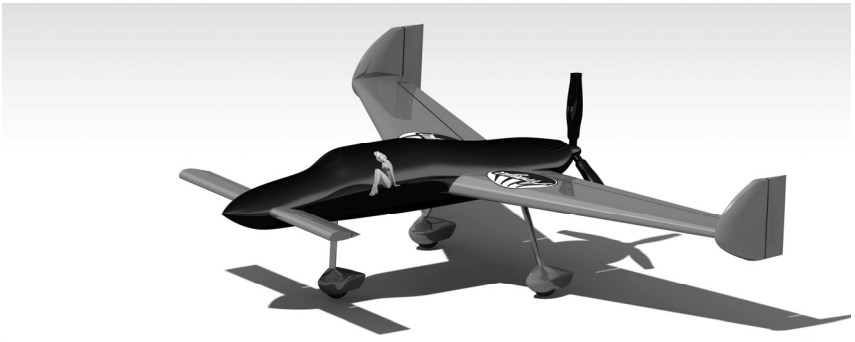

Figure 23.5: Render of the final aircraft design

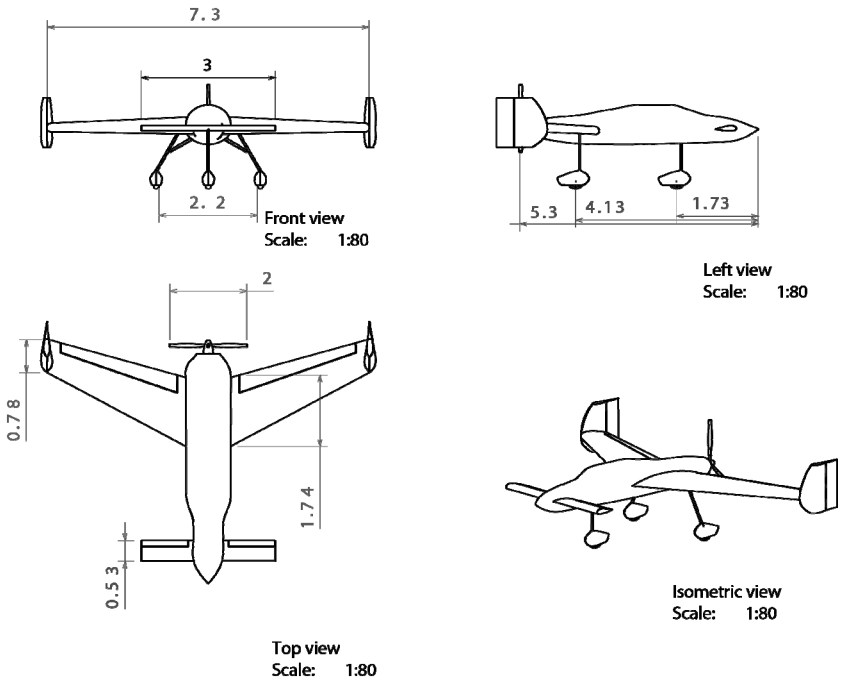

Figure 23.6: Aircraft views

Table 23.5: Results of two designed wings on two separate tracks

Wing	Track	Total time [sec]
Wing 1	Sample	29.6989
Wing 2	Sample	29.4795
Wing 1	Abu Dhabi	24.1683
Wing 2	Abu Dhabi	24.4462

23.10 Sustainability

The design is now finished, though the important concept of sustainability is not yet analysed. Although the Red Bull Air Race itself is not very sustainable, during the manufacturing, operations and end-of-life disposal it can be taken into account.

Firstly, most important during the manufacturing phase is the use of carbon fibres made from the waste that is produced during fractional

distillation of oil. Furthermore the use of existing facilities would be explored, in order to save building a new factory. Secondly, concerning the operations of the aircraft, it has to produce smoke during the race. Currently this is done by burning not less than 2.5 litres of oil per minute. Though Avinya will use an alternative solution, the easiest option is to replace the oil by a bio-diesel option, however replacing it by water is even more sustainable. Currently no such system is available which could be directly implemented into a RBAR type aircraft, thus this technology will have to be designed and incorporated in the next stage and is left as a future development discussion. Besides the smoke to be produced, research is done into the use of an electric engine. Due to the short mission times this seems to be a feasible option. More research has to be done before it can be actually implemented, but it is possible to replace the engine in a later stage. Finally, concerning the last phase, end-of-life disposal. Steel is one of the major components of the aircraft, this can be easily recycled by melting and re-using. The carbon fibre used is harder, though there are techniques to recycle carbon fibre as well. This will be researched more in the future.

23.11 Conclusion and recommendation

The final design of Avinya is based purely on aerobatic racing and hence flying the challenging courses featured in the RBAR competition in the fastest possible time. Therefore performance and trajectory optimisation has been an integral part of the aircraft design. Ultimately a design with modular wings was chosen to have the fastest aircraft on different types of tracks. The design features a canard with an elevator, a sweptback main wing with vertical tails mounted at the wingtips and a pusher propeller at the rear. The propeller is powered by a piston engine, standardised in the current RBAR season. It is found, however, that the engine can be replaced by an electric model without major implications on the overall design, greatly improving the sustainability of the design, especially if combined with a less wasteful alternative for the current smoke system.

Although a promising conceptual design is made, several steps have to be undertaken before the aircraft can actually compete. These steps include a CFD analysis followed by wind tunnel tests to validate the aerodynamic characteristics, especially the stall angle. Structural analysis methods need to be refined and static tests performed to validate the structural integrity. Additionally, balancing tabs have to be designed to reduce the stick force and research has to be done in replacement of more sustainable systems than the current smoke system. Finally, the aircraft has to be certified for both wings and Red Bull has to be convinced that Avinya is safe and of additional value to compete. Once the aircraft is certified it is ready to beat the competitors.

24. HOTFIRE

Students: S. Baar, J. van den Berg, D. Huang, M. Kaandorp, T. Keil, J. Lee, F. Lindemann, J. Rojer, J. Rose

Project tutor: dr.ir. F.F.J. Schrijer, dr.ir. A.H. van Zuijlen

Coaches: dr. D.I. Gransden, A.C. Jimenez MSc

24.1 Introduction

During the first flights of the Space Shuttle, it was found that the pressure in the base region of the Solid Rocket Boosters had been underestimated. This resulted in 453.6 kg of additional payload that could be launched in later missions. The cause of the mismatch was due to lack of knowledge of phenomena such as the base flow and the resulting back pressure on the base plate.

In addition to that, large safety factors were taken into account for thermal protection, resulting in redundant mass to be launched. Again, this was caused by a lack of knowledge of the base flow physics. Until now, only very limited progress has been made on the prediction of base pressure and temperature loads.

Previously, wind tunnel experiments have been performed where an exhaust plume consisting of cold gases was used to investigate the base flow physics of a launcher. However, it has been found that there is a large difference between using a hot and cold plume in terms of

aerodynamic behaviour. For example, in cold plume experiments, the base pressure is underestimated, resulting in an over prediction of the vehicle drag. Furthermore, cold plume experiments are, by definition, incapable of reproducing temperature effects. Therefore, for an accurate experimental investigation of the base flow phenomena, a wind tunnel model that includes a hot plume generator is needed. This leads to the following mission statement:

"The hot plume test facility 'HotFire' will investigate the interaction of the hot exhaust plume with the external flow in the base region of a launcher model."

24.2 Requirements

To achieve the abovementioned mission, the following requirements must be met:

- The hot plume shall be similar to the plume of a launcher in terms of similarity parameters.
- The system shall be able to generate a cold plume for reference purposes.
- The cold plume shall be similar to the hot plume in terms of similarity parameters.
- The system shall allow for constant visual access to the base region.
- The system shall allow for the use of non-visual measurement equipment.
- The shock waves shall not enter the base region of the model.
- The system shall operate for at least 5 s.
- The plume diameter shall be at least 2 cm.
- The plume conditions shall not vary by more than 1% over time.
- The wind tunnel blockage shall not exceed 5%.
- The system shall comply with regulations set forth by Delft University of Technology.

24.3 Concept selection

In order to fulfil these requirements, a number of concepts are conceivable. Clearly, generating a hot plume requires some sort of heating process. Because the nature of the heating process will determine the necessity for and design of any other subsystem, the initial trade-off focused on the different options to raise the temperature of the working gas to the required level.

Various options were considered, including the use of electric heaters or the compression and energy increase of the free stream flow by means of a ramjet. Several types of rocket engines were also added to the trade-off, in particular those using liquid, solid, and hybrid propellants. Selecting the most promising one amongst these options took place based on feasibility considerations as well as the flow similarity that can be achieved by a given concept. Another trade-off criterion of crucial importance was the safety of the whole system.

Flow similarity is the core of "HotFire". Without appropriate flow similarity, the scientific objective of investigating the base flow characteristics of a rocket launcher cannot be reached. It was judged using the so-called similarity parameters. These parameters follow from the fundamental aerodynamic equations governing the transport of, for example, mass or energy, as well as the plume geometry. It still remains unclear how the physical phenomena in the base region are affected by the various similarity parameters. Therefore, decades of experiments using cold plumes have been conducted to determine the exact influence of each parameter and to reproduce plumes of the same size, shape, and flow conditions as a real launcher.

For "HotFire", it was attempted to match the initial inclination angle of the exhaust plume, as well as the pressure, mass flux, momentum flux, and kinetic energy ratios of plume to free stream. The reference launcher was an Ariane 5, selected amongst a number of possible launchers because of its relevance as a modern-day launcher and its relatively easily achievable plume similarity. Previous testing has

shown that closely matching the similarity parameters with a cold plume still does not yield the correct base pressure results. Therefore, it was desired to evaluate the influence of plume temperature on the base flow phenomena. To single out temperature effects on base pressure, the "HotFire" hot plume and the cold reference plume had to be similar to one another, as well as being similar to the Ariane 5 plume.

Electric heaters, a ramjet, and solid and hybrid propellants were quickly eliminated from the possible concepts due to issues with energy addition capability, complexity, and size limitations imposed by the TST-27 wind tunnel at Delft University of Technology, in which the "HotFire" test facility will be used. The remaining concept of using a liquid propellant rocket engine outperformed the others in terms of flow similarity, flexibility of operation, and safety.

A closer look at the combinations of fuel and oxidizer options for this concept revealed that an exact match of all similarity parameters is not possible. The required temperatures and pressures exceed the limits of such a miniature version of a rocket engine. Therefore, the similarity parameters were re-evaluated using the method of Weighted Least Absolute Derivations, emphasizing parameters that govern the behaviour of the plume close to the base region such as the pressure ratio and initial inclination angle.

Eliminating propellant combinations based on their toxicity, safety aspects, and flow similarity, resulted in a hot plume created by combusting kerosene in gaseous oxygen. In addition to that, a cold plume generator using helium as the working gas was selected to provide the best reference conditions for a comparison of differences in base flow characteristics between hot and cold plume.

This resulted in the deviations in similarity parameters presented in figure 24.1. The corresponding combustion chamber and nozzle exit conditions of the selected hot and cold plumes as well as those of the Ariane 5 reference launcher are shown in figure 24.2.

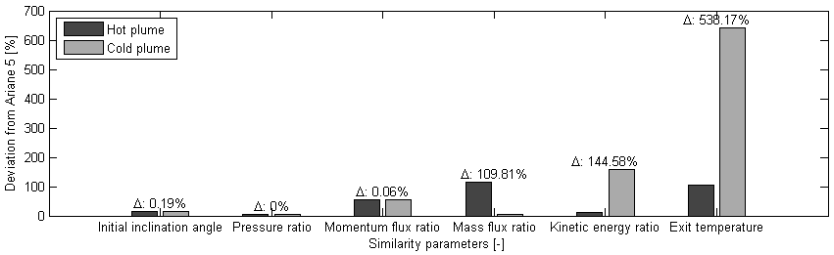

Figure 24.1: Hot and cold plume similarity parameter deviations from launcher conditions

Deviations of up to an order of magnitude are acceptable considering that they still constitute an improvement over the majority of cold plume experiments. A better hot plume would have been possible; however, in that case, no similar cold plume could be found. In addition to that, the main focus was a design that is conservative, yet certainly feasible, rather than the best possible design in terms of similarity. This stems from the large challenges associated with miniaturizing a rocket engine sufficiently to be operated inside a wind tunnel, resulting in the fact that no successful tests have been made so far.

Hot and cold plume deviate from each other and from the Ariane 5 reference launcher only minimally for initial inclination angle, pressure ratio, and momentum flux ratio. The major differences between hot and cold plumes show in kinetic energy and exit temperature. These two parameters were not matched in previous experiments. The mass flux of the hot plume deviates significantly from both the cold plume and the reference launcher. This was accepted for the sake of closely matching the remaining parameters, and because matching the mass flux exactly in previous cold plume experiments proved not to result in the correct base pressure conditions.

Using the large mismatches in kinetic energy and exit temperature, the effects of those two similarity parameters on base flow phenomena will be investigated by the 'HotFire' test set-up.

24.4 Final design layout

The final design of HotFire with the combustion chamber, exit, and free stream conditions can be seen in figure 24.2. It consists of the following subsystems: nose cone, injector, combustion chamber, nozzle, mount, feed system, and instrumentation. Figure 24.3 depicts their arrangement with respect to one another.

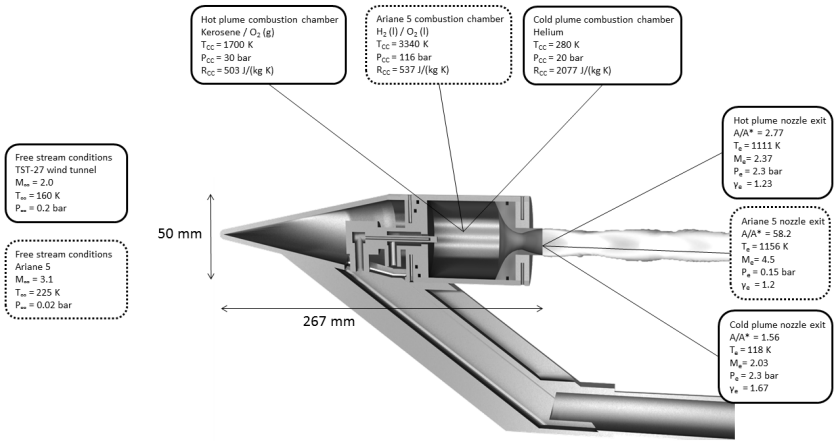

Figure 24.2: Hot plume, cold plume, and reference launcher combustion chamber and exit conditions

Most of the subsystems are located within the wind tunnel. However, part of the feed system such as the feed lines and the storage tanks will be outside of the test section. The model (nose cone, injector, combustion chamber, and nozzle) can be disassembled to accommodate both cold and hot plume experiments.

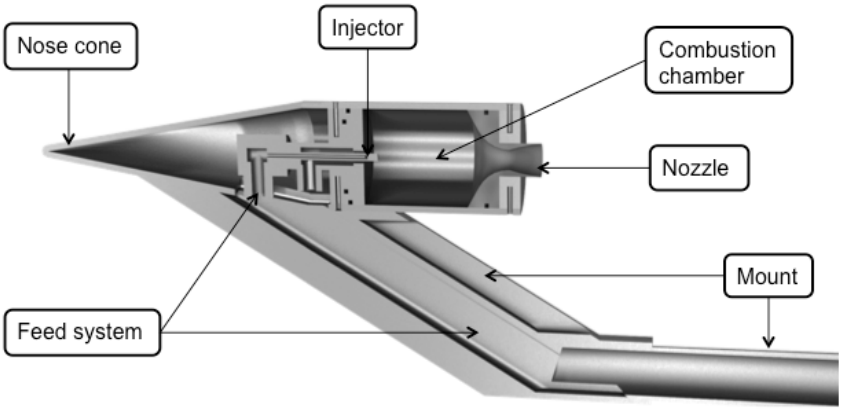

Figure 24.3: Overview of components of the final design

24.5 Model design

The model subsystem of the "HotFire" system is a miniaturized rocket to fit in the TST-27 wind tunnel. Three main components can be identified for the model: aerodynamic shape, combustion chamber, and nozzle. Their dimensions are pictured in figure 24.4.

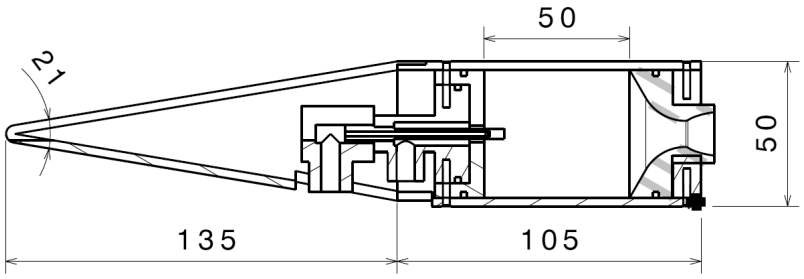

Figure 24.4: HotFire nose cone, combustion chamber and nozzle dimensions

Aerodynamic shape

Starting from the outside, the geometry of the rocket has to be designed, which is basically a cone attached to a cylinder. This shape must ensure flow conditions that are similar to those around the launcher. Therefore, the function of the aerodynamic shape is to avoid flow instability and shock wave interaction with the base region. An analysis on the velocity field inside the test section has been performed both analytically and numerically to optimize the

aerodynamic shape of mount and nose cone. The geometry of the nose cone has been optimized to maximize the distance between the reflected shock waves and the base region.

Figure 24.5 shows the flow pattern determined by the CFD software NUMECA. Together with ANSYS Fluent, it was used to determine the distance between base region and reflected shock wave as well as the size of the exhaust plume. The straight black lines show the result of analytical calculations of the shock wave position. Clearly, they are slightly conservative but agree very well with the CFD results. This confirmed that analytical calculations could be used to speed up iterative processes.

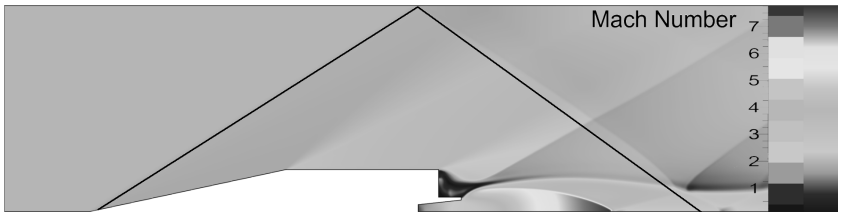

Figure 24.5: Shock wave interaction with base region - comparison of NUMECA results and analytical solution

The outcome of the optimization was a nose cone angle of 21 degrees, resulting in a distance of 3.06 times the model diameter between the base of the model and the reflected shock waves. The length of the nose cone was directly influenced by the diameter of the thrust chamber. Furthermore, the tip of the nose cone is rounded with a radius of 3 mm. This makes it easier to manufacture and is also aerodynamically desired; a too sharp nose cone will create flow separation, while a too blunt nose cone will create a bow shock. Lastly, zig-zag tape will be placed directly after the nose cone in order to make the flow entering the base region turbulent.

Combustion chamber and nozzle

On the inside, this model has a combustion chamber, where the propellants are combusted and expelled through the nozzle at the back to create a hot exhaust plume. Both the combustion chamber and

nozzle must have a certain geometry to perform their function. Moreover, the combustion chamber and nozzle must not fail thermally and structurally. To optimize the structural and thermal aspects of these subsystems, several materials have been analysed to select the most suitable one.

The concept of a cylindrical chamber was selected as it provided the minimum cross-sectional area and length. For the nozzle, the concepts of bell shaped and conical nozzles for the hot plume were studied. From the estimation of their lengths, the conical nozzle was found longer compared to the bell shaped nozzle. Moreover, the lip angle of 7 degrees resulted in an unconventional divergence angle which was not desired for the efficiency of the nozzle. Therefore, a bell shaped nozzle was selected. For the cold plume nozzle, an interchangeable nozzle with the hot plume combustion chamber was judged to be the best option as it does not require a new model that results in higher additional costs.

The wall thickness of the combustion chamber was determined by structural and thermal analysis. Iteration was performed over different materials to compute the optimum thickness for the corresponding materials. The results of the analysis showed that steel and titanium with a thickness of 2.5 mm can be used for the combustion chamber with sufficient design margins. Steel S355 was selected as the combustion chamber material since it is cheaper and weight optimization was not required for the project. For the nozzle, graphite was selected due to high temperatures at the throat and uncertainty of the base heating for the divergent region of the nozzle. Lastly, a CFD-based estimation on the plume size showed that the current design of the combustion chamber and nozzle can produce the required plume size.

24.6 Mount design

The mount is the connecting element between the model and the wind tunnel. It keeps the model in its place and provides the space for the propellant lines, electrical wiring, and instrumentation. For the

concept selection, a sting mount was selected over a window mount to enable Schlieren visualization and minimize its wind tunnel blockage.

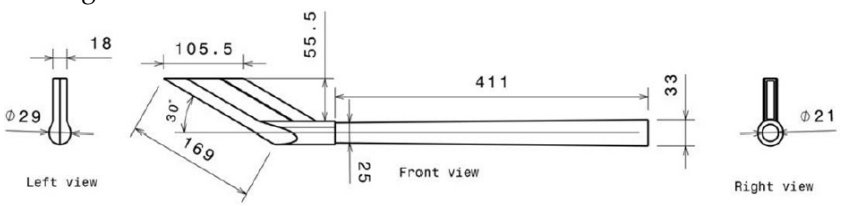

Figure 24.6: Mount dimensions

For the geometry, an angle of 30 degrees of the mount beam was found to be optimum in minimizing the cross-sectional space for blockage. Furthermore, the aerodynamic optimization of the front section of the mount resulted in a sharp angle of 16.7 degrees to ensure a low deflection angle of the oblique shock. This will result in a reduction of the Mach number across the shock, which yields less static pressure acting on the front of the mount, reducing the drag. The width of the inclined beam was designed to be 18 mm due to the size of the fuel lines. The length of the sharp frontal section of the mount was designed to have a length of 30 mm.

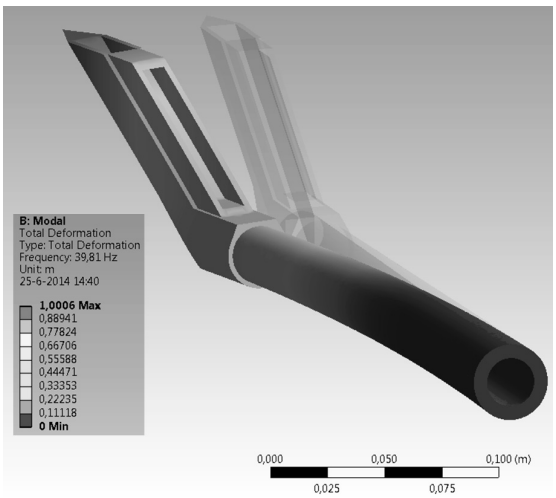

Figure 24.7: Deflection of mount due to start-up loads

The mount was analysed for static, dynamic, and thermal loads. The static and dynamic analysis is done both analytically and using FEM

software (ANSYS). Using a safety factor of 2, the mount was designed to sustain a maximum von Mises stress of ca. 440 MPa, which is below the specified 450 MPa for the chosen 'Uddeholm Impax Supreme' steel with a yield stress of 900 MPa. The lowest eigenmodes were found to be approximately 40 Hz. The base pressure pulsation frequency was calculated to be about 1200 Hz, but experimental research is needed to validate the result and to determine other frequencies caused by the aerodynamic behaviour and the engine. The maximum temperature to which the mount heats up was calculated to be 504 K for the worst case scenario.

24.7 Feed system design

The feed system is a crucial part of "HotFire", as it will supply the combustion chamber with the propellants. A drawing of the overall system is shown in Figure.

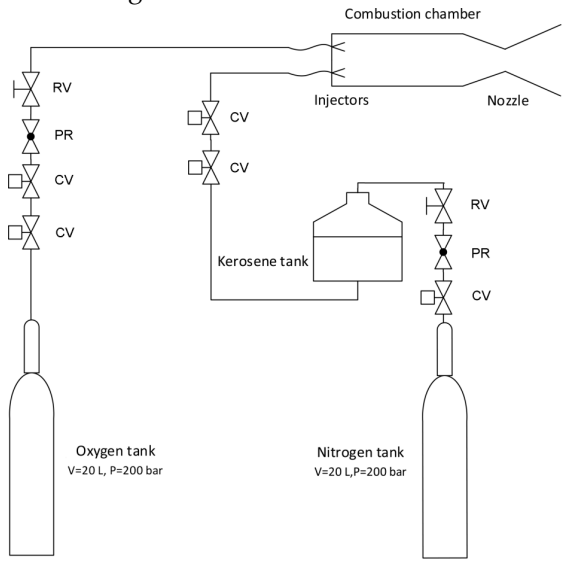

Figure 24.8: Feed system layout

Combustion chamber conditions such as mass flow and pressure as well as safety considerations drive the design. The feed system is designed as a blow down system using commercially available pressurized tanks to ensure safe operation while storing a minimum amount of propellant. An oxygen tank is selected with a pressure of

200 bar and a volume of 20 litre. The kerosene tank is pressurized by means of a nitrogen tank, which also has a pressure of 200 bar and a volume of 20 litre. Commercially available feed lines able to withstand the pressure and handle the respective propellants, are selected to connect those tanks to the combustion chamber of "HotFire". The kerosene feed line has an inner diameter of 3.81 mm and the oxygen feed line has an inner diameter of 6.35 mm.

The tanks and the feed lines are connected via two electronically operated valves (CV) to enable remote control and via pressure regulators (PR) to adjust the tank pressure to the required value. Relief valves (RV) were added to the system to avoid single points of failure. In this special set-up, the system can be controlled and shut down remotely in case of failure and will also turn to a safe state in case of power outage. Optimal mixing and minimal complexity of the injector is obtained by using a combination of a coaxial and splash injector. The injector itself will consist of three separately designed parts: the injector casing, an oxidizer injector, and a fuel injector. These parts are connected to each other by threads and bolts. Seals will ensure that the combustion chamber is pressure tight. In the end, the total pressure loss over the whole system was calculated to be 9.25 bar for the kerosene branch and 15.68 bar for the oxygen branch. With a chamber pressure of 30 bars, this results in mass flows of 0.063 kg/s 0.075 kg/s of kerosene and oxygen, respectively, yielding the desired oxidizer to fuel ratio of 1.2.

24.8 Instrumentation

In order to measure the phenomena in the base region of the model, pressure sensors, temperature sensors, mass flow sensors, and Particle Image Velocimetry (PIV) have been identified as the required measurement equipment. These measurements will be taken in a visual and non-visual way. Two pressure sensors of types "HI2200" and "Parker ASIC" will be placed at the base plate and inside the combustion chamber to measure the chamber pressure and unsteady pressures at the base region, respectively. A K-type thermocouple will be placed at the base plate to measure the base heating. Furthermore,

a load cell will measure the mass flow of propellants by measuring the change in weight of the tanks over time, and a thermal camera will determine the chamber wall temperature for safety reasons. Lastly, PIV equipment will measure the velocity of the base region flow field, the actual scientific measurement.

24.9 Conclusion and recommendations

The wind tunnel simulation of the base region of a launcher has been historically accomplished by using cold plumes. In the 1980s, the use of hot gases has been deemed unfeasible due to cost and complexity, despite of its high accuracy. However, with the recent advancements in computational fluid dynamics (CFD), finite element methods (FEM) and measurement techniques, the development of a plume test facility has become feasible.

During the DSE, the design of the hot plume test facility "HotFire" has proven to be not only feasible but also valuable due to its capability to better reproduce the base region of a launcher in real flight. The challenging aspects of the project, namely miniaturizing the plume generator and addressing the safety issues, have been met successfully through in-depth analysis and the use of advanced computational tools.

Following the successful demonstration of its feasibility, the aerodynamics chair of the Aerospace Faculty at Delft University of Technology will continue to develop the design of the hot plume test facility. Upon completion of this project, hopefully the base flow physics of the launchers will be better understood, resulting in more efficient future launchers.

Several tests have been proposed to further verify the requirements and validate the system. Due to the complex nature of the rocket propulsion system, it is recommended to perform tests to optimize the "HotFire" design.

25. FX15 - AEROBATIC RACING AIRCRAFT

Students: N.T. Andriesse, R.J. Baaij, J.A. Bellekom, A.M. Berkel, I.A. Gennissen, T. Hendrikx, G.R. Poeran, M.A. Robijns, I. van Teeseling, B.M. Verhagen

Project tutor: ir. S. Schroff

Coaches: dr. B.F. Santos, ir. M.F.M. Hoogreef, prof. dr. A. Rothwell, ir. D. Barazanchy

25.1 Introduction

The Red Bull Air Race is one of the most challenging air racing competitions in the world, and is a great opportunity for a company to gain publicity. FlashCo. is a young energy drink manufacturer and aims to gain a significant market share by beating Red Bull in its own competition.

This project revolves around the design of a new aerobatic racing aircraft that will enable FlashCo. to win the Red Bull Air Race. The aircraft that has been designed pushes the limits of what is possible and has performance unlike any other aerobatic racing aircraft. A combination of high speed, a strong design and extreme manoeuvrability make the FX15 the aircraft that will win the Red Bull Air Race. Figure 25.1 shows one of the extreme racing tracks the FX15 has to fly.

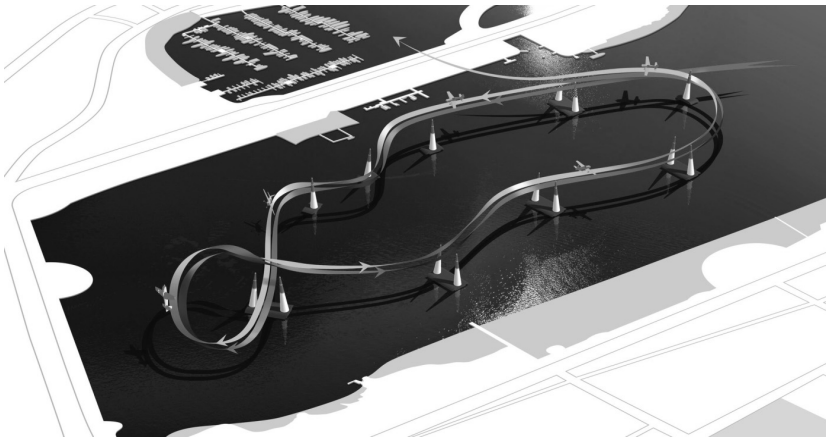

Figure 25.1: The Abu Dhabi Race Track

25.2 Mission need statement

The mission need statement summarizes the main requirements and constraints for the product that is designed. The mission need statement for the FX15 reads:

"Design an aircraft that can win the Red Bull Air Race World Championship 2017. The aircraft shall have a total cost lower than 275 000 euro. It shall comply with CS23 regulations, as well as Red Bull Air Race regulations. Furthermore, it shall be home-built and disposable in a sustainable manner."

25.3 Design requirements and constraints

The main design requirements and constraints for this project were issued by FlashCo. and Red Bull. A summary of the most important requirements is given below.

- The aircraft shall have a unit cost below € 275 000.
- The aircraft shall make its first flight in 2017.
- The aircraft shall have a modular design.
- The aircraft shall be home-built using facilities provided by TU Delft or other external parties within Europe.

- The aircraft shall have a maximum load factor of 12 with a safety factor of 1.5.
- The aircraft shall have a design cruise speed of 450 km/h.
- The aircraft shall have a service ceiling of 5000 m.
- The aircraft shall have a rate of climb of 18 m/s.
- The aircraft shall have a wing span between 7.0 and 8.5 m.
- The aircraft shall comply with CS23 regulations.
- The aircraft shall comply with Red Bull Air Race regulations.

25.4 Design options and trade-offs

In the first stages of the FX15 design, the possible design options were investigated and trade-offs were performed between them. The design options were highly limited by Red Bull Air Race regulations, which state that the aircraft must have a conventional layout and that it must use a Lycoming Thunderbolt AEIO-540-D engine with a 3-bladed Hartzell 7690 composite propeller. It was chosen to push these limits by experimenting as much as possible within the given bounds. The most interesting trade-off that was performed was between a front-mounted engine configuration and a mid-mounted engine configuration. It is traditional in aerobatic racing aircraft to mount the engine in the front of the plane, right behind the propeller. However, mounting the engine in the centre of the plane offers large advantages. The advantages and disadvantages of this mid-mounted engine configuration are listed below.

Advantages

- Lower mass moment of inertia, because the mass of the engine is closer to the centre of gravity of the entire aircraft.
- Lighter fuselage structure, because the bending moment due to the engine is significantly reduced and because all main loads are located in one area.
- More streamlined fuselage, because the front of the fuselage can be thinner.

Disadvantages

- Engine located away from the propeller, so a transmission system is needed to transfer the power from the engine to the propeller.
- A mid-mounted engine configuration was chosen, because of the abovementioned advantages. The disadvantage of needing a transmission system seemed challenging but surmountable, since it has also been done in reference aircraft.

Another interesting trade-off was that of the wing structure. A wing box design and a monocoque design were considered. It turned out that a wing box design is the better option but that a traditional wing box design was not the answer. Instead, a main spar that consists of a carbon fibre laminate shell with a high strength foam core was chosen to carry all wing loads, with a small rear spar that has the sole purpose of avoiding deformation of the aerofoil. The main spar uses a carbon fibre laminate because it is very stiff and light, so it does not deform much under the high loads encountered during the race and weighs as little as possible. The high strength foam core of the spar is intended to prevent buckling and deformation of the spar, which is usually the job of ribs and stiffeners.

Trade-offs were performed for all other subsystems as well. In all cases the focus was on reducing weight and drag, because this improves acceleration that is crucial for race performance.

25.5 Final design

The wing of the FX15 final design features a custom NACA 0011-61MOD aerofoil. The combination of this aerofoil and the optimized wing planform give the wing a maximum lift coefficient of 2.07, with minimum drag and safe stall characteristics. The wing contains large ailerons that span more than half of the wing to achieve a roll rate of 440 °/s. The aerodynamic loads of the wing are carried by a carbon fibre laminate spar with a Divinycell HT131 foam core. The carbon fibre laminate is a custom design made of HexPly 8552 with 65% IM7 fibre. The wing spar was optimized using a sophisticated geometric

optimization algorithm, resulting in a structure that weighs only 60 kg but is able to handle 18g turns.

The innovative engine location, just above the main spar of the wing, results in a fuselage with its heaviest and bulkiest components in the central section. This enables a smooth and streamlined fuselage shape with a zero-lift drag coefficient of 0.0063. The loads on the fuselage are carried by a truss structure that uses AISI 410S stainless steel tubes. The truss structure weighs 49 kg and does not fail despite loads of up to 18 g, as confirmed by FEM analysis.

The ability to perform a ±12g turn within a quarter second is assured by the horizontal stabilizer and its elevator with an area of 2.1 m^2. The vertical stabilizer and its rudder with an area of 1.7 m^2 are designed to allow safe crosswind landings and to enable the aircraft to recover from spin in less than 3 seconds.

The undercarriage of the FX15 consists of two main gears and a small tail wheel in a tail dragger configuration. The shape of the two main gear struts was optimized for low weight and low drag using an advanced optimization algorithm. The main landing gear with struts made of aluminium 2014-T6 contribute 19 kg to the total aircraft mass and increase the aircraft drag coefficient by only 0.0031, as a result of shaping the struts as NACA 64-020 aerofoils.

The unconventional engine location requires a reliable system to transmit the engine power along the cockpit to the 3-bladed Hartzell 7690 composite propeller. A system of shafts, chains and sprockets turned out to be the lightest, simplest and most durable solution. A combination of shafts made of AISI 4130 steel, aluminium 6061-T6 sprockets, and Triathlon HT chains guarantees a reliable transmission of the 315 hp generated by the Lycoming Thunderbolt AEIO-540-D engine. Air for cooling and combustion is supplied to the engine through air inlets conveniently located in the wing roots, keeping intake drag to a minimum. The power output of the engine can be increased to 350 hp using a Hartzell Engine Technologies turbocharger.

Performance analysis shows that the maximum speed of the FX15 is 127 m/s, which is slightly more than the required speed of 125 m/s. The highest rate of climb is 25 m/s, which greatly exceeds the required rate of climb of 18 m/s. The FX15 needs 145 meters of runway to get off the ground from standstill, which is well below the 500 meter requirement. An overview of the final design is shown in figure 25.2.

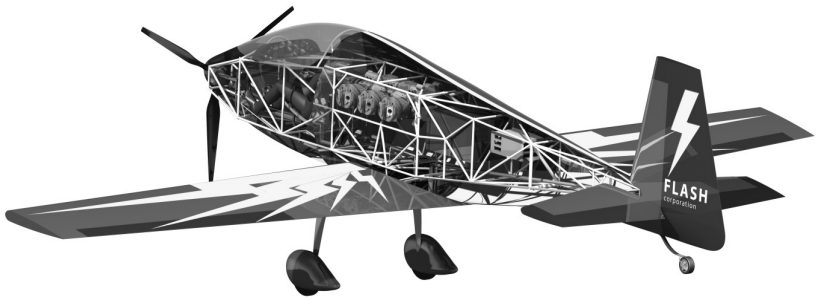

Figure 25.2: Final design of the FX15

25.6 Conclusion and recommendations

Designing the FX15 was not an easy task. The aerodynamic solver that was used to design the wing was unable to compute viscous drag for complex wing geometries, forbidding the design of using winglets. However, winglets could benefit the performance of the aircraft, so it is recommended to investigate their use in the future. Due to time constraints, the fibre layout in the custom carbon fibre laminate of the main spar could not be optimized. It is recommended to optimize this fibre layout in the future, because it offers an opportunity to save weight. It proved to be challenging to fit the transmission system in the confined space of the fuselage and to protect the pilot from fast moving components in the event of a failure, but a good result was obtained. The aerodynamic design of the undercarriage was troubled by large amounts of time necessary to run the CFD simulations. A particularly challenging aspect of the design of the empennage was to ensure the ability to quickly recover from a spin.

The final design of the FX15 weighs only 556 kg and can be produced at a unit cost of € 192 100. The aircraft can handle 12 g loads with a safety factor of 1.5, can climb at 25 m/s, has a service ceiling of 6000 meters, only stalls at 31 m/s and has a cruise speed of 450 km/h if a turbocharger is used. The aircraft has a modular design, allowing for easy maintenance and efficient transportation.

It can be concluded that the FX15 complies with all FlashCo., CS23 and Red Bull regulations and has a significant chance of winning the Red Bull Air Race World Championship 2017

26. THE TORERO T-16: AN AEROBATIC RACING AIRCRAFT DESIGN

Students: K. Capiot, W.F. Datema, R.R. Duivenvoorden, N.H.M. van den Dungen, J. Heijink, M. van Horssen, T. Hylkema, J.H. Klingelhoefer, L. Mengyang, L. Verheij

Project tutor: ir. S. Schroff

Coaches: ir. D. Barazanchy, dr.ir. J. Ellerbroek, ir. E. Ferede

26.1 Introduction

The Red Bull Air Race© World Championship is a series of air races, where pilots manoeuvre their aircraft through an obstacle course as fast as possible. Being the fastest and most exhilarating motorsport series in the world, the race draws a great deal of attention. Several million spectators being on site each season and another half a billion following the event on TV makes it a significant event in terms of advertising.

Being in the middle of launching a new product, the energy drinks company FlashCo. sees this event as the perfect opportunity to promote their product. By beating Red Bull in their own competition, FlashCo. intents to accomplish that their new product, the Flash Energy Drink, gets established and makes a mark in the energy drinks

market. FlashCo. has invited Torero to design and develop an aircraft fit to compete in the Red Bull Air Race© World Championship.

26.2 Requirements

The project objective statement is Design and optimise an aerobatic racing aircraft that is capable of competing in the Red Bull Air Race© World Championship. Based on the objective statement and the requirements set by FlashCo., the mission statement is stated as:

"Beat the current records in the Red Bull Air Race© World Championship by designing an aerobatic racing aircraft with a group of ten students within ten weeks."

The design shall, comply with the CS-23 and Red Bull Air Race regulations, be within budget of €275,000.- and shall have its first test flight in 2017. A sustainable approach by the Torero design team is taken without compromising for technical performance.

The aircraft shall comply with both the Red Bull Air Race regulations and CS-23 certification specifications, and be ready to have its first test flight in 2017. With a unit cost below €275,000.- including development costs, the aircraft should be capable of beating the current record times. Furthermore, the aircraft shall be transportable to the race site without flying it to the location. A single pilot will fly the aircraft and, in case of an emergency, shall be able to abandon the aircraft within ten seconds. On top of this, four technical requirements are specified. The aircraft shall withstand a maximum load factor of 12 g, have a minimum empty mass of 540 kg and a race mass not less than 698 kg. Lastly, a service ceiling of 5,000 m should be achieved.

26.3 Concept study

Before starting the concept study, the Torero design team was split up into four departments: Aerodynamics, Control & Simulation, Flight Performance & Propulsion and Structures. Each department worked

on subsystem level to design different concepts. These concepts are traded off and a final concept is made combining all choices.

Initial weight estimation

Before starting subsystem design, an initial weight estimation was performed based on parameters of existing aircraft. By making these weight estimations, it is possible to create a preliminary aircraft design which will be used for further detailed calculations. Using the requirements, a Class-I weight estimation resulted in an empty weight of 540 kg and a maximum take-off weight of 698 kg. Based on this estimation, the subsystem concept design was done.

Fuselage

Three fuselage structure options are considered, namely a truss, semi-monocoque and monocoque structure. For material selection, both metals and composites are taken into consideration.

Wing

The aerofoil is the starting point for the aerodynamic wing design. Different Eppler and NACA aerofoils were selected as a base for modification, as seen in figure 26.1. The variables sweep and taper can be adjusted. Dihedral and twist are discarded, since the aircraft needs to be able to fly inverted and their effects reverse. Backward sweep is also discarded because of its unwanted tip stall behaviour, making the aircraft uncontrollable.

Two types of internal wing structure are considered: a wing box or beams and ribs. The skins do not take any loads, and can be optimised for aerodynamics. In order to make the aircraft transportable, two options were considered feasible: the wing could either be foldable or dismounted.

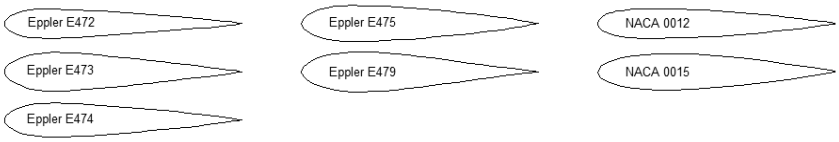

Figure 26.1: Aerofoil selection

Empennage

A selection of different aerofoils for the empennage were selected. The horizontal tail aerofoils can either be NACA 0012 or NACA 0015. The vertical tail profiles are thin NACA profiles: 0006, 0008, 0009, 0010 and 0012. T-tail, fuselage mounted and cruciform are three possible options for the horizontal stabiliser. A dual vertical stabiliser is discarded as it makes the structure too heavy and deteriorates rolling capabilities, resulting in a single vertical stabiliser.

Landing gear

Two landing gear configurations are possible: a tail dragger or tricycle configuration. The tail dragger is the most favourable option, since the front wheel in a tricycle configuration requires a heavy strut and increases aerodynamic drag. Two types of main gear are considered: a rigid axle or single-piece leaf spring. The tail wheel simply consists of a single leaf spring.

26.4 Trade-off

In order to come up with the final design, a trade-off is performed. Each subsystem trade-off is done separately, but the interactions between the subsystems are also taken into account.

Fuselage

Two trade-offs are done for the fuselage, regarding structures and materials. Cost, mass, impact safety and maintainability are considered for both cases. For fuselage material, flammability, availability, recyclability and smoothness are additional criteria. For fuselage structure, wing-fuselage integration, design effort, inspection and post-mission modification are taken into account.

Wing

Starting off with the aerofoil trade-off, stall speed, fuel storage, stall characteristics, low drag at low lift and low drag at high lift are considered. For wing planform, the longitudinal and lateral control, profile and induced drag, stall characteristics and aileron effectiveness

are useful criteria. The wing structure takes into account shipping size, mass and structural loads.

Empennage
For the empennage aerofoil and planform trade-off, its mass, drag and stall behaviour are weighed.

Landing gear
Last but not least, the criteria for landing gear trade-off are mass, cost, integration into fuselage and maintainability.

26.5 Preliminary design

After having done the trade-off and a detailed design phase, the preliminary design of the Torero T-16 is now unveiled. Three-viewings of the Torero T-16 can be found in figure 26.2.

Fuselage
The fuselage consists of a truss structure with treated jute reinforced Biopol composite skin for curved skin sections and Stits Poly-Fiber fabric for straight skin sections. The material ASTM A541 steel alloy is used for the truss structure resulting in a mass of 72 kg.

Wing
The aerofoil that has been selected is the Eppler E479. This aerofoil was modified in order to give the best possible properties for the Red Bull Air Race. The properties of the Eppler E479Mod can be found in table 26.1 as a comparison to the original Eppler. A second modification was made to allow variable aerofoil and thus improve the stall behaviour. The most important wing planform parameters are shown in table 26.2.

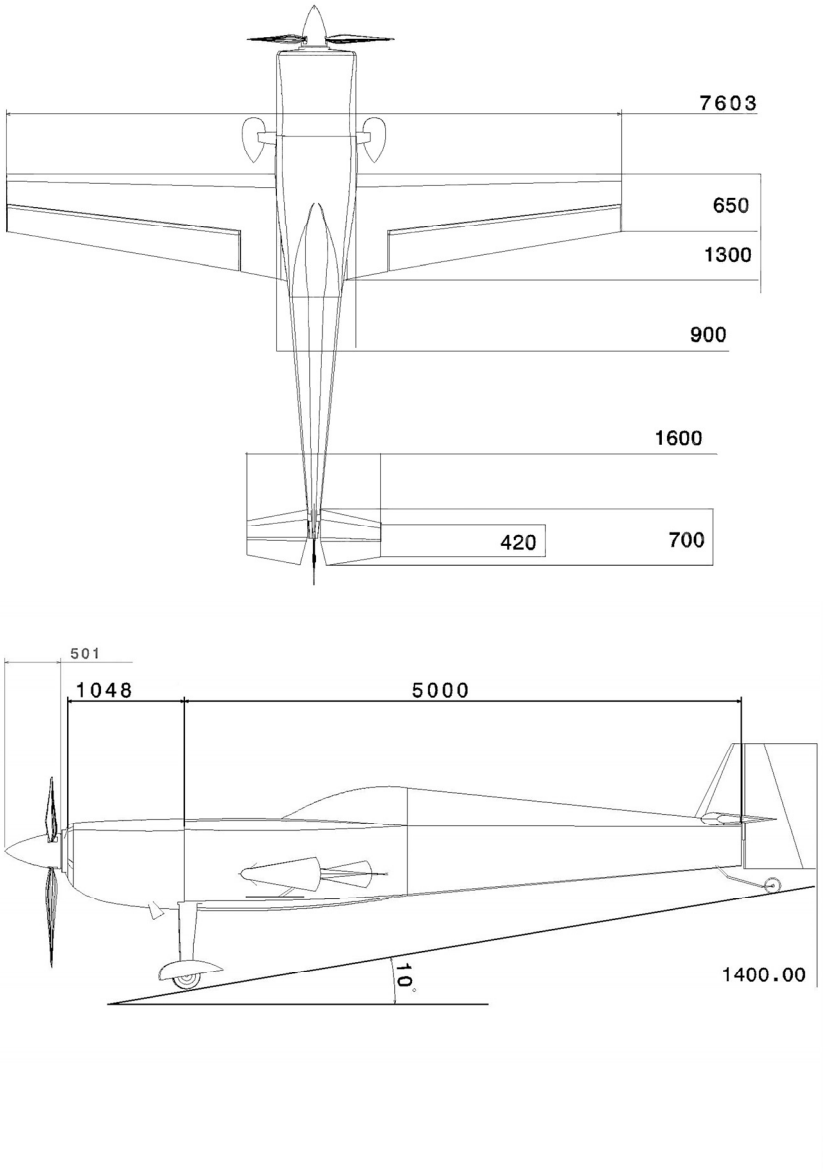

Figure 26.2: T-16 Drawings including dimensions in mm

Additionally, the T-16 wings feature endplates at both the root and tip of the aileron. These devices prevent a vortex of air rolling from one side of the aileron to the other, increasing the aileron effectiveness and thus the roll rate.

Table 26.1: Aerofoil data

Parameters	E479	E479Mod
$C_{l_{max}}$ [-]	1.66	2.29
$C_{l_{max_{tip}}}$ [-]	1.36	2.13
αstall [°]	18.1	23.1
C_{d_0} [-]	0.0059	0.0072
$C_{m_{max}}$ [-]	0.0314	0.06651
$\left(\frac{c_l}{c_d}\right)_{max}$ [-]	121	146
$\left(\frac{t}{c}\right)_{0.01225c}$ [-]	3.44%	4.66%

Table 26.2: Wing planform data

Parameters	Symbol	Value
Wing span [m]	b	7.6
Wing surface area [m^2]	S	7.3
Wing aspect ratio [-]	A	7.9
Wing taper ratio [-]	λ	0.5
Wing root chord [m]	c_r	1.3
Wing tip chord [m]	c_t	0.6
Wing leading edge sweep angle [°]	Λ_{LE}	0.0
Wing half chord sweep angle [°]	$\Lambda_{0.5c}$	-4.8
Wing quarter chord sweep angle [°]	$\Lambda_{0.25c}$	-2.4
Wing mean aerodynamic chord [m]	MAC	1.0

For the wing structure, a full wing box structure has been selected. This choice has been made in order to cope with additional torsional

loads on the wing. The wing box has been made from carbon fibre reinforced plastic and results in a mass of 68.3 kg. To transport the aircraft, an innovative plug-and-fly system was invented. This will be elaborated in the section Sustainability.

Empennage

The horizontal stabiliser is fuselage mounted, since a T-tail can cause deep stall and a cruciform tail needs heavy structural reinforcements to cope with the maximum load factor. The aerofoil of the horizontal tail is the NACA 0012 and a taper ratio of 0.6 has been used as it gives a result to approximate the ideal elliptical lift distribution.

From the stability analysis it follows that the horizontal tail should have an area of 11% of the area of the wing. The vertical tail size is determined mainly by the size of the rudder and by the wake of the horizontal tail. This results in a vertical tail size of 1.1 m^2 using a NACA 0009 aerofoil. The structure of the empennage is selected to be a single load carrying beam. This results in a mass of 18.7 kg and 12 kg for the horizontal and vertical tail respectively.

Landing gear

As has been decided in the concept study, a tail dragger is used for the T-16. Both the main gear and tail wheel consist of a single-piece leaf spring to reduce weight. Instead of designing a landing gear, an off-the-shelf product has been selected. The reason for this is that the structure is fairly simple and the costs and time for validation, testing and certification are high. The selected landing gear is the Pitts S2S manufactured by Grove Landing Gear Inc. with a mass of 15.7 kg.

Controls

Having designed the wing and empennage, the three control surfaces are designed: aileron, elevator and rudder. The control surfaces are limited by the lifting surface, and by the maximum control forces as defined by CS-23. Table 26.3 shows the control surface parameters.

Table 26.3: Control surface parameters

Aileron	Elevator	Rudder

Parameters	Value	Parameters	Value	Parameters	Value
Chord ratio aileron	0.3	Elevator chord ratio	0.53	Rudder chord ratio	0.7
Inboard aileron span [m]	0.76	Elevator span [m]	1.62	Rudder span [m]	1.43
Outboard aileron span [m]	3.8				
Maximum aileron deflection [o]	25	Maximum elevator deflection [°]	29	Maximum rudder deflection [°]	30
Maximum control force [N]	290	Maximum control force [N]	743	Maximum control force [N]	890

An extraordinary feature of the T-16 is the non-linear aileron control. A linear control stick input results in an exponential aileron deflection. The slow deflection of the aileron in its initial stage reduces the drag.

Performance

After the design of the aircraft has been fixed, the performance of the aircraft at sea level has been analysed. It was found that the maximum velocity the aircraft can reach, limited by the engine power, is 134 m/s and the stall speed is 29 m/s. The range is 404 km and the endurance 1.4 hours. The rate of climb and climb gradient are 24.5 m/s and 62% respectively. When looking into the turning performance it could be seen that the minimum turn radius and time to turn are 28 m and 3.3 s respectively.

Sustainable design

Different options have been taken into account to ensure a durable design. During the mission phase, the main approach was to look into recyclable materials. As mentioned before, a steel alloy was used for the fuselage structure and a biodegradable composite was used for the fuselage skin. For the post-mission phase, a modular design has been considered. This works according to the plug-and-fly system. The engine can be replaced by a less powerful engine, and the race wings can be replaced by cruise wings which are optimised for range and endurance. This leads to an increase of up to 28%. Additional fuel

can be stored in the cruise wings to increase range and endurance up to 240%. The fuel is replaced by a less polluting fuel.

26.6 Conclusion and recommendations

Multiple features on the aircraft make the T-16 stand out from other aircraft currently competing in the Red Bull Air Race: first of all, the aileron control system is non-linear, which reduces drag as the ailerons are deflected. Secondly, wingtip devices are used to increase aileron effectiveness. Also special attention is paid to sustainability, resulting in the use of biodegradable composites for the fuselage skin.

The aircraft zero ballast weight is 489 kg, which is 51 kg lighter than the 540 kg required to compete in the Red Bull Air Race and thus ballast weight is required. Its maximum take-off weight including ballast is 698 kg, which is equal to the minimum race weight defined by Red Bull. The total production cost of the T-16 is €115,900.-, which means that the remainder of the €275,000.- budget, can be used for development costs.

To improve the aircraft's practical purposes by doing post-mission commercial flights, a revolutionary modular plug-and-fly design has been developed. The high performance racing engine can be replaced by a more fuel efficient engine, while the race wings can be replaced by cruise wings, optimised for range and endurance. This enables the aircraft to fly promotional banner flights for FlashCo. or towing gliders, without significantly changing the structural elements of the fuselage. To increase the recyclability of the aircraft, the truss structure is designed as a tubular steel truss structure and part of the fuselage skin is made from a fully biodegradable natural composite.

With the current technology it is not possible to convert the aircraft from piston powered to electrically powered. Therefore this is not suitable to implement in the T-16 now, but it is an interesting design option for the aircraft's post-mission purposes.

For next design phases, a number of recommendations are made. To further analyse the aircraft's aerodynamic performance, Computational Fluid Dynamics (CFD) analyses are recommended. The main goal of this is to analyse the effect of the propeller wake on aerodynamic performance, which cannot be modelled accurately without an advanced CFD program such as Fluent. Wind tunnel tests for both small scale and full scale are recommended, for instance to study aerofoil hysteresis effects.

Instead of the current linear, time-independent state-space model, a non-linear, time-dependent state-space model should be developed, to analyse the aircraft's dynamic behaviour more accurately. It is recommended to also build a simulator, to evaluate the aircraft's handling. Finally, the influence of the propeller on the tail control surfaces should be investigated. To improve the performance analyses, it is recommended to perform detailed analyses on the variation of efficiency with altitude of the engine and propeller. By improving the accuracy of the available power provided by the propulsion system, the resulting performances become more realistic.
For the structural analysis, the current models include simplifications. It is advised to develop less simplified models. An investigation into fatigue is recommended to be initiated.

27. NEW AIRLINE WORKHORSE

Students: D.P. Eijpe, G.J. de Haan, J. Haverkamp, J.Y.S. Ip, S.A.W. Moreels, K.M. Simoiu, B.M. Streck, J.L. The, M.P.A. Zondag

Project tutor: ir. J. Sinke

Coaches: ir. P.L. Blinde, X. Liu MSc

27.1 Introduction

Rising oil prices and increasing awareness of sustainability drive the commercial aviation industry towards more fuel efficient designs. Simultaneously, the aviation market is growing significantly, with the Asia-Pacific region expected to dominate future demand in the mid-size, mid-range aircraft class. Current market leaders are the Airbus A320 and Boeing 737, both of which are metal aircraft. Technology improvements in the domain of composite materials allow for lighter airframes. However, large scale application of composites in primary structures has not yet been used for high volume production.

The objective of the A3200-NeMO (New Materials Option) project is to design a successor of the A320 'workhorse'. Main goal is to:

"reduce fuel consumption and to cut operational costs, primarily by minimising airframe weight with the use of composite materials."

Emphasis is put on optimisation of assembly for high volume production.

27.2 Requirements

Starting point of the design process is to understand the requirements which need to be met in order to fulfil the project's objective and goals. A total of 39 requirements is established, where 13 of them are classified as key requirements. They must be met without any compromises in order for the A3200-NeMO design to be successful. The following set of ten requirements provides a representative scope of the complete requirements list.

- The aircraft shall be able to operate on all ICAO class 4C airports.
- The aircraft shall comply with all regulations specified in EASA CS-25.
- At least 50% of the airframe's volume shall be constructed of laminated materials.
- The aircraft shall have an airframe weight reduction of at least 15% compared to the current A320.
- The aircraft's seating capacity shall be 180 passengers in single class highest density configuration.
- Maximum range shall be at least 3,700 km with design payload on board.
- Fuel consumption shall be at least 10% lower in comparison to the current A320 on a 1,000 km flight at cruise altitude of 35,000 ft with a load factor of 85%.
- Production rate shall be at least 50 frames per month with an option to increase to 75.
- Production costs shall not exceed an additional 25% in comparison to the current A320.
- The aircraft shall be in service in the first quarter of 2025.

27.3 Configuration

In aircraft design, the very first trade-off and decisions concern configuration. It includes engine type, engine position, fuselage class, wing location, empennage type and gear configuration. A total of 19

possible concepts are explored, with the term 'possible' interpreted in the broadest sense.
First, preliminary filtering narrows down the list of concepts by eliminating obviously unfeasible ones and those which cannot be developed yet. Also, concepts with no aerodynamic improvements and configurations which require airport adjustments are taken out, as are concepts which are unsuitable for the mid-size aircraft class.

Remaining concepts after filtering are traded-off through qualitative assessment of six weighted criteria: aural signature (3/5), manufacturing (4/5), customer appearance (2/5), maintainability (3/5), aerodynamic performance (4/5) and ground operations (3/5). Overall best scoring concept is an elliptical body with aft open rotor engines and fuselage mounted undercarriage. Figure 27.1 illustrates the A3200-NeMO's configuration, as well as its cross section in high density configuration.

The elliptical cabin allows for two aisles in an 8-abreast (2-4-2) configuration. As such, passengers are never more than one seat away from the aisle. Moreover, two aisles quicken loading and unloading, reducing turnaround time. Pressurisation however, results in larger hoop stresses within the elliptical hull.

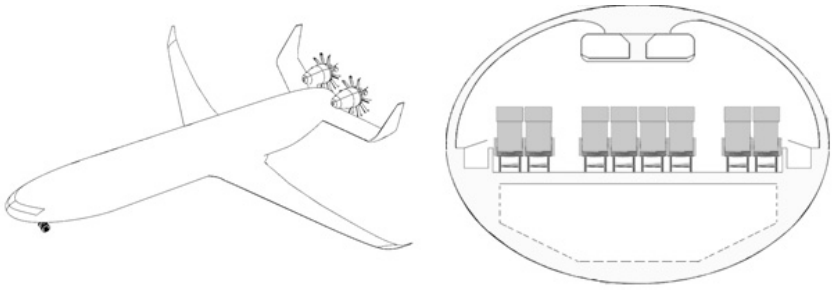

Figure 27.1: A3200-NeMO concept illustration and cross section sketch

The selected fuselage serves as a lift generating body, making the fuselage into an aerodynamically beneficial section rather than just a parasite drag generator. Aft mounted engines have two main advantages. First, larger fan blades are allowed, because engine ground clearance is significantly larger compared to wing mounted

engines. Second, the body and C-tail shield both passengers and environment from noise. On the other hand, a far aft centre of gravity and the engine certification are points of attention.

Initial sizing and first weight estimations are established according to Roskam's Class I approach. Enhancements in aerodynamics and structures are assumed to be 5% each. The propulsion system accounts to a 10% improvement in fuel economics, although cruise Mach number is decreased by 5%. On a typical A3200-NeMO mission the corresponding additional flight duration is expected to be compensated by faster turnaround. Final Class I design parameters are presented in table 27.1. Fuel consumption on a 3,700 km flight is cut by 19%.

Table 27.1: Class I design parameters

	A3200	A320	Units		A3200	A320	Units
MTOW	68.8	78.0	tonnes	Cruise Mach	0.741	0.780	-
OEW	35.3	42.6	tonnes	Max thrust	231	230	kN
Mission fuel	15.2	18.7	tonnes	Wing area	109.3	122.6	m^2
Design payload	19.8	19.8	tonnes	Aspect ratio	11.8	9.5	-

Elaborating on Class I design, a more detailed set of aircraft characteristics is determined through Torenbeek's Class II method. Weight of various components and their corresponding centre of gravity (c.g.) are computed. In addition, the shift in centre of gravity location during loading is analysed. Class II output is used to ensure stability and controllability of the aircraft during operations. Table 27.2 displays Class II design results.

Table 27.2: Class II design parameters. All locations are specified with respect to the aircraft's nose.

	A3200	A320	Units		A3200	A320	Units
Fuselage length	33.0	37.6	m				
Most aft c.g.	22.4	n.a.	m	OEW c.g.	22.3	16.6	m
Most forward c.g.	19.7	n.a.	m	MTOW c.g.	20.6	n.a.	m

The A3200-NeMO has a design range of 3,700 kilometre at a payload of 180 passengers. Trading payload for range is possible according to the payload-range diagram presented in figure 27.2. A comparison to the A320 is included as well. Differences are mainly due to the A3200-NeMO's improved aerodynamics and enhanced engine performance.

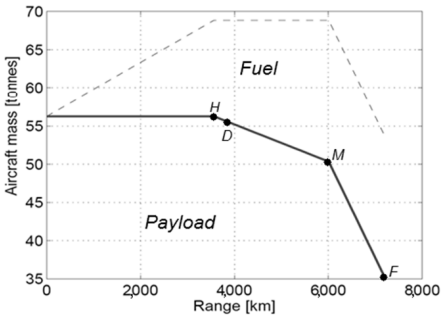

Range[km]	*A3200*	*A320*
Harmonic	3,560	2,960
Design	3,700	3,500
Max. fuel	6,000	5,560
Ferry	7,200	6,850

Figure 27.2: A3200-NeMO payload-range diagram

27.4 Aerodynamics and control surfaces

Among the aerodynamic surfaces are the systems needed for the aircraft to fulfil all flight phases within the flight envelope. First, a suitable aerofoil is selected. The NASA/LANGLEY LS(1)-0413 is favoured over others, because of its high lift to drag ratio in cruise conditions. The aerofoil geometry is the same throughout the wing, but a twist of 3.3 degrees is introduced to prevent tip stall.

Due to insufficient lift generation at low speeds during take-off and landing, high lift devices (HLDs) are investigated. Simplicity of the HLDs is a key factor during selection, ensuring low weight and limited maintenance. The chosen concept is a combination of single slotted Fowler flaps and downward deflecting spoilers. Figure 27.3 illustrates the A3200-NeMO's aerofoil with high lift devices deployed. The flap-spoiler system provides the same additional lift as more complex double slotted Fowler flaps. Since the spoilers are incorporated in the flap system, they are placed along the same wingspan as the flaps, namely 70%. In order to compensate for the higher ground effect due to the A3200-NeMO's lower wing, spoiler area will be larger than on the A320.

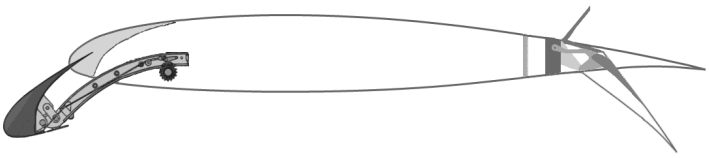

Figure 27.3: A3200-NeMO airfoil with high lift devices deployed (not to scale)

Of the remaining 30% wingspan, 21% is used for ailerons. These control surfaces enable the A3200-NeMO to comply with banking regulations during take-off at MTOW. Both the ailerons and flaps are limited in width, due to the aft spar location of the wing structure. The flaps and ailerons are no wider than 30% of the local chord, which satisfies both the spar constraint and high lift device size requirement.
For longitudinal stability and controllability, the vertical tail volume is determined based on reference aircraft. For the horizontal stabiliser, the extreme front and aft centre of gravity locations are used. Final results are the general dimensions of the empennage.

The rudder is sized to ensure a sufficiently large flight envelope during cross-wind landings. Cross-wind landing is the driving requirement, rather than a one engine inoperative situation, because the fuselage mounted engines create a smaller moment during engine failure than wing mounted engines. In addition, recall that the A3200-NeMO has a twin tail, resulting in two smaller rudders.

The elevator is sized such that it provides enough pitching moment to rotate the aircraft during take-off. Also, its deflection at different centre of gravity locations is investigated. Final results show that trim conditions may be optimised in future.

Finally, aerodynamics of the fuselage is considered. Most aircraft have a circular fuselage. However, the A3200-NeMO has an elliptical body. Using a Computational Fluid Dynamics tool, the fuselage is found to generate 18% more lift, at a 5 degree angle of attack in comparison to a circular fuselage. Overall, 17.5% of all lift is generated by the fuselage.

27.5 Structures and materials

For the design of the A3200-NeMO, structural loads are analysed and appropriate materials are selected. For analysis, an ultimate manoeuvre load factor of 2.5 is assumed. Additionally, a safety factor of 3.0 is taken into consideration to account for the use of composites and calculation uncertainties.

Wing and fuselage design

The main airframe components to be redesigned are the wing and fuselage. For analysis, one wing half is modelled as a cantilever beam; the fuselage is modelled as two cantilever beams attached to each other at the quarter root chord.

The loads acting on the structure cause shear stresses and normal stresses in longitudinal and transverse direction. These stresses are used to size the primary structural components such as stringers and skins.

For both skin and stringers, carbon epoxy is used as material. Since it is assumed that stringers cope with axial loads only, their fibre content in axial direction should be as high as possible. It was chosen to have 70% of all fibres in 0° longitudinal direction, 15% in 90° transverse direction and 15% in ±45° direction. Since the skin has to cope with both axial and shear stresses, more isotropic properties are desired. Therefore, a fibre orientation of 40% , 40% and 20% in 0°, 45° and 90° direction, respectively, is chosen. The 0° orientation refers to axial direction.

Using carbon epoxy as material, the wing weight amounts to 7.1 tonnes. For a constant thickness fuselage of 4 mm, the weight would amount to around 6.5 tonnes.

Detailed fuselage design

For the A3200-NeMO, 27% wider and 47% higher windows as compared to the A320 are chosen to be in line with market trends. Cut-outs result in a redistribution of stresses in their proximity,

yielding a locally reinforced structure that is around 11% heavier than without cut-outs.

Also, a varying skin thickness is considered. More specifically, the fuselage front section from nose to wing root is redesigned. A thickness ranging from 2.4 to 3 mm throughout the front fuselage is found, resulting in a fuselage mass of 5.8 tonnes.

Airframe weight
Adding the weight estimates of empennage, surface controls, nacelles and undercarriage to the calculated wing and fuselage weight, results in an airframe of 18.8 tonnes. Applying a contingency value of 5% to account for joints and floor supports, the airframe weight amounts to 19.7 tonnes, yielding a 16% weight reduction in airframe as compared to the A320.

27.6 Manufacturing and assembly

High volume production is one of the top level requirements of the A3200-NeMO. In order to achieve the required production rate of at least 50 aircraft per month, current manufacturing and assembly procedures are explored.

Manufacturing
Manufacturing of the A3200-NeMO focusses on the manufacturing of stringers, spars, ribs and frames. Starting point is a number of manufacturing processes, from which twelve candidates are selected. This first selection focusses on cost and feasible production quantities of the manufacturing processes. Subsequently, a trade-off is performed with criteria such as production speed, cost, shape and safety. From the trade-off, pultrusion is selected as manufacturing process for the stringers and spars. The skins, ribs and frames are manufactured using lay-up of prepregs. Skin and stringers are co-cured

For aircraft assembly, joining and corresponding processes are crucial aspects. Adhesive bonding has a number of advantages, such as a

better load distribution over the joint. However, the use of adhesive bonding in primary structures is not yet possible due to strict regulations. Consequently, stringers in the primary structure are joined to the skin by co-curing through Quickstep, a new process which rapidly cures the parts using liquids instead of gas to transfer heat. Since expandable joints should be avoided in composites, the remaining structural elements are joined by titanium HI-LOKs.

Assembly

Recall that 50 aircraft will be delivered per month, with an option to increase to 75 aircraft. Boeing and Airbus currently deliver 47 737s and 42 A320s per month, respectively, each using three separate final assembly lines.

The parts delivered to the final assembly line are already sub-assembled and tested. Among the major parts delivered to the line are the front- , mid- and aft fuselage sections, the wings, empennage and engines. Producing 50 aircraft per month means that approximately two aircraft need to be assembled per day. Due to the high volume production and associated risks, it is chosen to use two moving final assembly lines divided over two factory sites. Boeing already incorporates a moving line that shortens corresponding assembly time by multiple days. For the A3200-NeMO it is aimed to have a final assembly line that takes ten days to produce an aircraft. Subsequent painting of the aircraft requires three days. The final assembly factory will operate for 20 hours per day effectively, five days per week, leaving two days for reserve purposes. Work is divided among two day shifts and one night shift.

The final assembly process is split up into three parts. The first one is the fuselage line, where all three fuselage sections are joined and several components are installed, such as the undercarriage and the overhead bin lockers. The complete fuselage is then transported to the major assembly line by crane. On the major assembly line, empennage, wings and engine pylons are added. The final step is the addition of the engines. They are installed last, being the aircraft's most expensive and fragile part.

For the moving assembly line, a default speed of 5.1 cm per minute is chosen, which results in 50 aircraft built within 19 days using two moving assembly lines. 75 Aircraft are produced within 28 days. For contingency purposes, a faster line speed is preferred. Line speed can be increased according to the figures in table 27.3.

Table 27.3: Moving assembly line speed comparison

	Speed 1	Speed 2	Speed 3
Speed of line [cm/min]	5.1	5.8	6.8
50 aircraft [days needed]	19	17	14
75 aircraft [days needed]	28	25	21

The two assembly lines are divided among two geographically different factory sites. Taking into account the highest speed of the final assembly line, each factory site has six hangers. This also includes a spare hangar to use in case of delays. In case one factory is out of order due to unforeseen circumstances (e.g. strikes, fire), the line speed can be increased to 6.8 cm per minute. That speed is required for the remaining factory to still be able to produce 50 aircraft per month. Note that it is impossible for the sole operating factory to output 75 aircraft per month.

27.7 Conclusions and recommendations

The A3200-NeMO's project objective was to design an A320 successor with a reduced airframe weight, through innovative materials and corresponding manufacturing principles, optimised for high volume production. Due to enhanced aerodynamic and propulsive properties, a fuel reduction of 19% on a 3,700 km trip is achieved, resulting in a CO_2 reduction of 11.1 tonnes per flight. The use of carbon epoxy in the primary structure allows for an airframe weight reduction of 16%. With two moving assembly lines, the minimum required 50 aircraft per month as well as the option to increase to 75 can be achieved.

In terms of operational profits, preliminary estimates have been made. Selling price will be USD 120 million, thus around 28% more expensive than the current A320. The higher selling price is compensated for by 12% lower annual operating costs. In order to

obtain better insight into economic benefits for the manufacturers, it is recommended to determine manufacturing and assembly costs in greater detail.

At the end of the project, none of the 39 requirements are violated. However, one third of them could not be validated. Nevertheless, all results are satisfactory at this design stage. The A3200-NeMO is safe, sustainable and satisfies customers.

Figure 27.4: A3200-NeMO isometric view

Figure 27.5: A3200-NeMO rear view

28. WORLD'S LARGEST DIRIGIBLE BILLBOARD

Students: M. Corvers, B. De Vogel, A.F. van Geel, W.B.A. Grimme, N.J.F.P. Guillaume, M.G.M. Jans, B.C.P. Jongbloed, A.J.P. Knol, C. Patrizi, N.J. Schutteman

Project tutor: ir. D. Steenhuizen

Coaches: dr.ir. A.C. in 't Veld, Y. Guo, MSc

28.1 Introduction

In order to be able to reach a broad audience for commercial announcements, increasingly complex strategies are being developed by marketers to catch the attention of their intended audience. A new method of advertising has been conceived by having large video displays positioned at considerable height, viewable from several kilometres away. In addition, a commercial opportunity is envisioned by exploiting this system for sightseeing.

The decision was made to name the project "Diamond of Dubai". Following the requests of the company "United Balloon" (UB), the Diamond of Dubai team developed a 95 meter high dirigible, supporting three large video screens and a gondola. The video screens are visible from a distance of four kilometres and the gondola provides sightseeing to the tourists in the city of Dubai.

Figure 28.1: Diamond of Dubai logo

The mission need statement is:

"In order to reach a broad audience for advertising and commercial purposes, a dirigible billboard having large video-displays, positioned at considerable height, providing sight-seeing, initially deployed at the Wafi shopping mall in Dubai and viewable from Dubai's airport needs to be developed."

28.2 Requirements

Customer requests provided the team with the following important requirements:

- The system shall operate continuously for an operational life-time of 10 years.
- The system shall be certifiable under Dubai's airworthiness regulations.
- The system shall be able to get into safety mode within 24 hrs.
- Video broadcasts shall be displayed at a height of at least 250 m.
- The display shall cover 360 degrees in azimuth.
- The display shall display video broadcasts from 06:00 to 03:00 on a daily basis.
- Display's visibility shall not be hampered by vibration due to atmospheric turbulence.
- The system shall transport 50 persons to and from a height of 200m for sightseeing.
- The system shall have the capacity for continuously repeating the sightseeing task 4 times per hour on a daily basis from 10 AM till midnight.
- Display video broadcasts shall be visible from Dubai's airport.

28.3 Design concepts

In order to provide UB with the best possible design, six different design concepts were created. Before creating these six designs, trade-offs were performed on every subsystem of the aerostat. In these trade-offs, the clearly infeasible options were discarded and a ranking was made for the feasible options. From these feasible options, the six design concepts were then created.

The "1st choice" design was based on the subsystem trade-offs, incorporating as many subsystem options that were ranked first. Only when a certain choice for a subsystem was incompatible with another first choice, the subsystem option that was ranked second was used. The "balanced" design was created as a team effort and tried to incorporate the systems that were most likely to work well together and create an optimal design. The "cost" design incorporated all subsystem options that would require the smallest investment. This resulted in a design that was very attractive from a financial point of view. The "safety" design incorporated all the subsystem options that were considered the safest option in that category, resulting in a design that would have no problems in getting certified. The "stability" design was created using all subsystem options that would result in the most stable design, as stability is a major concern. Finally, the "aesthetics" design incorporated all the subsystem options that were considered to be the most aesthetically pleasing, resulting the most eye-catching design.

These designs were then analysed on different characteristics, such as finances, reliability, safety, design risk and sensitivity. A final trade-off was then performed and the "balanced" design turned out to be the best design option. This design is shaped like a three-sided diamond, is reinforced with an internal structure and its lift is provided by helium. The advertisement system consists of three large LED arrays on the sides of the diamond and sightseeing is provided by a gondola that is suspended from the aerostat by cables.

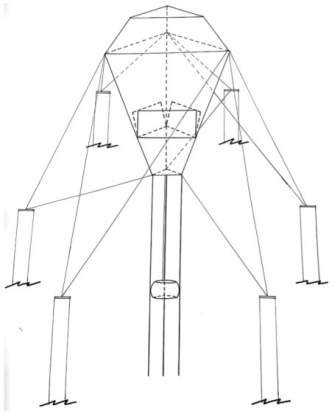

Figure 28.2: Preliminary layout of the billboard

28.4 Payload design

The payload of the aerostat consists of the advertisement screens and the sightseeing mechanism. This section covers the design of both systems.

Advertisement screens

As the advertisements need to be visible from a distance of 4 km, the screens need to be large enough to guarantee this visibility. After research and conference with UB, a screen height of 18 meters was chosen. As advertisements are standardly made for screens with an aspect ratio of 16:9, the screens on the aerostat will have the same aspect ratio. This results in three screens of 32x18 m.

In order to limit the size of the aerostat, the payload weight should be kept as low as possible. This was an important deciding factor in selecting the screen technology. LED curtains are the lightest screens currently available. These can provide sufficient brightness to even allow the advertisements to be visible during the day, when the sun in Dubai is very bright. The second important aspect of the screens is the resolution. The image should be clear and individual pixels should not be visible to any viewer. To guarantee this, it has been determined that a pixel spacing of 50 mm is sufficient.

Because LED curtains are not rigid, a structure is needed to connect these curtains to the dirigible. An aluminium structure of crossbeams was designed to this end. The total weight of the screens including structure is 9,000 kg.

Sightseeing mechanism

The sightseeing mechanism consists of a gondola which is stabilized by three cables on its sides and lifted by a cable that is connected to an engine on the aerostat. The size of the gondola is 8*8*3 m, it provides room for 50 tourists and 10 staff members and weighs approximately 2,300 kg. In figure 28.3, the internal structure of the gondola can be seen.

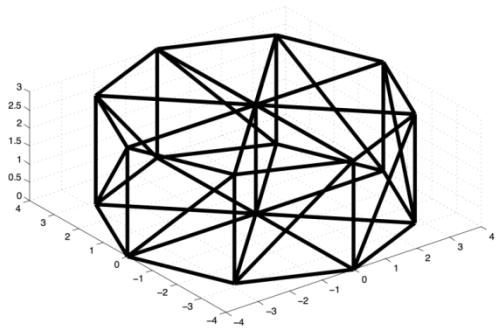

Figure 28.3: Internal structure of the gondola

The stabilization and lifting cables are Dyneema cables, designed with a safety factor of 12, which is a commonly used safety factor for elevator cables. A 35 kW engine is located on the aerostat and will provide the power for the ascent and descent of the gondola, which will be at a speed of 0.83 m/s. A passenger weight of 100 kg is assumed, to account for variations in passenger weight and possible carry-on luggage. This results in a total weight of around 9,000 kg for the sightseeing mechanism.

28.5 Structures and materials

MATLAB was chosen to perform the structural sizing calculations. Once the preliminary structural configuration was put in MATLAB, it was found to be statically indeterminate. As a result, the first step was

to change the configuration, until it was statically determinate. Next, the internal forces in each member needed to be calculated. These internal forces are a result of the external applied loads, such as gondola attachment cables or drag on the surface. For sizing, the worst load cases were used. After this, the truss members needed to be sized on their internal load. By only sizing the structure on its internal loads, the total mass, when using aluminium, was found to be unrealistically low at 1,200 kg. Further investigation showed that the buckling of the members would have the largest impact on the structure. Next, a second sizing process was performed to size the members for buckling. These calculations resulted in a required cross sectional area far larger than the first required area. As a result, the structure was now optimally designed for buckling, but a lot overdesigned for internal failure. As a consequence of this, the resulting structure would be heavier than required.

The optimum design configuration would be such that the two failure modes occur at exactly the same time. In order to ensure the optimum design, the material area for tensile failure was taken and the cross sectional area was adjusted to change the moment of inertia. This way, both failures would happen at the same time, resulting in a minimum structural weight. Unfortunately, the required diameter of some members exceeded 3.5 m, which is not feasible for production. This option was therefore discarded. Another design parameter that could be adjusted was the length of the members. An effective alternative to influence the buckling of the structure was adding members. When aluminium would be used, this resulted in a far too heavy structure which took up nearly 90% of the aerostat's MTOW. Therefore, using aluminium was no longer an option, the only material that was still eligible seemed to be carbon fibre reinforced plastics (CFRP). Manufacturability was also taken into account: realistic maximum member diameters were chosen, as well as minimum manufacturable wall thicknesses. The mass of the final internal structure is 32,000 kg.

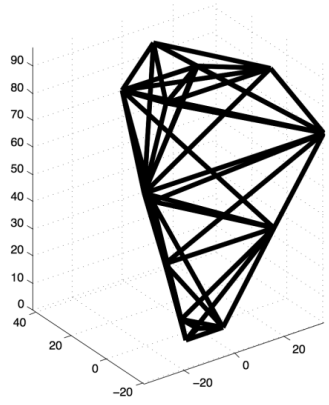

Figure 28.4: Internal structural layout of the aerostat

From the inside to the outside, the dirigible will consist of an internal envelope, the internal structure, fishnet cabling and an external envelope. The function of the internal envelope is to contain the helium and to withstand any pressure differences. The internal structure will ensure that the aerostat retains its shape and it handles the loads that act on the aerostat. The fishnet cabling will ensure further retainment of the shape, by ensuring that the external envelope cannot bend towards the inside of the aerostat. The function of the external envelope is to protect the components inside the aerostat from the harsh environmental conditions. The entire structural weight of the aerostat is 48,000 kg.

28.6 Aerodynamic stability

Disturbance of the aerostat consists of displacement, rotation and vibration. To prevent displacement and rotation of the aerostat, cables will be used to tether it. With the use of cables, a balance needs to be found. The more cables, the more stable the system. However, the more cables, the more ground space required, which is undesired. In the end, full stabilization must be ensured with the least ground space required.

The tetrahedron has three corners. These corners are structural nodes and are therefore strong points. This structural argument is the reason that the cables will be connected to the three corners.

The next step is determining how the cables need to be directed to prevent destabilization. Inspired by a recently published master thesis, it was concluded that pointing three cables in the three directions of the corners was not sufficient. Two of the three cables would be hanging loosely and one cable would have to cope with all forces. A better configuration to cope with wind force from one side and directly prevent rotation to a certain extent was to have one cable in the direction of the wind and two other cables, connected to the other corners, pointing diagonally into the direction of the wind.

Wind is unpredictable and can originate from all possible directions. The concept of figure 28.5 is a good way of coping with wind forces. This concept solves for displacement as well as for rotation. To reduce the amount of required ground connections and ground space, every two diagonal cables are connected to one ground station and these ground stations are placed on top of 50 m high poles.

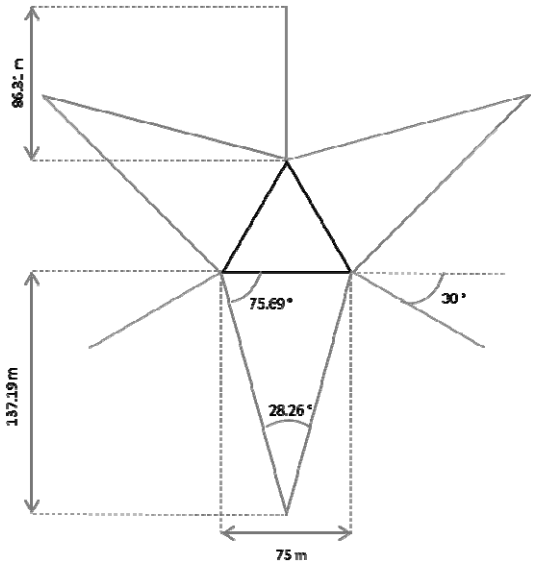

Figure 28.5: Cable layout and ground area

Vibration is caused by vortex shedding. When the frequency of this vortex shedding approaches the natural frequency of the aerostat, resonance will occur. This will cause loads way beyond the structural

capacity and should thus be avoided. To avoid resonance, the eigenfrequencies of the aerostat should be higher than the vortex shedding frequencies.

The flight envelope of the aerostat can be seen in figure 28.6. The average ground wind speed in Dubai is 5 m/s. The aerostat is able to operate at an altitude of 280 m up until a ground wind speed of 5 m/s. Up to a ground wind speed of 12 m/s, the aerostat can remain in operation, but at a lower altitude.

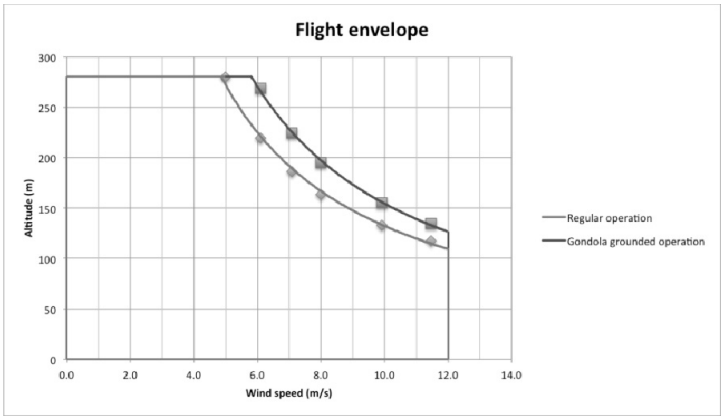

Figure 28.6: Flight envelope

28.7 Safety mode

When the ground wind speed exceeds 12 m/s, the aerostat has to be lowered to the ground. This lowering is achieved by retracting the stability cables for the aerostat and gondola. The aerostat can be lowered at a speed of 0.5 m/s, which ensures that the aerostat reaches the ground within 10 minutes. After being lowered, the bottom of the internal structure of the aerostat will be secured to the ground. Stabilization of the aerostat will be achieved by tightening the stability cables. At higher wind speeds, the stability cables are not sufficient to stabilize the aerostat, so extra cables will be added to structural joints as the wind speed increases. Above a wind speed of 25 m/s, the amount of cables needed would exceed the number of

structural joints. Extra cables could then be added to the structural members themselves or the outer envelope of the aerostat.

28.8 Final layout and performance

Figure 28.7 shows the final layout of the aerostat. The most important performance characteristics can be seen in table 28.1 and in figure 28.8, the dimensions of the aerostat are shown.

Figure 28.7: Final layout of the Diamond of Dubai

Table 28.1: Performance characteristics of the Diamond of Dubai

Performance characteristic	Value
Payload weight/total weight	0.21
Lift/MTOW	1.40
C_L (at α=0)	0.16
C_D (at α=0)	0.84

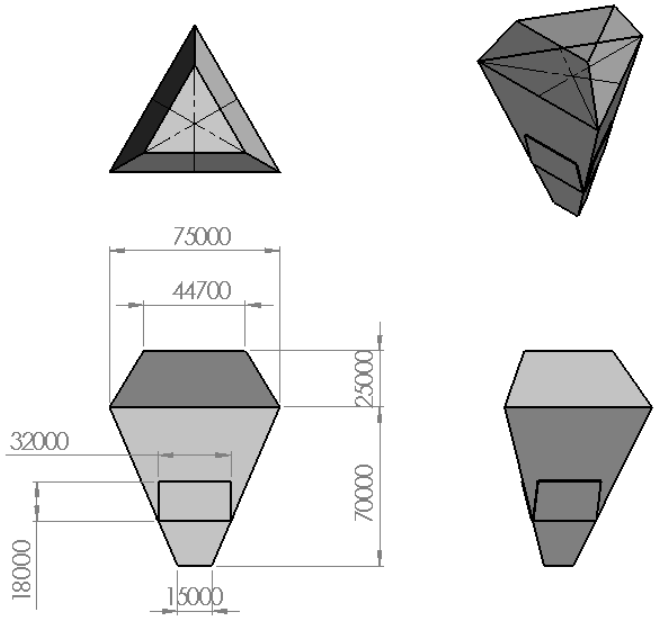

Figure 28.8 Dimensions of the billboard

28.9 Cost

The cost has been evaluated for the design lifetime of 10 years. The cost is broken down into development and production costs and operational costs. The development cost is estimated to be in between 6 and 10 million euro and the operational cost is estimated to be in between 3 and 5 million euro per year. When this is compared with the estimated revenue, the return on investment is commercially attractive.

28.10 Conclusion and recommendations

The most important outcome of this report is that a technical feasibility is confirmed, provided that assumptions made correspond with reality to a sufficient extent. A preliminary layout shows that, with a correct material choice, it is possible to build a structure light enough to lift with helium, yet strong enough to withstand wind forces. Furthermore, calculations into aerodynamics and stability show that it is possible to keep the dirigible stable and upright in the

air. Although the required ground space is currently out of bounds, no large redesign is thought to be necessary to resolve this issue. Finally, it has also been found possible to realize the plan of attaching a gondola to the base of the balloon for sightseeing purposes.

It is recommended that wind tunnel tests and dynamic CFD analyses are performed in a further design of the aerostat. This should yield the actual loads on the structure and enable structural and aerodynamic optimization. The eigenfrequency of the structure should also be determined, to ensure that vortex shedding does not destroy the structure.

29. AEGIR: MARITIME MONITORING OF THE NORTH SEA USING A BI-STATIC SAR SATELLITE NETWORK

Students: T. Buijs, D. Ju, N.M. de Kogel, S.P. van der Linden, A. Melaika, T.D. van den Oever, D. Petković, B.T. van Putten, C.W.M. Verhoeven

Project tutor: ir. P.P. Sundaramoorthy

Coaches: A ir. M.C. Holtslag, X. Mao MSc

29.1 Introduction

The North Sea is a relatively small body of water through which a large amount of ships travel to one of the important ports in North-Western Europe, such as Rotterdam and Hamburg. Approximately 34% of the worldwide shipping trade travels through the North Sea, and this high shipping density necessitates reliable continuous monitoring. A system called Automatic Identification System (AIS) is already in place to monitor and guide these ships. However, this system is limited to detecting sea vessels equipped with AIS transponders and currently restricted by ground receivers to monitoring vessels close to the coast. Furthermore, there is significant legal and environmental interest in detecting oil spills and illicit fishing in the North Sea. A solution is offered by the Aegir

constellation that can enhance maritime monitoring to meet current and future needs.

This chapter elaborates on the design of the Aegir constellation. First the mission objectives will be clarified, followed by a description of the initial conceptual designs. Thirdly, the final design will be presented, along with a description of the individual subsystems. Finally, conclusions will be drawn, which will be used to state recommendations for further research and design actions.

29.2 Mission objectives

The Aegir constellation consists of a network of bi-static Synthetic Aperture Radar (SAR) satellites. As the name implies, radar is used with this technique. In normal radar, a pulse is transmitted by an antenna and reflected by a target. This echo is received back at the same antenna, where the time between the transmission and echo results in the distance to the target. SAR involves using radar to create images of the terrain that lies within the beam of the (moving) transmitter. In the Aegir mission, it is used to detect and track ships in the North Sea. The objective of the mission is:

"to detect at least 90% of all vessels in the North Sea."

This is primarily to be performed by using the so-called PanelSAR instrument provided by the Dutch company SSBV, the main customer of the project. It is required that the monitoring is as continuous as possible, hence the temporal resolution must be low. For the Aegir constellation, the target temporal resolution is set to 100 minutes.

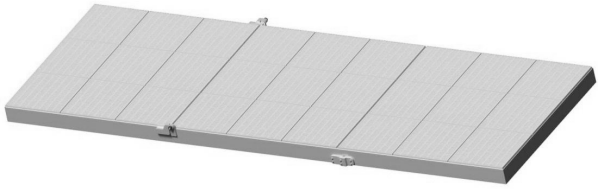

Figure 29.1: The PanelSAR provided by SSBV

In accordance with these requirements the first conceptual designs were created, which are described in the next section.

29.3 Conceptual design

For the initial design of the satellite pair, four different design options were examined. These four designs differ with respect to cost, reliability, and other major design parameters.

The first option consists of two identical satellites. Each of these satellites is capable of transmitting the SAR signal down to Earth, as well as receiving it. Furthermore each of the two satellites is also capable of sending the payload data generated by the SAR instrument down to Earth. Due to the fact that each satellite is able to perform all the required functions to perform the mission, this proves to be a very reliable design.

The second option was designed in order to be able to provide the most inexpensive satellite pair that would still be able to perform the mission. The first satellite, designated the transmitter satellite, is used to send the SAR signal down to Earth. A second satellite designated as the receiver satellite has the responsibility to measure the response and communicate this data down to the ground.

The third option differs from the previous ones in the fact that here the main focus of the design was to provide most inexpensive downlink solution for the transmission of the payload data. To this end, the receiver satellite is capable of processing part of the data generated by the payload. This results in a lower amount of data that needs to be sent down to Earth. However with the use of this method, a lot of the measured information is lost, since only images are sent down to Earth.

The last design makes use of a single transmitter and two or more receivers. By adding multiple satellites capable of receiving the response from the SAR signal sent to Earth, more information can be obtained on the area measured. This includes a velocity map. Due to

the extra receiver, this design is a more expensive option with enhanced performance.

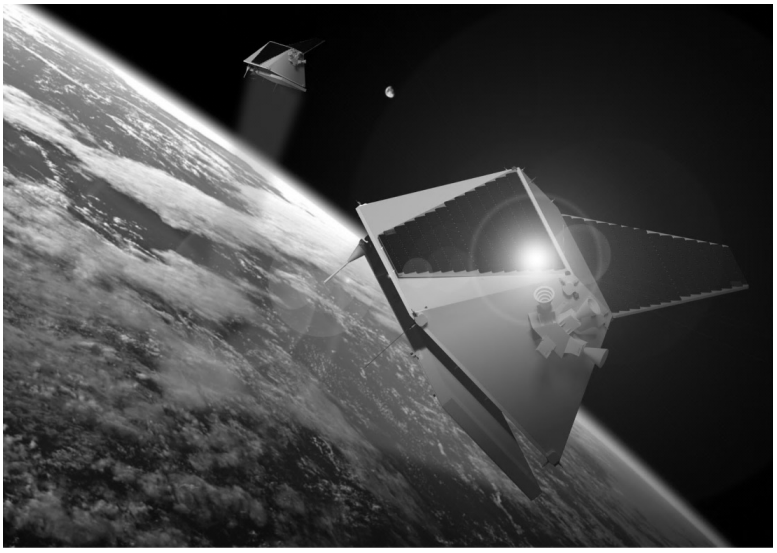

Figure 29.2: A satellite pair consisting of a transmitter and a receiver satellite

Since the focus of the mission is to create a feasible design, the final choice is the option that results in the lowest cost for the mission, which is option two.

29.4 Final design

With an idea on the general layout of the satellite, the detailed design of each of the subsystems could be performed.

Astrodynamics

The PanelSAR has a swath width of approximately 120 km, but it differs with the side-looking angle. The satellite pairs will be placed in an Earth repeat orbit at an altitude between 510 km and 517 km. The satellites will be placed at five different inclinations between 58 and 63 degrees. The advantage of the selected Earth repeat orbit is that the ground track of the satellite repeats on a daily basis. The ground track can be aligned with areas of interest, such as fishing areas and

shipping routes. The selected Earth repeat orbit has five daily flyovers over the North Sea, which is more than polar or Sun synchronous orbits. In order to obtain a 100 minutes temporal resolution of the North Sea, 20 satellite pairs are launched using four Soyuz 2-1b launchers. The entire constellation consists of 40 satellites of which six satellites are redundant with respect to the temporal resolution.

Launcher

The chosen launcher is the Soyuz 2-1b. The Soyuz rocket has already performed over 800 successful launches with a success rate of 97.4% and can easily fit 5 satellite pairs inside the fairing. A major advantage is the provided frigate which can act as the orbital insertion module. This frigate is able to put all the satellite pairs in their different orbits. Therefore no extra ΔV is required from the spacecraft for this part of the mission. A cylindrical support structure on which the satellites will be mounted is placed in the middle of the fairing. On the bottom, 6 satellites are placed around this support structure, at the top there are 4.

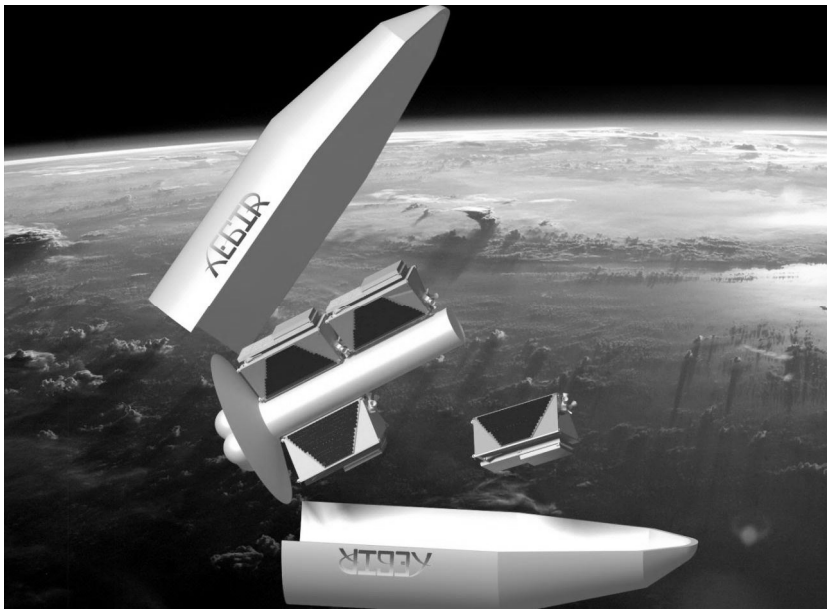

Figure 29.3: The launcher fairing, support structure and insertion module

Propulsion

The propulsion system is responsible for the orbital maintenance and attitude control, such as insertion into orbit, formation keeping, momentum dumping, altitude and differential drag corrections. Extra simulations were made for the de-orbiting stage and if de-orbiting might create space debris, due to the transmitter and receiver degrading orbits. These simulations proved to be positive, which implies no extra propellant is needed to achieve them and the satellites meet the international 25 year de-orbiting regulation. To perform the previously mentioned orbital and attitude functions, a total ΔV of 143.07 m/s is required over 5 years of the mission. For each of the mentioned functions, a range of 0.23 to 1.1 N thrust is required.

This leads to calculating the needed propellant mass for different stages, which is a total of 36.23 kg. The off-the-shelf 1 N Aerojet MR-103G thrusters are taken, which use hydrazine as a propellant. A total number of 20 thrusters are used to cover 3 degrees of freedom and are grouped into 2 thruster clusters and 3 thruster clusters. From the total propellant mass value, the required volume is calculated and is found to be 0.046 m3. A pressure fed blowdown system is considered due to its simplicity and structural requirements of the satellite's bus. The total volume of the propellant is split for two tanks which have their own assigned components, such as latch valves, one cross-latch valve, pressure transducers, fill/drain valves, as well as orifices with filters. All these components are off-the-shelf like the thrusters. The propellant tanks are made out of aluminium and have a cylindrical shape. They contain propellant and pressurant gas, which is nitrogen. A rubber diaphragm as an expulsion device for propellant will be used.

ADCS

To achieve a pointing accuracy of 10 arcsec a real time Attitude Determination and Control Subsystem is implemented. There are five different sensor types that are chosen. They will be used at specific times during different modes. For the first mode after the launch, the de-tumbling mode, the satellite is going to use magnetometers positioned at 90 degrees to each-other and a fine sun sensor. The

required accuracy for the scanning mode is the highest out of all. This is why the attitude determination sensors must be the most precise and reliable in AEGIR satellite. For the scanning mode satellite is going to use two star trackers along with an inertial measurement unit. Last attitude determination sensor type that is going to be used is the coarse sun sensor. This attitude determination sensor is going to be used for orientation of the solar panels with respect to the Sun. All these sensors are connected with the main on-board computer, while only the fine sun sensors and the magnetometers are going to be connected with the pre-processing unit. This pre-processing unit will be used during de-tumbling and safe modes.

During the de-tumbling mode, a low power attitude control components is required. Therefore three magnetorquers are used. During the scanning mode more accurate components are required. For 3-axis control, a 4-reaction wheel configuration designed by Honeywell have been taken which are placed at a 45 degree pyramid configuration, in which one wheel is used as redundancy. At the operating altitude of 500 km, four main disturbances are present which act on the satellite. This includes gravity gradient, magnetic, aerodynamic and solar radiance torque in order of magnitude. To unload the momentum stored due to these disturbances, the satellites have been equipped with 20 thrusters capable of 0.19 - 1 N developed by Aerojet.

A control process has been added in which PD controller has been added to control the roll, pitch and yaw performances of the satellite. This resulted in stable conditions for the roll and the pitch movement. For the yaw motion however instability has been resulted after 45,000 seconds which should be sufficient to counteract the unstable motion.
GNC

The Guidance, Navigation and Control, or GNC, subsystem is responsible for determining the location and orbit of the spacecraft (Navigation), calculating future manoeuvres to change or maintain the orbit (Guidance) and finally performing the calculated actions (Control). For each Aegir spacecraft, the propulsion system is

responsible for actuating the orbital control of the spacecraft, and has already been treated. Three Septentrio PolaRx2 GPS receivers are responsible for the navigational part of the GNC, complemented by the Satellite Laser Ranging (SLR) network. The PolaRx2 is able to determine the position of the spacecraft within 2 cm and its velocity with an accuracy value between 1.5 mm/s and 1.9 mm/s. The latter characteristic is critical for SAR operations: for the highest quality images, an accuracy in velocity determination of at least 1 cm/s is required. The choice for the PolaRx2 was made because of its low costs: approximately 10,000 euros per unit.

Maintenance of the formation flying is also performed by the GNC. The main method chosen for the formation is the Chief-Deputy method, where one spacecraft is designated chief and one as deputy. It is the chief's responsibility to maintain the orbit, where it is assumed that it is able to maintain a near circular orbit. The other spacecraft, designated as deputy, is responsible for maintaining the separation between the two spacecraft within the formation. For modelling the separation, the same method as developed for the TerraSAR-X/TanDEM-X formation is used. Here, the deputy follows an ellipsoidal motion around the chief within the chief's local reference frame.

The size and orientation of the ellipsoid can be changed by creating a slight variation in eccentricity and inclination between the chief and the deputy. Because it is the deputy's responsibility to maintain the separation, it must carry extra ΔV. For this reason, the receiver satellite is chosen as the deputy because of its slightly lower mass. Extra ΔV must also be added to account for orbital perturbations, which also change the characteristics of the ellipsoid. The J2 effect is by far the largest perturbation, and hence is the one used in the design. The total ΔV found to create the formation and the ΔV to counter the effects due to the J2 perturbation are 2.43 m/s and 10.95 m/s respectively, both not very significant compared with the rest of the ΔV budget.

TT&C

The TT&C subsystem was designed to handle the big amounts of data (2.4 Gb/s) which are produced by the PanelSAR. A simulation of the downlink data rate showed that a combination of two X-band transmitters (0.5 Gb/s) suffice to take care of payload data. This simulation was based on three existing ground stations in the vicinity of our area of interest: the North Sea. These are: Kiruna (Sweden), Matera (Italy), and Neustrelitz (Germany). For the telemetry and command simple S-band transponders are chosen. A redundancy component was added for all of these transmission devices. Additional instruments consist of a GPS component for accurate time synchronization, a data management system for the storage of data in case of surpluses and a central processing unit which handles all of the incoming and outgoing commands and signals.

Power

All the systems especially the payload and the TT&C need a lot of power. To provide this the power system consists out of three parts: the solar cells, the battery and the Power Distribution and Conditioning Unit. The solar cells used are the Ultra Triple Junction cells of Spectrolabs which has an efficiency of 28.3%. The solar arrays are designed for average power and the worst case scenario was used for the design, this is during an eclipse. The longest eclipse is 32.52 % of the total orbit. A total area of 3.47 m2 and 3.68 m2 for the transmitter satellite and receiver satellite respectively. The battery will consist out of 4 batteries of which 1 is for redundancy and the battery will be designed for peak power. The Ves 16 batteries cell chosen lead to a battery weight of 18.4 kg. The PCDU exist out of a modular design which is based on the number of exits needed for all systems. In total this were thirty one 28 V connections, twelve 5 V connections and 20 connections for the thrusters.

Thermal Control

Each component has a temperature range in which it needs to operate, the thermal system is designed for the component which has the smallest range. The batteries had the smallest temperature range of 10 to 40 ∘C. There are two cases analysed of which one is the situation

where the satellite is always in sunlight and where the satellite is in eclipse 35 % of the orbit. To do this it was assumed that 20 % of the peak power is dissipated into heat. In the first case the temperatures are between 22.9 and 26.6 °C and the second case the average temperature is between 17.8 and 22.4 °C. The temperatures in the second case will fluctuate, to prevent components getting too cold polyimide strip heaters are added. This is done for the batteries, the thrusters, and the hydrazine tank.

Structures and mechanisms

The structure of the satellite must be able to withstand the launch forces, protect the satellite components from the environment, and provide attachment points for all the components. The structure of each satellite consists of a bottom plate, on which most of the components are mounted, two solar panels, and a truss structure that carries the loads applied on the bottom plate to the support structure in the launcher. The bottom plate is a 2.5 cm thick aluminium honeycomb panel. Beams with a cross section of 10 cm and thicknesses ranging from 1.5 to 4 mm will be used in the truss structure. Lightweight honeycomb panels are used for the solar panels. A total of 4 small electromotors are used in order to make sure that the solar panels can be pointed towards the sun. The SAR panel will be deployed with the help of a prewound torsional spring.

29.5 Conclusion and recommendations

Conclusion

The aim of this project was to check the feasibility and if possible to create a design for the monitoring of the North Sea using a bi-static SAR satellite configuration. This configuration should be able to monitor the sea with a temporal resolution of 100 minutes. In order to achieve this, it was found that 20 satellite pairs are required. The satellites will have an Earth repeat orbit which repeats every 15 revolutions.

To cover the North Sea efficiently, the satellites have to be spread out over inclinations between 58 and 63 degrees. The satellites will be

launched into orbit using four Soyuz-2 launchers. The Soyuz-2 launcher, combined with a fregat upper stage is used to launch all the satellites into a single orbital plane, so that the fuel required on-board of the satellites is minimized. This will result in different starting values for right ascending node per group launched. A scanning pattern was derived that results in a good coverage of the busiest areas in the North Sea.

The payload of the satellites, the PanelSAR provided by SSBV, is used to scan the North Sea in order to detect ships. By employing side-looking SAR, combined with single-pass interferometry, the required resolution to detect the ships is reached. The addition of AIS to the satellite allows for the combination of the two systems to have a higher chance to detect ships.

The total mass for the transmitter satellite is found to be 471 kg while the receiver has a mass of 483 kg. The transmitter satellite has an average power consumption of 347 W and a peak power consumption of 823 W. The receiver satellite has an average power consumption of 355 W and a peak power consumption of 793 W.

The final cost for the transmitter satellite is equal € 15.2 million, while the receiver satellite has a costs of €17.2 million. The launch costs of the Soyuz-2 is equal to € 40 million. The costs of a the entire constellation would be equal to €1012.5 million. It has been estimated that €315.15 million can be earned directly by saving costs of current monitoring systems.

Current solutions have a lower coverage with respect to a space based SAR mission and can only cover areas efficiently near the coastline. The Aegir project can provide a temporal resolution of 71, 88, 118, 178 or 355 minutes depending on the area, because some areas are covered more often than others. Since space based SAR has a better temporal resolution compared to ground based systems, it is likely that more money would be available for this project than for current solutions.

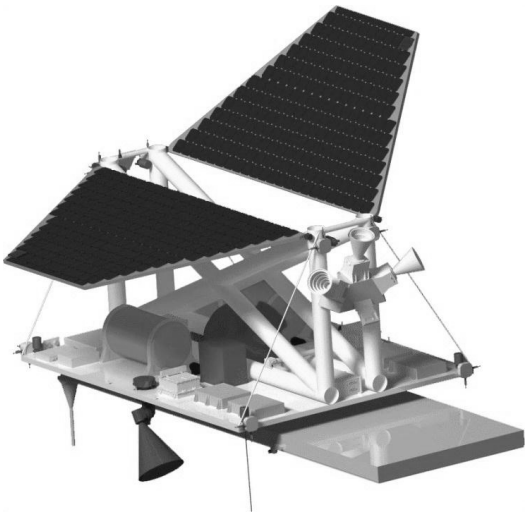

Figure 29.1: The layout of the receiver satellite

The North Sea can be monitored efficiently with a space based SAR system, however the size of the constellation remains dependent on the amount of available resources of North Sea monitoring organizations.

Recommendations

In order to further improve the design, several different steps can be taken. First of all, because it was decided to give the orbits different altitudes and inclinations, these orbits have different orbital periods. This results in the fact that the satellites in the different orbits drift apart during the mission life. More investigation can be done into this phenomenon, since it leads to a variable temporal resolution. A more in depth market analysis can be performed linking the return on investment with respect to temporal resolution. The current market analysis does not take the temporal resolution into account while the temporal resolution is a major performance parameter. Furthermore, the design for the different subsystems that have been presented in this report have not yet been fully optimized with respect to mass and cost. These subsystems can be further improved upon in order to improve the final design of the satellite.

30. ANTARCTIC WIND TURBINES

Students: M.P.C. Bontekoning, S.J.P. Callens, D.A.M. De Tavernier, S.M. Haasdijk, A. Koshias, S.P. Niemansburg, J. Reinders, A.S. Moreiro Ribeiro, N.J.C. Tange, M.F.M, Weerdesteijn

Project tutor: ir. W.A. Timmer

Coaches: dr. D. Stam, W. Zheng MSc

30.1 Mission statement

The Antarctic region, covering twenty percent of the Southern Hemisphere, is a priceless asset to the world with its unique wildlife and can provide great insight for all those studying climate change and the climate systems of the Earth. The Arctic regions are very important for regulating the climate and sea level rise, as they hold a huge reservoir of water. Due to its importance, thousands of scientists and supporting staff live and work in research stations at various locations in Antarctica. One of these research stations is the Signy Research Station located on Signy Island. The station has been occupied since 1947 and mainly biological research is performed. For the research operations, a proper energy source is required. For this purpose, the Windpulse is designed.

The mission statement of the DSE group 20 is defined as follows:

"The DSE group of the TU Delft will design a wind energy system to meet the power demand of the Signy Research Station in a sustainable way"

30.2 Signy Island

Signy Island is an island of the South Orkney Islands, within the Antarctic region, situated in the South Atlantic Ocean. The South Orkney Islands lie on the southern limb of the Scotia Ridge. Signy Island is located at a latitude of 60°43' S and a longitude of 45°37' W. Figure 30.1 presents a map of a part of Antarctica and a closer view on the South Orkney Islands where Signy Island is located. The square on the left and square on the right represent the Signy Research Station on Signy Island controlled by Great Britain and the Orcadas Base on Laurie Island controlled by Argentina, respectively. Laurie Island is not covered by this project. Signy Research Station is located in Factory Cove, Borge Bay, close to the waterfront where the surface is characterised by a rock bottom.

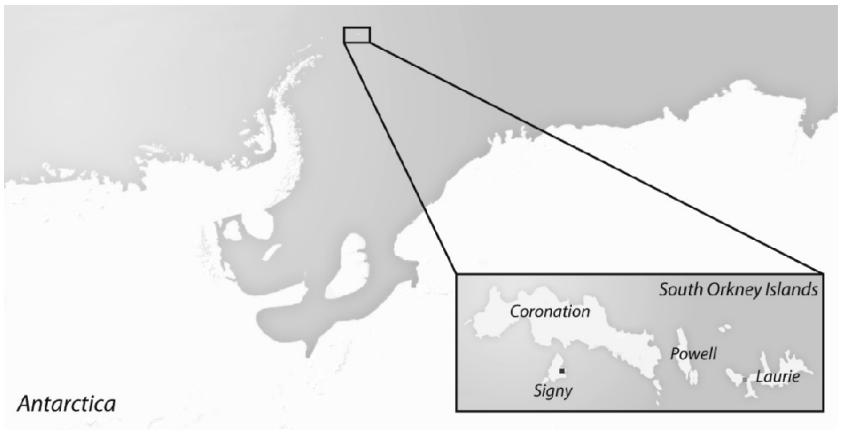

Figure 30.1: Partial map of Antarctica and the South Orkney Islands

Signy is usually covered with ice and attached to the continent of Antarctica by ice. This makes the climate more continental than if it was not connected. Signy deals with strong winters with low temperatures and clear skies. The brightest sunniest days occur in November and December with increased levels of UV light. The

summer is from November to March. The high icy plateaus on the island remain even in high summer times when the climate of Signy becomes more a maritime climate and the ice packs retreat. Low clouds cover the sky and cause frequent, but no heavy rainfall. Since Signy lies north of the Antarctic circle, it is never subjected to 24 hour of day or night. The Sun is below the horizon for a minimum of 4-5 hours at midsummer. These Antarctic conditions with minimum temperatures of -38 °C and wind speeds reaching up to 58 m/s presents an interesting challenge to realise wind turbines on Antarctica.

30.3 Requirements

The driving and killer requirements of the project are a part of the total requirements that the system was designed to adhere to. The requirements are taken into account during the entire design process.

Driving requirements

- REQ-CO-4: The wind energy system shall leave no visible trace above the surface of the Antarctic continent after its end-of-life.
- REQ-CO-5: A waste management plan shall be constructed for the entire life cycle of the wind energy system.
- REQ-CO-6: The wind energy system shall have a carbon footprint with a CO2 equivalent smaller than the current power system averaged over its entire life cycle.
- REQ-TE-1: The wind energy system shall be able to continuously meet the power demand of the Signy Research Station.
- REQ-TE-12: The wind energy system shall have an energy storage system capable of providing power at 65% of the average power for three consecutive days.
- REQ-TE-15: The maintenance of the wind energy system shall be limited to one major session per year.

Killer requirements

- REQ-CO-3: The wind energy system shall adhere to the legal constraints and regulations imposed by the Protocol on Environmental Protection to the Antarctic Treaty.

- REQ-CO-7: The total cost of the wind energy system shall not exceed €500,000 excluding the battery systems.
- REQ-TE-2: The structure shall withstand the aerodynamic loads obtained at an average wind speed of 15 m/s with gusts of maximum 75 m/s during its entire lifetime.
- REQ-TE-3: The structure shall withstand a temperature range of minimum -50° and maximum 20° during its entire lifetime.

30.4 Horizontal axis wind turbine

Since Signy Island is one of the most windy locations in the world, the free available wind is a perfect source to base the energy production on to power the research station. Wind energy systems appear in different shapes and configurations. By performing a trade-off, a base design is selected on which the whole design process is established.

The configuration selected to operate within the hostile Antarctic environment was that of a horizontal axis wind turbine (HAWT). The selected HAWT design is a lift driven device and as such is the most commonly implemented wind turbine system around the world. This configuration was deemed to be the optimum design given the environmental conditions and defeated vertical lift driven devices, vertical drag designs, airborne turbines and jet engine turbine configurations in the detailed trade-off phase. The different configurations are visualised in figure 30.2.

Figure 30.2: Trade-off configurations: Horizontal axis wind turbine (a), airborne turbines (b), vertical axis wind turbine (c), jet engine turbine (d)

In terms of feasibility and reliability the HAWT was seen as the best choice of all the options. This was because the HAWT design has already been successfully implemented in Antarctica and has been

applied numerous times in various configurations all around the world. Due to the wealth of experience associated with this design being implemented on such a vast scale, in addition to the steady refinement of design methodology within the wind energy sector, the HAWT is deemed to be the safest choice in terms of reliability. The HAWT benefits from the experience curve resulting in a reduction of cost each year. Furthermore, this design has the highest maximum theoretical efficiency and performs well in terms of maintainability of the system. Finally, in terms of sustainability and environmental concerns, the HAWT is seen to have a relatively low carbon footprint. Since the wind speeds found at the Signy location are so high, the noise of the turbine is not seen as a prohibitive factor. In conclusion the lift driven HAWT system was taken to form the basis of the design with further configuration changes applied during the detailed design of the turbine.

30.5 Turbine design

The estimated power of approximately 50 kW can be produced by one large turbine or by multiple small turbines. For this project, it turned out that 3 turbines each producing 17 kW is preferred based on reference Antarctic research stations and criteria such as redundancy, maintenance, manufacturing, transportation, installation and cost. For each turbine, the main components of the rotor, nacelle and tower are designed where the largest attention is put on the most risky components.

The counter clockwise rotating turbine is operative within a velocity range of 3 to 30 m/s. The designed wind turbine is a variable pitch/variable speed downwind oriented turbine with a diameter of 8.8 m. Based on its downwind configuration, a passive yaw system is implemented on the turbine combined with a yaw limitation to avoid cable twist. The aerofoil shaped rotor blades have an optimum twist and chord distribution and are internally supported by a stiffening box which is able to withstand all forces exerted on the blades. The blade deflection is limited to 50 cm in all situations. The blades are made out of a hybrid composites using flax and bio-based epoxy in

combination with glass or carbon fibres. The rotation of the blades is converted into electrical energy by use of the shaft and a gearless permanent magnet direct drive generator cooled with a passive cooling system. The cooling system of the generator uses the Antarctic climate to its advantage. The other nacelle components are protected from the environment by a nacelle housing which creates the least amount of drag. The system is provided with an aerodynamic and mechanical brake and is designed taking into account fail safe design methods. The bedplate made of highly recyclable steel alloys transfers the loads of the other components into the tower.

A tapered 8.8 m tower going from a diameter of 0.64 m up to 0.16 m, is supporting the complete rotor and is designed in such a way that it can handle all load cases. A rock anchor foundation fixes the wind energy system to the ground with 8 anchors with a length of 2 m. The wind turbine design was subjected to fatigue and vibrational analysis as well as an intensive verification and validation. In figure 30.3, the final configuration of the Windpulse is shown. Taking into account the electrical component losses of 5% and the yaw limitation losses of 15%, the AEP of one 17kW turbine is calculated to be approximately 101,790 kWh. For the design of the wind turbine, the capacity factor based on the extremely high wind speed distribution corresponds to 0.68.

Figure 30.3 Visual impression of the designed wind turbine

By adding special features to the turbine, the system is suited to the Antarctic environment. The bird impact is minimized by using one solid black blade and two blank blades to reduce the effects of motion smear. Moreover to ensure that no animals would be hit by the blades and also for aerodynamic purposes, a ground clearance of 4.4 m was used. All power transfer cables are placed into insulated tubes to avoid any shocks to the wildlife. To account for the extremely low Antarctic temperatures, an electric pulse de-icing system is implemented to keep the blades free from ice formation. A capacitor is installed on the blade that creates micro-thermal pulses in order to meld the ice created on the leading edge. Due to the height of the wind turbines they are vulnerable to the effects of direct lightning strikes which is dealt with by installing a lightning system. The design is completed by adding sensors used to provide environmental and operational information.

30.6 Batteries

Batteries are vital in the provision of power from the electrical system to the research station. In that way, energy can be stored and used when the wind speeds are too low to produce the required power demand.

For the design of the energy storage system lead acid, as opposed to lithium or nickel based batteries, was selected as the battery of choice. One of the dominant reasons for selecting this type of batteries were the low costs per Wh of 0.17 USD. Furthermore as they account for 40-45% of all battery sales worldwide and have a well-established recycling process, bringing the recycling rate of such batteries to more than 97%, and as such lead acid batteries are a safe and sustainable choice for such storage systems. Due to the expected cycling of the system, deep-cycle, VRLA (Valve-Regulated Lead-Acid) maintenance free batteries will be used in order to achieve a longer lifetime with least maintenance possible. The battery system is required to provide 65% of installed power for an extended period of time to the station. Two size options are presented, with future clients to select one for their specific purposes. One option provides energy for one day and

as such would require the back-up system to be turned on around 30 times a year. This option is the recommended choice as it provides a balance between costs and sustainability. The second option provides energy for three days with the generator needed to be turned on 4 times a year, and may be an option for clients who wish to minimize carbon emissions at a higher cost. The design results of the two options are presented below in table 30.1. It should be noted that in order to increase the lifetime of the batteries the maximum depth of discharge is limited to 50%, and thus the battery capacity must be twice as large as the usable energy.

Table 30.1: Battery properties

	1 Day Energy Option	3 Day Energy Option
Energy Capacity [kWh]	1,600	4,800
Mass [kg]	39,000	118,000
Cost [$]	270,000	810,000
Back-up Generator On [days/year]	30	4

The battery system will be located in an insulated enclosure with heating elements which can be used to keep the operating temperatures above the operating temperature of -20°C. The heating elements in the enclosure can also be used as an energy dumping load. Further confirmation of lead acid batteries being a viable and implementable choice in the Antarctic environment can be found by considering the Belgium Antarctic station where lead acid batteries are implemented successfully as an energy storage system.

30.7 Back-up

In the case the battery system does not have enough energy stored to meet demand at any given time or in case of emergencies, a back-up power system must be selected. Three types of back-up systems were considered, namely diesel, bio-fuel and hydrogen fuel cell systems. When evaluating possible designs for costs, reliability and sustainability, it emerged that converting the diesel (Marine Gas Oil) generator, currently used as the primary source of energy on the BAS station, to a back-up generator setup would be the best option.

Using the current generator would reduce costs, as no new generator would be purchased, also saving on transportation and installation of a new system. Furthermore, such generators are very reliable, as can be seen by the use of such generators as primary energy sources, and so a good choice for an emergency system. Moreover although such a system still causes greenhouse gas emissions, by using the currently stationed generator, the greenhouse gases that would be used to produce and transport a new generator can be offset.

In addition reusing the generator would promote the 'Reduce, Reuse, Recycle' motto of waste management hierarchy and as such promote a sustainable future. The generator currently stationed is a 40 kW generator and as such can be used both to meet peak power and provide a margin for possible increase. It is the recommendation of this group that a hydrogen fuel cell system should be explored for future replacement of the generator, when the cost of storing and producing hydrogen have reduced, and the technology has reached a level of maturity to safely and reliably be implemented as both a back-up system and an energy storage system. Such a future change is recommended in order to create an emissions free energy system for the Signy station.

30.8 Cost

The Signy station is controlled by the British Antarctic Survey. This organisation will own the power generation system to perform biological research on Antarctica and therefore there is no need to make profit out of the energy production of the wind turbine system. To present the project to potential investors, the total project cost and the electricity cost are determined. The whole turbine investment should be captured by the price paid for the energy over the entire lifetime. Assessing the wind energy cost requires careful research.

The levelised cost is of primary importance to determine the cost of electricity at a later stage. The key parameters that determine the levelised cost are the investment costs, the operations and maintenance costs and the lifetime of the wind system. The

investment costs are a one-time expense that occurs in the beginning of the lifetime and is around 55% of the entire project cost. Combining studies, the market analysis and a detailed estimation of separate components, this cost is estimated to be 6,882 €/kW and € 351,000 in total, which meets the requirements. The most expensive components of the turbine are found to be the tower, blades and generator and these parts together account already for 60 % of the whole wind turbine cost.

For this project a large battery system needs to be implemented. It accounts for 31% of the total costs. Throughout the entire lifetime, the wind turbine will undergo maintenance checks which require trained personnel and specific tools. The operations and maintenance costs typically account for 14% of the total costs of the entire project. Finally it is also important to consider the lifetime of the wind turbines to be able to describe the levelised cost. For the wind energy system designed in this report, the lifetime will be minimum 15 years.

The total project cost is found to be € 642,000 for the lifetime of 15 years. Dividing this by the entire lifetime, the levelised cost is determined to be € 42,800. The estimated cost of wind power varies significantly, depending on the capacity factor, which in turn depends on the quality of the wind resource and the technical characteristics of the wind turbines. The electricity cost for the Signy station is estimated to be € 0.1402/kWh.

30.9 Environmental impact

In order to meet the United Nations definition of sustainable development, defined as 'the ability to make development sustainable to ensure that it meets the needs of the present without compromising the ability of future generations to meet their own needs', a number of factors were considered throughout the design process. The environmental impact of the energy system has to be reduced as much as possible and therefore the carbon footprint, noise impact and visual impact of the wind turbines are studied.

With regard to carbon footprint a complete analysis of the lifecycle of the turbine was conducted. This analysis included manufacturing and transportation of all the parts, as well as the carbon emissions from the operation of the system. It was found that the carbon footprint of the system was found to be 974,800 kg and 782,600 kg for the one-day energy storage system and the three-day energy storage system respectively. These numbers highlight the sustainable nature of the design since the wind energy system results to have 71% reduction in carbon emissions when compared to the current diesel generator during the entire lifetime of the system.

Both noise and visual impact of the wind turbine system were considered so as to minimize their effect on the environment and the humans. Noise reduction was achieved by reducing the number of moving components by selecting a direct drive generator, and as such avoiding noise from having a generator gearbox. Furthermore the wind turbines were placed at 70 m away from the research station and as such avoiding announce to the researchers by keeping the noise produced by the turbine below 40 dB(A). In addition the location selected for the turbines ensured that even on the longest day of the year, no shadows were cast onto the research station and so avoiding any problems with shadow flicker.

30.10 Conclusion and recommendations

A lot of different power generating systems are available on the market. However, our wind energy system, The Windpulse, is very notable and outstanding compared to others. The turbines are designed especially for the Signy application and as such that they are as efficient as possible taking into account the cost, sustainability and environmental impact. The main conclusion is summarized in figure 30.4.

Power producing systems using wind energy as main source are an optimum choice to use on the Antarctic Island Signy. A lot of configurations are just not feasible taking into account the environment and weather conditions. Based on the sustainability,

safety requirements and the demand to be a zero emission generation plant, wind energy and eventually solar panels are the only suitable and already developed systems. These systems are no longer in a conceptual phase and thus very reliable. The importance of the energy system cannot be underestimated especially for such a remote location. Comparing wind energy with solar energy, it is clear that wind energy is by far the most favourable. At Signy, the wind speeds are so high which makes wind energy very attractive. In the winter period at Antarctica, the sun is only available for 4 hours a day with a very low solar intensity. During these hours, the system has to be able to produce the power demand for the whole day and therefore 1,800 m^2 of solar panels is required. This makes solar energy unlikely to power the research station. The panels can easily be destroyed by the 4,000 kg elephant seals living on the Island and also disturb the living area of the animals. Additionally, due to the large number of animals, the solar panels might become extremely dirty and decrease the efficiency significantly. Based on the maintenance requirement of one day, this might be a decisive criterion.

The Windpulse distinguishes itself from already existing and developed wind turbines based on multiple aspects. The size of the wind turbine of both the rotor, tower and nacelle correspond to found reference turbines which proves the validity of the design. The turbine is uniquely customized to power the research station of Signy Island and is adapted to withstand the harsh environment. Already designed and tried wind turbines are not provided by such features which will decrease its efficiency and thus the performance significantly when operating on the Antarctic continent. Since Signy Island is an important bird area, the protection of the wildlife is taken into consideration with a lot of care. The implemented black blade reduces the bird impact and will interrupt the normal life of the animals as limited as possible. Beside the electrical efficiency, the de-icing system also does not damage the aerodynamics of the blade aerofoil. The environment is also used as an advantage to cool down the generator. By using the outside temperature, a very precise passive system can be used. The system is much cheaper than the ones implemented on other turbines and these complex cooling

systems are of no use for our application. Even though the Windpulse is designed especially for this application, the system costs are acceptable and within the range of other available wind turbines. The same can be said from the carbon footprint of the turbines taking into account the manufacturing and transportation.

To conclude it can be said that the Windpulse is of great importance and can serve as a very suitable solution to power the Signy research station. It is shown that the Windpulse performs superior with respect to the competitors. Signy Island is a perfect location to implement wind turbines and the Windpulse respects all requirements and important aspects of the barely touched and seen continent. The Antarctic region is a priceless asset to the world with its unique wildlife and this should be protected as much as possible.

DSE group 20 recommends to continue the design with more research since the group has confidence in the project. More effort needs to be put into the research and development of wind turbines in harsh environments in order to help contribute to the fight against climate change. The design should be finalised and a prototype should be tested. An intensive analysis of the test should be done to make the system more reliable. Finally the manufacturing and integration of the system can be initiated.

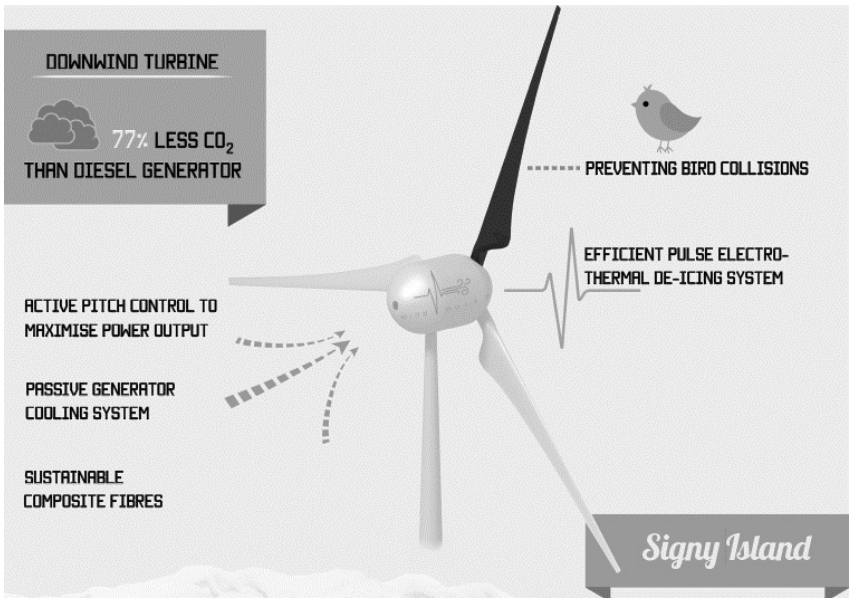

Figure 30.4: Main conclusion DSE Antarctic wind turbines

31. PHOENIX 5600: DESIGNING A PREMIUM LIGHT BUSINESS JET

Students: W.F.J.P. Brugmans, J.H. Bussemaker, M.B.P. Claeys, R.J. Groot, E. Kireeva, K.C. Leung, R.F. Mollee, S.S. Ng, F.M. Sickler, Y. Tigchelaar

Project tutor: dr.ir. W.J.C. Verhagen

Coaches: V. Gentile MSc, N. Koutras MSc

31.1 Introduction

In an era where 'time is money', an opportunity exists to offer a unique proposition to customers by developing a Premium Light Business Jet: the Phoenix 5600. There are a number of benefits by using business jets as a transportation mean. Firstly, the business jets are not constrained by airliner schedule and can depart at any required time. Furthermore, business jets have the capability to fly point-to-point and can be integrated relatively straightforwardly into door-to-door solutions. This saves a lot of valuable time of travellers with business purposes. Additionally, the Phoenix 5600 allows meetings and conference calls during flight, which greatly increases the business productivity.

Between 2013 and 2023, 9,250 new business jets will be produced globally, which is worth $260 billion. From the market analysis, it has been concluded that a significant growth in the last two decades has occurred, driven by an increasing demand of corporations for

business jets and the global recognition of the utility of business jet travel. The North American and Asian regions will be the main market focus. In general, extended range is the top priority for business jet customers.

Phoenix 5600 sets itself apart from the competition by combining flight speed in the transonic domain with short take-off and landing capability. Together, these aspects are expected to result in a significant decrease in travel time. Another outstanding aspect is the extended range and unparalleled cabin altitude compared to the other competitors. Simultaneously, sufficient capacity and comfort should be retained to be competitive in the light business jet market.

31.2 Mission objectives and requirements

The mission objective of the Phoenix 5600 was formulated as follows.

"Design a light business jet offering premium value through unparalleled in-class performance."

A set of requirements, provided by the customer, has to be met. Some of the requirements are subjected to be updated after an extensive market analysis has been done. The top-level requirements are listed in table 31.1. Each requirement is shown with its initial value.

Table 31.1: Summary of the top-level requirement of the Phoenix 5600

Requirement	Value
Range	4200 km
Nominal cruise speed	Mach 0.90
Maximum speed	Mach 0.95
Payload	2 crew 4 passengers (typical) 8 passengers (max) Passenger baggage
Service ceiling	41000 ft
RAMS	Similar to competition
Specific fuel consumption	0.5 lb/(lbf · h)
Take-off & Landing distance	1000 m 800 m
Pressurization	1500 m ISA equivalent

Noise level in aircraft	Exceed competitors
List price	$16 – 20 Million
Direct operating cost	2500 $/h
Entry into service	2020

31.3 Concepts and trade-offs

In the earliest stages of the design process, it is essential to consider all possible design solutions. These solutions include a variety of conventional and unconventional configurations, which are assessed systematically with respect to the most important design characteristics. This is done by means of trade-off tables which include criteria with corresponding weight factors. In this way, it is ensured that an unbiased decision is made, while the final choice is fully justified by its advantages with regard to the criteria and requirements set.

First trade-off

During the preliminary design process of the Phoenix 5600, two major trade-off procedures have been conducted. Initially, thirteen possible configurations were defined, after which a trade-off was made to find the four best designs. Brainstorm sessions with the entire group were hold to find the initial thirteen configurations. Possible designs for each component of the aircraft was defined individually, after which thirteen logical configurations were composed. Literature studies and individual research was part of the process and the goal was to include a large variety of design solutions. For example, both subsonic and supersonic type aircraft were considered. The used criteria in the first trade-off are listed below from the most important to the least important:

- Originality
- Cabin Noise & Cabin Space
- Fuel Storage, Aerodynamic Interference, Controllability & Risk
- Stability & Complexity
- Accessibility, Landing Gear Integration
- Engines & Time
- Cockpit Integration
- Ground Operations

This trade-off narrowed the number of optional configurations down to four. These four designs were then designed by Class I methods. Of these four configurations, three were designed to fly in the subsonic speed region and one for supersonic speeds. Design 1 is a subsonic three surface aircraft with forward swept wing. Design 2 is a subsonic delta wing with canard. Design 3 is similar to Design 1, only without horizontal tail. Finally, Design 4 is the supersonic aircraft. 3D images of all designs can be found in figure 31.1.

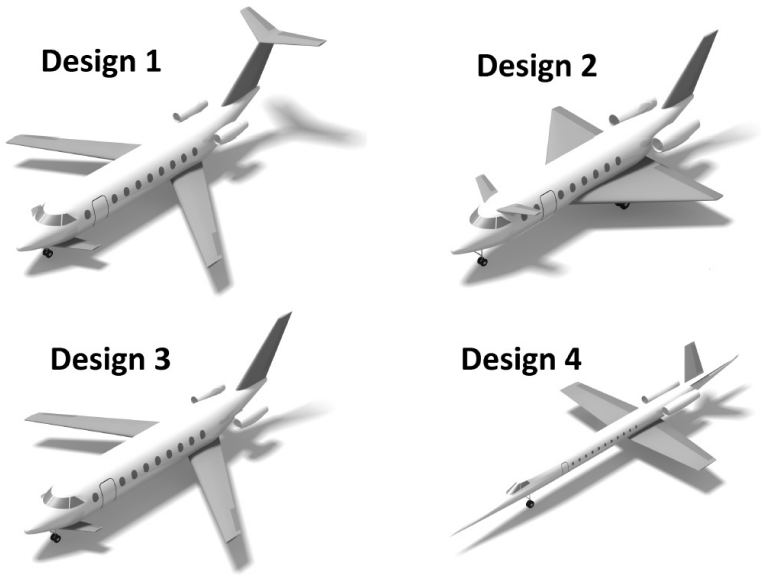

Figure 31.1: The configurations selected for Class I sizing

Second trade-off

The stated four configurations went through a Class I sizing method, in which a general design is generated. This means that the major components, such as the wing, are sized with limited resources available. Also, characteristics such as list price, drag polar and maximum take-off weight are estimated. From the preliminary four designs, one was found to be most suitable for further design. Again, a trade-off was conducted using various criteria. From most important to least important (detailed parameters are stated between brackets):

- Comfort (Cabin Noise, Seat Size, Facilities, Accessibility)
- Structural Characteristics (Fuselage, Empennage, Wing)
- Aerodynamic Characteristics (Lift & Drag Polar)
- Cost (List Price, Operating Cost)
- Risk (Feasibility)
- Stability (Static Margin, C.G. Range)
- High Lift Devices (Complexity, Efficiency)
- Weight (Maximum Take-off Weight)
- Empennage (Empennage Size)
- Sustainability (Engine SFC, Engine Emissions)
- Performance (Cruise Speed)
- Landing Gear (Size, Location)
- RAMS (Supportability)
- Fuel Storage (Location)

Overall, Design 1 was found to be the best performing configuration on the stated criteria. It is therefore the configuration that was designed according to Class II sizing methods.

31.4 Final concept

The final concept which was chosen in section 31.3 can now be designed in more detail. The aircraft features a canard, a forward swept, low mounted wing and a T-tail aft empennage configuration. The design of each part of the aircraft is discussed in this Section. The final concept is shown in figure 31.2.

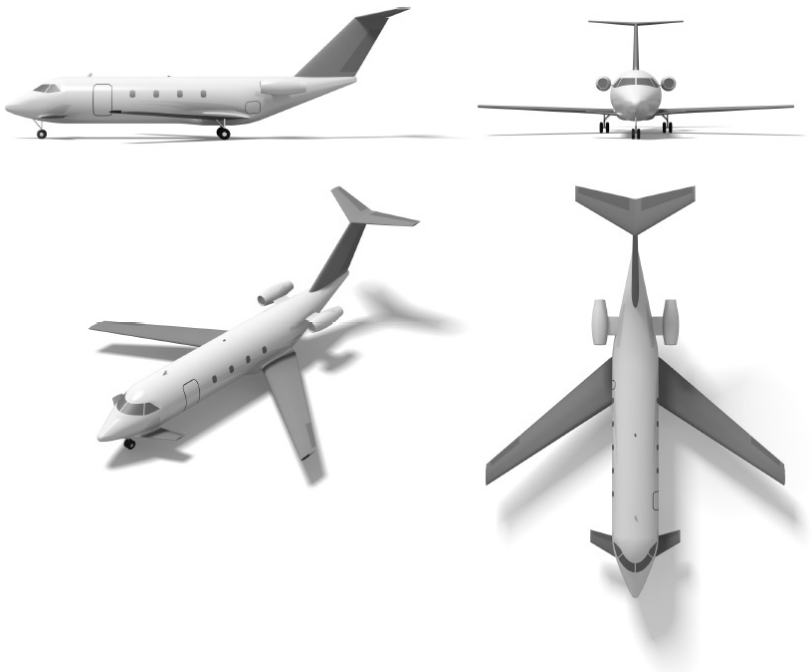

Figure 31.2: The final configuration selected for Class II sizing

Forward swept wing

A forward swept wing with a sweep angle of 35 degrees was chosen. This high sweep angle is required to ensure that no sonic speeds are reached on the surface of the wing for this will cause an increment of drag. The forward swept wing was chosen based on its reduced induced drag and its good controllability characteristics. From the aerodynamic analysis, the NACA 64212 Mod B was chosen as aerofoil type. In order to meet the landing distance requirement, fowler flaps were chosen as high lift device. Fowler flaps also have the advantage of their high efficiency, combined with relatively low mechanical complexity.

A big challenge that arose in using the forward swept wing was the occurrence of structural divergence. This effect is especially significant in this design due to the high forward sweep angle. The structural divergence causes a positive feedback system which induces high structural loads on the wing. During the design, it was decided to use aluminium material for the wing box. The divergence

was countered by shifting the shear centre in front of the aerodynamic centre. Although this can be done successfully for every cross section of the wing, the sweep angle is too significant to eliminate divergence entirely.

Empennage

The empennage of the aircraft consists of a canard in combination with a T-tail configuration. Adding the canard reduces the required size of the T-tail and besides this advantage, the added canard moves the centre of gravity forward. It will also reduce the size of the main wing since a part of the lift can be carried by the canard. For longitudinal and directional stability and control, the T-tail features elevators and a rudder, and the canard a canardvator.

Fuselage

It was chosen to size the fuselage such that a person with a height of 2 meters would be able to stand up straight in the cabin. A certain ratio was chosen between the diameter and the length of the fuselage to reduce the profile drag. The requirement for the interior of the fuselage states that it should support the possibility of holding meetings and presentations. Figure 31.3 shows the three final lay-outs which are offered for the customer of the Phoenix 5600.

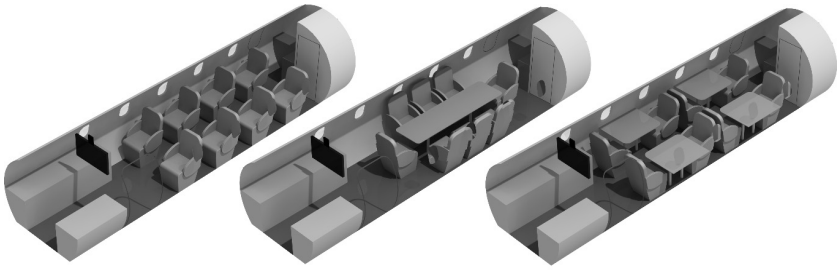

Figure 31.3 The interior design of the Phoenix 5600 business jet

The aircraft is internally pressurized from the cockpit until the baggage compartment, which is located behind the passenger cabin. The cabin itself is very spacious and features large windows, a large access door, a galley, a lavatory and state-of-the-art air conditioning, entertainment system, electrical systems and more. The cockpit floor

is raised slightly compared to the cabin floor for cockpit visibility and nose shape reasons. The cockpit windows allow excellent visibility for the pilots to ensure safe operations, also during high pitch flight.

Material selection

It was chosen to use aluminium alloys as material for the wing box, fuselage and landing gear. The exact alloy are determined by selecting the best combination of weight and cost, while still being able to cope with the loads of the structure. The materials for the wing box, fuselage and landing gear can be seen in table 31.2. Aluminium is the most conventional material choice available since its properties and structural behaviour are well known and predictable. Although compared to composite structures, aluminium weighs more and has a lower yield stress, the strength-to-weight ratio is still significantly high.

Table 31.2: The material selected for the different structures

Structure	Material	Yield strength [MPa]
Fuselage	Aluminium 7075-T6	503
Wing	Aluminium 7150-T77	570
Landing Gear Struts	Aluminium 6061-T6	276

Engine

The engines are attached high on the aft of the fuselage at the position of the aft pressure bulkhead. This ensures that engines are as far away from the cabin as possible (reducing inside noise), that the engine inlets are not positioned in the wing wake and that the engine exhaust flow does not interfere with the aft empennage surfaces. A total required take-off thrust of 37 kN was calculated. After a trade-off, the Pratt and Whitney 545C turbofan engine was chosen based on the high by pass ratio which results in a low specific fuel consumption.

Performance

After the main systems have been sized, it has to be verified that the aircraft will still meet the requirements which were set at the start of the project. It turned out that all the requirements have been met, and some even have been exceeded. The final performance characteristics are once more summarized in table 31.3.

Table 31.3: The performance characteristics of the Phoenix 5600 business jet

Performance Characteristics	Value	Unit
Take-off Distance	819	m
Landing Distance	746	m
Range	5686	km
Endurance	40.4	min
Glide Range	159	km
Glide Time	14.6	min

Finance

It is important for a new aircraft to eventually be profitable. Following from the market analysis, estimations have been made on how many aircraft will be sold. From the amount of aircraft sold, a list price could be obtained of $ 15.9 Million. Using the estimated production cost of the aircraft, the break-even point is calculated to be reached in 2026. Eventually the target of obtaining a profit of 24% is reached in 2036. With the list price of $ 15.9 Million, the aircraft will be located at the higher price range of the business jet market, but it will pay itself back by offering premium quality.

31.5 Conclusions

Starting with thirteen optional configurations, four designs were selected for Class I design. One design was chosen to perform a Class II design on; a forward swept, three lifting surfaces aircraft with the NACA 64212 Mod B aerofoil. Furthermore, the aircraft has Fowler flaps as high lift devices. The maximum take-off weight is still only 9,100 kg with a maximum payload of 980 kg, consisting of 4 passengers, but this can be extended to 8 passengers, with 2 crew members and 180 kg of baggage.

With the aft placed double Pratt & Whitney PW 545C engines in combination with an isolated fuselage, a cabin noise of 60 dB should be ensured which is equivalent to an average meeting room. With the comfort of a silent cabin a high-tech interior can be placed providing an opportunity for meetings and conference calls during the flight. The Phoenix 5600 is expected to be ready for operation in 2020 and with a list price of only $ 15.9 million and an operating cost of only

2400 $/h it is relatively cheap to operate. With a low noise and emission exhaust the Phoenix 5600 also complies with all the ICAO regulations. In the future, a detailed design can be conducted followed by testing, certification and production. For example, the wing needs to be redesigned in order to have a divergence free aircraft. Given a forward sweep angle of 35 degrees, aeroelastic tailoring using composites is the most promising solution.

According to the market analysis, between 2013 and 2023, 9250 new business jets are expected to be produced which is worth $260 Billion. The highest selling potential will be in Asia and North America and therefore these will be the target markets. With a range of 5600 km, all continental destinations of Asia and America can be reached, as well as all inter-continental destinations between America, Asia and Europe. With a cruise speed of Mach 0.90 and a maximum speed of Mach 0.95 the competition is overruled to ensure the shortest travel time as possible for our customers. With a short take-off and landing distance of 819 m and 746 m respectively, 3% more airports can be reached than the aircraft of the competition ensuring point-to-point travelling. Flying at a cruise altitude of 41,000 ft, no nuisance of the commercial airlines will be experienced and with a cabin altitude of 1,500 m ISA equivalent maximum comfort is guaranteed for our customer.

31.6 Recommendation

During the design process, several times design steps could not be performed in an optimal way. Sometimes data had to be estimated due to a lack of data, other times lack of resources or time caused inaccuracies. Some of most important recommendation are mentioned here.

For the main wing design, it is recommended to increase the complexity of the structural analysis. Further research can be done into torsional divergence by applying the described method to all positions on the wing instead of at the resultant lift force. For a metal wing box, using different thicknesses along the span or adjusting the

rib, spar and stiffener configurations can still optimize the geometry. Other solutions include making the leading edge of the wing load carrying or shifting the wing box structure forward. The use of composite materials is still an potential solution as its properties are unique and very suitable for countering torsional divergence. Therefore, it is strongly recommended to explore the composite coupling effect on the divergence matrix.

Furthermore it is advised to perform a more detailed market analysis. This will increase the accuracy of the predicted sale number. Besides this, a more extensive literature study would be helpful in finding more manufacturing and reference data. This will be result in making more accurate estimations for the aircraft design parameters. Especially for the engine performance characteristics, a lot of data is still missing.

32. SOTERIA MULTI-UAV OPERATIONS

Students: E. den Boer, J.T. Booms, H.J.A. Engwerda, A.P. Feenstra, C.R. Fonville, L.R.J. Hellenthal, R.H. Lenssen, R.C. van 't Veld, S. Verbist, J.J. Vroom

Project tutor: ir. C. de Wagter

Coaches: ir. J. Chu, ir. D. Deutz

32.1 Introduction and problem statement

Natural disasters can strike at any time and in any place. Due to their sudden nature, they often catch local residents unaware, resulting in extensive damage to the area along with casualties and injuries. In the ensuing chaos, it is often difficult for search and rescue (SAR) teams to coordinate the relief effort and reach survivors quickly. This leads to the mission need statement for this project:

"To improve SAR capabilities in the topics of surveillance and recognition in urban areas."

A project objective statement can be derived from this statement, based on the international micro aerial vehicle (IMAV) competition 2014. This competition simulates an area in the aftermath of a natural disaster and is set in a military training village in the Netherlands. Competing teams are challenged to perform some tasks that are common in SAR missions by designing an unmanned aerial vehicle

(UAV) system. It is tailored for participation with multiple UAVs, leading to the following project objective statement:

"With ten students in ten weeks, design a multi-UAV system with autonomous capabilities, which will prove itself to be useful in disaster scenarios in urban areas by winning the IMAV 2014 competition with a budget of 5,000 euro."

The system is called Soteria, after the ancient Greek goddess of safety, and it consists of an aerial segment and a ground station. The aerial segment is comprised of four UAVs, while the ground station is formed by two computers.

32.2 Requirements

From the project objective, seven top level requirements were formulated:

- The design shall win the IMAV 2014 competition.
- The design shall comply with the safety rules and the requirements of the IMAV 2014 competition set by its organisation.
- The total cost for production of the design shall not exceed € 5,000.
- The design shall comprise at least two UAVs.
- The design shall be completed within 10 weeks with 10 students.
- The design shall demonstrate autonomy.
- The design shall be functional in disaster scenarios in urban areas.

32.3 IMAV mission design

Within the international micro aerial vehicle (IMAV) competition there are ten mission elements that can be performed. Participants in this competition can choose freely what elements they want to do and in which order. Because the goal of Soteria is to win the most points within the competition, the most optimal combination needs to be chosen. In table 32.1 an overview of all mission elements is presented.

Table 32.1: Overview of mission elements

Mission Element	Description
1	Take-off from ground station position
2	Create a photomap of the competition area
3	Indicate roadblocks on a map
4	Perform a quick inspection of house numbers in a specified area
5	Scan the rooms in those houses for survivors
6	Create an overview of the rooms in a building
7	Identify items in the rooms of that building
8	Land on top of a building with a flat roof
9	Read the numbers on a panel across the street from the landing site
10	Perform a precision landing

In order to converge from the initial 2047 possible mission element combinations, an analysis was performed on the time, cost and points per mission element. After this analysis, the best three mission concepts were found. They are shown in table 32.2.

Table 32.2: Top three mission concepts

Mission Concept	Mission Element Numbers	Mission Points	Total Points
Concept I	1 4 6 7 (3 8 10)	12 120 252 60 (48 36 24)	444+
Concept II	1 3 4 8 10	12 48 120 36 24	240
Concept III	1 2 3 4 8 10	12 72 48 120 36 24	312

This is optimised exclusively for points gained. However, at this stage it was already known that performing indoor flight (mission elements 5, 6 and 7) will be very difficult. Therefore, although the indoor missions yield the most points by far, two outdoor-only concepts were also considered. For all three mission concepts, five points were analysed in detail: point sensitivity, operational risks, points per euro, technical feasibility and SAR capabilities. For the total score and point sensitivity, concept I performs best; the other two concepts perform similarly. However, due to the low feasibility and the operational risks of indoor flight, concept I was eliminated. Since concept III also performs the photomap mission element, it has more SAR applications. Therefore this mission concept was chosen.

Mission strategy

The mission elements presented in the previous section are performed in a certain order to minimise operational risks. The UAVs will perform a take-off (mission element 1), take the photos for the photomap (ME 2) and then return to the ground station, performing a precision landing (ME 10). Here, the SD card is removed and plugged into one of the ground station computers. The computer starts stitching the photos into one map, and will subsequently use recognition software to find the roadblocks to mark them on the map. Meanwhile, the UAVs will proceed to the rooftop landing (ME 8), ending with the house number recognition (ME 4). This mission scenario yields some driving requirements. Furthermore, the IMAV safety rules add some constraints to the design:

- The system shall execute its mission in less than 30 minutes.
- The system shall only use electric propulsion.
- The system shall store the last reliably known position of all UAVs
- The system shall be able to receive manual control inputs at any moment

32.4 Final design

With the mission and adjacent strategy known, the UAV can be designed that has to perform this mission. In the figure 32.1 the final design can be found. The next sections describe the multiple subsystems the UAVs consist of.

On-board computer

The on-board computer will process any data collected by the payload subsystem. This data may contain the numbers to be recognised, the command to take a picture for the photomap, the detection of an object or a check whether the UAV has landed. By looking at processing power, power usage, mass and costs, a trade-off was performed. Since computer vision requires a lot of resources, a lot of on-board computers could be crossed out. Due to its limited cost and weight and the extensive documentation, the Raspberry Pi, model B was chosen.

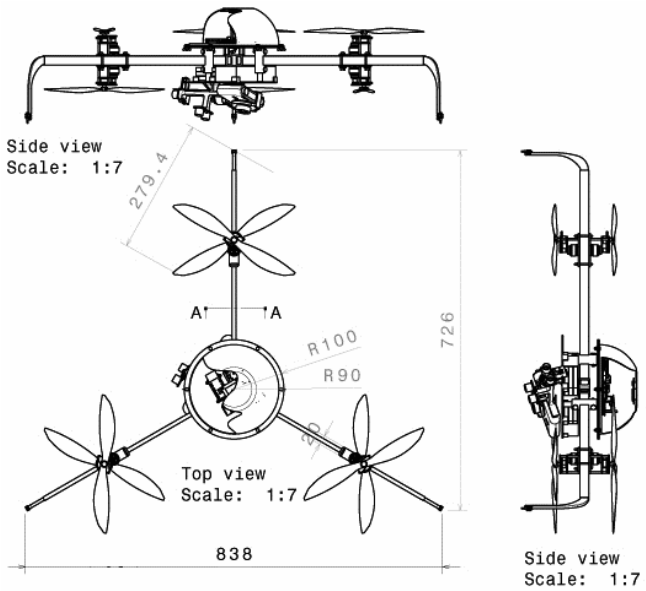

Figure 32.1: Three-view drawing of the Soteria UAV

Navigation, location and attitude control

Navigation involves the strategy with which a UAV moves from one location to another. It is an aspect of the design relevant to every mission element, since every mission element requires the UAV to be on a certain location, which on its turn must always be known due to the IMAV rules. From analysing several design options, the use of a GPS receiver in combination with flying towards pre-specified way-points was selected. Due to multipath errors and limited satellite coverage when flying at ground level, it is required to fly above houses. Besides navigation, the attitude has to be controlled as well. An Internal Measurement Unit (IMU) can be used to determine the attitude, where an autopilot can be used to process the generated data. The Paparazzi software is known for its extensive options regarding flight plans and is quite user friendly. The hardware which it operates upon was chosen from an analysis to be Lisa/m v2.0 due to its weight, size, documentation and connectivity with i.e. the Raspberry Pi. The combination of the IMU and GPS with a filter even enhances the performance. For the landing mission elements, three push buttons are chosen to give input whether the ground is touched.

In order to find the distance with respect to the ground, an ultrasonic range finder is used which is directed nadir.

Object detection and number recognition

Object detection will be needed to complete mission element 4 and 8, the house number recognition and roof landing respectively. For the house number detection, a camera has to be present as well as software in order to apply the recognition of the paper sheet were the number is printed upon. The Raspberry Pi camera module was selected as well as a script that uses Red-Green-Blue (RGB) colour values to detect a white sheet. Experiments with this script showed that the detection is working at a distance of at least 3 metre. When the sheet of paper has been detected, the number printed upon it can be recognised. In order to do this, the Camera Module is used with a script that uses a Hough transform and an OpenCV library containing reference numbers. Due to its free availability and ease of programming, this combination was found favourable. Several experiments were performed to verify that this software behaves as expected and from these experiments, an optimal distance with respect to the sheet was found. In order to fly at this distance, another ultrasonic range finder will be used which detects the distance with accuracy.

Data transmission

All the data processed in the UAV must either be transmitted to the ground station or stored locally. Also the IMAV rules state that the position of the UAVs must be available at the ground-station at any time during the competition. Another safety rule states that the UAV must be able to be manually switched off. For this last requirement, a Spektrum remote receiver was selected which can be used in combination with the hardware present on the ground station. Since the photos from the photomap require a vast amount of data to be transmitted, a simple SD card turned out more viable. For the communication with the UAV a radio frequency transmitter was chosen, namely the XBEE series 1 pro.

Map stitching

For the second mission element, a photomap must be created. This map comprises of multiple photos that have to be stitched together. In order to obtain points for this mission element, a certain ground resolution has to be obtained. It was found with calculations that a Sony Cybershot is able to cover the whole area with an overlap, including attitude error margins, such that the software is able to make an accurate stitch. The software used is the freeware Microsoft ICE. Several photo stitching experiments have been performed in order to validate this software. The attitude of the camera has to be controlled quite accurate for this mission element, even so accurate that the autopilot cannot perform adequate enough. Therefore an additional stabilising structure has to be introduced in terms of a gimbal. A self-developed gimbal structure is used together with a Mobius control board and motors. On this structure, the Sony camera as well as the range finders are mounted in order to always point respectively nadir and horizontally.

Blockade mapping

The main requirement of mission element 3 states that the UAV should be able to recognise an unknown number of blockades during its mission. These blockades then have to be indicated on the map already obtained in the previous mission element. The same colour detection is used for this purpose as in the object detection part. The roads will be distinguished from the surroundings by this recognition method and consecutive the blockades are found by this means. The ground station will perform this mission element due to its larger processing power.

Ground station

The ground station will consist of two computers. One will be used to perform the map stitching and blockade detection, marking its findings on the map. Its operating system will be Windows 7 or 8. The second ground station, using a Linux operating system, will run the ground station software necessary to use the Paparazzi software that will control the UAVs. Using an Xbee telemetry modem, it will send commands to the UAVs when necessary and receive their GPS

coordinates. These must be displayed to the IMAV committee at all times. Two laptops owned by team members will be used to reduce costs.

Flying concept

Multiple flying concepts were investigated and from these a trade-off was performed. Flapping wings were found to be infeasible due to the lack of proven concepts. Balloons were found to lack controllability which leaves only three feasible design options, namely airships, aircraft and rotorcraft. The dimensions, performance, controllability and feasibility of these three design options were investigated. The airship could be crossed out due to exceeding maximum dimensions specified by IMAV. Vertical take-off aircraft were found to be infeasible due to the transition between the different flight modes and conventional take-off aircraft have problems with autonomous take-off as no industrial proof of concept was found. The control algorithms for a multicopter are less complicated than those of a helicopter, hence the multicopter concept was selected.

Propeller

To select a propeller, two conflicting considerations need to be taken into account: a larger propeller has a high efficiency than a small propeller, but a small propeller yields increased controllability. Furthermore, the scoring system of the IMAV competition rewards smaller UAVs. After research, it was determined that a maximum thrust-to-weight ratio of 2:1 is required, while the nominal thrust-to-weight ratio was found to be 3:2. With these values in mind, the smallest size propellers that generate sufficient thrust are 11 inch (28 cm). Among these, the APC Slow Flyer 11x4.7 propeller was found to be optimal. To generate the required thrust, six propellers are required, making the design a so-called hexacopter.

Motor

The motor selection process was performed by selecting one motor from a database containing 3748 options from 65 different manufacturers. After verification of the database, the revolutions per minute (RPM) at maximum thrust and efficiency at nominal thrust

were found for each motor. In order to match the RPM of the motor with that of the propeller, a gearbox was designed. Including the cost and weight of the gearbox as well as the power supply subsystem, since these vary per motor, the Tiger MN1806-2300 was selected, with a gearbox with a gear ratio of 3.61:1.

Electronic speed controller

With the motor selected, the next step of the iteration is to select the electronic speed controller (ESC). This ESC converts the direct current from the battery to alternating current for the motors. Furthermore, the ESC uses the signal from the autopilot to control the engine RPM and power. The most important parameter for the ESC is the motor current. The maximum current the motor can draw from the ESC should be lower than the rating of the ESC. Naturally, the ESC must be compatible with the autopilot. The lightest ESC which can handle the current of the motor was found to be the Afro Slim 20Amp Multi-rotor Motor Speed Controller, which was duly selected.

Power supply

For the propulsion and payload subsystems, a power supply is needed that can provide a total of 178 Wh, including a contingency factor of 5%. First sustainable energy harvesting is investigated, but this was found infeasible for the UAVs due to size and weight constraints. The ground station might be able to make use of this energy source, but this has not been part of the design since two standard computers can form a functional ground station for the competition. Battery packs are chosen as the power source for the UAVs. By looking at specific energy and cost efficiency, a list of feasible design options could be made. Finally a trade-off between power, mass and price was performed and a large and a smaller Lithium-polymer battery pack were selected that provide a total of 180 Wh.

Airframe

The airframe is needed to support all subsystems and transfer all loads generated by other subsystems. First the airframe configuration was determined as being a double-deck central platform that supports

the payload and three arms that each have two engines attached in a push-pull set-up. This so-called Y6 configuration yields a lighter airframe than using six arms, like a conventional hexacopter. Dimensions can be found in figure 32.1.

Secondly, a landing gear was designed. The UAV should be able to withstand a landing with 1 m/s vertical speed at 45°. The landing gear was designed to be located at the tip of each arm, which provides protection of the propellers. Various shapes were researched, which resulted in the choice for a simple strut. A pressure switch is attached to the tip of each strut in order for the UAV to know when it has touched down, allowing for direct thrust cut down.

To have an efficient system, mass is to be minimised. This is achieved by using materials with a high strength-to-density ratio. Multiple materials were examined and the optimal material for the airframe arms was found to be carbon fibre. The landing gear should be impact resistant, which carbon fibre is not. In order to withstand the rough landing load, 3D printed material was chosen, as this allows for certain bending and can thereby absorb impact energy.

The airframe should allow the six engines to be mounted. The engines are to be mounted using bolts. However, the carbon fibre airframe loses strength when holes are drilled into them, therefore it was chosen to glue 3D printed plates on the upper and lower side of the beams. The engines are then bolted onto these plates.

32.5 Subsystem integration

All subsystems are designed and the integration into one complete design is shown in figure 32.2. It displays the push-pull configuration of the propellers and the Y-shaped frame. It can also be seen that payload is attached both on top of and underneath the centre of the frame. This is done to separate the systems that generate strong currents from the sensitive electronic circuits. For example, the batteries are mounted on the lower deck, while the autopilot and GPS module are on the top platform. The gimbal is also mounted below

the airframe. This is done to give the ultrasonic rangefinder, the Raspberry Pi camera and the Sony Cybershot camera a clear field of view.

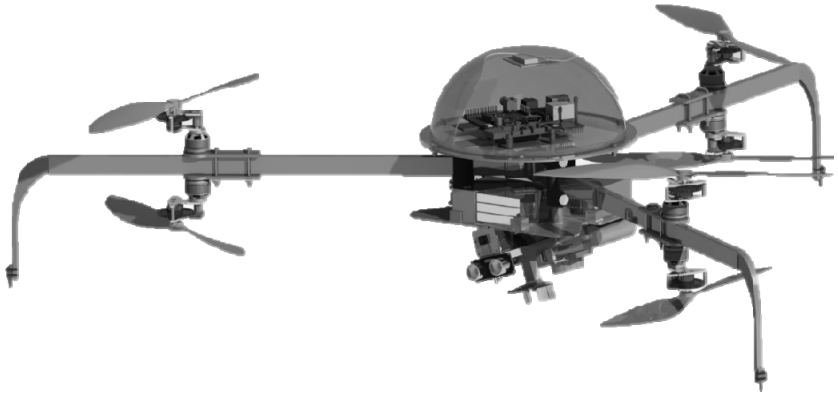

Figure 32.2: Computer aided drawing of one Soteria UAV

Cost and power budget

The total mass and power budget of each UAV can be graphically represented. In figure 32.3, all subsystems and unforeseen costs are represented by their respective percentage of total mass and total cost of the system.

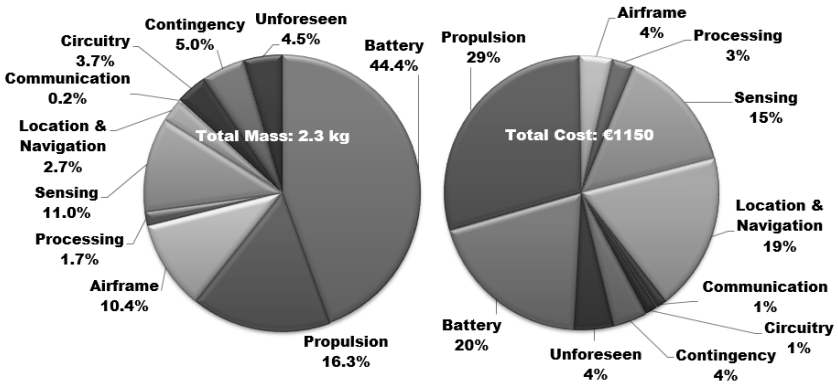

Figure 32.3: Mass and cost budgets

From these figures it can be seen that the batteries and propulsion are the biggest subsystems in terms of mass and cost. Next to these costs,

also a ground station mass and cost is present which consists of respectively 2.0 kilograms and €300.

Table 32.3: List of important design parameters

Parameter	Value	Unit
Number of UAVs	4	-
Range	20	km
Flight Time	20	min
Maximum Speed	17	m/s
Dimensions	830 x 777 x 208	mm (l x w x h)
Total Weight	2.3	kg
Centre of Gravity	0.12 x -0.13 x -22	mm (l x w x h)
Power Supplied	180	Wh
Cost	1150	€
Ground Station Weight	2.0	kg
Ground Station Cost	300	€

Listing of most important design parameters

The performance of the UAVs can be represented by parameters listed in table 32.3. Note that the total weight includes unforeseen and general elements such as wires, connectors and fuses which are not represented by the payload or propulsion group.

32.6 Conclusion

This project was initiated with the objective to design an autonomous multi-unmanned aerial vehicle (UAV) system that can be used to aid in search and rescue (SAR) missions after natural disasters and can be tested at the international micro aerial vehicle (IMAV) competition, while keeping production costs within a budget of €5000. Such a design has been generated and it is named Soteria. It comprises four UAVs, distinguishable by their colour scheme, and two laptops that act as ground station to give the operator an overview of the ongoing mission.

Soteria is specialised in autonomous performance. After the UAVs have taken off from a local command centre (LCC), the system is able to create a photomap of the area of interest. Using this map it will detect and mark any road blockades. It is also able to identify the numbers of all houses in a specified section of the area. This allows for

a rapid increase in situational awareness of the area and its accessibility. If one wants to continually observe a static object, the UAVs can fulfil this need, as they are able to land on a flat roof which can act as a perching location. When their mission is done, all UAVs will return to and perform a precise landing at the LCC. All these capabilities are to be tested in the IMAV 2014 competition.

The design of the UAVs was split up in two parts: design of the payload and design of the airframe with the propulsion system attached. A three-armed configuration with six engines and propellers was designed. The centre of this configuration features a double-deck platform, covered with a dome to protect its payload against rain and impact. This payload consists of a processor, cameras, ultrasonic rangefinders and a navigation module.

A market analysis has shown that Soteria offers a greatly reduced price in comparison with similar systems and increased functionality in comparison with other systems in the same price category, making it a valuable system to be used in search and rescue operations.

32.7 Recommendations

The hardware selection of the design has been completed, but further testing is required to verify and validate all subsystems and their integration. This includes researching the optimal distance for the camera module to recognise numbers and the reliability of the rangefinder measurements, allowing further optimisation of the mission approach. Furthermore, testing is to be performed on the use of colour detection for the detection of roads and road blockades in a photomap. If unforeseen complications arise during these tests, further research into edge detection is recommended. More research into availability of multi-constellation satellite receivers is stimulated; as such a receiver will further enhance the performance of Soteria in dense urban areas. Finally, the impact of the environment, such as dust and particles, on the UAV is recommended to be researched, in order to quantify and prolong the lifetime of the Soteria system.